University of Southampton

Faculty of Environmental and Life Sciences

School of Biological Sciences

Investigating the role of MHC class I molecules in immune evasion by transmissible tumour cells

DOI:

by

Kathryn Anne Hussey

ORCID ID 0000-0002-8882-1502

Thesis for the degree of Doctor of Philosophy

June 2024

University of Southampton

Abstract

Faculty of Environmental and Life Sciences
School of Biological Sciences

Doctor of Philosophy

Investigating the role of MHC class I molecules in immune evasion by transmissible tumour cells

by

Kathryn Anne Hussey

Downregulation of Major Histocompatibility Complex (MHC) molecules is often key to evasion of the immune system by tumours and viruses. Transmissible cancers transmit between individuals, in a manner akin to a metastatic event, providing a unique opportunity to study the evolution of MHC loss in the face of selective pressure from the immune system. Tasmanian devils are infected with two genetically distinct transmissible cancers which transmit via biting behaviours. Devil Facial Tumour Disease (DFT1) emerged over 25 years ago and has spread across most of Tasmania, while DFT2 was identified in 2014 and is still limited in geographical range. In contrast to DFT1, which has epigenetically downregulated MHC class I expression, DFT2 tumours express MHC class I molecules, but recent evidence shows some DFT2 tumours have lower MHC class I expression, suggestive of evolving immune escape by this cancer. In this thesis, I investigate how MHC expression is changing in DFT2 as it spreads through the population and encounter hosts with disparate MHC class I genotypes, and how non-classical MHC class I molecules may be modulating immune escape by DFT1.

DFT1 (n=76) and DFT2 (n=34) tumour biopsies were stained by immunohistochemistry (IHC) for classical MHC class I molecules, and non-classical, Saha-UD and Saha-UK. An expression score was generated using semi-automated image analysis to quantify IHC staining. To investigate host immune responses to MHC class I expression, tumours were also stained for IFNγ (DFT1, n=51; DFT2, n=25) and CD3 (DFT1, n=42; DFT2, n= 20). Two antibodies previously generated in our lab were validated for use in this thesis, Saha-UD (α-UD_14-37-3) and IFNγ (α-IFNγ_13-44-6). Hosts (n=10) were genotyped using deep sequencing at three classical MHC class I loci to study whether mismatch between host and tumour drives MHC class I loss in DFT2.

In this thesis I have confirmed classical MHC class I expression is highly variable among DFT1 and DFT2 tumours. In DFT2, classical MHC class I expression correlated with IFNγ expression, therefore it's expression in DFT2 may be immunogenic. However, there was no correlation between classical MHC class I expression and host-tumour mismatch. A ubiquitous and likely fixed allele, SahaI*27, is expressed within the population and DFT2 cells, which may assist DFT2 immune evasion. In DFT1, the finding of classical MHC class I expression in primary tumours is surprising and challenges our understanding of immune escape by DFT1, as it was presumed all DFT1 tumours had downregulated MHC class I from the cell surface. For the first time, non-classical, Saha-UD expression has been confirmed in DFT1 tumours. Interestingly, DFT1 tumours are heterogeneous for expression of non-classical, Saha-UD and Saha-UK, and their expression is positively correlated with classical MHC class I expression. Therefore, their expression may be immunosuppressive, to prevent host immune activation.

These results demonstrate that DFT2 is evolving immune evasion mechanisms as it transmits between individuals in the population, with the potential for more rapid dispersion if MHC-negative subclones gain dominance. Expression of a dominant MHC class I in the population likely facilitates DFT2 spread in this area. While non-classical Saha-UD expression by DFT1 tumours *in vivo* may be a mechanism for immunosuppression, further work is needed to characterise its ligand on immune cells. This data can be used to inform more effective management of the population and vaccine design. Further, this study provides a platform to investigate the mechanisms behind MHC loss in a cancer under sustained pressure from the immune system.

Table of Contents

Table of Tables

Table of Figures

Table of Figures

Table of Figures

List of Accompanying Materials

Hussey, K., Caldwell, A., Kreiss, A., Skødt, K., Gastaldello, A., Pye, R., Hamede, R., Woods, G.M. and Siddle, H.V. (2022) 'Expression of the Nonclassical MHC Class I, Saha-UD in the Transmissible Cancer Devil Facial Tumour Disease (DFTD)', *Pathogens*, 11(3), 351. https://doi.org/10.3390/pathogens11030351

Data DOI: https://doi.org/10.5258/SOTON/D3092

Research Thesis: Declaration of Authorship

Print name: Kathryn Hussey

Title of thesis: Investigating the role of MHC class I molecules in immune evasion by transmissible tumour cells

I declare that this thesis and the work presented in it are my own and has been generated by me as the result of my own original research.

I confirm that:

1. This work was done wholly or mainly while in candidature for a research degree at this University;
2. Where any part of this thesis has previously been submitted for a degree or any other qualification at this University or any other institution, this has been clearly stated;
3. Where I have consulted the published work of others, this is always clearly attributed;
4. Where I have quoted from the work of others, the source is always given. With the exception of such quotations, this thesis is entirely my own work;
5. I have acknowledged all main sources of help;
6. Where the thesis is based on work done by myself jointly with others, I have made clear exactly what was done by others and what I have contributed myself;
7. Parts of this work have been published as:-

Hussey, K., Caldwell, A., Kreiss, A., Skødt, K., Gastaldello, A., Pye, R., Hamede, R., Woods, G.M. and Siddle, H.V. (2022) 'Expression of the Nonclassical MHC Class I, Saha-UD in the Transmissible Cancer Devil Facial Tumour Disease (DFTD)', *Pathogens*, 11(3), 351. https://doi.org/10.3390/pathogens11030351

Signature: ..... Date: 06/06/24

Acknowledgements

I dedicate my thesis to my Grannie, whom we lost in the midst of a pandemic. She was one of my strongest supporters, and the most loving, generous, and kind person I have ever known. She would be so proud.

Thanks be to God; my comforter, my strength, and my guide. Through a difficult four years I have been held and observed many blessings.

Extra special thanks to my primary supervisor, Dr Hannah Siddle. Thank you for believing in me, teaching me, and supporting me. Thank you for your feedback and your encouragement. I feel very blessed to have you as my PhD supervisor. I am not sure I would have made it to the end without you.

Thank you to my co-supervisors, Prof Edd James and Dr Emma Reeves, for your feedback and support. Thank you to my Siddle lab mates over the course of my PhD: Dr Rachel Owen, thank you for your humour, advice, and always being there to answer questions; Anne-Lise Gerard, thank you for your kindness and illustration of work ethic; Dr Annalisa Gastaldello, thank you for your teaching.

Massive thanks to my family for their endless support. To my parents for their love, comfort, and always rooting for me. And for proofreading my thesis despite not understanding a lot of what I was talking about. Thank you to my brother, Daniel, for your constant encouragement and for making me laugh.

Thanks to my friends for keeping me sane! Firstly, my PhD pals. Belle, Jacob, and Lloyd, I am so blessed to have you as my friends. We started our PhDs together and I am so proud of us all for what we have achieved. You are all amazing. Thank you for being there through the highs and lows. Beatriz, you have the biggest heart of anyone I know. Thank you for making me smile.

To my oldest friends, Avery, and Naomi, thank you for being a consistent source of friendship and support in my life. To my newest friends from FMS (you know who you are), thank you for bringing so much joy into my life, I am so thankful to have met you.

Thank you to colleagues and collaborators, without whom this thesis would not exist. The Gerald Kerkut Trust and the University of Southampton Presidential Scholarship for funding my PhD project. Rodrigo Hamede (University of Tasmania) for supplying Tasmanian devil tissue samples. Jon Ward and Jenny Norman (Histochemistry Research Unit, University of Southampton) for paraffin embedding tissue samples, providing coated slides, and assistance with FFPE cell lines.

Acknowledgements

Jacob Trend (University of Southampton) for lending your image analysis expertise to creating a semi-automated image analysis technique for expression scoring. Nicola Pratt (National Oceanography Centre, University of Southampton) for amplicon library preparation and Illumina sequencing. Dr Jane Gibson (University of Southampton) for drafting a script for assignment of Tasmanian devil classical MHC class I alleles from NGS reads. And the IRIDIS High Performance Computing Facility (University of Southampton), which was used for NGS data analysis.

Abbreviations

APP ..... Antigen Presentation Pathway

β_2m β2-microglobulin

BTN ..... Bivalve Transmissible Neoplasm

CAFs ..... Cancer Associated Fibroblasts

CCL22 ..... CC Chemokine Ligand 22

CTLA-4 ..... Cytotoxic T-lymphocyte-associated Protein 4

CTVT ..... Canine Venereal Transmissible Tumour

DFT1 ..... Devil Facial Tumour Disease 1

DFT2 ..... Devil Facial Tumour Disease 2

DFTD ..... Devil Facial Tumour Disease

DFTs ..... Devil Facial Tumours

DPIPWE ..... Tasmanian Government Department of Primary Industries, Parks, Water and the Environment

ECM ..... Extracellular Matrix

EED ..... Embryonic Ectoderm Development

EMT ..... Epithelial-to-Mesenchymal Transition

ER ..... Endoplasmic Reticulum

ERAP ..... Endoplasmic Reticulum Aminopeptidase

FFPE ..... Formalin-Fixed Paraffin-Embedded

IFNγ ..... Interferon-γ

IHC ..... Immunohistochemistry

IL-6 ..... Interleukin-6

IPTG ..... Isopropyl β-D-1-thiogalactopyranoside

KIR ..... Killer Cell Immunoglobulin-like Receptor

MAIT cells ..... Mucosal-Associated Invariant T cells

MHC ..... Major Histocompatibility Complex

Abbreviations

MDSCs..... Myeloid Derived Suppressor Cells

NGS ..... Next Generation Sequencing

NK Cell..... Natural Killer Cell

NLRC5..... NOD-like Receptor Family CARD Domain Containing 5

PCR..... Polymerase Chain Reaction

PD-1 ..... Programmed Cell-death Protein

PD-L1..... Programmed Death-ligand 1

PIR..... Paired Ig-like Receptor

PLC ..... Peptide Loading Complex

PRC2..... Polycomb Repressive Complex 2

SDS-PAGE ..... Sodium Dodecyl Sulphate Polyacrylamide Gel Electrophoresis

SNPs ..... Single Nucleotide Polymorphisms

TAP..... Transporter Associated with Antigen Processing

TCR..... T Cell Receptor

TGF-β ..... Transforming Growth Factor β

T regs ..... T Regulatory Cells

Chapter 1 Introduction

1.1 Cancer evolution

Cancer is caused by cellular mutations leading to uncontrolled cell growth and is a common occurrence in multicellular organisms. Most cancers emerge and remain in a single individual, which are termed 'somatic cancers' in this thesis. However, some cancer cells have gained the ability to survive outside of their original host and transmit among a population, like a pathogen, termed transmissible cancers. Transmissible cancers should be recognised by a mammalian immune system due to differing major histocompatibility complex (MHC) molecules on the cell surface, and thus represent a valuable phenomenon for the study of cancer evolution and immunology as they avoid the immune systems of multiple hosts.

Broadly, there are requirements that all cancer cells need to fulfil to survive and progress. These requisites are summarised by the Hallmarks of Cancer (Hanahan, 2022; Hanahan and Weinberg, 2011, 2000), illustrated in Figure 1.1. The original hallmarks defined in 2000 (Hanahan and Weinberg) included 6 conditions: resisting cell death, sustaining proliferative growth, evading growth suppressors, inducing angiogenesis, enabling replicative immortality, and activating invasion and metastasis. Two additional hallmarks were proposed in 2011, reprogramming cellular metabolism and avoiding immune destruction. Along with the hallmarks, 'enabling characteristics' were defined, which are overarching mechanisms that support the development of cancer's functional traits (hallmarks); these were genome instability and mutation (2000), and tumour-promoting inflammation (2011). Further hallmarks and enabling characteristics were proposed in 2022, unlocking phenotypic plasticity and senescent cells for the former, and non-mutational epigenetic reprogramming and polymorphic microbiomes for the latter; while the hallmarks suggested in 2011 had been validated since they were first proposed (Hanahan, 2022).

The continual modification of the Hallmarks of Cancer highlights the development in our understanding of how cancer operates and progresses. Particularly with regard to the role of the immune system, with 'avoiding immune destruction' and 'tumour-promoting inflammation' proposed and confirmed in later publications (Hanahan, 2022; Hanahan and Weinberg, 2011). The ability of cancer cells to evade the immune system is the central topic of this thesis and will be the focus going forward.

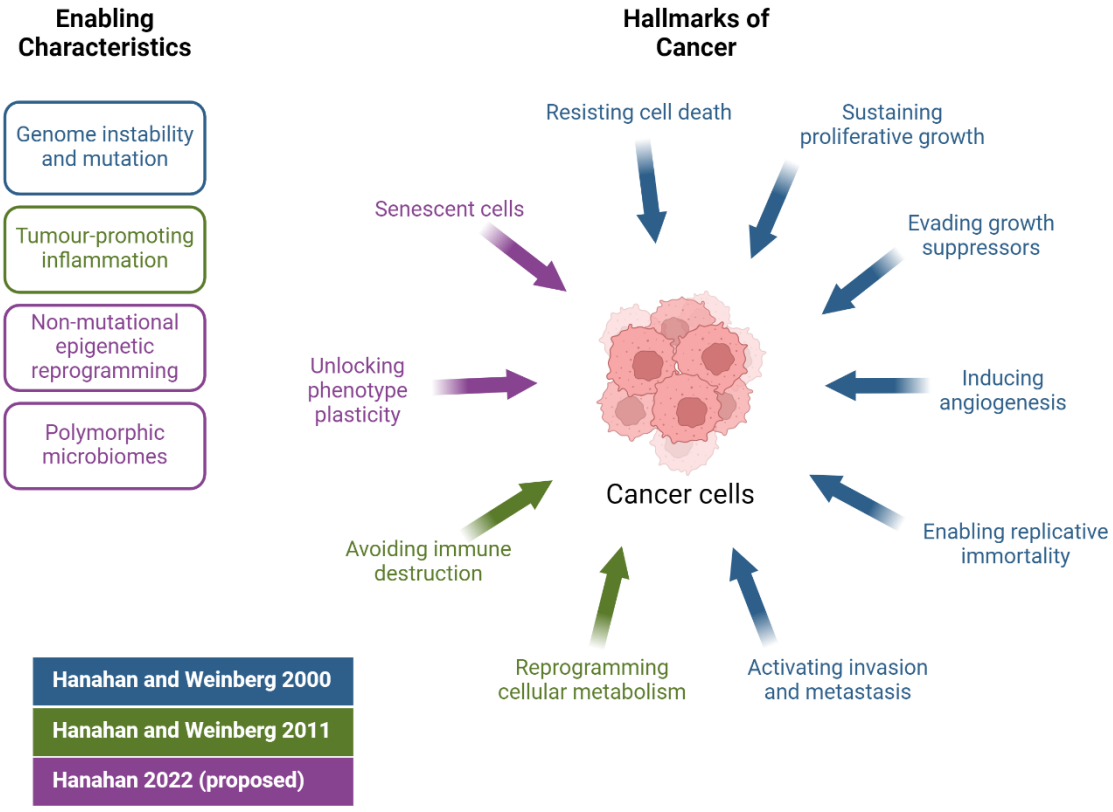

Figure 1.1 Hallmarks of cancer

The hallmarks of cancer and enabling characteristics that apply to all cancer cells, first put forward by Hanahan and Weinberg in 2000 (shown in blue). Additional hallmarks were proposed by Hanahan and Weinberg in 2011 (in green) and by Hanahan in 2022 (purple), though the latter have yet to be validated by further studies. Figure was adapted from Hanahan (2022). Created with BioRender.com.

1.1.1 Cancer immunoediting

The immune system is an important driver of cancer evolution. The immune system can detect cancer cells, largely due to their high mutational burden via peptide presentation by MHC class I molecules, which often results in cell killing, such as cytotoxic killing by CD8+ T cells. As a result, recognition of cancer cells by the immune system provides a selective pressure for the development of immune escape mechanisms by the cancer. This is described by the theory of immunoediting (Dunn et al., 2004, 2002; Schreiber et al., 2011), consisting of 3 stages: elimination, equilibrium, and escape (explained below and illustrated in Figure 1.2). One of these immune escape mechanisms is MHC class I loss, to prevent recognition of cancer cells. Recently, more detailed mechanisms of how MHC class I loss occurs during clonal evolution of cancer has

been elucidated, aided by detailed sequencing projects on primary cancers (McGranahan et al., 2017).

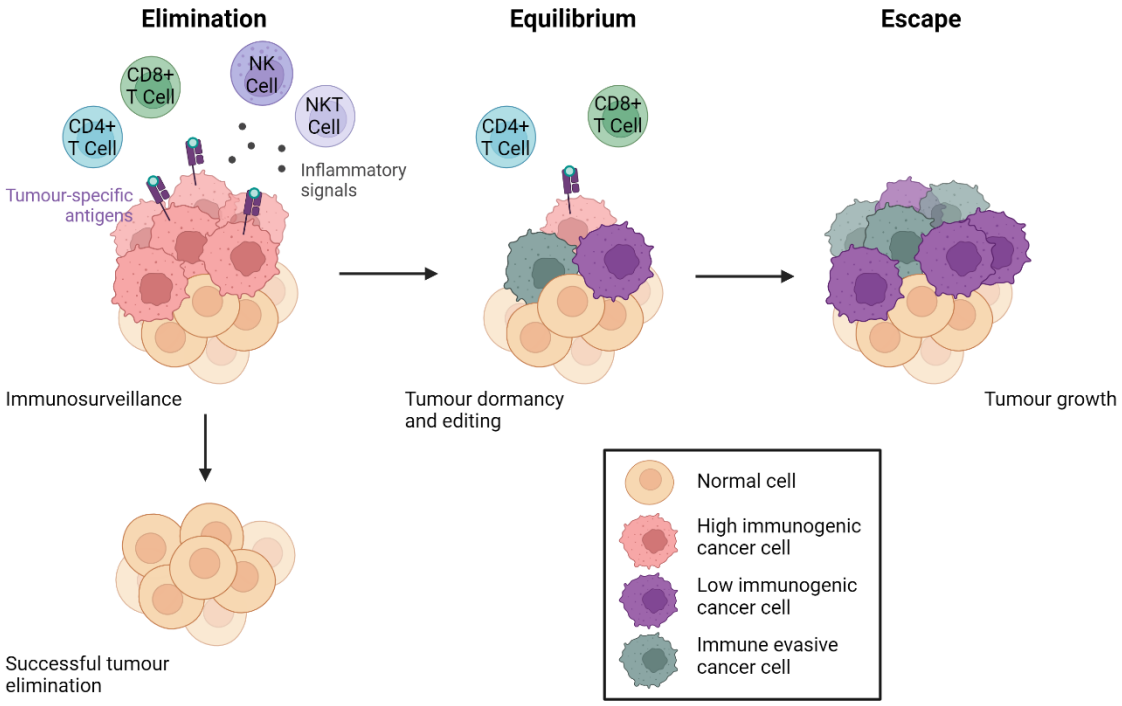

Figure 1.2 Cancer immunoediting

Illustration of the theory of cancer immunoediting, adapted from Shankaran et al. (2001). Cancer immunoediting occurs in 3 stages. Elimination: The innate and adaptive immune systems can respond to inflammatory signals and tumour-specific antigens, resulting in cytotoxic killing of tumour cells. Equilibrium: If the immune system fails to eliminate all tumour cells, the tumour becomes dormant, with the adaptive immune system preventing tumour growth. The immune system creates selective pressure for the development of immune evasion mechanisms by the tumour cells. Escape: Tumour cells with mutations enabling evasion of immune recognition or immune destruction can proliferate, enabling tumour growth and immune escape. Created with BioRender.com.

Stages of Cancer Immunoediting:

Elimination: Also known as cancer immunosurveillance (Burnet, 1970; Dunn et al., 2002). Inflammatory signals and tumour-specific markers are recognised by innate and adaptive immune systems in tandem and initiate cell killing of developing tumours, through cytotoxicity of T cells and NK cells (Shankaran et al., 2001).

Equilibrium: If the previous step fails to kill all tumour cells, the tumour enters a state of equilibrium (dormancy), where the adaptive immune system prevents tumour progression. The immune system continuing to act on cancer cells creates a selective pressure for the development of immune evasive clones.

Escape: Due to genomic instability of cancer cells, cells with beneficial mutations for avoiding immune recognition or immune destruction survive. This can be achieved through several different mutations, which are discussed in Section 1.2. These mutated cells are able to proliferate, progressing the tumour and escaping the immune system.

1.2 Immune evasion by cancer cells

There are many mechanisms employed by cancer cells to evade detection by the immune system. The most common mechanisms are discussed in this section and summarised in Figure 1.3.

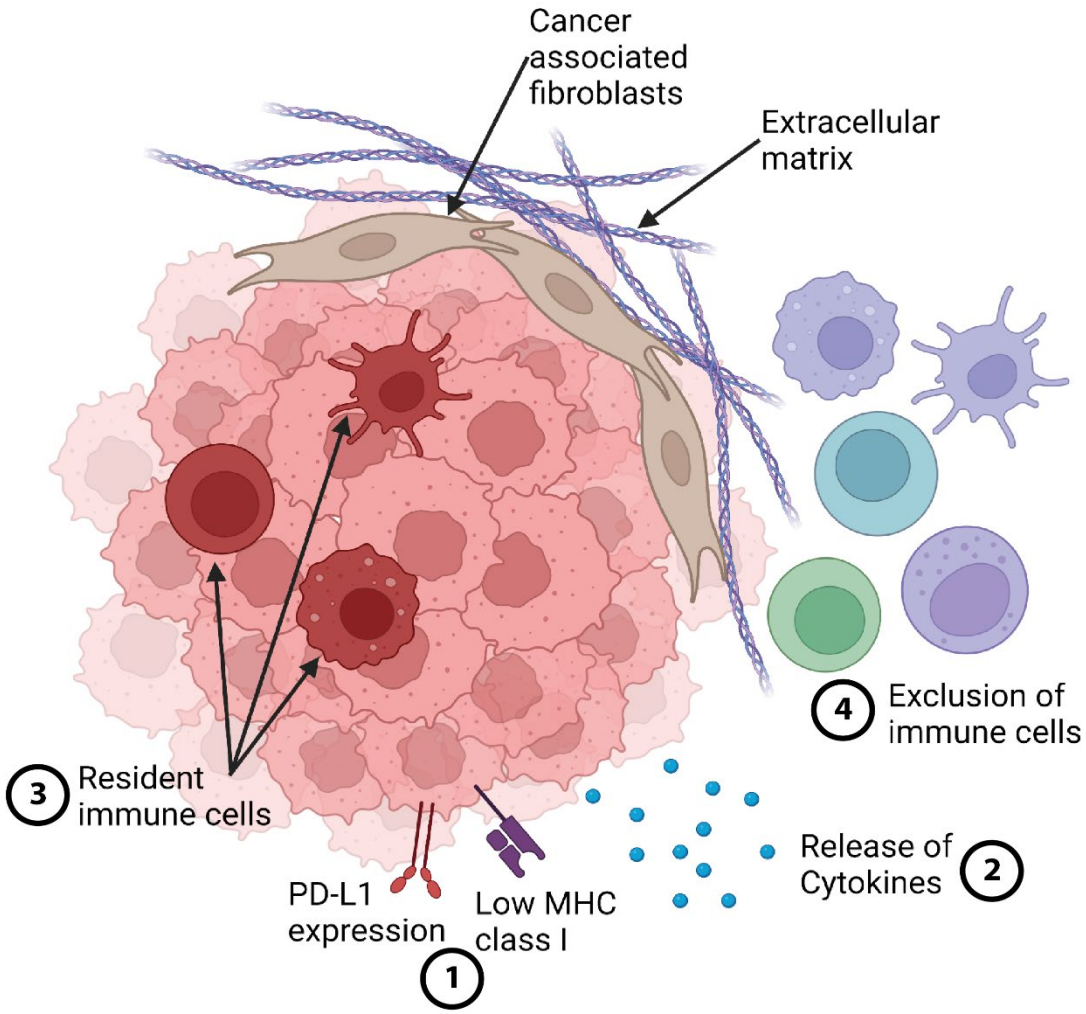

Figure 1.3 Summary of major immune evasion mechanisms by tumours

Illustration of common immune evasion mechanisms utilised by tumours. (**1**) Cancer cells can modulate cell surface expression of proteins, including downregulation of MHC class I to prevent CD8+ T cell recognition, and upregulation of immunosuppressive proteins, non-classical MHC class I, and PD-L1. (**2**) They can also release cytokines, either to directly suppress immune cells or to recruit (**3**) immunosuppressive resident immune cells, which will prevent immune activation. (**4**) Tumour structure also plays a role in tumour immune evasion; the recruitment of

cancer-associated fibroblasts (CAFs) and the development of an extracellular matrix forms a physical barrier to the entry of immune cells. Created with BioRender.com.

1.2.1 Major histocompatibility complex (MHC) class I

MHC class I molecules are expressed on the surface of most cells and play an important role in immune recognition. There are two broad categories of MHC class I molecules: classical and non-classical, which have different functions and expression patterns (summarised in Table 1.1 and discussed below). Most MHC class I molecules consist of a heavy chain, which binds intracellular self or non-self peptides for presentation to immune cells, and a β2-microglobulin (β2m) molecule (shown in Figure 1.4).

Table 1.1 Major differences between classical and non-classical major histocompatibility complex (MHC) class I and the associated genes in humans

MHC Class I	**Classical**	**Non-classical**
Expression	Ubiquitous (except red blood cells)	Tissue-specific
Interacts With	$CD8^+$ T cells	$CD8^+$ T cells, NK cells, NKT cells
Polymorphisms	High	Limited
Genes in Humans	HLA-A, HLA-B, HLA-C	HLA-E, HLA-G, HLA-F CD1, MR1

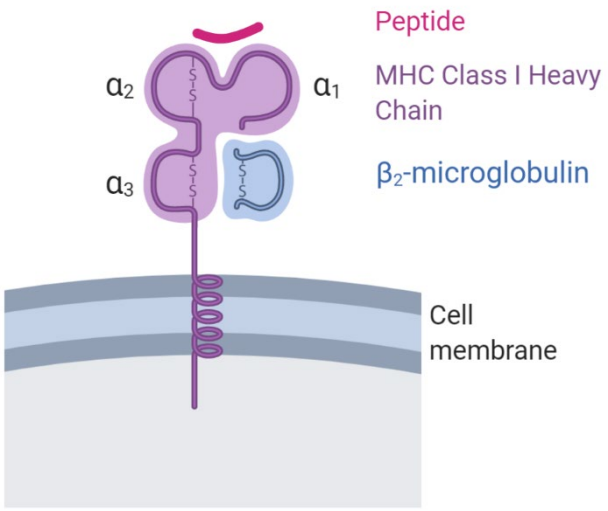

Figure 1.4 Major Histocompatibility Complex (MHC) Class I Structure

The basic structure of MHC class I molecules, which is a trimer consisting of a MHC class I heavy chain, β_2-microglobulin, and an intracellular peptide for presentation to immune cells. Created with BioRender.com.

1.2.1.1 Classical MHC class I

Classical MHC class I molecules are highly polymorphic genes expressed on the surface of all nucleated cells, and present intracellular peptides to CD8+ cytotoxic T cells via the T cell receptor (Alberts et al., 2002; Neefjes et al., 2011), illustrated in Figure 1.5.

Interaction of classical MHC class I with T cells is important in cellular immunity and can generate an immune response in two ways. The first is recognition of a foreign MHC class I molecule by the T cell receptor (TCR) (often referred to as direct recognition), which is important in distinguishing between self and non-self (Lin and Gill, 2016). The second is recognition of the MHC class I-bound peptide by the T cell (often referred to as indirect recognition of a minor histocompatibility antigen), which may have originated from a viral, mutated, or non-self protein (Lin and Gill, 2016). Recognition of a foreign or mutated peptide, or MHC class I molecule, results in activation of the CD8+ T cell and transition into an effector T cell. This promotes clonal expansion of the T cell (Gudmundsdottir et al., 1999) and cytotoxic killing, by inducing apoptosis in cells presenting the offending antigen (Alberts et al., 2002; Janeway et al., 2001).

Classical MHC class I molecules are also an inhibitory ligand for natural killer (NK) cells (Lu et al., 2010). By binding to killer cell immunoglobulin-like receptors (KIRs), lectin-like Ly49 family, or paired Ig-like receptor (PIR) on NK cells (Lanier, 2005; Moretta et al., 1996; Yokoyama, 1995), inhibitory signalling is maintained, preventing activation of the NK cell. If cells lack MHC class I

expression, or do not express high enough levels on the surface of a cell, there is less inhibitory signalling, therefore the NK cell will activate, leading to cytotoxic killing of the target cells (Ljunggren and Kärre, 1990; Lu et al., 2010). The recognition of a lack of MHC class I molecules on the cell surface is termed 'missing self' (Kärre et al., 1986; Ljunggren and Kärre, 1990, 1985) and is an important immune mechanism for detection of virally infected or mutated cells that have downregulated MHC class I to evade T cell recognition. As with CD8+ T cells (Barnes and Amir, 2017; Idos et al., 2020; Sun et al., 2023), high levels of NK cell infiltration correlates with a positive prognosis in some tumours (Xue et al., 2022; Zhang et al., 2020).

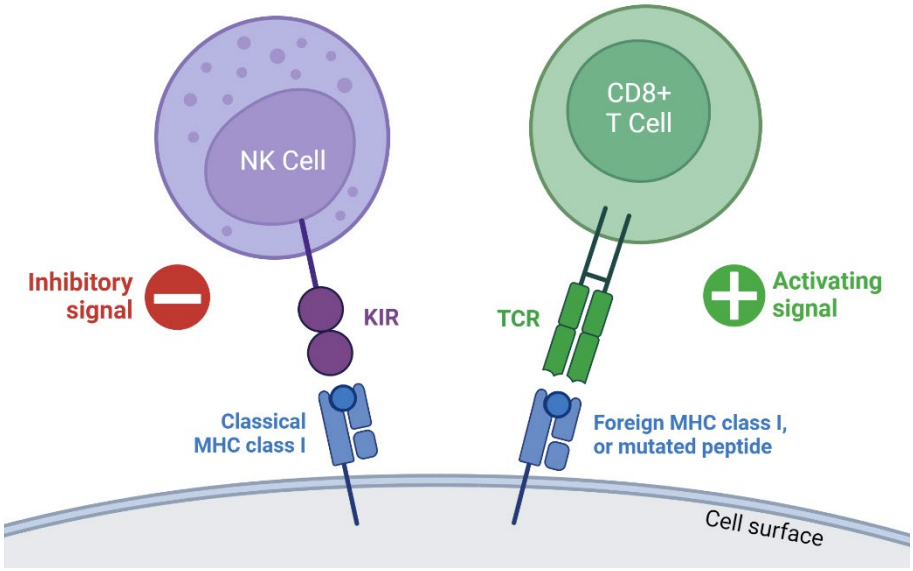

Figure 1.5 Immune cell interactions with classical MHC class I molecules

Two major immune cell interactions with classical MHC class I molecules are CD8+ T cells and natural killer (NK) cells. Classical MHC class I molecules present on a cell bind to killer cell immunoglobulin-like receptors (KIRs), lectin-like Ly49 family, or paired Ig-like receptors (PIRs) on NK cells. This creates inhibitory signals, preventing NK cell activation. If classical MHC class I is downregulated from the surface of a cell, there will be fewer inhibitory signals, resulting in NK cell activation and cytotoxic killing. Classical MHC class I molecules bind CD8+ T cells via the T cell receptor (TCR). T cells can recognise a foreign MHC class I heavy chain, and/or mutated or foreign peptides bound to the MHC class I heavy chain. Recognition by the T cell activates effector functions, including cytotoxic killing. Created with BioRender.com.

1.2.1.2 Non-classical MHC class I

Non-classical MHC class I genes also play important roles in the immune system but are not ubiquitously expressed. Their tissue-specific expression varies between genes, and for many of these our understanding of their function is still developing. Non-classical MHC class I molecules share the same basic structure as classical MHC class I, though some are expressed at the cell surface without β_2m (Allen and Hogan, 2013).

The non-classical genes have few alleles (often subject to purifying selection), are less polymorphic than classical MHC class I, and bind fewer peptides. While some non-classical MHC class I bind peptides for presentation to CD8+ T cells (Allen and Hogan, 2013; Blum et al., 2013), some bind other antigens, such as lipids, and have additional immune cell interactions, such as being a ligand for NK, γδ, and invariant T cells (Braud et al., 1999; Chancellor et al., 2018; D'Souza et al., 2019).

While non-classical MHC class I molecules can have a role in activating the immune response to cancers and pathogens, there is also evidence molecules such as HLA-E, HLA-F, and HLA-G, have a role in inhibition of effector cells, acting as inhibitory ligands (Allen and Hogan, 2013). Though mechanisms for non-classical MHC class I immunosuppression are still being elucidated, they have been shown to interact with a wide range of immune cells for this function. This includes: inhibition of NK cells, CD8+ T cells, and macrophages via CD94/NKG2A, KIRs, and killer cell lectin-like receptors (Kochan et al., 2013; Lanier, 1998; Vance et al., 1998), expansion of myeloid derived suppressor cells (MDSCs) (Agaugué et al., 2011), preventing maturation of myeloid dendritic cells, which become tolerogenic dendritic cells that can inhibit function of CD8+ and CD4+ T cells (Ristich et al., 2005), and they have been shown to interact with CD8+ T cells to induce production of CD8+ T regulatory cells (T regs) (Jiang et al., 2010). In both cancer and pregnancy, expression of non-classical MHC class I, by tumour and placental cells respectively, is associated with an immunosuppressive environment (Kochan et al., 2013; Rapacz-Leonard et al., 2014); and in tumours, non-classical expression is associated with poor prognosis (Bossard et al., 2012; Menier et al., 2008; Wolpert et al., 2012).

1.2.1.3 Antigen presentation pathway (APP)

In its role of antigen presentation to T cells, MHC class I molecules are a trimer, consisting of a heavy chain, β2-microglobulin, and a peptide (illustrated in Figure 1.4). The process of peptide presentation involves many different proteins, which are all required for correct loading of the peptide onto the MHC class I heavy chain and the subsequent expression of MHC class I at the cell surface.

The process of assembling the MHC class I trimer and transporting it for expression at the cell surface is called the antigen presentation pathway (APP) (Blum et al., 2013), illustrated in Figure 1.6. Intracellular proteins are cleaved in the cytosol by the proteasome following ubiquitination and a subsection of these peptides are transported into the endoplasmic reticulum (ER), via transporter associated with antigen processing (TAP). Once in the ER, peptides are trimmed by endoplasmic reticulum aminopeptidase (ERAP) 1 and 2 to the correct size for loading onto the MHC class I heavy chain (between 8-11 amino acids in humans). If the peptides remain too long, they can undergo further trimming by ERAP1/2. A peptide is loaded onto the MHC class I heavy chain, bound to β_2m, by the peptide loading complex (PLC), consisting of TAP, tapasin, ERp57, calreticulin and the MHC class I (Blees et al., 2017; Hulpke and Tampé, 2013). Once assembled and stable, the MHC class I trimer disassociates from the PLC and is transported through the Golgi for expression to immune cells at the cell surface.

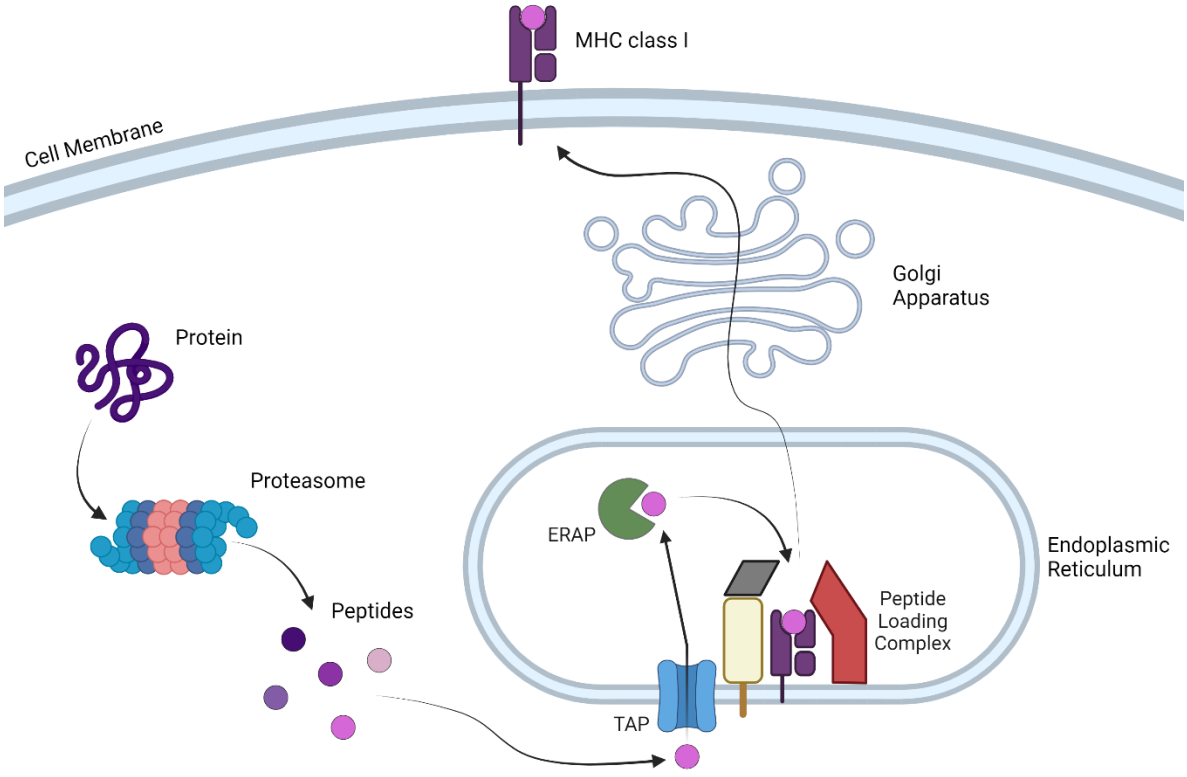

Figure 1.6 Summary of the antigen presentation pathway (APP)

Illustration of the antigen presentation pathway, which assembles MHC class I molecules for expression at the cell surface, adapted from Reeves and James (2017). Intracellular peptides are cleaved by the proteasome and the resulting peptides transported into the endoplasmic reticulum via transporter associated with antigen processing (TAP). Peptides are further cleaved by endoplasmic reticulum

aminopeptidase (ERAP) 1 and 2, then loaded onto MHC class I heavy chain, bound to β_2m, by the peptide loading complex: consisting of TAP, tapasin, ERp57, calreticulin and the MHC class I heavy chain. Following assembly, the MHC class I trimer dissociates from the peptide loading complex and is transported through the Golgi for expression to immune cells at the cell surface. Created with BioRender.com.

1.2.2 Modulating expression of cell surface markers

A major mechanism utilised by cancer cells to avoid recognition by the immune system is the modulation of molecules expressed on the cell surface. This is either by removal or downregulation of molecules that would initiate immune responses against the cancer cells, or upregulation of molecules that will suppress immune responses.

1.2.2.1 MHC class I loss in tumours

In cancer cells, classical MHC class I molecules will bind peptides that originated from mutated proteins. Mutated peptides can be recognised by CD8+ T cells triggering a cytotoxic immune response. As a result, a common mechanism for immune escape by cancer cells is downregulation, or total loss, of classical MHC class I from the cell surface (Campoli and Ferrone, 2008; Dhatchinamoorthy et al., 2021; Hicklin et al., 1999), which is associated with poor prognosis (Hicklin et al., 1999; Mehta et al., 2008). MHC class I downregulation is due to selective pressure from the immune system (cancer immunoediting), as cancer cells expressing classical MHC class I bound to mutated peptides will be detected and eliminated by cytotoxic CD8+ T cells.

One method to reduce MHC class I expression on the cell surface is total MHC class I loss. This can be achieved through structural mutations (Dhatchinamoorthy et al., 2021), which is a permanent loss of MHC class I expression, or epigenetic modifications to genes (Campoli and Ferrone, 2008; Mehta et al., 2008), 'switching off' MHC class I expression, which is reversible. Both structural and epigenetic mutations occur at drivers of MHC class I heavy chain expression or components of the APP to prevent MHC class I expression at the cell surface, therefore preventing expression of all MHC class I genes.

While effective at preventing T cell-mediated responses, total loss of MHC class I expression risks activation of other immune responses, such as by NK cells. Therefore, other mechanisms utilised by cancer cells, which reduce the chance of recognition by CD8+ T cells and prevent an NK cell response to 'missing self', are selective loss and loss of heterozygosity for classical MHC class I. Selective loss involves the downregulation or loss of a specific MHC class I allele or locus that is

immunogenic (Campoli and Ferrone, 2008; Hiraki et al., 2004), such as alleles that bind mutated peptides that will be recognised by T cells, called 'neoantigens'. Loss of heterozygosity is a type of selective downregulation where an MHC class I gene or haplotype is structurally mutated on one chromosome (McGranahan et al., 2017; Tran et al., 2016); therefore, the cancer cell only has one copy of the gene(s) and there is a reduction in MHC class I expression.

1.2.2.2 Non-classical MHC class I expression

As mentioned in Section 1.2.1.2, non-classical MHC class I is upregulated in many cancers (Campoli and Ferrone, 2008; Rouas-Freiss et al., 2005) and its expression is associated with poor prognosis (Bossard et al., 2012; Ye et al., 2007; Yie et al., 2007, 2007), due to its immunosuppressive functions. In some cancers, soluble forms of non-classical MHC class I are released to induce immune suppression (Derré et al., 2006; Morandi et al., 2007; Sebti et al., 2007), rather than or in addition to cell surface expression. Studies have shown that blockade or inhibition of non-classical MHC I in tumours correlates with increased immunogenicity of cancer cells (Wischhusen et al., 2005; Wolpert et al., 2012) and has been shown to prevent tumour formation (Agaugué et al., 2011). Non-classical MHC class I expression in tumours suppresses immune cells by preventing effector cell activation, such as NK cells and CD8+ T cells (Derré et al., 2006; Lin et al., 2007; Wischhusen et al., 2005; Wolpert et al., 2012), and induction of suppressive immune cell phenotypes (Agaugué et al., 2011; Ristich et al., 2005; Rouas-Freiss et al., 2007).

The mechanisms by which cancer cells upregulate non-classical MHC class I are still being elucidated, as historically non-classical MHC class I molecules have received less focus than classical MHC class I. Current evidence suggests epigenetic upregulation of non-classical expression in cancer cells. A study found non-classical, HLA-G could be upregulated by demethylation of gene promoters, mediated by 5'-aza-2-deoxycytidine, or treatment with interferon-γ (IFNγ) in some cell lines already expressing HLA-G, however these treatments could not induce expression in HLA-G-negative cell lines (Dunker et al., 2008). Other studies found HLA-G expression regulated in tumours by other environmental factors, such as hypoxic factors and TNFα (Rouas-Freiss et al., 2007). Additionally, in leukaemia cell lines an increase in cell surface expression of non-classical, HLA-E correlated with downregulation of classical MHC class I heavy chain expression (Marín et al., 2003).

1.2.2.3 Expression of PD-L1

In addition to modulation of MHC class I expression, cancer cells can also mutate to upregulate molecules associated with immunosuppression. A molecule widely expressed by tumour cells is programmed death-ligand 1 (PD-L1), also named B7-H1 and CD274, expression of which is

correlated with malignancy and poor prognosis (Han et al., 2020; Hino et al., 2010; Maine et al., 2014; Muenst et al., 2014). PD-L1 is the ligand for the receptor, programmed cell death protein 1 (PD-1), expressed by activated T cells. Binding of PD-L1 results in suppression of T cell effector functions, inducing anergy or apoptosis (Freeman et al., 2000; Gibbons Johnson and Dong, 2017; Jiang et al., 2010), thus preventing recognition and killing of tumour cells by T cells. As such, blockade of PD-L1 is commonly used in combination with other immunotherapies against cancer (Han et al., 2020; Hudson et al., 2020; Wang et al., 2019), though not effective in all patients. Unresponsive patients appear to lack pre-existing T cell responses against the tumour (Iwai et al., 2017), highlighting the multifaceted nature of anti-tumour immune responses and cancer immune evasion.

1.2.3 Tumour microenvironment

Instead of, or in addition to, modulating expression of cell surface markers, tumours can also evade the immune system by modifying the tumour microenvironment. This is mainly achieved by creating an immunosuppressive environment or through exclusion of immune cells (discussed below).

1.2.3.1 Immunosuppressive environment

Cancer cells can alter the immune environment within a tumour by releasing cytokines and other small molecules to directly suppress immune cells or to recruit/induce regulatory immune cells. Cancer cells can release immunosuppressive cytokine, interleukin-6 (IL-6), which recruits myeloid derived suppressor cells (MDSCs) (Jiang et al., 2017) for suppression of CD8+ T cells (Gabrilovich and Nagaraj, 2009). Cancer cells can also release growth factor, granulocyte macrophage colony stimulating factor (GM-CSF), which decreases macrophage effector functions (Lin et al., 2002; Sotomayor et al., 1991). CD4+ T regs can be recruited into the tumour via release of chemokine, CC chemokine ligand 22 (CCL22) by cancer cells (Curiel et al., 2004; Lee et al., 2005). T regs become resident or tumour-associated immune cells, which interact with and inhibit tumour-antigen specific responses by T cells (Yokokawa et al., 2008) to maintain a suppressive immune environment. Recruited immune cells also contribute to immunosuppression by producing their own cytokines, for example MDSCs produce transforming growth factor β (TGF-β) (Bierie and Moses, 2010), which suppresses anti-tumour immune responses (Pasche, 2001) and induces T cell conversion to suppressive T regs (Zou, 2006).

1.2.3.2 Exclusion of immune cells

Tumour cells can also prevent immune activation by modulating the physical structure of the tumour, to create a barrier to entry of immune cells. Cancer associated fibroblasts (CAFs), mainly fibroblasts activated by contact with cancer cells or inflammatory signalling (Sahai et al., 2020), and extracellular matrix (ECM), deposited by CAFs and tumour cells (Popova and Jücker, 2022), are common in solid tumours. CAFs have a role in immunosuppression, for example, by the release of cytokine, TGF-β (Arpinati and Scherz-Shouval, 2023; Calon et al., 2012; Hawinkels et al., 2014). However, through deposition of the ECM, they also function to provide structure and support for cancer cells, while also creating a dense matrix that forms a physical barrier to infiltration of immune cells (Koppensteiner et al., 2022; Salmon et al., 2012). As a result, even if there is a strong immune response against tumour antigens, tumour cells are protected from immune killing.

1.3 History of transmissible cancers

Though rare, some cancer cells have escaped the individual they emerged in, to spread among a population. Unlike oncoviruses, such as human papillomavirus (HPV), where the virus passes between individuals, causing DNA damage and consequently cancer formation; the cancer cells themselves are the infective agent, acting as an allograft to form a tumour in the new host.

Very few transmissible cancers have been found in nature. Six have been discovered in bivalves since 2015 across six species (Metzger et al., 2016, 2015; Yonemitsu et al., 2019), and there are two mammalian species that are known to harbour transmissible cancers, one occurring in dogs and two in Tasmanian devils (Sarcophilus harrisii). The timeline summarising transmissible cancers is shown in Figure 1.7.

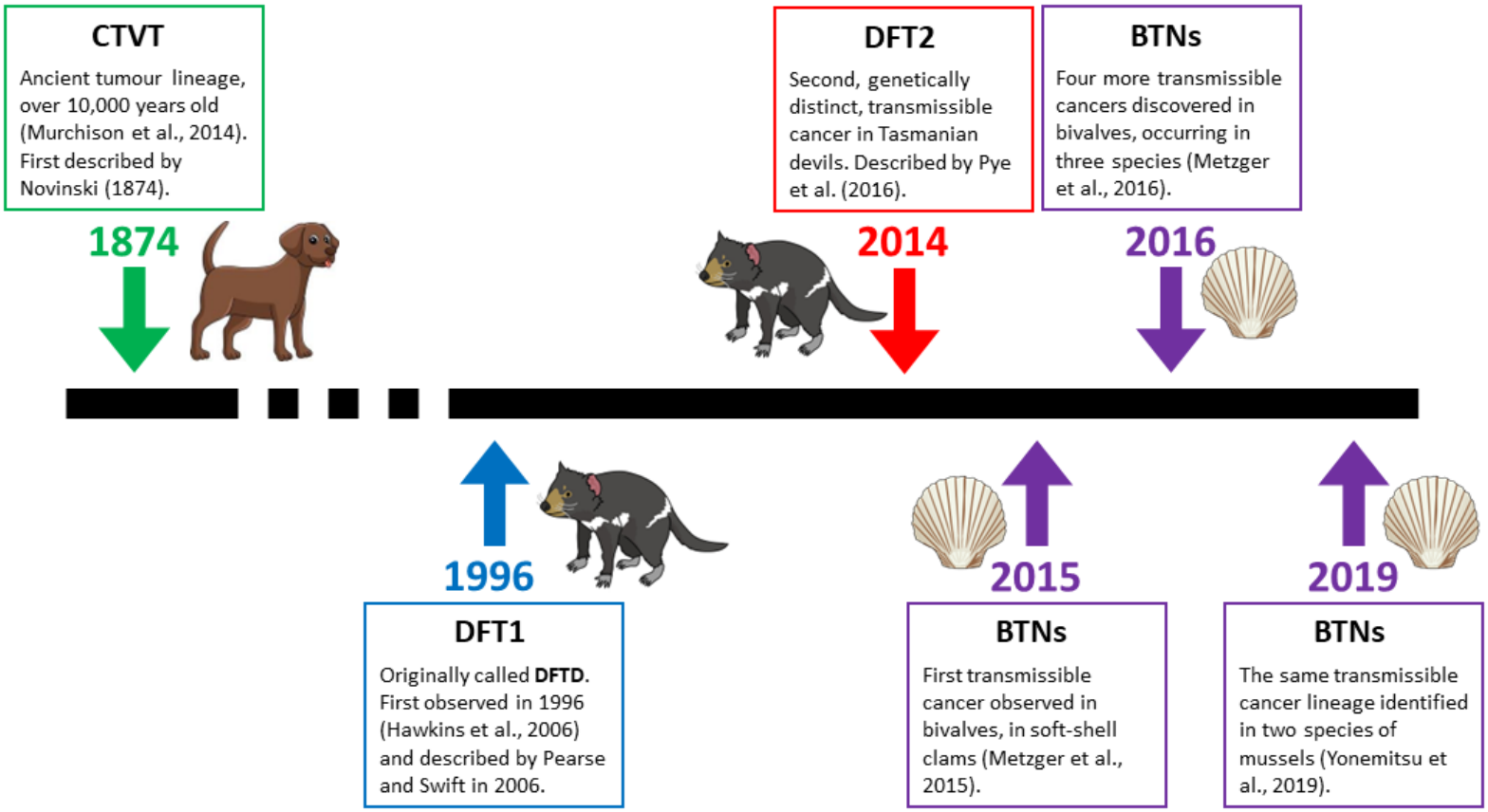

Figure 1.7 Timeline of transmissible cancers

Transmissible cancers have been discovered in 2 mammalian species, dogs and Tasmanian devils, and 6 species of bivalves. The oldest transmissible cancer, Canine Transmissible Venereal Tumor (CTVT), predicted to be over 10,00 years old (Murchison et al., 2014) occurs in dogs and was first described by Novinski (1874). Two genetically distinct transmissible cancers occur in Tasmanian devils; the first, Devil Facial Tumour Disease 1 (DFT1), was first observed

in 1996 (Hawkins et al., 2006) and was first described by Pearse and Swift (2006). The second transmissible cancer was identified in 2014 (Pye et al., 2016b). Most recently, since 2015, 6 transmissible cancers have been identified in 6 species of bivalves (Metzger et al., 2016, 2015; Yonemitsu et al., 2019).

1.3.1 Canine Transmissible Venereal Tumor (CTVT)

The oldest known transmissible cancer is Canine Transmissible Venereal Tumour (CTVT), also referred to as Sticker's sarcoma and Canine Transmissible Venereal Sarcoma, an ancient clonal lineage infecting dogs (*Canis lupis*), which is estimated to be over 10,000 years old (Murchison et al., 2014). CTVT was first described in 1874 (Novinski, 1874) and is predicted to have arisen in a wolf ancestor (Rebbeck et al., 2009). This cancer exists worldwide (Cohen, 1985; Das and Das, 2000; Ganguly B et al., 2016), with high prevalence in countries with large populations of stray/wild dogs or where neutering is less common (Strakova and Murchison, 2014). Copy number analysis across samples from seven countries found significant deviation from normal cells, but remarkable similarity to each other (Rebbeck et al., 2009), supporting clonal lineage and suggesting CTVT genome is relatively stable, supported by other studies (Murchison, 2009; Murchison et al., 2014; Murgia et al., 2006).

CTVT is thought to derive from a macrophage, due to its expression profile and ability to be infected by a macrophage parasite (Murchison, 2009). Tumours usually occur on the external genitalia of the host and cancer cells transmit between dogs through sniffing, licking and sexual contact. Tumours start as small, localised nodules and grow to become large, noduled, ulcerated tumours, but rarely metastasise (Murchison, 2009). Mortality from CTVT infection is low in immune-competent adult dogs, with most tumours regressing (Cohen, 1985; Ganguly B et al., 2016).

1.3.2 Devil Facial Tumours (DFTs)

In contrast to CTVT, the cancers in Tasmanian devils have occurred much more recently; with the first observed in 1996, called Devil Facial Tumour Disease 1 (DFT1) (Pearse and Swift, 2006), and the second identified in 2014, called DFT2 (Pye et al., 2016b), which is thought to have emerged close to this time. DFT1 originated in the North East of Tasmania, first observed at the Mount William National Park (Hawkins et al., 2006), and since then has spread across most of the population of mainland Tasmania, see Figure 1.8. In contrast, DFT2 emerged in the d'Entrecasteaux peninsula and has continued to circulate in this population (see Figure 1.8).

DFT1 and DFT2 have the same gross morphology, growing as tumours on the face and neck of infected devils, but are genetically distinct and arose in different individuals (Pye et al., 2016b; Stammnitz et al., 2018). Both cancers transmit as an allograft between devils due to fighting behaviours during feeding and mating, where lesions are often caused around the face (Hamede et al., 2013, 2008; Loh et al., 2006), with tumours forming on the face and/or neck of the new

host. Tumours start as small nodules, but often grow to become large, ulcerated tumours (shown in Figure 1.9).

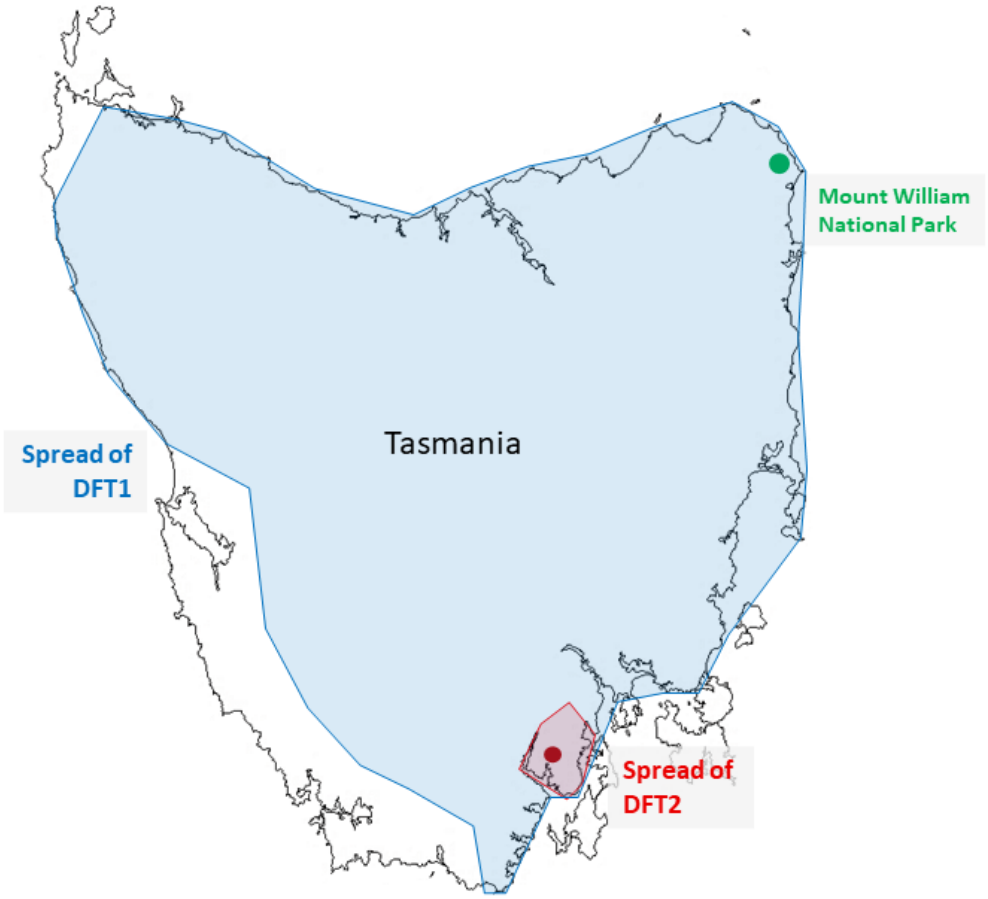

Figure 1.8 Map of Tasmania showing spread of Devil Facial Tumour Diseases

Map of Tasmania marked with the spread of DFT1 (blue), as of 2020 (Kozakiewicz et al., 2021), and DFT2 (red). DFT1 was first observed at the Mount William National Park in 1996 (Hawkins et al., 2006), marked in green. The site where DFT2 was first detected in 2014 (Pye et al., 2016b) is marked by the red dot.

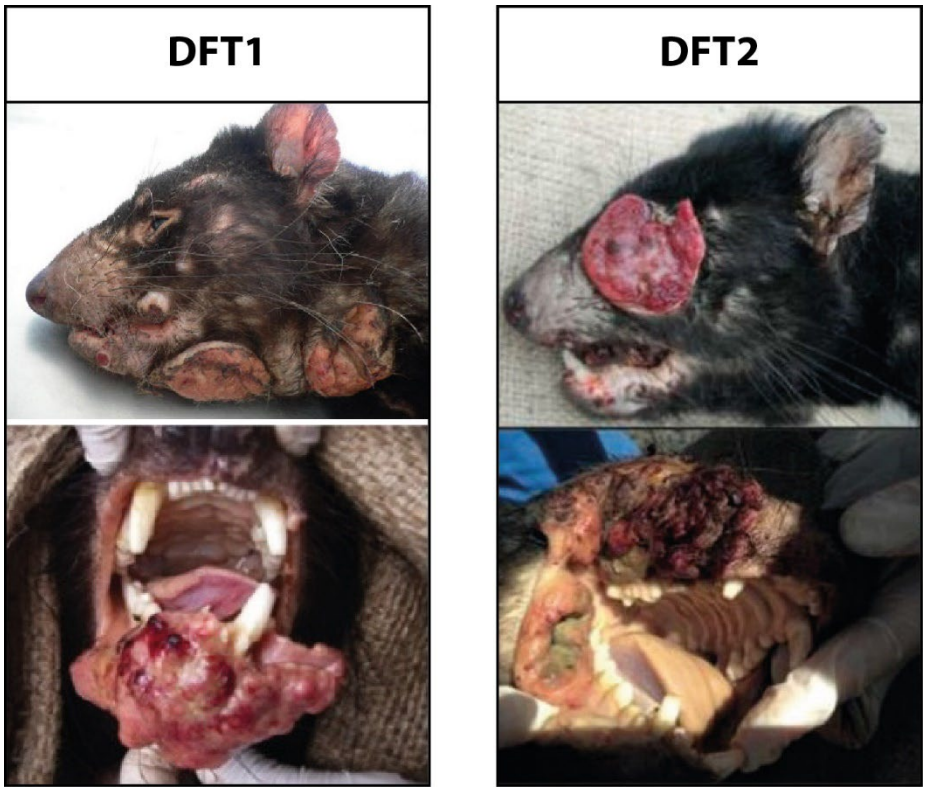

Figure 1.9 Photographs of DFT1 and DFT2 tumours

Pictures of DFT1 (**left**) and DFT2 (**right**) tumours at a late stage of development. Most DFTs occur on the face, neck, and mouth of their host, Tamanian devils (*Sarcophilus harrisii*). Images were first published by (**top left**) (Murchison et al., 2012), (**bottom left**) (Siddle and Kaufman, 2015), and (**right**) (Pye et al., 2016b).

1.3.2.1 DFT1

DFT1 is a transmissible cancer circulating in the Tasmanian devil (*Sarcophilus harrisii*), a marsupial species endemic to the Australian island of Tasmania (Pearse and Swift, 2006). Originally named DFTD (Devil Facial Tumour Disease), prior to the emergence of a second transmissible cancer called DFT2 (Pye et al., 2016b). DFT1 is derived from a myelinating Schwann cell (Murchison et al., 2010; Owen et al., 2021) and tumour cells are clonal, originating in the same devil, as cells taken from tumours infecting different individuals share the same karyotype, which is distinct from their hosts (Pearse and Swift, 2006).

The disease was first observed in 1996 (Hawkins et al., 2006), predicted to have emerged around 1986 (Stammnitz et al., 2023), and has since spread across most of the island. The cancer cells grow to become large, ulcerated and necrotic tumours that can affect the structure of the jaw and often metastasise (Loh et al., 2006; Siddle et al., 2013). There is a near 100% mortality rate, with

infected devils dying of starvation, secondary infection, or metastasis to vital organs leading to organ failure (Murchison, 2009). The spread of DFT1 across Tasmania (see Figure 1.8) led to an average devil population decline of 77% (Lazenby et al., 2018) and up to 90% in some areas (McCallum et al., 2009, 2007), resulting in Tasmanian devils being listed as an endangered species in 2008 (Hawkins et al., 2008). However, recent phylogenetic analysis of DFT1 indicates the cancer is becoming endemic, with reduced transmission rates compared with the outbreak of the disease (Patton et al., 2020).

There is disagreement in the literature about the stability of the DFT1 genome (James et al., 2019; Kwon et al., 2020), however the development of distinct DFT1 lineages has been observed (Kwon et al., 2020; Stammnitz et al., 2023). As DFT1 has spread across Tasmania, clades (or subclones) have developed, based on phylogenetic analysis of mitochondrial mutations, copy number variations, and genome analysis (Kwon et al., 2020; Stammnitz et al., 2023). Some clades have disappeared over time, while others have become dominant in different geographical areas (Kwon et al., 2020). There has been no investigation into the phenotypes of clades, but they may confer functional differences in DFT1 cells, though due to their convergent evolution, these differences are predicted to be limited (Kwon et al., 2020).

1.3.2.2 DFT2

DFT2 is the second transmissible cancer identified in Tasmanian devils. It was discovered in 2014 during routine screening of tumour samples for DFT1 markers (Pye et al., 2016b). Despite forming tumours with a similar gross morphology to DFT1, these cancer cells are genetically distinct (Pye et al., 2016b; Stammnitz et al., 2023). DFT1 and DFT2 vary from each other at microsatellite loci and have different marker chromosomes (Pye et al., 2016b). Additionally, DFT2 cells contained a Y chromosome, indicating the cancer originated in a male devil, while DFT1 originated in a female (Pye et al., 2016b). Despite not sharing genetic markers with DFT1 or their hosts, the five tumours shared markers with each other (Pye et al., 2016b), therefore they marked the emergence of a new transmissible cancer. As devil captures were carried out regularly to monitor DFT1 progression, DFT2 is thought to have emerged close to these first observations in 2014, supported by phylogenetic analysis, predicting DFT2 emerged close to 2011 (Stammnitz et al., 2023).

DFT2 emerged in the d'Entrecasteaux peninsula in the South East of Tasmania, marked on Figure 1.8. Since then, it has spread among the devil population within this area but has not expanded its range beyond this (James et al., 2019). It has been suggested this may be due to the geographical area DFT2 emerged in, which it confined by water and urban landscape, and/or the lower population densities due to DFT1 (Durrant et al., 2021). Another possibility is that DFT2 spread has been limited due to host immune responses (Caldwell et al., 2018), discussed in Section 1.4.5.

DFT2 emerged from an immature Schwann cell (Owen et al., 2021; Stammnitz et al., 2018). As both DFT1 and DFT2 came from a Schwann cell, this suggests this cell type is more prone to transformation into a transmissible cancer, due to the cellular phenotype and/or frequent damage caused to these cells during biting behaviours. It has been observed that DFT2 is replacing DFT1 in the d'Entrecasteaux peninsula (R Hamede 2022, personal communication), which may be the result of higher growth (Gerard, Owen et al., 2023 (in review)) and mutation (Stammnitz et al., 2023) rates in DFT2 cells. Less is known about the mortality of DFT2, and therefore impact on the devil population. However, the emergence of a second transmissible cancer within an endangered species is of concern and suggests Tasmanian devils may be susceptible to generation of transmissible cancers.

1.3.3 Bivalve Transmissible Neoplasms (BTNs)

Bivalves, a class of molluscs (including clams, mussels, and oysters), appear to be particularly prone to transmissible cancers. Six distinct transmissible cancers have been identified since 2015 (Metzger et al., 2016, 2015; Yonemitsu et al., 2019), collectively known as Bivalve Transmissible Neoplasms (BTNs). All six transmissible cancers vary genetically from their hosts but share mitochondrial single nucleotide polymorphisms (SNPs) and DNA markers (Metzger et al., 2016, 2015; Yonemitsu et al., 2019).

BTNs are hypothesised to transmit through sea water, picked up by a new host via filter feeding (Metzger et al., 2015; Sunila and Farley, 1989). Infection with these cancers is fatal, causing large population losses (Metzger et al., 2015). These transmissible cancers are disseminated neoplasia, a leukaemia-like cancer, which are common in bivalves. Wide prevalence of disseminated neoplasia in soft-shell clams (*Mya arenaria*), the species in which the first BTN was identified, was first described in the 1970's (Brown et al., 1978; Yevich and Barszez, 1977), therefore it is possible this cancer lineage is over 50 years old.

BTNs have been found globally, in North America (Metzger et al., 2016, 2015), South America, and Europe (Yonemitsu et al., 2019). *Mytilus edulis* (Europe) and *Mytilus chilensis* (South America) were infected with BTN lineages that are highly similar to each other, and are thought to have originated from the same host, *Mytilus trossulus* (Yonemitsu et al., 2019). It has been suggested that the spread of BTNs across broad geographical areas may have been facilitated by anthropogenic activity, due to translocation of bivalves by attachment to shipping vessels (Yonemitsu et al., 2019) and transplantation of seed stocks between sites (Metzger et al., 2015).

In addition to the BTN infecting mussels (*M. edulis* and *M. chilensis*), which originated in a different species, the BTN in golden carpet shell clams (*Polititapes aureus*) was found to originate

in *Venerupis corrugata* (Metzger et al., 2016). Additionally, no infections of either cancer were found in the original host (Metzger et al., 2016; Yonemitsu et al., 2019). These results suggest BTNs can easily transfer between species, however, transmission experiments of other BTNs between species were unsuccessful (Kent et al., 1991; Mateo et al., 2016), therefore transfer of transmissible cancer from one species to another may be dependent on mutations within the cancer.

1.4 Immune evasion by transmissible cancers

As transmissible cancers transmit as allografts, those circulating in mammalian populations should be easily recognised by host immune systems due to disparate MHC class I molecules between tumour and host. All three cancers have spread through their respective populations, often showing limited signs of immune activation. Therefore, these cancer cells must be employing immune evasion mechanisms. Our current understanding of immune evasion by these cancers is discussed in this section.

1.4.1 Immune evasion by CTVT

CTVT is an unusual cancer, which has evolved to co-exist with its host and is rarely fatal. As an ancient cancer lineage, less is known about the evolution of CTVT than other transmissible cancers. However, since it has spread worldwide, the cancer must have mechanisms for evading, or being tolerated by, the host immune system.

Studies of CTVT have observed its tumours have three distinct phases: growth, stasis, and regression (Cohen, 1985; Murchison, 2009). In most cases all three phases are observed, though there are some cases where the tumour grows then regresses, without entering a state of stasis, or the tumour enters stasis and does not regress. During early stages of infection (growth phase), CTVT cells downregulate MHC class I expression (Belov, 2011; Hsiao et al., 2002; Murchison, 2009), preventing T cell responses, and express TGF-β, which inhibits NK cells, B cells and dendritic cells (Liao et al., 2003; Liu et al., 2008). Tumour infiltration by lymphocytes upregulates MHC class I expression via release of IFNγ (Hsiao et al., 2008; Pérez et al., 1998). IL-6 and IFNγ expression by lymphocytes also antagonises TGF-β production by CTVT (Hsiao et al., 2008; Pérez et al., 1998). This triggers an inflammatory immune response within the tumour, leading to stasis and/or regression.

Presumably CTVT has evolved with its host species to avoid immune detection during the early stages of infection but transmits to another host before it is eradicated by the host immune system. Thus, enabling both host and pathogen to survive.

1.4.2 Tasmanian devil MHC class I genes

Due to rapid evolution, MHC class I gene families are generally highly divergent between species, with little orthology between classical genes (genes identified for humans and marsupial species are listed in Table 1.2). In Tasmanian devils, three classical genes have been identified, Saha-UA, Saha-UB and Saha-UC (Cheng et al., 2012), and six non-classical genes; *Saha-UD* (Cheng et al., 2012; Siddle et al., 2007b), *Saha-UK* (Cheng et al., 2012), *Saha-UM*, *Saha-CD1* (Cheng and Belov, 2014), *Saha-MR1* (Tsukamoto et al., 2013), and *Saha-UT* (Papenfuss et al., 2015) (summarised in Table 1.3).

Table 1.2 MHC class I genes identified for humans, Tasmanian devils, and other marsupial species.

Species	**Classical MHC class I genes**	**Non-classical MHC class I genes**	
Human (*Homo sapiens*)	HLA-A HLA-B HLA-C	HLA-E HLA-F HLA-G	HLA-MICA HLA-MICB
Tasmanian devil (*Sarcophilus harrisii*)	Saha-UA Saha-UB Saha-UC	Saha-CD1 Saha-MR1 Saha-UD	Saha-UK Saha-UM Saha-UT
Tammar wallaby (*Macropus eugenii*)	Maeu-UA Maeu-UB Maeu-UC	Maeu-UE Maeu-UK Maeu-UM	Maeu-UO
Grey short-tailed opossum (*Monodelphis domestica*)	Modo-UA1	Modo-UE Modo-UG Modo-UI	Modo-UJ Modo-UK Modo-UM

Table 1.3 Summary of Tasmanian devil MHC class I genes

Type of MHC class I	Gene	Polymorphisms	Tissue expression	Described by
Classical	Saha-UA	High	Ubiquitous	Cheng et al. (2012)
Classical	Saha-UB	High	Ubiquitous	Cheng et al. (2012)
Classical	Saha-UC	High	Ubiquitous	Cheng et al. (2012)
Non-classical	Saha-CD1	Low	Restricted	Cheng and Belov (2014)
Non-classical	Saha-MR1	None	Restricted	Tsukamoto et al. (2013)
Non-classical	Saha-UD	Low	Restricted	Siddle et al. (2007) Cheng et al. (2012)
Non-classical	Saha-UK	None	Restricted	Cheng et al. (2012)
Non-classical	Saha-UM	None	Ubiquitous	Cheng and Belov (2014)
Non-classical	Saha-UT	Low	Restricted	Papenfuss et al. (2015)

Classical MHC class I molecules in Tasmanian devils were assigned based on their high level of polymorphism and ubiquitous expression. The three classical MHC class I genes, Saha-UA, -UB, and -UC, are highly similar to each other, resulting from gene duplications (Cheng et al., 2012; Lane et al., 2012), which makes assigning alleles to gene loci difficult (Caldwell and Siddle, 2017). Based on three classical MHC class I genes, is it expected that Tasmanian devils will have six alleles; however, it is important to note that a 1.646kbp deletion was found in *Saha-UA*, rendering it a pseudogene (Cheng et al., 2012), therefore the number of functional classical MHC class I alleles will be lower in some devils. Across populations in Tasmania there is limited MHC class I diversity. A study in 2010 with 387 devils found there was a difference between classical MHC class I genotypes of devils in the East compared to the North West (Siddle et al., 2010), but low diversity overall. A recent study using long-read sequencing found no significant difference between MHC class I alleles across Tasmania, aside from the geographically isolated South Western population (Cheng et al., 2022), highlighting the restricted MHC class I diversity in Tasmanian devils.

Non-classical MHC class I alleles in Tasmanian devils were assigned based on low polymorphisms, tissue-specific expression, and orthology with genes in other species of marsupials or humans.

Saha-UD alleles identified have high nucleotide sequence similarity (>97.7%) and putative peptide binding residues are not under positive selection (Cheng and Belov, 2014). Amino acid differences between these alleles due to single nucleotide polymorphisms is low and only a few of these residues are predicted to interact with peptides or the TCR (Bjorkman and Parham, 1990) (see Figure 1.10). Saha-UD, while it is in a separate phylogenetic clade (Cheng et al., 2012), is closely related to the classical MHC class I genes (Cheng and Belov, 2014) and binds β2m (Gastaldello et al., 2021), therefore it is hypothesised that Saha-UD molecules bind peptides for antigen presentation at the cell surface. *Saha-UK* is monomorphic (Cheng and Belov, 2014); therefore, its immunogenicity in allograft rejection is expected to be low. However, it has not been found to bind β2m (Gastaldello et al., 2021), and is predicted to have a marsupial-specific function (Cheng et al., 2012). As a result, Saha-UK is not predicted to bind peptides for antigen presentation at the cell surface.

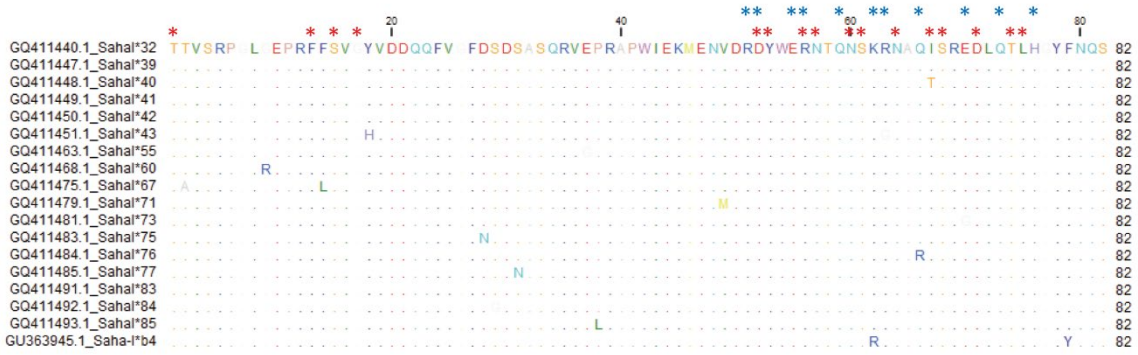

Figure 1.10 Amino acid alignment of non-classical, Saha-UD alleles

Blue asterisks indicate residues predicted to interact with the TCR, red asterisks indicate residues predicted to bind the peptide. Residue predictions were calculated by referencing Bjorkman and Parham (1990), Figure 4. Alignment created in CLC Main Workbench 22.0.

Saha-CD1 and *Saha-MR1* are orthologous with CD1 and MR1 genes, respectively, in eutherian mammals (Cheng and Belov, 2014; Tsukamoto et al., 2013), so are predicted to serve a similar function in Tasmanian devils. This would mean Saha-CD1 would bind glycolipids and lipoproteins for antigen presentation to T cell and NKT cells (Brigl and Brenner, 2004), while Saha-MR1 binds vitamin derivatives for presentation to mucosal-associated invariant T (MAIT) cells (Krovi and Gapin, 2016). The function of Saha-UM and Saha-UT in the Tasmanian devil immune system is currently unknown, due to their orthology with genes in other marsupials, these genes are

predicted to perfume a marsupial-specific function (Cheng and Belov, 2014; Papenfuss et al., 2015).

1.4.3 Immune responses against DFT1

Transmitting as an allograft, DFT1 should elicit an immune response due to disparate major histocompatibility complex class I (MHC class I) molecules between the cancer and its host. In most cases, devils produce little to no immune response to DFT1. The lack of immune response was initially thought to be due to reduced genetic diversity in the devil population (Siddle et al., 2007a; Woods et al., 2007), specifically, due to low genetic diversity at classical MHC class I loci (Cheng et al., 2012; Siddle et al., 2010). However, experiments have shown that devils can produce an immune response against both matched and mis-matched skin grafts (Kreiss et al., 2011), therefore the level of genetic diversity at major and minor antigens should initiate an immune response.

Lymphocyte infiltration is rarely observed in wild devils infected with DFT1 (Loh et al., 2006). Immune responses to DFT1 were only recently identified in a small number of wild devils (Pye et al., 2016a). Six wild devils have been found to produce serum antibodies against DFT1, four of these associated with regressions (Pye et al., 2016a), but these cases are rare, with most devils appearing ignorant of DTF1 infection. Interestingly, some devils can tolerate DFT1 infection, with increased survival in females associated with host SNPs in genes linked to cell-cycle regulation, cell adhesion and immunity, though no link was found in males (Margres et al., 2018). It has also been found that males infected with DFT1 have a greater decline in body condition based on body weight than females (Ruiz-Aravena et al., 2018). These results are supported by broader host evolution of Tasmanian devils in response to DFT1, particularly in genes associated with immunity and cellular processes (Epstein et al., 2016; Hubert et al., 2018). Increased reports of tolerance in the devil population correspond with reduced transmission rates and DFT1 becoming endemic (Patton et al., 2020), therefore evolution of the devil immune response may be a contributing factor.

Vaccination trials have shown that immune responses can be generated against DFT1 (Kreiss et al., 2015; Pye et al., 2018; Tovar et al., 2017). Out of six devils immunised with sonicated or freeze-thawed cells, five produced antibody and/or cytotoxic responses; however, this did not provide long-term protection when two of these devils were challenged with live DFT1 cells (Kreiss et al., 2015). Two studies immunised devils with DFT1 cells that expressed MHC class I, with 86% (n=7) (Tovar et al., 2017) and 95% (n=52) (Pye et al., 2018) of devils producing antibodies against MHC class I positive and negative DFT1 cells. Additionally, antibody responses

were found to be higher in juveniles compared to adults in both studies by Pye et al. (2018), and females compared to males in one of the two studies. Devils immunised by Pye et al. (2018) were released, but recapture rates were low, therefore conclusions cannot be made about the protection of this immunisation, however, three devils were captured with natural DFT1 infection. Of the seven devils immunised by Tovar et al. (2017), six were challenged with live DFT1 cells; only one of these remained tumour free and two had delayed onset, therefore immunisation offered little long-term protection. Three of these tumours were treated with DFT1 cells (expressing MHC class I) as immunotherapy, which resulted in tumour regression, mediated by T cells (Tovar et al., 2017). DFT1 cells were taken from biopsies from two of these tumours, and one non-immunised control. Analysis found DFT1 cells from regressing tumours had a de-differentiated mesenchymal phenotype (Patchett et al., 2021), having undergone an endothelial to mesenchymal transition, which is a common mechanism utilised by cancer cells (Hamilton et al., 2018; Pastushenko and Blanpain, 2019; Terry et al., 2017), presumably in response to recognition by the host immune system. These vaccination trials show Tasmanian devils can generate immune responses against MHC class I molecules expressed by DFT1 cells, therefore, based on the lack of immune responses observed in wild DFT1 hosts, the cancer cells must have evolved immune evasion mechanisms.

1.4.4 Immune evasion by DFT1

As DFT1 transmits as an allograft, it typically has a different MHC class I genotype to the host. MHC class I molecules that are different to the host and are expressed on the cell surface of DFT cells should initiate a robust immune response. However, in DFT1 components of the peptide presentation pathway, including TAP and β_2m, have been epigenetically downregulated, resulting in the loss of MHC class I on the cell surface (Siddle et al., 2013). These genes can be upregulated by treatment with the inflammatory cytokine interferon-γ (IFNγ) (Siddle et al., 2013) or overexpression of transcriptional co-activator, NOD-like receptor family CARD domain containing 5 (NLRC5) (Ong et al., 2021). This parallels modulation of MHC class I expression in Canine Transmissible Venereal Tumour (CTVT), which in laboratory models has low MHC class I on the cell surface during initial infection, with expression upregulated in response to cytokines (i.e. IL-6) during immune infiltration (Hsiao et al., 2008, 2002; Pérez et al., 1998) (discussed in Section 1.4.1). More recently it has been found that DFT1 expresses polycomb repressive complex 2 (PRC2), which is a conserved mechanism for transcriptional silencing of the APP in tumours with extremely low MHC class I expression (Burr et al., 2019). DFT1 also has a hemizygous deletion in β_2m (Stammnitz et al., 2018), resulting in lower cell surface expression of classical MHC class I than normal cells, even when gene expression is upregulated, which may have been an early mutation in DFT1 prior to total MHC class I downregulation.

Total loss of MHC class I on the cell surface should prevent recognition by T cells but may activate a natural killer (NK) cell response through 'missing self' (Ljunggren and Kärre, 1990, 1985). It is important to note that devil NK cell markers are not well defined, making study of these cells difficult. However, it has been found that devils have functional NK cells that engaged in cytotoxic killing of human HLA-null cancer cell line, K562, though this response was not seen against DFT1 cells (Brown et al., 2011). Thus, it is predicted that DFT1 is employing additional mechanisms to avoid host immune responses. Tasmanian devils have PD-1 and PD-L1 proteins, which can be transiently upregulated in DFT1 cells in response to IFNγ, but were not constitutively expressed (Flies et al., 2016). PD-L1 was also expressed in DFT1 tumours infecting immunised devils (Patchett et al., 2021). Therefore, this could be a method for immunosuppression by DFT1 cells. Also, non-classical MHC class I, Saha-UD and Saha-UK were expressed in a DFT1 tumour biopsy (Cheng and Belov, 2014) and are expressed in DFT1 cell lines (Caldwell et al., 2018; Gastaldello et al., 2021). Due to the potential of Saha-UD for peptide presentation, the low polymorphisms for *Saha-UD* in the population, and lack of polymorphism in *Saha-UK*, their expression may be immunosuppressive; therefore, expression by DFT1 could be a mechanism for host immune evasion.

1.4.5 Immune evasion by DFT2

With DFT2 emerging more recently, less is known about host immune responses to DFT2. Six DFT2 biopsies have been stained by immunohistochemistry (IHC) for CD3, a marker for T cells (Caldwell et al., 2018). Four had CD3+ cells, two of these were localised to the stroma, while the other two had some infiltration among tumour cells. The remaining two tumours had no CD3+ cells, though this may vary in a different section of the tumour. This shows devils can generate immune responses against DFT2 cells, but that immune responses are variable. Therefore, DFT2 may be evolving immune evasion mechanisms.

In contrast to DFT1, DFT2 expresses classical MHC class I on the cell surface (Caldwell et al., 2018), which should be immunogenic to hosts with disparate MHC class I genotypes. Though little is known about the immune response to DFT2, it has been observed that DFT2 has been limited to circulation within devil populations in the d'Entrecasteaux peninsula (South-Eastern Tasmania) (James et al., 2019; Kwon et al., 2018), where the cancer was discovered. DFT2 was found to share several alleles that appear to be common in the d'Entrecasteaux peninsula, as shown in Table 1.4 (from Caldwell et al., 2018). This may have resulted in less pressure from host immune systems for the development of immune escape mechanisms, such as MHC class I loss.

Table 1.4 MHC class I alleles expressed by DFT1 and DFT2 cell lines and DFT2 host samples.

From Caldwell et al. (2018). Grey boxes indicate alleles identified for each sample. Numbers indicate the number of clones identified for each allele when amplifying classical MHC class I genes with pan-specific primers. Non-classical alleles, SahaI*32(UD) and SahaI*UK, were amplified with gene specific primers. DFT1 and DFT2 alleles were identified using cell lines, DFT2 host (Red Velvet, 818, and Snug) alleles were identified from spleen or kidney biopsies.

NCBI allele name	DFT1	DFT2	Red Velvet	818	Snug
SahaI*46					
SahaI*27		22	22	14	2
SahaI*27–1		13		25	13
SahaI*74/88		9			
SahaI*35		13		10	
SahaI*90		4			1
SahaI*49/82				7	
SahaI*97			6		2
SahaI*33			6		2
SahaI*36			2		
SahaI*37			5		1
SahaI*29				2	2
SahaI*32(UD)					
SahaI*UK					

In addition to recognition of mismatched classical MHC class I alleles, CD8+ T cells can recognise mutated peptides. However, investigation into peptides expressed by DFT2 cells and a fibroblast cell line, found DFT2 cells expressed a restricted range of peptides, and expression of a common peptide motif across devil classical MHC class I, potentially reducing the number of mutated peptides presented by MHC class I molecules on DFT2 cells (Gastaldello et al., 2021). That said, loss of Y chromosome has been reported in DFT2 cells (Stammnitz et al., 2023, 2018). Previously there was bias towards DFT2 infection in males (James et al., 2019; Kwon et al., 2018) and loss of the Y chromosome was first observed in DFT2 cells infecting a female devil (Stammnitz et al., 2018). This fits with the expectation that the Y chromosome is immunogenic in female hosts, suggesting MHC class I molecules are able to present antigenic peptides, such as those from the Y chromosome. Additionally, DFT2 cells have been shown to upregulate PD-L1 expression in response to IFNγ, thus providing a potential immune suppression mechanism (Flies et al., 2016).

While classical MHC class I is still expressed by DFT2 cells, across the six tumour biopsies stained for MHC class I expression, expression levels were variable (Caldwell et al., 2018). Therefore, the retention of MHC class I may be limiting the cancer to circulation among devils with a similar MHC class I genotype (Caldwell et al., 2018). As DFT2 encounters devils with disparate classical MHC class I genotypes, greater selective pressure from the immune system is predicted and, consequently, we would expect evolution of immune escape mechanisms by DFT2.

1.5 Hypotheses and aims

1.5.1 Hypotheses

1) DFT2 is losing classical MHC class I expression during progression through the devil population.

DFT2 cells lines and tumours express classical MHC class I (Caldwell et al., 2018). As DFT2 has circulated in the d'Entrecasteaux peninsula where it first emerged, it is hypothesised that it has mostly encountered devils with similar MHC class I genotypes (Caldwell et al., 2018), therefore has not been subjected to host T cell responses, so there has been little pressure for downregulation of classical MHC class I. As the cancer continues to spread through the devil population it will encounter disparate MHC class I genotypes. As a result, we hypothesise that DFT2 will downregulate classical MHC class I alleles uncommon in the population in response to host T cell activation, via selective downregulation or total loss of classical MHC class I.

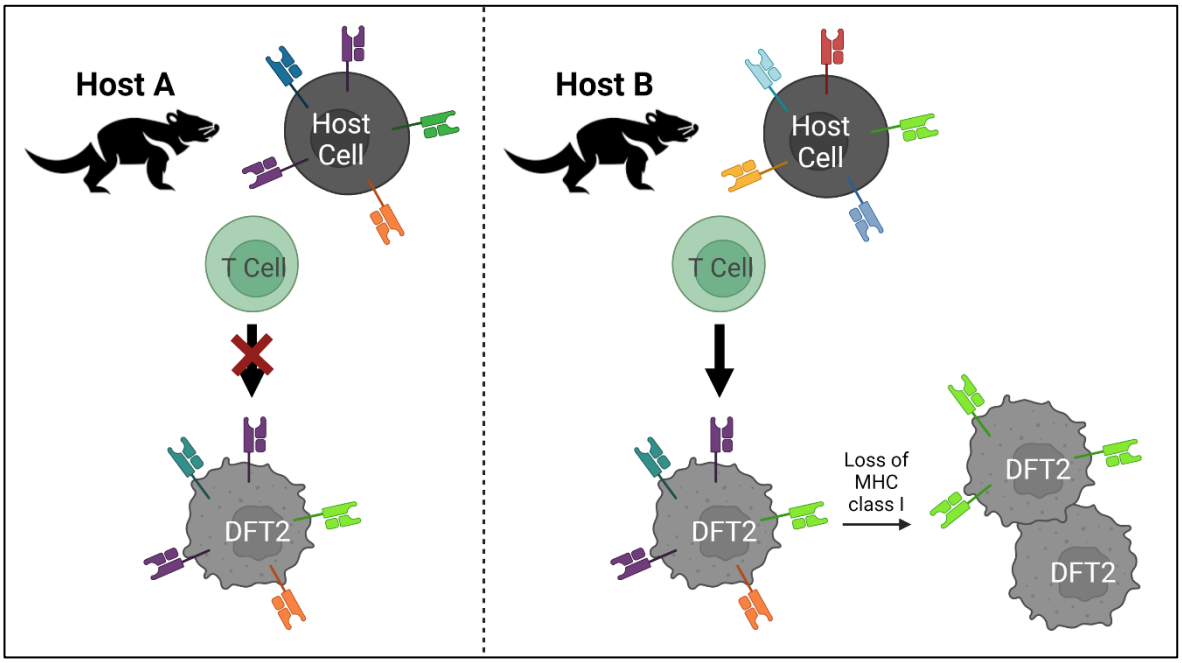

Figure 1.11 DFT2 hypothesis

(Left) DFT2 cells still express classical MHC class I and is hypothesised to circulate in devil populations with similar MHC class I genotypes (Caldwell et al., 2018), therefore has not been subjected to T cell responses. **(Right)** As the cancer continues to spread and encounters disparate genotypes, we would expect downregulation of alleles

uncommon in the population in response to host T cell activation, via selective downregulation or total loss of classical MHC class I. Created with BioRender.com.

2) DFT1 expresses non-classical MHC class I to evade the host immune response.

To evade the host immune system DFT1 has downregulated classical MHC class I expression via epigenetic mutations (Siddle et al., 2013). While this lack of classical MHC class I on the cell surface will prevent T cell recognition, it may result in the activation of NK cells due to 'missing self'. Non-classical MHC class I genes are expressed in DFT1 cell lines (Caldwell et al., 2018; Gastaldello et al., 2021) and a DFT1 tissue biopsy (Cheng and Belov, 2014). Due to their predicted immunosuppressive functions, we hypothesise that non-classical genes may be expressed by DFT1 tumours as a ligand to inactivate NK cells, while also avoiding a T cell response due to low polymorphisms.

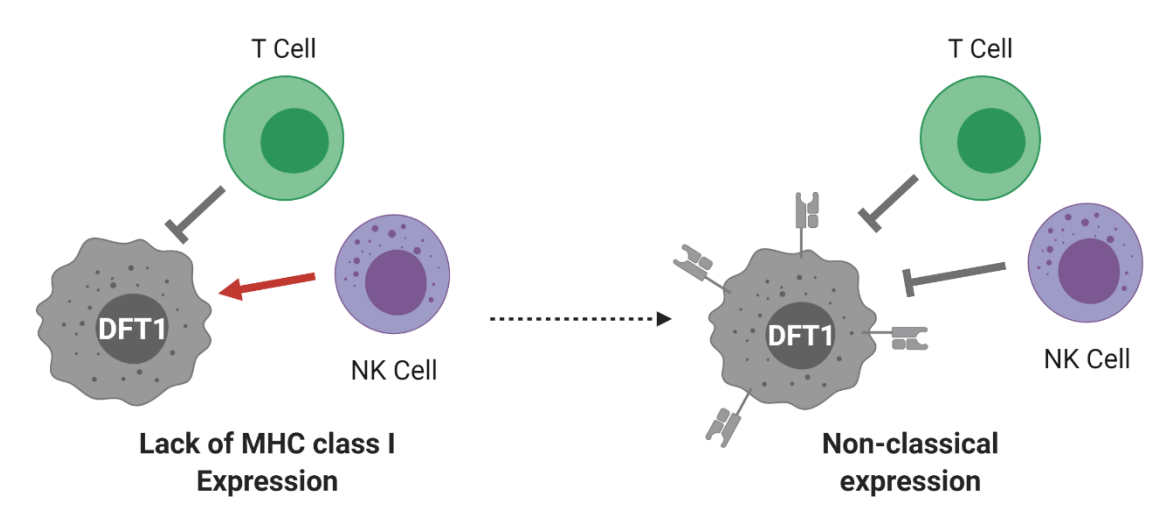

Figure 1.12 DFT1 hypothesis

In DFT1 there is a lack of classical MHC class I on the cell surface (Siddle et al., 2013). This prevents T cell recognition but should activate NK cells due to 'missing self'. Non-classical MHC class I molecules are often involved in immunosuppression and have been found expressed in DFT1 samples (Caldwell et al., 2018; Cheng and Belov, 2014; Gastaldello et al., 2021). Therefore, we hypothesise that non-classical genes may be expressed by DFT1 cells as a ligand to inactivate NK cells while also avoiding a T cell response due to low polymorphisms. Created with BioRender.com.

1.5.2 Aims

Hypothesis 1

Aim 1: Investigate whether classical MHC class I expression is being lost in primary DFT2 tumours.

Aim 2: Examine whether there is an immune response against tumours that express classical MHC class I.

Aim 3: Investigate classical MHC class I mismatch between tumour and host as a driver of MHC class I loss by DFT2.

Hypothesis 2

Aim 4: Determine whether loss of classical MHC class I expression is widespread in DFT1 tumours.

Aim 5: Investigate non-classical MHC class I expression in primary DFT1 tumours.

Aim 6: Investigate whether non-classical MHC class I expression correlates with a 'colder' tumour immune environment.

Chapter 2 Materials and methods

2.1 Collection and processing of Tasmanian devil samples

Tissue samples were collected by Dr Rodrigo Hamede (University of Tasmania), Prof Gregory Wood (Menzies Institute for Medical Research), or Dr Elizabeth Murchison (University of Cambridge). Wild Tasmanian devils were either trapped or found dead from road trauma or other causes. Tissue biopsies were collected post-mortem or from live devils, which were subsequently released, as part of other studies. Tumour biopsies were formalin fixed (10% neutral buffered formalin) for 2 to 4 days, and subsequently processed and embedded in paraffin blocks, or were stored in RNAlater. Ear biopsies were stored in RNAlater.

All animal procedures were performed under a Standard Operating Procedure approved by the General Manager, Natural and Cultural Heritage Division, Tasmanian Government Department of Primary Industries, Parks, Water and the Environment (DPIPWE), in agreement with the DPIPWE Animal Ethics Committee, or under University of Tasmania Animal Ethics Committee Permit A0014976, A0016789, or AEC 27141. Tasmanian devil samples used in this thesis are listed in Table A 1 and sample collection locations shown in Figure 2.1. A complete metadata spreadsheet for these samples is available at https://doi.org/10.5258/SOTON/D3092.

Two DFT1 tumour samples came from devils, Grommit and Tiarna, immunised with irradiated cell line DFT1_C5065 (protocol detailed in (Kreiss et al., 2015)). C5065 (RRID:CVCL_LB79) is a cell line established from a DFT1 biopsy in 2005. Despite irradiation of the cell line, tumours grew at the site of inoculation. Christine was inoculated with DFT1_C5065 as part of a transmission trial (A Kreiss 2022, personal communication). Immunisation and transmission trial procedures were approved by The University of Tasmania Animal Ethics Committee, under permit numbers A9215 and A11436.

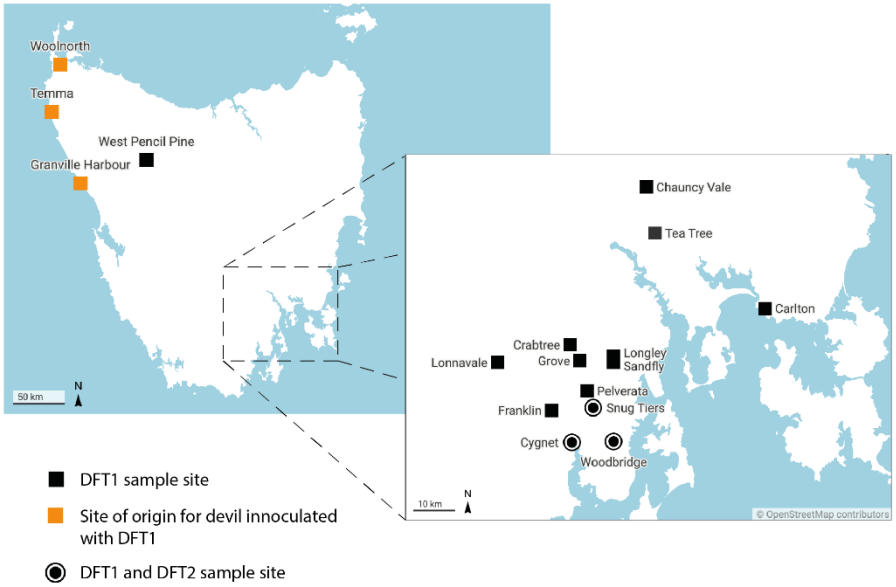

Figure 2.1 Map of sample locations

Map of Tasmania showing trapping locations for tissue samples used in this thesis. Due to proximity, Snug Tiers represents Snug Tiers and Snug, and Lonnavale represents Lonnavale and Southwood Road. Orange square markers represent sites from which devils were captured and later inoculated with DFT1 cell lines in immunisation and transmission trials (as detailed in Section 2.1 above); at all other sites DFT1 and/or DFT2 samples were taken from wild Tasmanian devils.

2.2 Cell Culture

The cell lines used in this thesis are detailed in Table A 2. Three DFT1 cell lines, 1426, 4906, and C5065, and two DFT2 cell lines, RV and SN, were used in this thesis (See Table A 2 for alternative names). DFT cell lines were cultured in RPMI 1640 with glutamine (Gibco 61870-010), with penicillin/streptomycin (100 units/ml penicillin and 0.1 mg/ml streptomycin) or 50 µg/ml gentamicin, 10% (v/v) foetal calf serum (filtered), at 35 °C and 5% CO_2. They were passaged 1:3 every 3 days or when 80% confluent.

Hybridoma cell lines producing antibodies against devil-MHC class I and IFNγ (Caldwell, 2018; Caldwell et al., 2018), were cultured in RPMI 1640 with glutamine (Gibco 61870-010) with penicillin/streptomycin (100 units/ml penicillin and 0.1 mg/ml streptomycin) or 50 µg/ml gentamicin, 10% (v/v) foetal calf serum (filtered), at 37 °C and 5% CO_2. Cells were passaged 1:5 every 3 days, into a 50:50 mixture of conditioned and fresh media. Once cells were at 80% confluence, the media was replaced and cells were incubated for 24-48 hours; after which the media was collected, centrifuged twice at 500 g for 5 min and the supernatant filtered through a

0.22 µm filter to remove any remaining cells. Hybridoma supernatant containing antibodies was used in IHC and Western blots as listed in Table A 3.

Chinese Hamster Ovarian (CHO) cell lines were previously transfected to produce devil IFNγ, CHO_SahaIFNγ (Siddle et al., 2013). Supernatant from culture of CHO_SahaIFNγ was used to upregulate β_2m expression in DFT1_4906, restoring classical MHC class I expression on the cell surface (see Section 2.2.1 below). CHO and CHO_SahaIFNγ cell lines were cultured in Hams F-12 with glutamine (Gibco 31331-028), and penicillin/streptomycin (100 units/ml penicillin and 0.1 mg/ml streptomycin) or 50 µg/ml gentamicin, 10% (v/v) foetal calf serum (filtered), at 37 °C and 5% CO_2. Cells were split 1:10 every 3 days. Supernatant was collected after 30 hr. The supernatant was centrifuged at 500 g for 5 min and filtered using a 0.45 µm filter before being applied to DFT cells.

2.2.1 IFNγ treatment of devil cell lines

To upregulate classical MHC class I expression on the cell surface of DFT cell lines, and investigate DFT phenotypes in an inflammatory immune environment, DFT1_4906 and DFT2_RV were treated with supernatant from culture of CHO_SahaIFNγ (see Section 2.2 above), containing devil IFNγ (Siddle et al., 2013). Once the DFT cells were 80% confluent, they were treated with 50% CHO_SahaIFNγ supernatant, 50% fresh RPMI media for 48 hr.

Upregulation of β_2m from IFNγ treatment was confirmed using flow cytometry (detailed in Caldwell, 2018 and Owen, 2019). Briefly, $2x10^5$ DFT cells per antibody or control, kept cold throughout, were incubated with 1 µg/ml anti-β_2m antibody (13-34-48; Caldwell et al, 2018) for 30 min, then incubated with 2 µg/ml secondary antibody (goat anti-Mouse IgG (H + L) Alexa Fluor 488; ThermoFisher Scientific) for 30 min in the dark, resuspended in 200 µl propidium iodide (1 µg/ml), and analysed on a Guava® easyCyte™ SL system (Millipore) using guavaSoft 3.3 software. DFT cells treated with supernatant from untransfected CHO cells were used as a control. IFNγ-treated cells were used for paraffin embedding (Section 2.2.3) and PCRs (Section 2.3).

2.2.2 Cell lysis

Media was removed, and DFT or CHO cells detached from the culture plate using TrypLE™ Express (Gibco 12605-010). Cells were centrifuged at 400 g for 5 min and resuspended in cold 1X PBS. Once harvested, cells were kept on ice.

Cells were counted using a hemacytometer, centrifuged and resuspended in cold lysis buffer (30 Mm NaCl, 50 mM Tris-Cl pH8, 1 mM $MgCl_2$, 1% NP-40, 1X Halt Protease Inhibitor Cocktail (Thermo

Scientific, 100X) in ddH_2O) at $1x10^7$ cells/ml. The tubes were inverted on a tube rotator at 17 rpm for 45 min at 4 °C. The resulting lysate was centrifuged at 12,000 rpm for 20 min at 4 °C. The pellet was discarded, and the supernatant kept for use in Western blots (see Section 2.4.4).

2.2.2.1 Bradford assay

Prior to use in Western blots, the protein concentration of cell lysates was determined by Bradford assay. Lysates were diluted 1:2, 1:5 and 1:10 in lysis buffer and 5 µl added to a 96-well plate (transparent bottomed). Protein standards were created using a 1 mg/ml BSA stock in lysis buffer as shown in Table 2.1 below. Two replicates were included for each protein standard and sample dilution. To each well, 250 µl of room temperature Bradford reagent (1X working solution, Thermo Scientific 1856209) was added, and the plate incubated for 5 min at room temperature. The absorbance at 585 nm was read on a POLARstar Omega plate reader (BMG Labtech).

Table 2.1 Bradford assay protein standards

Protein standard (mg/ml)	Volume of 1 mg/ml BSA stock (µl)	Volume of lysis buffer (µl)	Bradford reagent 1X (µl)
0	0	5	250
0.2	1	4	250
0.4	2	3	250
0.6	3	2	250
0.8	4	1	250
1	5	0	250

The mean absorbance for the protein standards was used to create an absorbance curve, which the mean absorbance for the sample dilutions was compared against, and the protein concentration multiplied by the dilution factor. If the sample dilution mean absorbances were higher than the mean absorbance for the 1 mg/ml protein standard, the Bradford assay was repeated with higher sample dilutions.

2.2.3 Formalin fixation and paraffin embedding

To test antibodies and investigate protein expression by DFT cells, cell lines were fixed in formalin, suspended in Cytoblock™ matrix (Epredia™ Cytoblock 10446640), and embedded in paraffin blocks for use in IHC. DFT or CHO cells detached from the culture plate using TrypLE™ Express (Gibco 12605-010) were centrifuged at 400 g for 5 min and resuspended in media for counting.

Once harvested, cells were kept on ice until fixed. $4x10^6$ cells were transferred to a 1.5 ml tube, centrifuged (400 g for 5 min) and resuspended in 500 µl of cold, sterile TBS (0.1 M TBS, 0.14 M sodium chloride, 2 mM potassium chloride, pH 7.4). Cells were fixed in 2% formaldehyde (adding 500 µl of 4% paraformaldehyde to the cell suspension) for 10 min at room temperature, before being centrifuged (500 g for 5 min) and washed twice in 1 ml sterile TBS. Finally, cells were centrifuged at 400 g for 10 min at 20 °C and the supernatant removed. The cells were resuspended in 1 drop of Cytoblock™ Reagent 2, following which 1 drop of Cytoblock™ Reagent 1 was added and the tube vortexed immediately. The cell matrix was embedded into paraffin blocks on the same day.

Varying cell numbers were trialled for the cell matrix: $2x10^6$, $4 x10^6$, $6 x10^6$, and $2 x10^7$. Following IHC staining (for protocol see Section 2.5.1), $4x10^6$ was determined to be the optimal number and was used for all experiments where possible, as listed in the protocol above. 4906, RV, CHO, and CHO_SahaIFNγ were used at $4x10^6$; however, IFNγ-treated DFT cell lines, 4906-gamma and RV-gamma, were embedded at $2x10^6$ and $1x10^6$ respectively, as they did not reach high enough cell numbers.

2.3 Polymerase Chain Reaction (PCR)

2.3.1 RNA extraction

2.3.1.1 Tissue samples

RNA from Tasmanian devil tissue samples was extracted using TRIzol™ Reagent (Sigma-Aldrich) according to the manufacturer's instructions. For tumours and spleen, 10-20 mg of tissue was used for extraction. As host ear biopsies were smaller tissue samples, between 0.8-10.2 mg of tissue was used, depending on the size of the sample. The tissue was homogenised in 500 µl TRIzol™ Reagent using a 2 cm^3 tissue grinder (Thermo Fisher). Homogenate was transferred to a 1.5 ml tube, centrifuged at 12,000 g for 10 min at 4 °C and the clear supernatant transferred to a fresh tube. At this point samples were either stored at -80°C for up to a month or processed immediately. Between uses tissue grinders were cleaned with detergent in hot water using a spout brush and sprayed with 70% ethanol.

Samples were incubated at room temperature for 5 min, after which 500 µl of 1-bromo-3-chloropropane was added. Sample were shaken vigorously for 15 s and left to stand at room temperature for 10 min. The mixture was centrifuged at 12,000 g for 15 min at 4 °C. This is phase separation, where the mixture separates into 3 phases: bottom red organic phase (protein), middle white interphase (DNA), and top colourless aqueous phase (RNA). The top aqueous phase

was transferred to a fresh 1.5 ml tube by pipetting, being careful not to pipette any of the white interphase, otherwise there would be DNA contamination. The organic phase and interphase could be stored at 2-8 °C for subsequent isolation of protein and DNA.

Due to the small size of the host ear biopsies, the aqueous phase was very thin, therefore it was difficult to obtain a sufficient volume without interphase contamination. For these samples, the aqueous phase was pipetted into Phasemaker™ tubes (A33248. Invitrogen) to remove contaminating DNA. Prior to use, the Phasemaker™ tubes were centrifuged at 14,000 g for 30 s. Once the aqueous phase was added, the tubes were centrifuged at 14,000 g for 5 min at 4 °C and the supernatant transferred into a fresh 1.5 ml tube.

To the isolated interphase, 250 µl of 2-propanol was added and mixed by inversion. Samples were incubated at room temperature for 8 min, then centrifuged at 12,000 g for 10 min at 4 °C. The supernatant was discarded, and the RNA pellet washed in 500 µl of 70% ethanol, vortexed, and centrifuged at 7,500 g for 5 min at 4 °C. Supernatant was removed by pipetting and the RNA pellet air-dried for 5-15 min. The RNA pellet was resuspended in 15 µl of RNase-free water (or 30 µl for tumour or spleen samples greater than 10 mg) by pipetting. RNA concentration was determined using a Nanodrop spectrophotometer at 260nm absorbance. Extracted RNA was kept on dry ice and reverse transcribed immediately or stored at -80 °C for future use.

2.3.1.2 Cultured cells

The NucleoSpin RNA kit (Macherey-Nagel) was used to extract RNA from cells lines according to the manufacturer's instructions. Cells were washed with PBS and centrifuged at 300 g for 5 min. The supernatant was removed and 350 µl Buffer RA1 and 3.5 µl β-mercaptoethanol added to $1x10^6$-$5x10^6$ cells in a 1.5 ml tube and vortexed vigorously. The lysate was filtered through a NucleoSpin® Filter at 11,000 g for 1 min. To the filtered lysate, 350 µl of 70% ethanol was added and mixed by pipetting. The lysate was added to a NucleoSpin® RNA Column and centrifuged at 11,000 g for 30 s, after which the column was placed in a fresh collection tube. The column membrane was desalted using 350 µl Membrane Desalting Buffer and centrifuging at 11,000 g for 1 min. To digest DNA, 95 µl rDNase reaction mixture was added to the column membrane and incubated at room temperature for 15 min. The membrane was washed 3 times, first with 200 µl Buffer RAW2, then 600 µl Buffer RA3, both centrifuged at 11,000 g for 30 s, and finally 250 µl Buffer RA3, centrifuged at 11,000 g for 2 min. RNA was eluted in 30-40 µl RNase-free water and centrifuged at 11,000 g for 1 min.

RNA concentration was measured using a Nanodrop spectrophotometer at 260nm absorbance. Extracted RNA was kept on dry ice and reverse transcribed immediately or stored at -80 °C for future use.

2.3.2 Reverse transcription

1 µg of RNA was reverse transcribed to cDNA, or up to 11 µl if the RNA concentration was 9 ng/µl or less, using the RevertAid First Strand cDNA Synthesis kit (Thermo Fisher) according to manufacturer's instructions. Reverse transcription reagents are detailed in Table 2.2 and reverse transcription reaction conditions are summarised in Table 2.3 below. Reagents for Step 1 were added to a 0.2 ml PCR tube, heated at 65 °C for 5 min, then chilled on ice. To the reaction mixture, reagents from Step 2 were added, heated at 45 °C for 60 min, then 70 °C for 5 min. The cDNA was stored at -20 °C for future use in PCR amplification (See Section 2.3.3).

Table 2.2 Reverse transcription reagents

Step 1	
Reagent	**Amount**
Template RNA	1000 ng
Oligo (dT) primer	8.33 µM
Water	To total
TOTAL	12 µl
Step 2	
Reagent	**Amount**
Mixture from Step 1	12 µl
5X reaction buffer	1X
RiboLock RNase inhibitor	20 U
dNTP mix	1 mM
RevertAid Reverse Transcriptase	200 U
TOTAL	20 µl

Table 2.3 Reverse transcription reaction conditions

Step	Temperature (°C)	Length (min)
1	65	5
Chill on ice		
2	45	60
	70	5

2.3.3 PCR amplification

To investigate expression of non-classical MHC class I, *Saha-UD*, Dev Men UD primers (Caldwell et al., 2018) were used to amplify *Saha-UD* by PCR. RPL13A primers (Siddle et al., 2013), amplifying a ribosomal protein, were used as a control. Primers and annealing temperatures are listed in Table 2.4. 500 ng of cDNA from tissue or cell lines was amplified using Phusion High-Fidelity DNA Polymerase (Thermo Fisher), according to the manufacturer's instructions (see Table 2.5 for PCR reagents and Table 2.6 for PCR conditions) and appropriate negative controls.

Table 2.4 Primer sets

Gene Amplified	Primer Names	Primer Sequence (5’ -> 3’)	Product Length (bp)	Annealing Temperature (°C)
Non-classical MHC Class I *Saha-UD* (exon 2-4)	Saha138	GCCATATGGGCTCTCACTCCTTGAGGTATTTCGGCACCAC	1044	63
	Saha48	ATGCAAGCTTGGCTTTGGCTGTCAGAGAGACATCTGACC		
RPL13A	Saha120	ACAAGACCAAGCGAGGCCAGG	300	60
	Saha121	GCCTGGTATTTCCAGCCAACCTCA		
Non-classical MHC Class I *Saha-UD*	Dev Men UD (F)	ATGGAGAATGTGGACCGGGAC	275	60
	Dev Men UD (R)	TGAGTTCACTGCCTCATTCACT		
Classical MHC class I *Saha-UA, -UB & -UC (addition of adaptors for Illumina MiSeq sequencing)*	Saha428	TCGTCGGCAGCGTCAGATGTGTATAAGAGACAGCCGTGGGCTACGTGGACGATCAGC	363	60
	Saha429	GTCTCGTGGGCTCGGAGATGTGTATAAGAGACAGGTCGTAGGCGAACTGAAG		

Table 2.5 PCR reagents

Reagent	**Final Concentration**
cDNA	250ng or 500 ng
DNA polymerase (Thermo Fisher *Phusion*)	0.5 U
Primers	0.6 µM each
dNTPs	200 µM
Phusion High Fidelity buffer	1X
ddH_20	To total volume of 25 µl

Table 2.6 PCR amplification conditions

Cycle Element	**Temperature (°C)**	**Time (s)**	**Number of Cycles**
Initial denaturation	98	30	1
Denaturation Annealing Elongation	98 Temperatures for primers in Table 2.4 72	10 30 30	 30
Final Elongation	72	300	1

2.3.4 Agarose gel electrophoresis

Following PCR amplification, PCR products were run on an agarose gel to confirm gene expression of *Saha-UD*. To the 25 µl PCR reaction mixture, 5 µl of 6X loading dye was added. For each sample, 13 µl was added per well. PCR products were run on a 1.2% (w/v) agarose gel with GelRed, at 110V for 35 min, or until the dye front reached the edge of the gel. Agarose gels were visualised using SynGene P*Xi* machine and SynGene software.

For host genotyping (see Section 2.6.1), 5 µl of PCR product per sample replicate was run on an agarose gel to confirm amplification prior to sequencing.

2.4 Antibody generation and validation

2.4.1 Antibodies against devil MHC class I

Antibodies against Tasmanian devil MHC class I molecules were previously designed and validated in our lab (Caldwell et al., 2018). These were against non-classical Saha-UK, using peptide sequence 'RITHRTHPDGKVTL' from the alpha-3 domain of the molecule, and a pan-specific antibody for classical Saha-UA, -UB and -UC, against peptide sequence 'WMEKVQDVDPGYWE' from the alpha-1 domain (Figure 2.2).

For generation of an antibody against non-classical Saha-UD, MHC class I transcripts representing all known devil MHC class I alleles (from Caldwell and Siddle, 2017) were aligned and translated into protein sequences using CLC workbench (Caldwell et al., 2018). The α1 domain was manually assessed for regions of low amino acid identity between Saha-UD alleles and the classical MHC class I (Saha-UA, -UB and -UC) and Saha-UK (Figure 2.2). Using this sequence, the peptide 'WIEKMENVDRDYWE' was synthesised for immunisations against Saha-UD (Caldwell, 2018). The protocol for immunization and hybridoma generation was undertaken by our collaborator, Prof Karsten Skjødt (University of Southern Denmark). Briefly, mice were immunised subcutaneously twice with a mixture of GERBU adjuvant and WIEKMENVDRDYWE-C coupled to diphtheria toxoid, with a final boost of antigen without GERBU given by intravenous injection. Three days later spleen lymphocytes were fused with the SP2 cell line and hybridomas selected based on reactivity in ELISA against the peptide.

Supernatant from the candidate antibodies was subsequently screened against Tasmanian devil spleen samples by IHC (for protocol, see Section 2.5) (Hussey, 2018) and verified against recombinant MHC class I by western blot. Two anti-Saha-UD antibodies selected by IHC screening (Hussey, 2018) were tested for specificity using Western blot on recombinant proteins for devil

MHC class I, classical Saha-UC, non-classical Saha-UD, and non-classical Saha-UK. Further details of recombinant protein production and Western blotting are included in Sections 2.4.3 and 2.4.4 respectively.

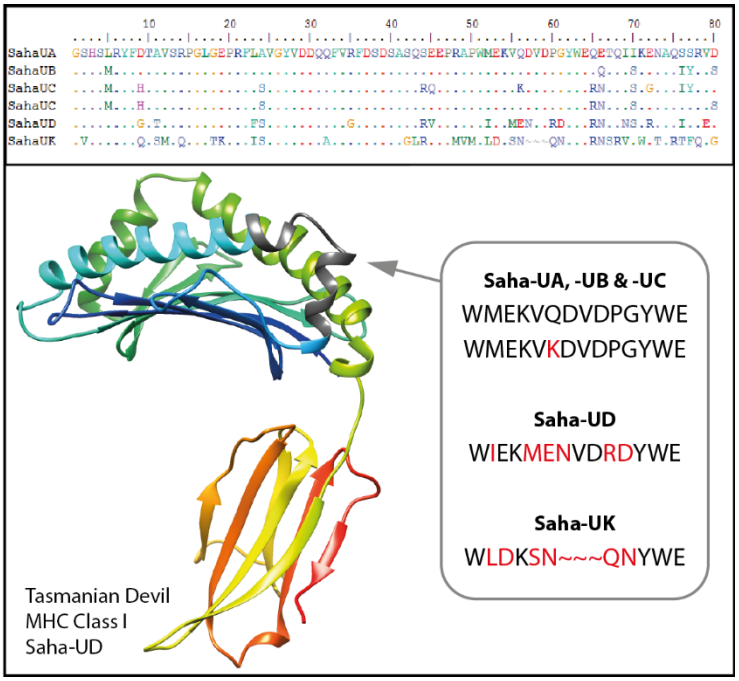

Figure 2.2 Devil MHC class I peptide sequences used for antibody generation.

Antibodies were generated against the peptide sequence 'WIEKMENVDRDYWE' from the alpha-1 domain of the non-classical MHC class I, Saha-UD heavy chain protein. This sequence differs from the classical MHC class I (Saha-UA, -UB, and -UC) and non-classical Saha-UK sequences, shown in the amino acid alignment. A putative model of the Saha-UD molecule is shown, with the antibody epitope in grey. In the grey box, red indicates where the sequences differ. An antibody against the Saha-UA-UB-UC was generated previously, using the sequence 'WMEKVQDVDPGYWE' from the alpha-1 domain (Caldwell, 2018).

2.4.2 Antibody against devil-IFNγ

Antibodies against devil-IFNγ have previously been generated in our lab (Caldwell, 2018). In summary, recombinant devil IFNγ protein was produced by Dr Hannah Siddle and used to immunise mice by Prof Karsten Skjødt, following a similar immunisation protocol to MHC class I antibodies (described above). Thirty-one antibodies against IFNγ were screened by Dr Alison Caldwell for use in Western blot, flow cytometry, immunocytochemistry, and IHC. All 31

antibodies recognised denatured devil IFNγ by Western blot. Antibodies were screened for IHC by staining devil spleen samples and a DFT1 tumour. One antibody, α-IFNγ_13-44-6, worked by IHC and was validated by blocking the antibody using IFNγ produced by CHO_SahaIFNγ, prior to use for further IHC staining.

2.4.3 Recombinant MHC class I protein production

Recombinant devil MHC class I heavy chain proteins were used to determine the specificity of anti-Saha-UD antibodies, specifically Saha-UC (SahaI*27), Saha-UK, and Saha-UD (SahaI*32). MHC class I, classical Saha-UC and non-classical Saha-UK full length recombinant proteins were previously generated in our lab (Caldwell, 2018; Caldwell et al., 2018). To validate anti-Saha-UD antibodies, a recombinant protein for non-classical Saha-UD was generated using the same method. In summary, exons 2 – 4 (α1, α2 and α3 domains) from Saha-UD were amplified from the full gene sequence (Ensembl identifier: ENSSHAG00000010776.2) using primers Saha-138 and Saha-48 (Table 2.4). The subsequent amplicons were cloned into the pET22b^{+} vector (Novagen), by digestion with NdeI (Promega R680A) and sticky end cloning with T4 ligase (Promega M180A), then transformed into competent dh5α E. coli cells. The resulting plasmid produces a recombinant Saha-UD protein with a 6xHis-tag at the C-terminal. Clones from single colonies were grown in LB with ampicillin (100 μg/ml) for 12 hours at 37 °C with shaking. To confirm dh5α colonies had been transformed with the plasmid, a colony PCR was performed using Dev Men UD primers (Table 2.4) and 2 μl of bacterial broth; PCR reagents are listed in Table 2.7 below and PCR conditions as detailed in Table 2.6, using 22 cycles rather than 30 cycles for denaturation, annealing, and elongation steps.

Table 2.7 PCR reagents for colony PCR

Reagent	**Final Concentration**
Bacterial broth	2 μl
2X master mix (VWR *Taq*)	1X
Primers	0.2 μM each
ddH_20	To total volume of 25 μl

Plasmids were isolated from positive colonies using the NucleoSpin Plasmid kit (Macherey-Nagel) and the transcripts sequenced in both directions by Eurofins genomics using T7 and sp6 vector primers. pET22b^{+}-SahaUD plasmids with the correct sequence were transformed into Rosetta pLysS cells (Novagen) using 3 ng/µl of plasmid. Bacterial colonies containing the plasmid were cultured with LB with ampicillin (150 µg/ml) at 37 °C with shaking to OD_{600} 0.6, and protein expression induced with 1mM isopropyl β-D-1-thiogalactopyranoside (IPTG). Following addition of IPTG, the bacteria were cultured for 4 hours at 37 °C with shaking. Samples were taken prior to protein induction and every 1 hr after by removing 1 ml of culture, which were used to confirm protein induction (see Section 2.4.4.1). The bacterial culture was analysed directly on a Western blot for anti-Saha-UD antibody validation (see Section 2.4.4.2).

2.4.4 SDS-PAGE and Western blotting

2.4.4.1 Confirming induction of non-classical MHC class I, Saha-UD protein production

To ensure that each bacterial culture analysed by Western blot had approximately the same number of cells, the samples were normalised to the turbidity of bacterial suspension prior to protein induction (T_0). The volume used from each sample was calculated based on its OD (600nm) using the following equation: $Volume\ of\ bacterial\ culture\ (\mu l) = \frac{T0}{Tx}\ x\ 250\ \mu l.$ Calculated volumes of bacterial culture were centrifuged at 13,000 rpm for 1 min, resuspended in 25 µl loading buffer (500 µl 2X Lamelli sample buffer, 50 µl β-mercaptoethanol and 450 µl dd-H_2O) and heated at 95 °C for 10 min. 20 µl of each sample was run by Sodium dodecyl sulphate polyacrylamide gel electrophoresis (SDS-PAGE). Gels were stained with Coomassie blue and used for Western blots with antibodies against myc and 6xHIS (which will recognise tags on the recombinant proteins; antibodies listed in Table A 3) to confirm induction of Saha-UD protein production (see Sections 2.4.4.4, 2.4.4.5 and 2.4.4.6 for protocols).

2.4.4.2 Testing the specificity of anti-Saha-UD antibodies

To test the specificity of anti-Saha-UD antibodies, recombinant MHC protein (see Section 2.4.3) was analysed on a Western blot (see Sections 2.4.4.4 and 2.4.4.6). 6 µg of Saha-UC or Saha-UK recombinant protein was added to a 1.5 ml tube, made up to a total volume of 25 µl with loading buffer (500 µl 2X Lamelli sample buffer, 50 µl β-mercaptoethanol and 450 µl dd-H_2O). The Saha-UD recombinant protein was used following protein induction but prior to protein purification; the IPTG-induced cell suspension was centrifuged at 13,000 rpm for 1 min and resuspended in 25 µl loading buffer. The volume centrifuged was calculated based on the OD (600 nm) of the

suspension, to give approximately the same number of cells as in 250 µl of a suspension at OD (600 nm) 0.6. Both preparations were heated to 95 °C for 10 min and 20 µl added per well.

2.4.4.3 Testing the specificity of anti-IFNγ antibodies

Anti-IFNγ antibody, 13-44-6, was previously screened and validated by antibody blocking for use in IHC (Caldwell, 2018), see Section 2.4.2 for more information. To validate the specificity of α-IFNγ_13-44-6, CHO_SahaIFNγ cell lysate, and untransfected CHO lysate as a control, were analysed on a Western blot (see Sections 2.4.4.4 and 2.4.4.6). 30 µg of cell lysate was added to a 1.5 ml tube and made up to a total volume of 25 µl with loading buffer (500 µl 2X Lamelli sample buffer, 50 µl β-mercaptoethanol and 450 µl dd-H_2O). Samples were heated to 95 °C for 10 min to denature the proteins and 20 µl added per well. Anti-IFNγ antibody, 13-44-6 was further validated using CHO and DFT FFPE cell lines by IHC (protocol detailed in Section 2.5.1).

2.4.4.4 SDS-PAGE

Samples were analysed on a 12% acrylamide gel (National Diagnostics ProtoGel® 30%), with a 4% stacking gel. Gels were loaded with 20 µl sample, 5 µl protein ladder (Fisher PageRuler™ or Sigma BLUeye), and 5 µl loading buffer (500 µl 2X Lamelli sample buffer, 50 µl β-mercaptoethanol and 450 µl ddH_2O) in unused wells to keep the shape of the gel. Gel was run using running buffer (2.5 mM Tris, 19.2 mM glycine, 1% SDS, ddH_2O) and Fisherbrand™ Vertical Gel Tank at 200 V for 1 hr, or until the appropriate protein marker had run to the bottom of the gel. Gels were either stained with Coomassie blue (Section 2.4.4.5) or transferred to a nitrocellulose membrane for Western blotting (Section 2.4.4.6).

2.4.4.5 Coomassie blue staining

To visualise proteins, SDS-PAGE gels were stained with Coomassie blue (45% (v/v) methanol, 45% (v/v) ddH_2O, 10% acetic acid, 121 µM Coomassie R-250) overnight; followed by fix/destain solution (7.5% (v/v) acetic acid, 10% (v/v) methanol, 82.5% (v/v) ddH_2O) until protein and ladder bands were clearly visible. Both steps were performed at room temperature with rocking.

2.4.4.6 Western blotting

Proteins were transferred from the SDS-PAGE gel to a nitrocellulose blotting membrane (Amersham Protran GE Healthcare Life Sciences) in 1X transfer buffer (2.5 mM Tris, 19.2 mM glycine, 20% (v/v) methanol, ddH_2O) using a vertical gel tank (Geneflow) on a magnetic stirrer. Transfer was run at 100 V for 1 hr at 4 ° C.

Non-specific binding was blocked for 1 hr with 5% milk powder in TBST (150 mM NaCl, 0.1% (v/v) Tween20, 5% (w/v) milk powder, 50 mM TrisCl (pH 8)). The membrane was washed in TBST (150 mM NaCl, 0.1% (v/v) Tween20, 50 mM TrisCl (pH 8)) 3 times for 10 min each, then incubated with neat hybridoma supernatant (antibodies listed in Table A 3) at 4 °C overnight on a roller. Membranes were washed with TBST (10 min x 3), incubated with secondary antibody (IRDye® 680RD Goat anti-Mouse IgG (H + L)) in 5% milk in TBST for 1 hr at room temperature, and washed in TBST (10 min x 3). All steps were performed on a roller and at room temperature unless stated otherwise. Membranes were visualised using the LI-COR Odyssey® scanner.

2.5 Immunohistochemistry (IHC)

Formalin-fixed paraffin-embedded (FFPE) tissue samples were cut using a microtome at a thickness between 4-6 µm, or up to 10 µm for some tissues if necessary, and mounted onto APES-coated slides.

Sections were deparaffinized in two changes of xylene for 10 min each, and rehydrated through graded alcohol (100% I, 100% II, 95%, 70%) for 5 min each. Antigen retrieval was performed by water bath (95 °C) in citrate buffer solution (10mM citric acid, 0.05% Tween20, pH 6) for 40 min, followed by cooling for 15 min. Endogenous peroxidase was blocked by incubation with 3% H_2O_2 (Sigma Aldrich) for 10 min and non-specific protein binding was blocked with 10% (vol/vol) goat serum in PBS for 30 min. Sections were incubated with primary antibodies (listed in Table A 3) at 4 °C overnight. Peroxidase-coupled secondary antibody (EnVision Peroxidase/DAB+ kit; Dako) was used to detect primary antibody binding; incubating sections with HRP for 30 mins and colour developed with DAB chromogen for 5 mins. Sections were counterstained with haematoxylin (Vector hematoxylin nuclear counterstain (Gill's Formula) or Sigma-Aldrich haematoxylin (Harris' Formula, Modified)) for 4 min, differentiated in 2% (vol/vol) acetic acid and blued in 0.2% (vol/vol) ammoniated water for 2min. Sections were dehydrated through graded alcohol (95%, 100% II, and 100% I) for 5min each, transferred through two changes of xylene for 5 min each, and cover-slipped (using National Diagnostics Omnimount Histological Mounting Medium). Images were captured using the Nikon Eclipse 400 microscope, Retiga 2000R camera and Q-capture pro 7 computer software. Scale bars were added to images using ImageJ software.

2.5.1 IHC for embedded cell lines

FFPE cell lines were cut using a microtome at a thickness of 2, 4, 6 and 10 µm. Following preliminary experiments, the optimal thickness was determined to be 4 µm, which was used for all experiments. Slides were stained following the protocol above, excluding the endogenous

peroxidase blocking step. The cytoblock matrix is removed during the PBS washes, leaving only the cells. To make visualisation of DAB staining clearer, a weak haematoxylin stain was used.

2.5.2 Expression scoring

To quantify IHC staining with MHC class I antibodies, expression scores were assigned based on strength of staining of tumour cells. Expression scores ranged from 0 – 4, where 0 indicates no staining of tumour cells and 4 very strong DAB staining (Illustrated in Figure 2.3). Initially scoring was assigned by eye, but to reduce subjectivity and streamline analysis, a script was created in Fiji to automate assignment of expression scores (IHC image processing is illustrated in Figure 2.4). The scripts for expression scoring are available at https://doi.org/10.5258/SOTON/D3092. In summary, images were separated into DAB and haematoxylin staining images in ImageJ using the IHC Profiler plugin (Varghese et al., 2014). Haematoxylin images were manually threshold-ed in Fiji (Image>Adjust>Threshold) to create an 8-bit binary black & white nuclei image, which was processed using the script. The nuclei image was distance mapped, where nuclei that were further apart (Threshold(0, 3)) were removed, to create a mask of the areas of tumour cells. The mask was set as a region of interest (ROI) and measurements taken from the DAB image (mean intensity and standard deviation). A subset of tumours previously assigned expression scores by eye, were used to produce a scoring system for the automated analysis from their mean intensity (Table 2.8); all other tumours were assigned expression scores using this quantification. Assignment of expression scores was checked against the raw images with mask applied, and a manual expression score assigned if not representative. All images analysed were taken at 200x magnification.

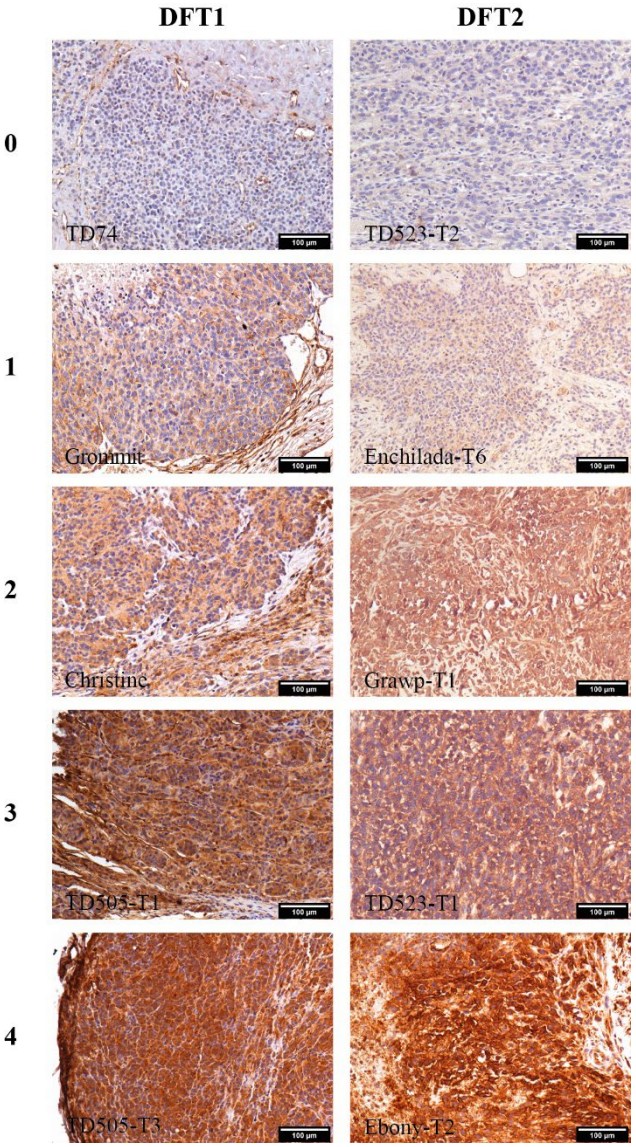

Figure 2.3 Expression scoring for MHC class I staining of tumour cells by IHC

Example images for expression scores, quantifying IHC staining, where 0 indicates no staining of tumour cells and 4 is very strong staining. Samples were stained for Tasmanian devil classical MHC class I (UABC_15-25-8). Images are taken at 200x magnification. Positive cells are stained brown and nuclei stained blue. Scale bars = 100 µm.

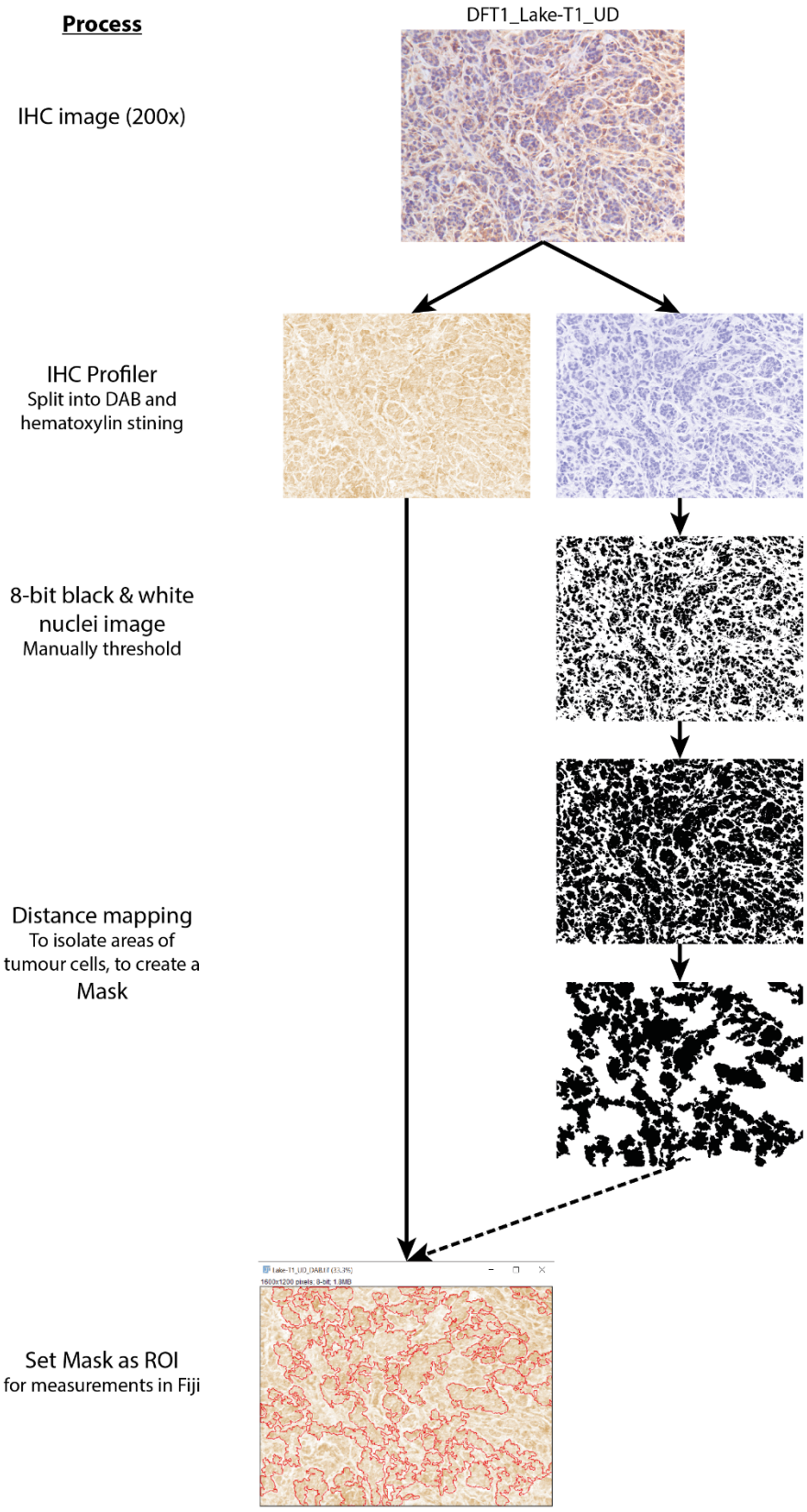

Figure 2.4 Processing pathway for IHC expression scoring

Table 2.8 IHC expression scores

Mean intensities, measured by Fiji, to assign expression scores to DFT samples stained by IHC. Expression scores were used to quantify strength of staining of tumour cells for MHC class I and IFNγ. '0' indicates no staining and 4 corresponds with very strong staining.

Expression Score	Mean Intensity
0	254.000 – 190.000
1	189.999 – 140.000
2	139.999 – 99.000
3	98.999 – 60.000
4	59.999 – 1.000

2.6 Host MHC class I genotyping

2.6.1 Amplification and addition of adaptors for Next Generation Sequencing (NGS)

For classical MHC class I genotyping of DFT hosts, classical MHC class I genes, *Saha-UA, -UB, and -UC*, were amplified by PCR. In total 31 samples were amplified: 12 DFT1 hosts, 17 DFT2 hosts, DFT1 cell line 4906, and DFT2 cell line RV, using the cell lines as controls. Primers Saha428 (F) and Saha429 (R) (listed in Table 2.4) were used to amplify classical MHC class I (exon 2-3); adapted from an established devil classical MHC class I primer set, Saha85 and Saha91 (Siddle et al., 2013), with the addition of Illumina adaptor sequences (forward adaptor sequence TCGTCGGCAGCGTCAGATGTGTATAAGAGACAG, reverse adaptor sequence GTCTCGTGGGCTCGGAGATGTGTATAAGAGACAG) for Next Generation Sequencing (NGS). PCR reagents are as listed in Table 2.5, with 250 ng of cDNA per sample, and PCR conditions are detailed in Table 2.9. Two PCR reactions were pooled for each sample to make one replicate for NGS library preparation (Section 2.6.2). 5µl PCR reaction for each replicate was analysed on an agarose gel (detailed in Section 2.3.4) to confirm gene amplification before sequencing.

Table 2.9 PCR amplification conditions for Illumina sequencing

Cycle Element	Temperature (°C)	Time (s)	Number of Cycles
Initial denaturation	98	30	1
Denaturation Annealing Elongation	98 60 72	10 30 30	28
Final Elongation	72	300	1

2.6.2 Library Preparation

Following PCR amplification and addition of Illumina adaptors (detailed in Section 2.6.1 above), two PCR reactions were pooled to make a single replicate. Three replicates were used for each sample; with 31 samples, this gave a total of 93 PCR amplicons for library preparation, which was performed by Nicola Pratt. (National Oceanography Centre, University of Southampton). 25 µl of PCR product was purified using AMPure XP beads and eluted in 50 µl 10 mM Tris (pH 8.5). A random selection of samples was analysed on an Agilent bioanalyzer to confirm presence of PCR product and removal of residual PCR primers and primer dimers. To add dual indices and Illumina sequencing adaptors to the PCR amplicons, an Index PCR was performed using 5 µl of cleaned up PCR amplicon, 25 µl NEBNext Ultra II Q5 PCR mastermix, Nextera XT Index kit (5 µl each Index primer), and 10 µl dH_2O (see Table 2.10 for Index PCR conditions). Index PCR products were cleaned up using AMPure XP beads, eluted in 25 µl 10 mM Tris (pH 8.5) and a selection of samples analysed on Agilent bioanalyzer to validate the libraries.

Table 2.10 Index PCR conditions

Cycle Element	Temperature (°C)	Time (s)	Number of Cycles
Initial denaturation	95	180	1
Denaturation Annealing Elongation	95 55 72	30 30 30	8
Final Elongation	72	300	1

The concentration of Index PCR products was quantified using a Qubit fluorometer and the concentration normalised across samples by diluting to 4 nM using 10 mM Tris (pH 8.5). 5 µl of each sample, each with unique indices, was combined to pool the libraries for a single MiSeq run. Prior to sequencing, the pooled library is denatured using sodium hydroxide and heat. To denature the DNA into single strands, 5 µl of pooled library was combined with 5 µl of freshly diluted 0.2 N sodium hydroxide and incubated at room temperature for 5 min. The denatured DNA was diluted to 4 pM using cold Hybridisation Buffer, first adding 990 µl of Hybridisation Buffer (MiSeq Reagent Kit v3), then aliquoting 120 µl and further diluting in Hybridisation Buffer to a final volume of 600 µl. The diluted library is mixed with PhiX control (4 pM, denatured with 0.2 N sodium hydroxide), 570 µl and 30 µl respectively, and kept on ice until heat denaturation. The combined amplicon library and PhiX control are heat denatured immediately before loading onto the Illumina MiSeq; the sample was heated at 96 °C for 2 min, then kept on ice for 5 min.

2.6.3 Illumina NGS

NGS was performed by Nicola Pratt on an Illumina MiSeq. Following library preparation, directly after heat denaturation, 600 µl combined amplicon library was loaded onto a MiSeq v3 sequencing reagent cartridge. MHC class I amplicons, excluding Illumina adaptors, were 296 bp. The library was sequenced using 300 bp paired end reads. Sequences were de-multiplexed based on sample specific indices, and forward and reverse reads for each sample output as fastq files.

2.6.4 Data processing and analysis

Forward and reverse reads for each sample replicate were analysed separately using fastq files. Illumina adaptor sequences were removed and the reads trimmed for quality using Trimmomatic (Bolger et al., 2014) v.0.39 (phred 33, sliding window, minimum length 150 bp). Read quality before and after trimming was assessed using FastQC (Andrews, 2010) v.0.11.9. An index for alignment was created from MHC class I, SahaI*27 (Ensembl identifier: GQ411435.1) and reads were aligned (local) using Bowtie 2 (Langmead et al., 2019; Langmead and Salzberg, 2012) v.2.4.2. Resulting sam files were converted to bam files, sorted, and indexed using SAMtools (Danecek et al., 2021) v.1.16.1.

Dr Jane Gibson (University of Southampton) drafted a script for variant calling MHC class I alleles. The aligned and sorted reads were variant called using FreeBayes (Garrison and Marth, 2012) v. 1.3.6, calling a ploidy of 6 (assuming 3 genes for classical MHC class I) across the whole 300 bp haplotype. Haplotypes were compared to a list of known Tasmanian devil classical MHC class I allele nucleotide sequences (Caldwell and Siddle, 2017) in FreeBayes, and the called alleles and read numbers for each replicate collated into an output file. NGS processing and data analysis is summarised in Figure 2.5.

Alleles called by FreeBayes were recorded in an Excel file for comparison between replicates. Where the alleles called for one replicate did not match the other two, the discordant replicate was discarded. Where the alleles called did not match across all replicates, the sample was discarded. Reverse reads called fewer alleles than the forward reads, as reverse reads did not always reach the variable region and more reads were lost through trimming due to lower quality; therefore forward reads were used for host genotype analysis. Scripts are available at https://doi.org/10.5258/SOTON/D3092

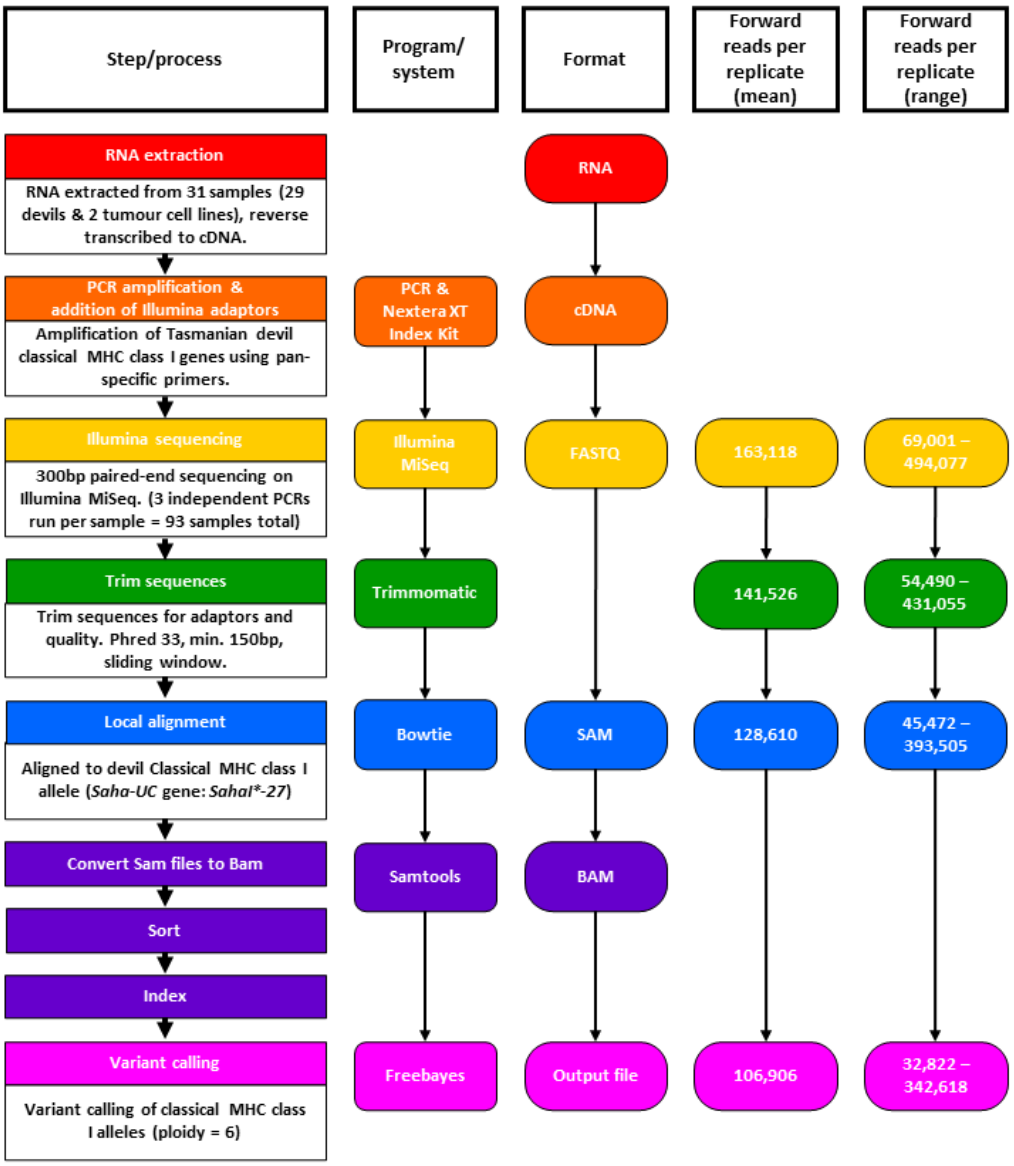

Figure 2.5 Flow diagram summarising NGS processing and data analysis for Tasmanian devil MHC class I genotyping.

Chapter 3 Investigation of classical MHC class I expression in DFT2

3.1 Introduction

Transmissible cancers transmit between individuals as allografts, therefore should be recognised by the host immune system due to disparate classical MHC class I molecules between tumour and host. DTF2 expresses classical MHC class I (Caldwell et al., 2018), which has the potential to elicit a host T cell response. Little is known about the host immune response to DFT2, but a study by Caldwell et al. (2018) found a small number of tumours are negative for CD3+ cells, despite expressing classical MHC class I, while others have low levels of infiltrating CD3+ cells.

Six DFT2 tumours were previously stained for classical MHC class I expression (Caldwell et al., 2018); some still had strong expression of classical MHC class I, while a few tumours had lower expression levels, suggesting MHC class I expression had been downregulated in these tumours. As downregulation or loss of MHC class I expression is a common immune evasion mechanism by cancer cells, and disparate classical MHC class I molecules expressed by DFT2 should elicit host immune responses, we predict a strong selective pressure for downregulation of MHC class I by DFT2. Therefore, it is hypothesised that as DFT2 continues to spread through the population, it will encounter hosts with different classical MHC class I genotypes, resulting in host immune responses against mismatched DFT2 alleles, creating selective pressure for classical MHC class I loss by DFT2.

To investigate classical MHC class I loss by DFT2 cells, classical MHC class I expression needs to be assessed in DFT2 tumours from across the timespan since emergence and the geographic range of this cancer. Thirty-four DFT2 tumour biopsies, collected between 2014 (close to the emergence of DFT2) and 2020, were stained by IHC, using a devil-specific classical MHC class I antibody, UABC, generated in our lab (Caldwell et al., 2018). Expression scores were assigned using novel semi-automated image processing developed during this project, to quantify staining for analysis.

The biopsies were also stained for CD3 (a T cell marker) and IFN-γ (an inflammatory cytokine) to assess the host immune response against the tumours. The anti-CD3 antibody has been used previously (Caldwell, 2018; Caldwell et al., 2018) and a devil-specific anti-IFN-γ antibody had been generated and screened in our lab (Caldwell, 2018). The anti-IFN-γ antibody was validated by Western blot and IHC, using formalin-fixed paraffin-embedded cell lines. Immune activation and

infiltration in the tumours was compared to MHC class I expression scores and host-tumour mismatch data, to assess the role of MHC class I expression in immune evasion by DFTs.

3.1.1 Aims and objectives

This chapter addresses Hypothesis 1, "DFT2 is losing MHC class I expression during progression through the devil population" (see Chapter 1 – Section 1.5):

> Aim 1: Investigate whether classical MHC class I expression is being lost in primary DFT2 tumours.
>
> Aim 2: Examine whether there is an immune response against tumours that express classical MHC class I.

The objectives of this chapter are:

1. Stain a range of DFT2 tumour biopsies by IHC using devil-specific classical MHC class I antibodies.
2. Investigate whether there is a loss of MHC class I over time in DFT2.
3. Validate a devil specific anti-IFNγ antibody for use by IHC.
4. Stain DFT2 tumours by IHC for immune markers (CD3 and IFNγ)

3.2 Classical MHC class I expression is highly variable in DFT2 tumours.

To investigate changes in classical MHC class I expression by DFT2, 34 tumour biopsies collected from 22 individuals (supplied by Dr Rodrigo Hamede, University of Tasmania and Prof Elizabeth Murchison, University of Cambridge) were stained by IHC for classical MHC class I (Saha-UA, -UB, and -UC) using an antibody previously generated in our lab, UABC (α-UABC_15-25-8) (Caldwell et al., 2018). Tumours stained for classical MHC class I were collected between June 2015 – May 2020 from the d'Entrecasteaux peninsula (shown in Figure 1.8). Some tumour sections were stained by master's students, Ella Milne and Neve Prowting, under my supervision. For analysis, six DFT2 tumour biopsies stained by Dr Alison Caldwell in our lab (Caldwell et al., 2018) were included, collected between March 2014 – June 2015.

Images were taken at 200x magnification and processed using Image J and Fiji to assign expression scores for quantification. Expression scores were calculated based on the strength of staining of DFT2 cells (see Section 2.5.2 for details), using a semi-automated image analysis pipeline, developed with Jacob Trend (University of Southampton). IHC images were separated into DAB and nuclei staining, with a mask for tumour cells created from the nuclei image using

distance mapping. The mask was then applied to the DAB image as a region of interest to measure the staining intensity in tumour cells. Example images for each expression score are shown in Figure 3.1.

To assess DFT2 classical MHC class I expression over time, expression scores for tumour biopsies were plotted against the date of capture (Figure 3.1). This shows classical MHC class I expression by DFT2 is highly variable, with some tumours expressing low levels (0 and 1) and some expressing high levels (3 and 4). At later time points (2017 onwards), the majority of tumours (23 out of 27) have an expression score of 1 or 2; though there are not enough samples at earlier time points to determine conclusively whether there has been a decrease in the number of tumours expressing high levels of classical MHC class I.

Looking at expression scores across all DFT2 tumours (Figure 3.2), most tumours express lower levels of classical MHC class I, with 19 tumours (55.9%) assigned an expression score of 1, and eight tumours (23.5%) an expression score of 2. Few DFT2 tumours have high expression, at 11.8% (4 tumours) and 2.9% (1 tumour) for 3 and 4 expression scores respectively. Interestingly, only two tumours (5.9%) lacked classical MHC class I expression, indicating few DFT2 tumours have total loss of classical MHC class I.

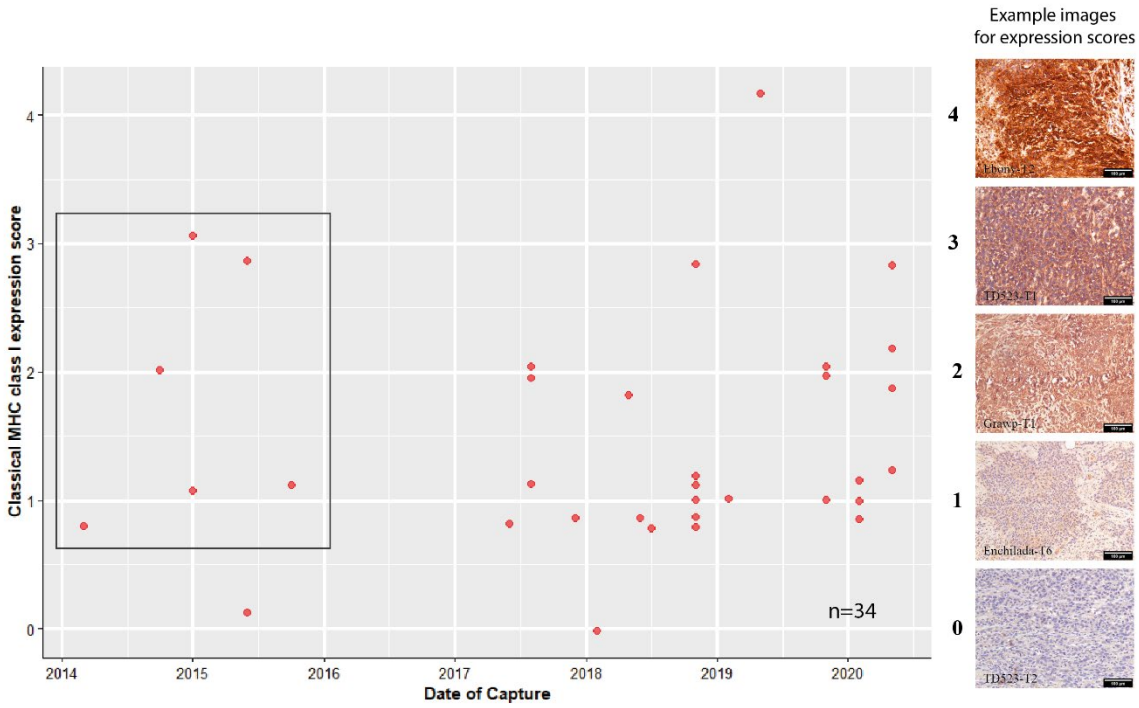

Figure 3.1 Classical MHC class I expression by DFT2 tumours is highly variable.

Classical MHC class I expression in DFT2 tumour biopsies over time (n=34) collected from 22 individuals. Classical MHC class I expression scores, based on the strength of IHC staining for Saha-UA, -UB, and -UC, are plotted against the sample collection date

(Date of Capture). Samples within the black box were presented in Caldwell et al. (2018). 0 = no staining for classical MHC class I, 4 = very strong staining. Expression scores are discrete variables – jitter has been applied to the data points for visualisation. Example images for expression scores are shown to the right of the graph. IHC images were taken at 200x magnification. Positive cells are stained brown; nuclei are stained blue. Scale bars = 100 μm.

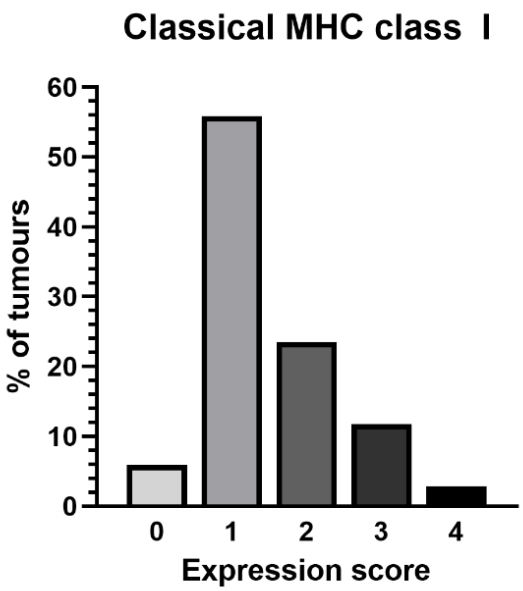

Figure 3.2 Few DFT2 tumours have complete loss of classical MHC class I expression.

Percentage of DFT2 tumours (n=34) assigned each expression score for classical MHC class I staining by IHC. 0 = no staining, 4 = strong staining.

3.2.1 Classical MHC class I expression by DFT2 tumours varies within an individual.

It is important to note that some of the tumours analysed come from the same devil. It is not known whether these tumours originate from different bites or metastasis of a primary tumour. Hosts with multiple tumours are highlighted in Figure 3.3A (n=7). Most tumours within the same host varied for classical MHC class I expression, but only by an expression score of 1. However, there were two devils with greater variation between their tumours. TD523, captured in June 2015, has two tumour biopsies, with expression scores of 0 and 3. While Enchilada from November 2018, a devil with a high tumour load (14 tumours counted during sample collection),

has six tumour biopsies stained; five of these samples had the same expression score, 1, and only one tumour varied, with an expression score of 3.

As multiple tumours from the same host have similar classical MHC class I expression scores, these samples may skew the data slightly, particularly Enchilada with five tumours assigned an expression score of 1. However, even when excluding these tumours, expression is still highly variable. In addition, from the data we can see that classical MHC class I expression is not necessarily the same between tumours taken from the same individual, therefore these samples are relevant to the analysis of classical MHC class I expression in DFT2.

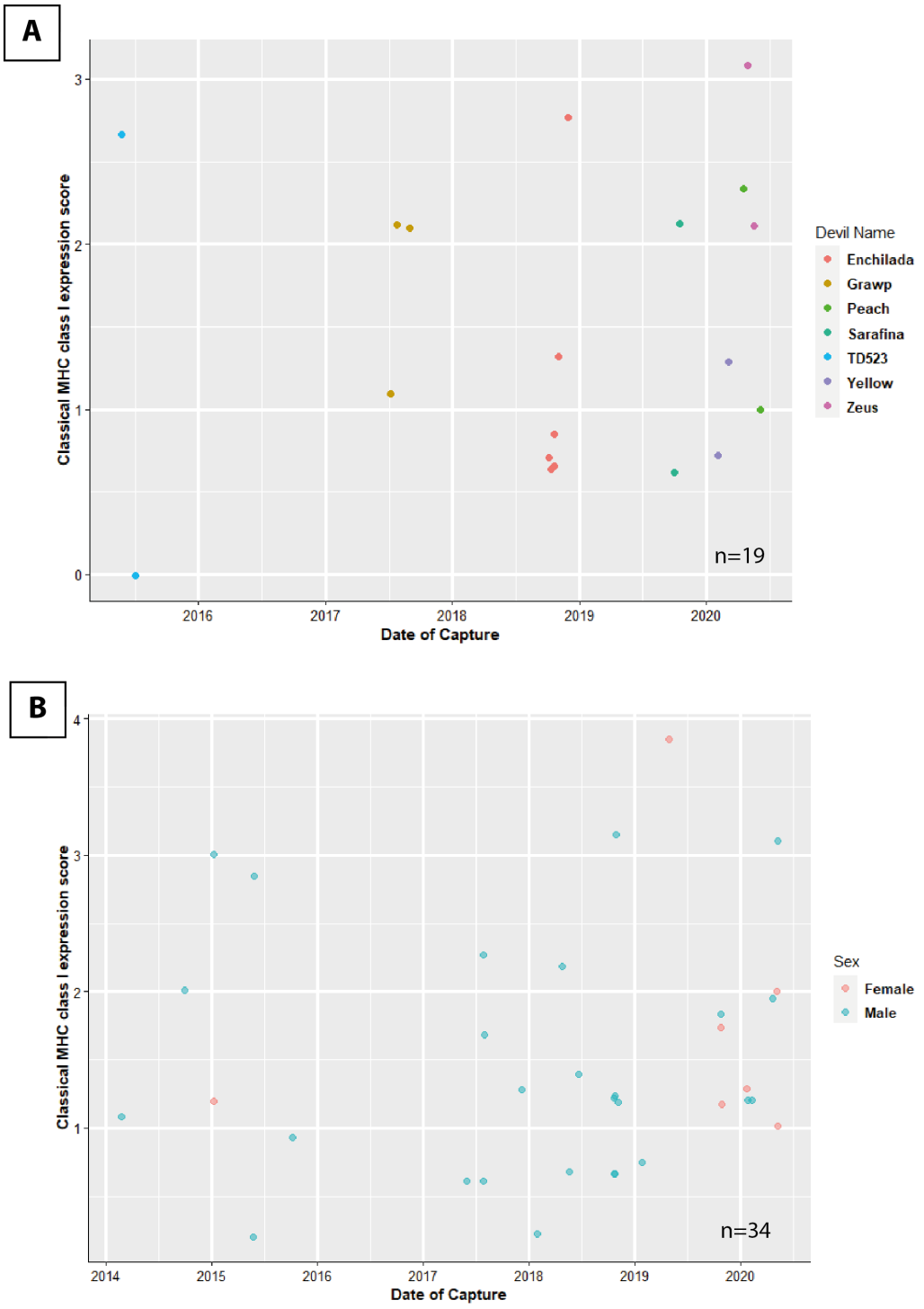

Figure 3.3 Classical MHC class I expression in DFT2 tumours varies within individuals.

Classical MHC class I expression in DFT2 tumour biopsies over time, showing **(A)** for samples (n=19) collected from the same host (n=7), and **(B)** sex of the host (tumours n=34, individuals n=22). Classical MHC class I expression scores, based on the strength of IHC staining for Saha-UA, -UB, and -UC, are plotted against the sample collection date (Date of Capture). 0 = no staining for classical MHC class I, 4 = very

strong staining. Expression scores are discrete variables – jitter has been applied to the data points for visualisation.

3.2.2 Sex of DFT2 hosts does not affect classical MHC class I expression by DFT2 tumours.

A factor of interest for studying classical MHC class I expression in DFT2 is sex of the host. As DFT2 originated in a male devil, the Y chromosome is expected to be immunogenic to female devils (Stammnitz et al., 2023, 2018); therefore, there may be reduced classical MHC class I expression by DFT2 in female hosts. The sex of DFT2 hosts is highlighted in Figure 3.3B.

There is no significant difference between classical MHC class I expression in male and female hosts (Wilcoxon rank sum test; t=0.636) (Appendix Figure B 1A), though there are not enough samples from female devils to make an effective comparison (female n=7 tumours, from n=5 individuals; male, n=27 tumours, from n=17 individuals). A significance level of $p<0.05$ was used for all statistical tests. However, it is interesting that of the samples analysed, there was only one sample collected from a female devil before May 2019, which had low classical MHC class I expression. While between May 2019 and May 2020, four female devils with DFT2 (with six tumours total) were captured (Figure 3.3B).

Classical MHC class I expression by DFT2 tumours was also assessed compared to other host factors (age and tumour load), as well as secondary infection, season, and tumour location (Appendix Figure B 1). Increase in age (shown in by Pye et al. (2018)) and host tumour load, the presence of secondary infection, and the season (as DFT1 transmission was more frequent during mating season in February-March (Hamede et al., 2008), which is late Summer and early Autumn in Tasmania) could all affect the ability of the host to produce an immune response against DFT2 tumours, thus higher MHC class I expression in these tumours would be predicted. Location of the tumours on the face could also affect the infiltration of immune cells, for example, whether they infect cutaneous (skin) or mucosal (mouth) tissue.

To investigate whether there was a significant difference in classical MHC class I expression by DFT2 tumours based on secondary infection, results were tested via Wilcoxon rank sum test (t=0.371), and age, season, and tumour location were assessed by Kruskal-Wallis rank sum test (t=0.556, t=0.147, and t=0.852, respectively). None of these factors were significant, though sample size likely limits assessment of the effect of secondary infection and tumour location. Host tumour load was tested for correlation with classical MHC class I expression using Spearman's rank correlation; no correlation was found (t=0.902).

3.3 Validation and classification of staining for immune markers

3.3.1 Validation of anti-IFNγ antibody

An antibody against devil IFNγ, α-IFNγ_13-44-6, was previously generated and tested by Alison Caldwell (Caldwell, 2018). Prior to application to additional samples by IHC, further validation of the antibody was carried out. The antibody was tested against cell lysates by Western blot and FFPE cell lines by IHC, used for the first time in DFT cell lines.

Lysates for CHO_SahaIFNγ (a CHO cell line transfected to produce devil IFNγ) (Siddle et al., 2013), and untransfected CHO as a control, were analysed on a Western blot, stained with IFNγ_13-44-6 (Figure 3.4A) (performed by masters student Humaira Islam). There is a strong band at ~25 kDa for CHO_SahaIFNγ, close to the expected ~20 kDa. A small dot also appears at the same weight for CHO, however, this is unlikely to be from the cell line as it does not cover the entire lane.

FFPE cell lines, CHO_SahaIFNγ, CHO, DFT1 cell line 4906, and 4906_IFNγ (4906 treated with devil IFNγ) were stained using α-IFNγ_13-44-6 by IHC (Figure 3.4B). These cell lines were used to replicate the fixation of cells in primary biopsies. CHO was used as an untransfected control for CHO_SahaIFNγ, therefore is not expected to stain for IFNγ; however, both cell lines were stained by α-IFNγ_13-44-6. This may be due to cross contamination of the cell lines, which were cultured at the same time. 4906_IFNγ stained strongly for IFNγ, while 4906 only stained weakly, potentially due to low levels of IFNγ in the cell line or weak non-specific staining. The increase in staining between 4906 and 4906_IFNγ is presumably due to binding of 4906_IFNγ cells to IFNγ, though antibody binding to other cytokines induced by IFNγ treatment cannot be ruled out.

These results, combined with previous antibody-blocking experiments (Caldwell, 2018), support the use of anti-IFNγ antibody, α-IFNγ_13-44-6 for staining of DFT samples for IFNγ by IHC. IHC staining of DFT samples for IFNγ was assessed using the same expression scoring system as developed for MHC class I staining.

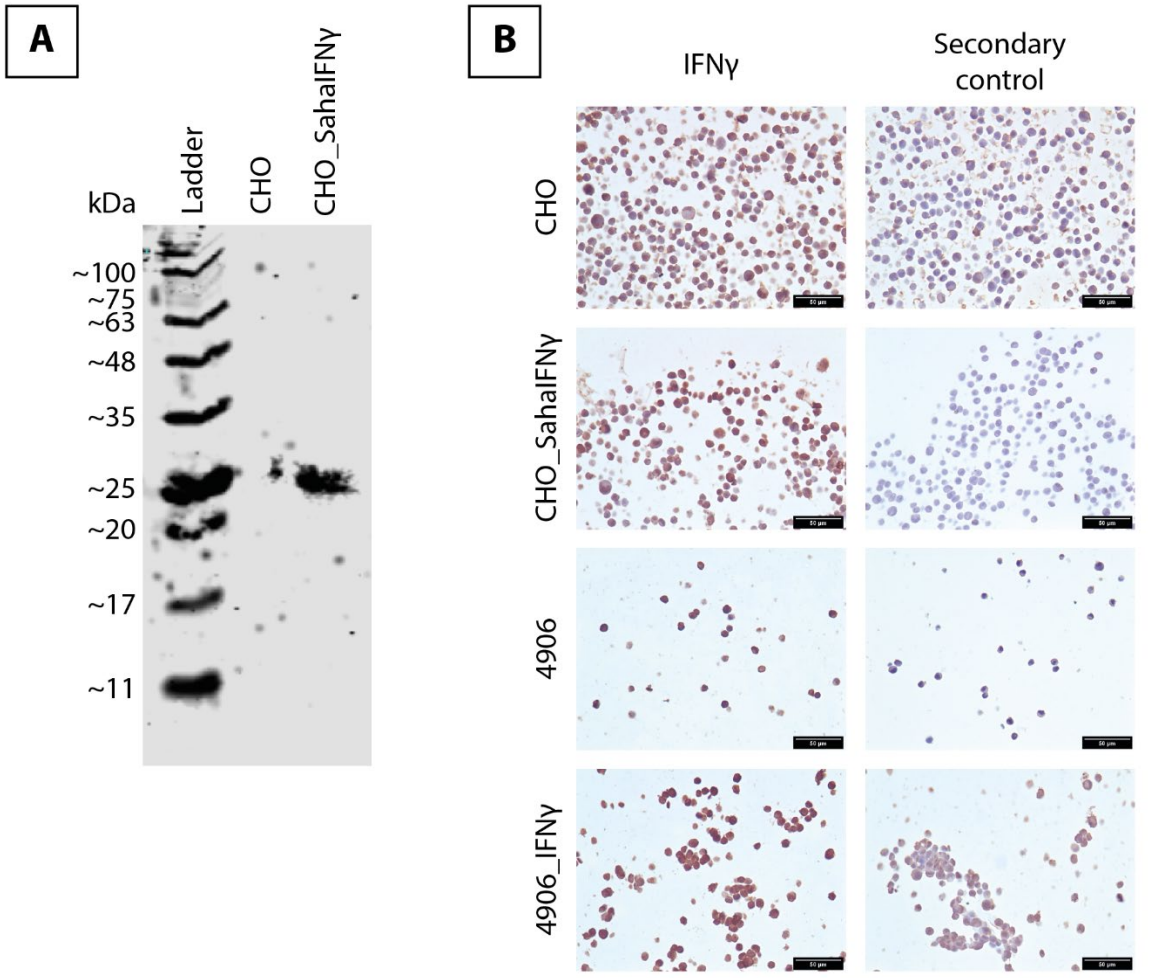

Figure 3.4 Validation of antibody against Tasmanian devil IFNγ

Anti-IFNγ antibody, α-IFNγ_13-44-6, generated by Dr Alison Caldwell (Caldwell, 2018) was validated by Western blot and IHC staining. **(A)** Western blot analysed with cell lysates; CHO_SahaIFNγ (CHO cell line transfected to produce devil IFNγ), and CHO (untransfected) as a control. **(B)** IHC images of formalin-fixed cell lines embedded in paraffin. CHO_SahaIFNγ (CHO cell line transfected to produce devil IFNγ), CHO (untransfected), 4906 (DFT1 cell line), and 4906_IFNγ (4906 treated with IFNγ). (**Left**) Cell lines stained with α-IFNγ_13-44-6, (**right**) control stained with secondary antibody only. Images were taken at 400× magnification. Positive cells are stained brown; nuclei are stained blue. Scale bars = 50 µm.

3.3.2 Classification of CD3 staining

To classify CD3 staining of tumours by IHC for analysis, a subjective scale was generated based on the number and density of CD3+ cells in the stroma and among tumour cells. Examples images of tumours in each classification are shown in Figure 3.5. Black arrows highlight examples of CD3+ cells within the area of interest.

The scale ranges from 'None' to 'Many', which was used to investigate immune activation in the tumour samples. No image is shown for 'Many' under tumour cells, as there were no DFT1 or DFT2 tumours that met this classification. This scale was created based on staining within DFT samples, therefore, while 'Many' is the highest classification, this does not indicate it is the highest CD3+ activation possible against a tumour.

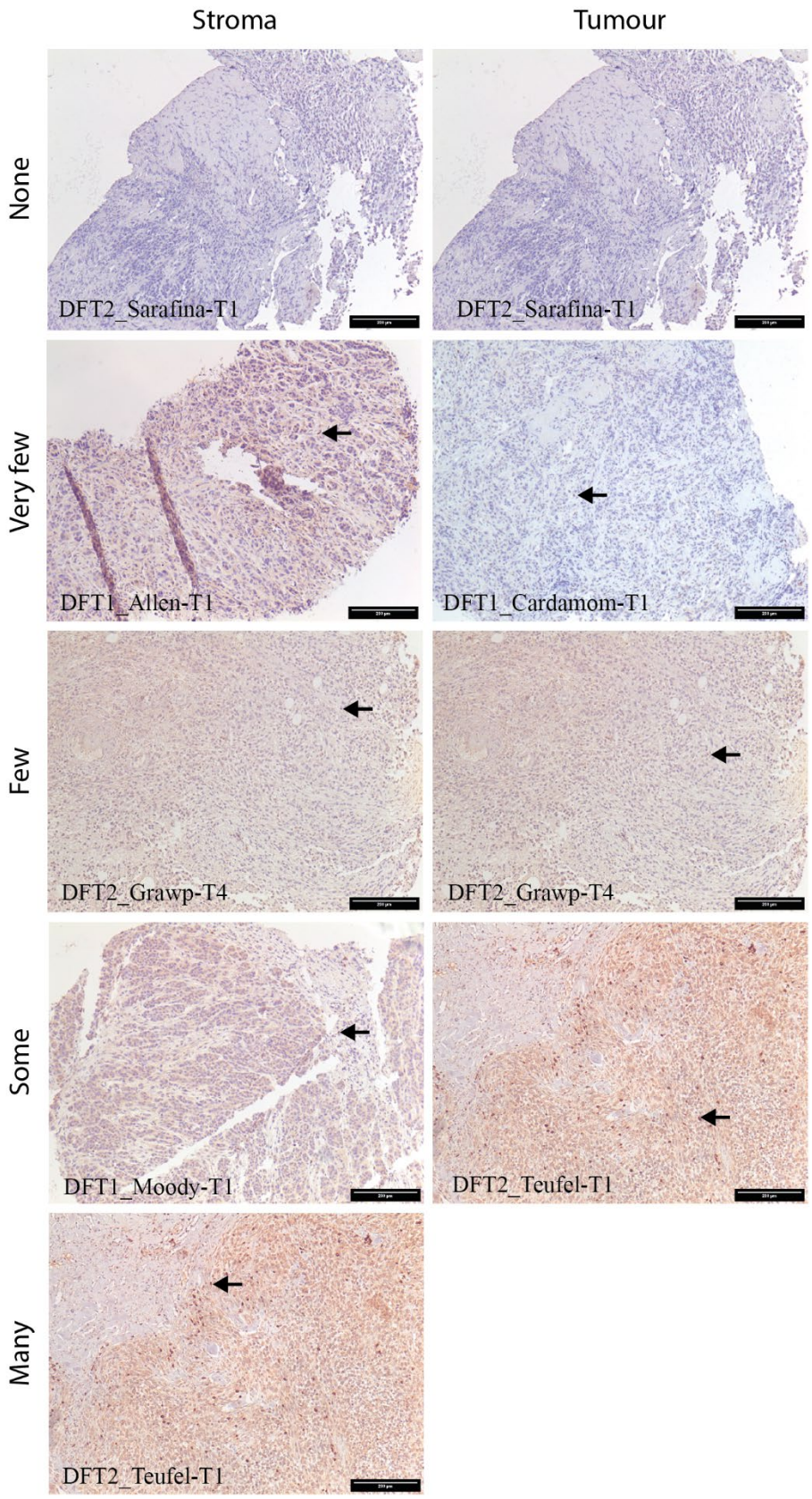

Figure 3.5 Classification of CD3 staining of DFTs by IHC

Example images of DFT samples stained for CD3 by IHC, assigned to a classification scale for analysis. Scale ranges from 'None' (no CD3+ cells) to 'Many' (the highest

level of CD3+ cells observed in the stained DFTs). Tumours were given two classifications based on the location of CD3+ cells in the biopsy, in the stroma and among tumour cells. No image is shown for 'Many' for 'Tumour' as there were no DFT samples within this category. Black arrows show examples of CD3+ cells. Images were taken at 100× magnification. Positive cells are stained brown; nuclei are stained blue. Scale bars = 200 μm.

3.4 There is little immune activation in DFT2 tumours.

To investigate immune activation against DFT2, of the 34 tumour biopsies stained for classical MHC class I (see Section 3.2), 25 were stained for IFNγ (α-IFNγ_13-44-6) (from 17 individuals) and 20 (from 15 individuals) were also stained for CD3. IFNγ is an inflammatory immune marker, while CD3 is a cellular marker of activated T cells. Some tumour sections were stained by master's students, Neve Prowting and Humaira Islam, under my supervision.

As shown in Figure 3.6A, most DFT2 tumours had IFNγ expression (88%). However, this expression is at a low level, with 64% assigned an expression score of 1, while only 20% and 4% were given scores of 2 and 3 respectively. Conversely, only 40% of DFT2 tumour samples had CD3+ cells (Figure 3.6B). Breaking this down by location of the CD3+ cells (Figure 3.6C), all samples with CD3+ cells (n=8) had these cells within the stroma, while only six had CD3+ cells infiltrating areas of tumour cells. Both stromal and tumour CD3+ cells were mostly categorised as 'Very few' or 'Few' Only two and one tumours (15% of all CD3 stained tumours) were classified as 'Some' and 'Many', respectively, for stromal CD3+ cells. While one tumour (5%) was classified as 'Some' for CD3+ cells within the tumour.

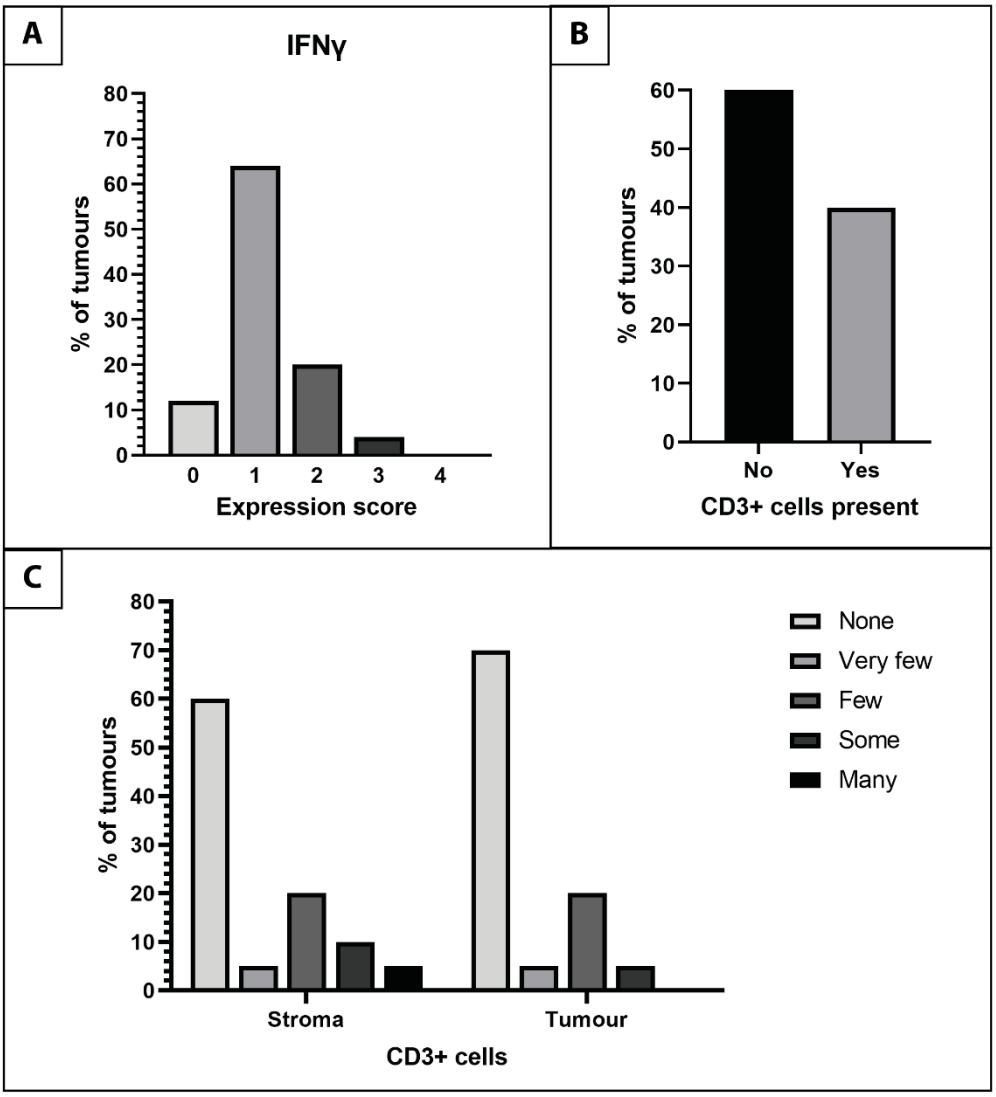

Figure 3.6 DFT2 tumours have limited immune activation.

Summary of immune markers for DFT2 tumours stained by IHC. **(A)** Percentage of DFT2 tumours (n=25) assigned each expression score for IFNγ staining by IHC. 0 = no IFNγ staining, 4 = strong IFNγ staining. **(B)** Percentage of DFT2 tumours (n=20) with CD3+ cells based on IHC staining. **(C)** Percentage of DFT2 tumours (n=20) for CD3+ cell classifications. Classifications were based on number and density of CD3+ cells in the stroma or among tumour cells.

3.4.1 IFNγ expression correlates with classical MHC class I expression by tumour cells.

To understand whether classical MHC class I expression by DFT2 tumours is antigenic in all hosts, a subsection of tumour biopsies were also stained by IHC for immune markers, IFNγ, an inflammatory cytokine, and CD3, a T cell marker. Staining for immune markers was compared to classical MHC class I expression scores (Figure 3.7). IFNγ staining was assigned expression scores, using the same method as classical MHC class I, and CD3 staining was categorised based on CD3+ cells.

No significant difference in classical MHC class I expression by DFT2 tumours was observed for the presence of CD3+ cells (Unpaired two-samples t-test; 0.325), CD3+ cells in the stroma (One-way ANOVA; t=0.594), or CD3+ cells within the tumour (Kruskal-Wallis rank sum test; t=0.0808); though sample size is a limiting factor for the CD3 categories. A significance level of $p<0.05$ was used for all statistical tests. However, IFNγ expression has a positive correlation with classical MHC class I expression by DFT2 tumour cells (Spearman's rank correlation: rho=0.435, t=0.0296, $p<0.05$). This indicates classical MHC class I expression is associated with an inflammatory tumour environment.

Release of inflammatory cytokines should trigger infiltration of immune cells, such as T cells. Therefore, IFNγ expression in DFT2 tumours was compared with presence of CD3+ cells (Figure 3.8). Infiltration by CD3+ cells was not associated with different IFNγ expression levels (Wilcoxon rank sum test; t=0.0911), regardless of whether CD3+ cells were stromal (One-way ANOVA; t=0.594) or among tumour cells (Kruskal-Wallis rank sum test; t=0.872); but, as previously mentioned, sample size is a limiting factor when assessing CD3+ cells.

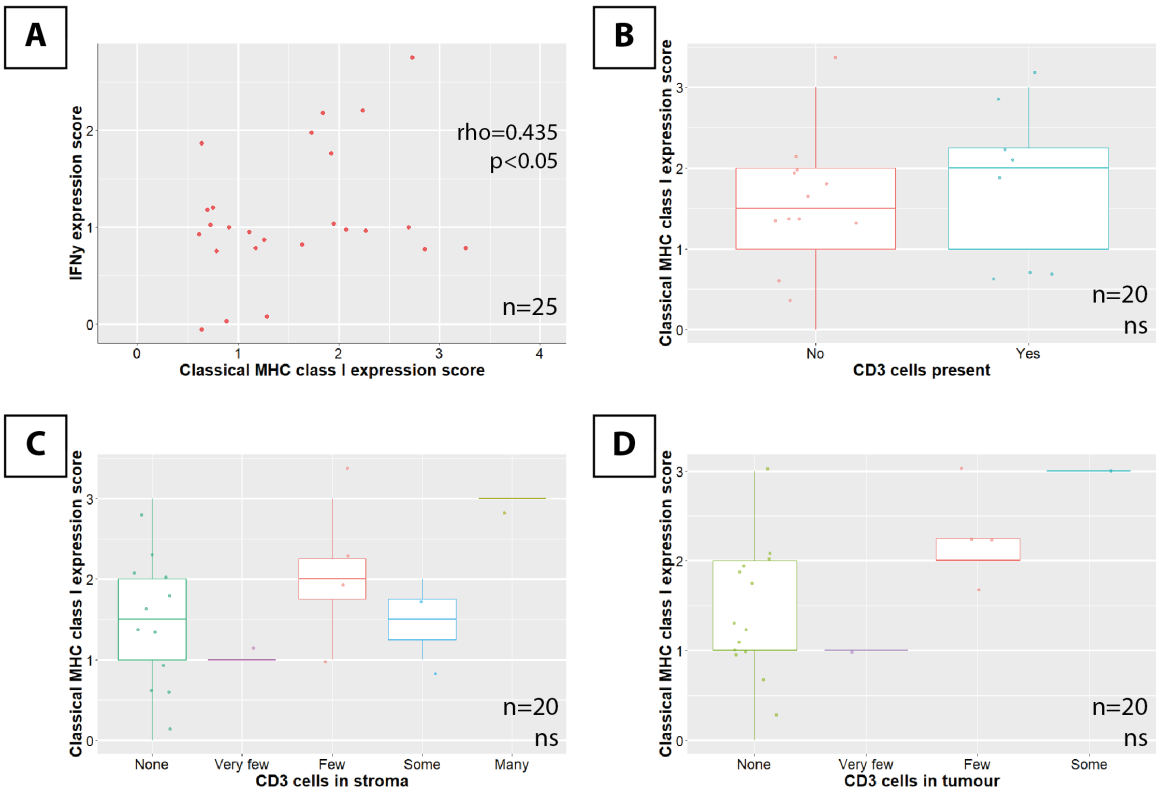

Figure 3.7 IFNγ expression correlates with classical MHC class I expression by DFT2 tumour cells.

Classical MHC class I expression in DFT2 tumour biopsies compared with **(A)** IFNγ expression scores (n=25), **(B)** presence of CD3+ cells (n=20), **(C)** CD3+ cells in the stroma (n=20), or **(D)** CD3+ cells among tumour cells (n=20). Expression scores are based on the strength of IHC staining; 0 = no staining, 4 = very strong staining. Expression scores are discrete variables – jitter has been applied to the data points for visualisation. There is a positive correlation between classical MHC class I and IFNγ expression scores (rho=0.435, t=0.0296, p<0.05). None of the CD3 classifications are significant for differences in classical MHC class I expression. 'ns' = not significant (p>0.05).

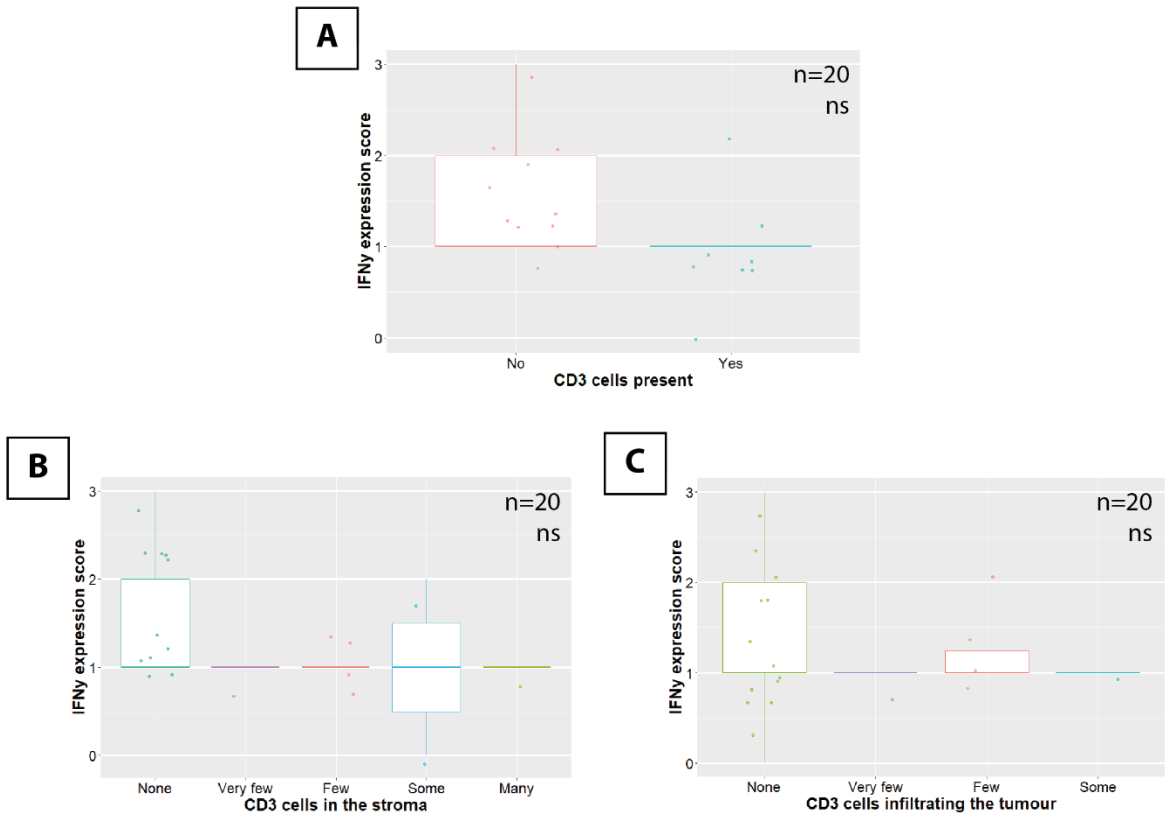

Figure 3.8 IFNγ expression does not correspond with infiltration of CD3+ cells.

IFNγ expression in DFT2 tumour biopsies by **(A)** presence of CD3+ cells (n=20), **(B)** CD3+ cells in the stroma (n=20), and **(C)** CD3+ cells among tumour cells (n=20). Expression scores are based on the strength of IHC staining; 0 = no staining for IFNγ, 4 = very strong staining. Expression scores are discrete variables – jitter has been applied to the data points for visualisation. There are no significant differences in IFNγ expression for the CD3 classifications. 'ns' = not significant ($p>0.05$).

3.4.2 IFNγ expression has little variation between DFT2 tumours in the same individual.

IFNγ expression in DFT2 tumours is highly variable (Figure 3.9A), as expected based on its positive correlation with classical MHC class I expression by DFT2 cells. Deviating from classical MHC class I expression slightly, there is very limited variation in IFNγ expression across tumours collected from the same individual (devils, n=6), shown in Figure 3.9B. All tumours within an individual had the same IFNγ expression score or only varied by a score of 1; except for Zeus, which had one tumour with an IFNγ expression score of 1 and the other a score of 3. Enchilada is interesting as it had one tumour with no IFNγ expression, while the other four stained positively, though expression was weak (expression score of 1).

As previously mentioned (Section 3.2.2), several host factors (sex, age, and tumour load), along with season, secondary infection of the tumour, and tumour location, could alter the immune response against DFT2. To investigate the effect of these factors on the inflammatory environment of DFT2 tumours, they were compared to IFNγ expression scores (see Appendix Figure B 2).

There was no significant difference in IFNγ expression scores for sex or secondary infection (Wilcoxon rank sum test; t=0.301 and t=0.137 respectively), season (One-way ANOVA; t=0.626), age or tumour location (Kruskal-Wallis rank sum test; t=0.476 and t=0.125), and there is no correlation between IFNγ expression and host tumour load (Spearman's rank correlation; t=0.430). A significance level of $p<0.05$ was used for all statistical tests.

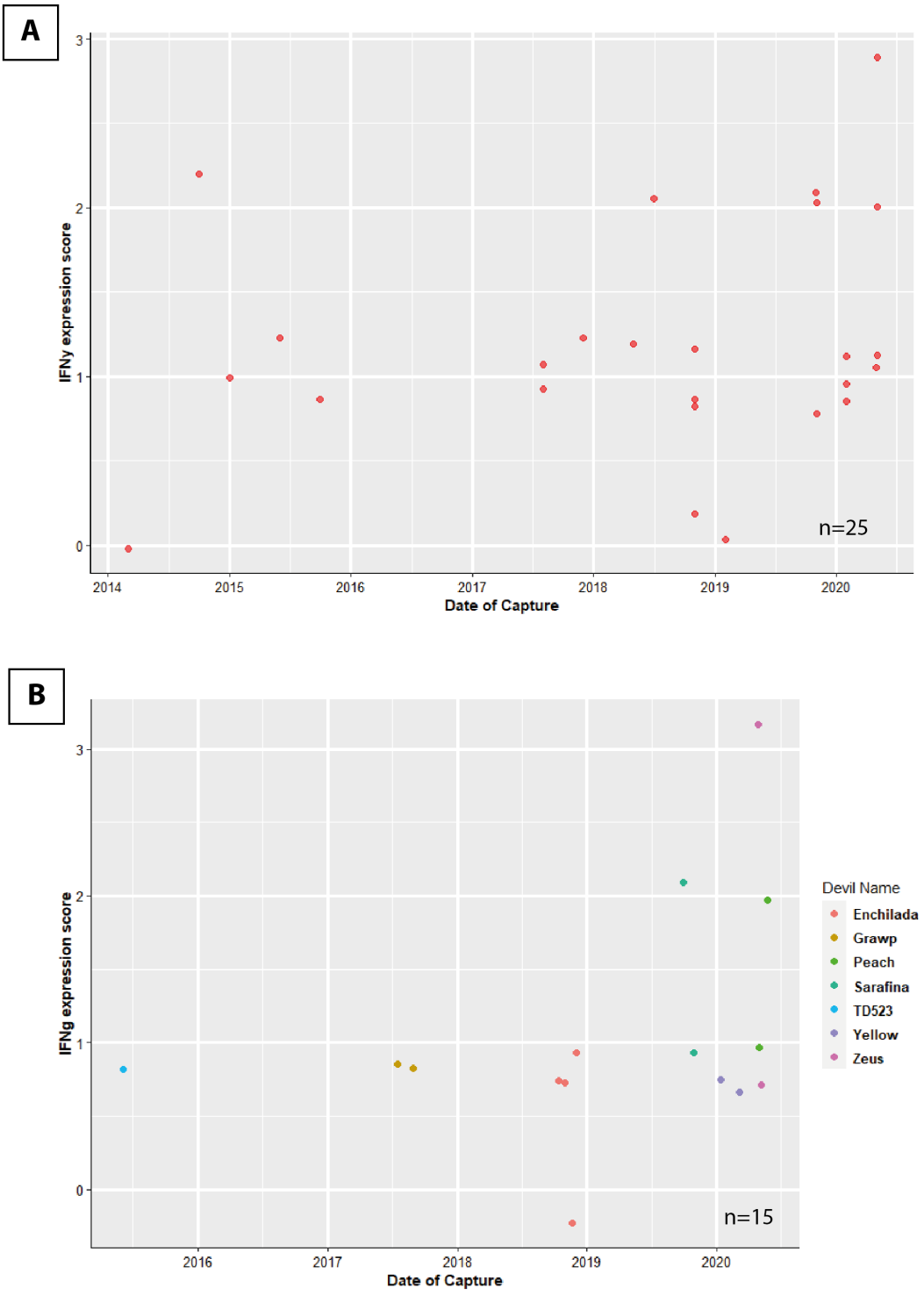

Figure 3.9 IFNγ expression in DFT2 tumours has little variation within an individual.

IFNγ expression in DFT2 tumour biopsies over time, plotted against the sample collection date. Showing **(A)** all stained DFT2 tumours (n=25), and **(B)** highlighting multiple tumours that came from the same host (n=15 tumours from n=7 individuals). Expression scores are based on the strength of IHC staining. 0 = no staining for IFNγ, 4 = very strong staining. Expression scores are discrete variables – jitter has been applied to the data points for visualisation.

3.5 Discussion

To investigate classical MHC class I expression by DFT2, 28 tumour biopsies (collected between June 2015 – May 2020) were stained by IHC. This significantly develops our understanding of classical MHC class I expression in DFT2 tumours, both in number and timeframe. Previous classical MHC class I staining for DFT2 covered six tumours from early in the emergence of DFT2 (March 2015 – October 2015) (Caldwell et al., 2018).

To quantify IHC staining, expression scores were assigned to each tumour based on the strength of staining using a novel semi-automated analysis pathway developed for this study. This is the first time IHC staining has been quantified for DFTs and enables the comparison of protein expression in FFPE samples between tumours and with factors, such as date of collection, age, and sex of the host.

Based on IHC expression scores, DFT2 tumours are variable for classical MHC class I expression and there is no observable correlation over time, which was expected from Hypothesis 1 - that DFT2 will lose MHC class I expression as it spreads through the population.

3.5.1 DFT2 may downregulate classical MHC class I to evade the host immune system.

In DFT2 tumours, IHC staining for classical MHC class I was highly variable. Some tumours have completely lost classical MHC class I expression, as expected from Hypothesis 1 (see Section 1.5.1), while others still show high expression. This variability over time suggests there is selective pressure for MHC class I loss in some tumours.

There may be a decrease in classical MHC class I expression over time, however, as shown in Figure 3.1, there are not enough samples from earlier years to draw firm conclusions. Regardless, the variation in classical MHC class I expression is of interest, as it expands our understanding of expression in DFT2 tumours and can be utilised to investigate the cause of classical MHC class I loss by DFT2 cells.

Most DFT2 tumours expressed low levels of classical MHC class I, with 55.9% assigned an expression score of 1 and 23.5% 2 (n=34), as illustrated in Figure 3.2. This fits with the hypothesis that DFT2 is losing classical MHC class I expression as it spreads through the devil population. Downregulation of classical MHC class I may be through downregulation of all alleles to reduce the chance of recognition by T cells, or downregulation of certain alleles that are more likely to be immunogenic (for example, due to low frequency in the population, or presentation of neoantigens). Only two tumours (5.9%) had complete classical MHC class I loss; indicating it may

be beneficial for the cancer to reduce the level of classical MHC class I on the cell surface, but not lose it completely. Selective downregulation is a known mechanism for immune evasion in cancer cells and virally infected cells (Dhatchinamoorthy et al., 2021; Taylor and Balko, 2022) and it has been shown that DFT1 downregulates MHC class I expression by overexpression of PRC2 (Burr et al., 2019). DFT2 lacks expression of embryonic ectoderm development (EED) protein, a component of PRC2 (Owen et al., 2021), therefore MHC class I expression is not modulated using the same mechanism as DFT1. However, DFT2 may be epigenetically modifying expression via different pathways, which is supported by variable expression of classical MHC class I in DFT2 tumours. By DFT2 preserving common classical MHC class I alleles, there would be fewer differences for T cells to detect on the DFT2 classical MHC class I, while preventing generation of an immune response against a total loss of MHC class I ('missing self') by NK cells.

Interestingly, classical MHC class I expression also varies between some tumours infecting the same devil (Figure 3.3A). While the variation is small in most individuals, some tumours vary by an expression score of 2. This indicates that classical MHC class I expression is not solely dependent on the current host. As DFT2 cells will have encountered multiple devils before their current host, it is possible that tumours that differ in expression were transmitted by different devils, though it is not known whether multiple tumours in the same devil originated from separate bites or metastasis of an established tumour. Alternatively, these tumours may be exposed to different immune pressures within their current host, such as tumour location. While no significant difference was found in classical MHC class I expression based on whether the tumour was mucosal or cutaneous (Appendix Figure B 1F), it could be that different locations on the head/body could affect immune recognition or infiltration. DFT2 has a higher proportion of tumours occurring on the body than DFT1, which mostly occurs on the face (James et al., 2019). The origin of tumours occurring on the body have not been confirmed, but they may be the result of direct transmission or have metastasised from tumours on the face. Sustained transmission of bodily tumours through the population is unlikely, therefore, metastasis of these tumours to the body may be more common than direct transmission. To metastasise, tumours will be exposed to different immune pressures as they move systemically and establish themselves in a new tissue. Therefore, their classical MHC class I and immune profiles would be expected to differ from primary tumours.

3.5.2 Host immune responses against DFT2 are limited.

As Tasmanian devils are capable of allorecognition and rejection of skin grafts (Kreiss et al., 2011), an immune response would be expected against DFT2 cells expressing classical MHC class I. Most tumours have IFNγ expression (88%; n=25), which indicates an inflammatory response from the

host. As IFNγ expression correlates with classical MHC class I expression by DFT2 tumour cells, this could indicate an immune response against DFT2 classical MHC class I. Alternatively, if DFT2 downregulation of classical MHC class I is epigenetic, as in DFT1 (Burr et al., 2019; Siddle et al., 2013), IFNγ expression may be upregulating classical MHC class I expression.

Most DFT2 tumours only had a low level of IFNγ expression, with an expression score of 1 (64%, n=25) (Figure 3.6A), this level may not be high enough to elicit an effective immune response. Low levels of IFNγ in the tumour microenvironment can be pro-tumorigenic, increasing metastatic potential of tumour cells and epithelial-to-mesenchymal transition (EMT) (Jorgovanovic et al., 2020). In an immune response against mismatched MHC class I, T cell responses are expected, however, IFNγ expression in DFT2 tumours does not result in infiltration by CD3+ cells (Figure 3.8). In addition, tumours that do have CD3+ cells (8 tumours, 40.0%) have low cell numbers, which rarely infiltrate areas of tumour cells, often restricted to the edge of tumour samples.

It is possible that as DFT2 spreads through the population it could be developing clonal lineages that evolve different immune evasion mechanisms. Phylogenetic analysis has shown that DFT1 has developed into multiple clades as it has spread through the population (Kwon et al., 2020; Stammnitz et al., 2023), and recently it has been discovered that early in the evolution of DFT2 it developed into two separate clades (Stammnitz et al., 2023). Therefore, it is possible that clonal evolution of DFT2 would develop subclones with different immune evasion mechanisms. Some clones may evade the host immune system by downregulating classical MHC class I expression. While clones with high classical MHC class I expression may employ other mechanisms to prevent immune responses against disparate classical MHC class I alleles.

3.5.3 Loss of Y chromosome may facilitate spread of DFT2 in female devils.

As DFT2 originated in a male devil (Pye et al., 2016b), the X chromosome is predicted to be immunogenic in female hosts, due to peptides presented by MHC class I. It has been observed that DFT2 has a bias towards infection of males, while DFT1 infection is equal across males and females (James et al., 2019; Kwon et al., 2018). Therefore, DFT2 tumours infecting female hosts are expected to have stronger pressures for downregulation of classical MHC class I than in males. Analysis of differences in classical MHC class I is limited due to number of samples from female devils (tumours in females = 7, tumours in males = 27). However, it is of note that from these samples there was only one tumour collected from a female devil before May 2019, and six tumours collected from four female devils between May 2019 – May 2020. This may be an artefact of our sample size, however, Stammnitz et al. (2018) found that a DFT2 tumour in a female host had lost its Y chromosome, and recently loss of the Y chromosome in DFT2 was traced

to an ancestor of clade B, occurring in 15 of 42 tumours analysed (Stammnitz et al., 2023). Therefore, this increase in DFT2 tumour samples from female devils from May 2019 may be linked to widespread loss of the Y chromosome by DFT2 or the increased spread of clade B, as the tumour cells will be less immunogenic to female hosts. In addition, the tumour from a female devil in January 2015 had a classical MHC class I expression score of 1, which may be due to immune recognition from this host.

3.5.4 Implications and future study

Understanding how DFT2 evades the host immune system is important for predicting disease spread, for the management of an endangered species, and for the design of therapeutic interventions, such as vaccines. As expected, some DFT2 tumours have lost classical MHC class I expression, which agrees with Hypothesis 1 - that DFT2 will lose MHC class I as it spreads through the population. However, few tumours have total loss of classical MHC class I, therefore low levels of classical MHC class I on the cell surface may be beneficial to DFT2 immune evasion.

To further understand immune evasion by DFT2, drivers of MHC class I loss, such as classical MHC class I mismatch between tumour and host, and mechanisms of MHC class I downregulation need to be investigated. Additionally, current DFT2 cell lines were established close to the emergence of DFT2 (see Table A 2). Therefore, these cell lines may not reflect the current mechanisms utilised by DFT2. Thus, the generation of new, low passage cell lines would be invaluable.

Chapter 4 Investigation of classical MHC class I expression in DFT1

4.1 Introduction

Downregulation of Major Histocompatibility Complex (MHC) molecules is often key to evasion of the immune system by tumours and viruses. As transmissible cancers transmit between individuals, they are under strong selective pressure from host immune systems to develop immune evasion mechanisms, to prevent recognition of disparate classical MHC class I alleles between tumour and host. In DFT1 the lack of an immune response is explained by a loss of classical MHC class I in tumour cells, through downregulation of components of the peptide presentation pathway; specifically, transporter associated with antigen processing (TAP) and β_2-microglobulin (β_2m) via PRC2 (Burr et al., 2019; Siddle et al., 2013).

Studies into epigenetic downregulation of MHC class I by DFT1 have largely been completed on cell lines, with only two tumour biopsies stained for classical MHC class I expression (Siddle et al., 2013). Additionally, as MHC class I expression is modulated epigenetically, upregulation of cell surface expression is possible via treatment with IFNγ or overexpression of NLRC5 (Siddle et al., 2013), and β_2m upregulation has been found in DFT1 cells originating from a regressing tumour (Pye et al., 2016a). Therefore, it is possible classical MHC class I expression varies in DFT1 tumours and expression needs to be investigated in a wider range of samples.

To investigate classical MHC class I expression *in vivo*, 76 DFT1 biopsies, from 2006 - 2022, were stained by IHC, using a devil-specific classical MHC class I antibody, UABC, generated in our lab (Caldwell et al., 2018). Expression scores were assigned using novel semi-automated image processing, to quantify staining for analysis. The biopsies were also stained for CD3 (a T cell marker) and IFN-γ (an inflammatory cytokine) to assess the host immune response against the tumours.

4.1.1 Aims and objectives

This chapter addresses Hypothesis 2, "DFT1 expresses non-classical MHC class I to evade the host immune response" (see Chapter 1 – Section 1.5):

> Aim 4: Determine whether loss of classical MHC class I expression is widespread in DFT1 tumours.

The objectives of this chapter are:

1. Stain a wider range of DFT1 tumour biopsies by IHC using devil-specific classical MHC class I antibodies.
2. Stain DFT1 tumours by IHC for immune markers (CD3 and IFNγ)

4.2 DFT1 tumours are not consistently negative for classical MHC class I expression.

Previously, two DFT1 tumour biopsies were stained for classical MHC class I expression by IHC, with both lacking expression (Siddle et al., 2013). However, it has been found that classical MHC class I expression can be upregulated in DFT1 cell lines by treatment with IFNγ or overexpression of NLRC5 (Ong et al., 2021; Siddle et al., 2013). Further, β_2m was found to be upregulated by DFT1 cells in fine needle aspirates from a tumour infecting a devil with an immune response against DFT1 (Pye et al., 2016a). To investigate whether total downregulation of classical MHC class I expression is widespread across DFT1 tumours, 76 tumour biopsies (supplied by Dr Rodrigo Hamede and Prof Gregory Woods, University of Tasmania), collected from 56 individuals between May 2006 – April 2022, were stained by IHC for classical MHC class I expression (Saha-UA, -UB, and -UC). Some tumour sections were stained by master's students, Ella Milne and Neve Prowting, under my supervision. It is important to note that three of these samples came from experimental tumours; two tumours, infecting Grommit and Tiarna (June and July 2010, respectively), developed in devils immunised with irradiated DFT1 cells, and the tumour infecting Christine (November 2008) was an induced tumour (A Kreiss 2022, personal communication). Expression scores were assigned based on strength of staining of tumour cells.

Unexpectedly, not all tumours were negative for classical MHC class I, challenging our understanding of how DFT1 tumours evade the host immune system. To assess expression over time, classical MHC class I expression scores were plotted against date of capture (Figure 4.1). Tumours expressing classical MHC class I are variable for expression scores. No correlation was

observed for classical MHC class I expression over time, however, there is a lack of samples from earlier dates.

It is important to note that many of the DFT1 hosts captured had multiple tumours. As a result, some of the biopsies stained were collected from the same host; these tumours are highlighted in Figure 4.2A (n=33 tumour samples, from n=14 individuals). Included in this figure are three biopsies taken from different depths in the same tumour (Savuti T1), though these are all negative for classical MHC class I expression. Many of these tumours have similar expression scores to each other, with either the same expression score or varying only by an expression score of 1. Two hosts are exceptions to this, Maui and Haloumi, whose tumours differed by an expression score of 2. Haloumi also had one negative tumour (expression score of 0) and one positive (expression score of 2). One devil, Orange, was captured twice (February 2020 and May 2020), with the same tumour sampled each time. Both tumours sampled had increases in their expression scores, by an expression score of 1. T1 increased from 0 to 1, and T2 increased from 1 to 2 (detailed sample information is available at https://doi.org/10.5258/SOTON/D3092). Therefore, it may be that classical MHC class I expression changes as the tumour grows and may correlate with tumour size.

The tumours with the highest classical MHC class I expression in 2015 were collected from two devils, TD505 and Crabtree, with expression scores of 3 and 4 (Figure 4.2A). As these are some of the highest expressing tumours across all DFT1 biopsies, this creates an 'artificial' peak in expression in 2015. However, this does not affect the distribution of classical MHC class I expression scores, shown in Figure 4.3. Classical MHC class I is not expressed in most DFT1 tumours (44.7%). Of the tumours that express classical MHC class I, 1 was the most common expression score (34.2% of all tumours), while only 7.9%, 9.2%, and 3.9% of tumours had expression scores of 2, 3, and 4 respectively.

Tolerance to DFT1 infection has been found in female, but not male, hosts (Margres et al., 2018; Ruiz-Aravena et al., 2018), therefore there may be differences in classical MHC class I expression in female hosts due to differing immune responses. To compare classical MHC class I expression in DFT1 tumours in female and male hosts over time, tumours from male (tumours n=21, individuals n=16) and female (tumours n=47, individuals n=32) hosts are highlighted in Figure 4.2B. However, there is no difference observed between expression scores in DFT1 tumours infecting male and female over time.

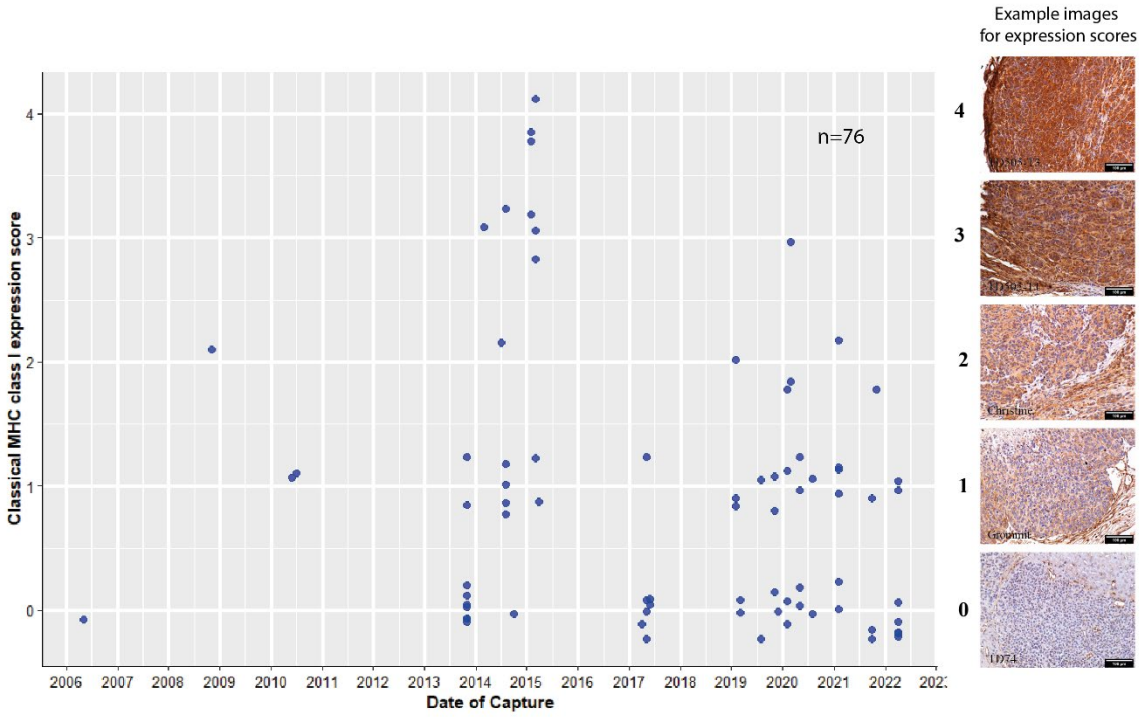

Figure 4.1 DFT1 tumours are not consistently negative for classical MHC class I expression.

Classical MHC class I expression in DFT1 tumour biopsies over time (n=76). Classical MHC class I expression scores, based on the strength of IHC staining for Saha-UA, -UB, and -UC, are plotted against the sample collection date (Date of Capture). 0 = no staining for classical MHC class I, 4 = very strong staining. Expression scores are discrete variables – jitter has been applied to the data points for visualisation. Example images for expression scores are shown to the right of the graph. IHC images were taken at 200x magnification. Positive cells are stained brown; nuclei are stained blue. Scale bars = 100 µm.

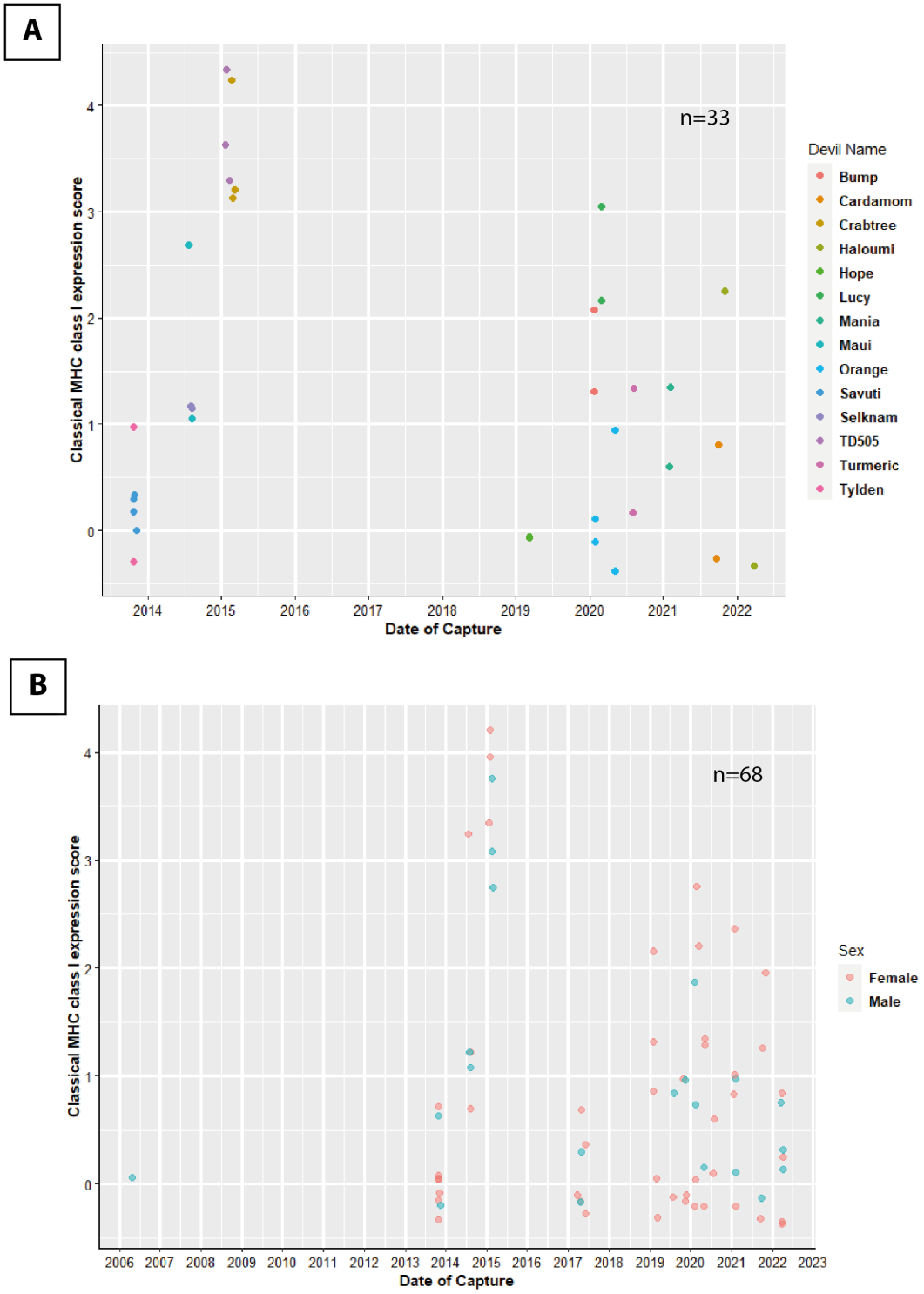

Figure 4.2 Multiple tumours in the same host have similar classical MHC class I expression.

Classical MHC class I expression in DFT1 tumour biopsies over time, showing **(A)** for samples collected from the same host (n=33), and **(B)** sex of the host (n=68). Classical MHC class I expression scores, based on the strength of IHC staining for Saha-UA, -UB, and -UC, are plotted against the sample collection date (Date of Capture). 0 = no

staining for classical MHC class I, 4 = very strong staining. Expression scores are discrete variables – jitter has been applied to the data points for visualisation.

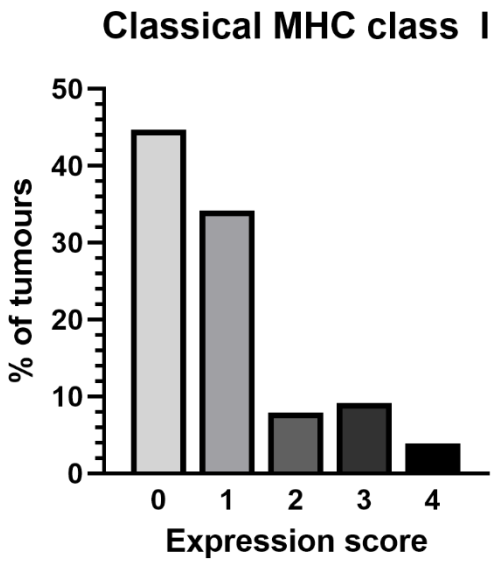

Figure 4.3 Most DFT1 tumours are negative for classical MHC class I expression.

Percentage of DFT1 tumours (n=76) assigned each expression score for classical MHC class I staining by IHC. 0 = no IFNγ staining, 4 = strong IFNγ staining.

4.2.1 Classical MHC class I expression by tumour cells does not vary by location.

As DFT1 has spread across most of Tasmania, there may be differences in classical MHC class I expression based on location; as different DFT1 clades have become dominant in different regions of Tasmania (Kwon et al., 2020). Variation of classical MHC class I expression in DFT1 tumours by location was investigated by assigning sample collection sites to broad areas of North-West (n=17 tumours, from n=11 individuals) and South-East (n=59 tumours, from n=45 individuals) (see Figure 4.4A). The South-East was further grouped into 'DFT2 Area' (n=5 tumours, from n=5 individuals), 'Channel' (n=51 tumours, from n=37 individuals), and North of Channel' (n=3 tumours, from n=3 individuals) (Figure 4.4A), to investigate whether there are any differences in classical MHC class I expression in the area where DFT2 is circulating. There was no significant difference in classical MHC class I expression by DFT1 (n=76) for either Broad Area (Wilcoxon rank sum test; t=0.820) or Area (Kruskal-Wallis rank sum test; t=0.713). A significance level of $p<0.05$ was used for all statistical tests.

Other factors were also investigated for effect on classical MHC class I by DFT1, sex of the host, age, host tumour load, season, secondary infection of the tumour, and tumour location (Appendix Figure C 1), as they could all influence the ability of the host to generate an immune response against DFT1 tumours. As expected from Figure 4.2B, there was no difference in classical MHC class I expression in DFT1 based on the sex of the host (Wilcoxon rank sum test; t=0.615). There was also no significant difference found for age (t=0.288), season (t=0.155), or tumour location (t=0.390) (Kruskal-Wallis rank sum test), or secondary infection (Wilcoxon rank sum test; t=0.783); and there was no correlation between classical MHC class I expression scores and tumour load (Spearman's rank correlation; t=0.902).

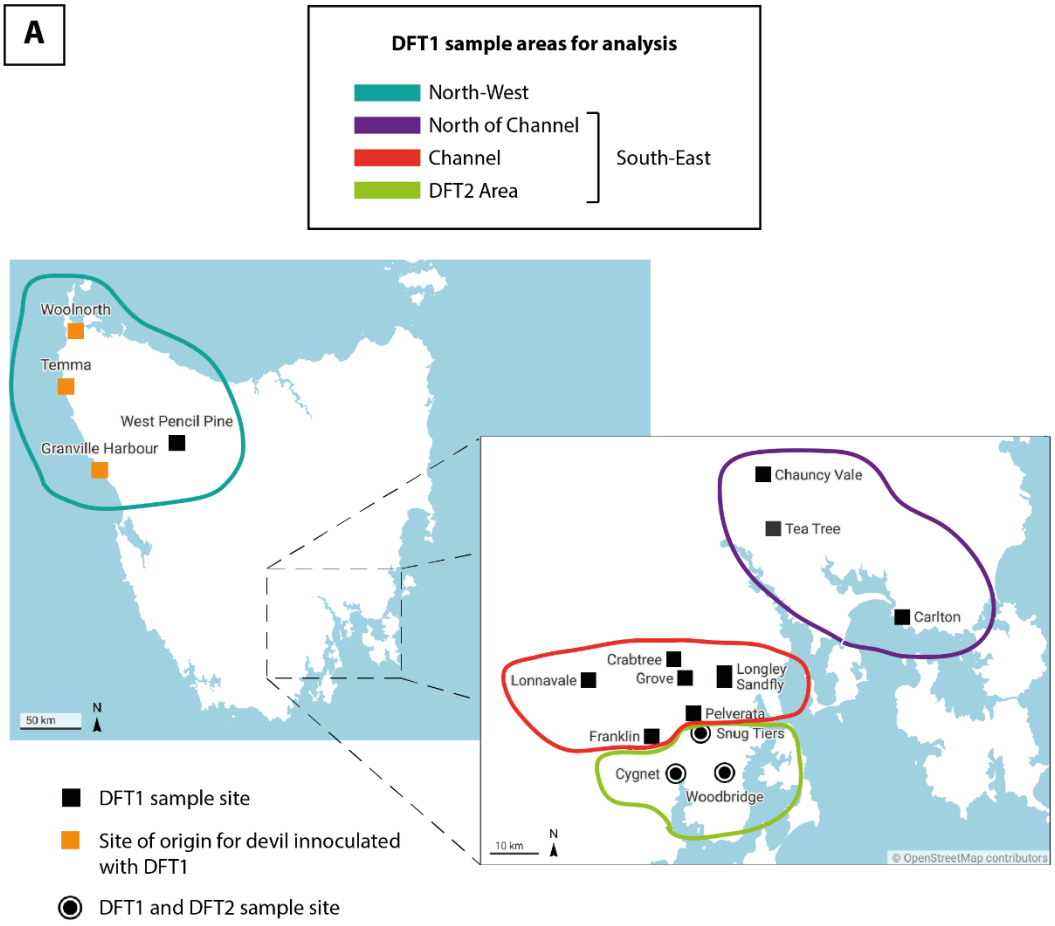

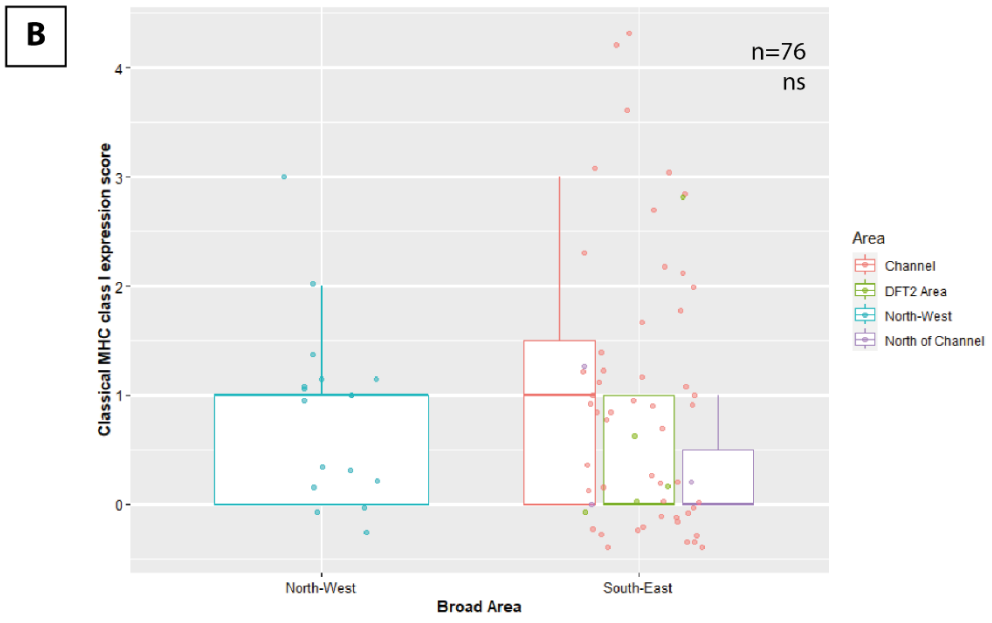

Figure 4.4 Classical MHC class I expression by DFT1 tumours does not vary by location.

Classical MHC class I expression by DFT1 tumours (n=76) based on the area of sample collection. **(A)** Map of Tasmania showing the sample sites included in the broad areas of North-West and South-East, for analysis. The South-East is broken down into

smaller areas, Channel, DFT2 Area (an area of the channel where DFT2 is circulating), and North of Channel. **(B)** Classical MHC class I expression is based on the strength of IHC staining for Saha-UA, -UB, and -UC. 0 = no staining for classical MHC class I, 4 = very strong staining. Expression scores are discrete variables – jitter has been applied to the data points for visualisation. There is no significant difference in classical MHC class I expression by Broad Area or Area. 'ns' = not significant ($p>0.05$).

4.2.2 DFT1 expression of periaxin is not consistently high.

Periaxin is used as a specific marker for DFT1 cells due to consistent high expression by DFT1 cells (Murchison et al., 2010). DFT1 tumour biopsies are routinely stained by IHC to confirm areas of DFT1 cells. However, staining of the 76 DFT1 tumour biopsies being studied for classical MHC class I expression found periaxin expression is highly variable in DFT1 tumours (example images shown in Figure 4.5). Some tumours strongly express periaxin as expected, but lower levels of expression were observed in some tumours, which is often variable through the tumour, and some are completely negative. Based on these findings, periaxin cannot be used to consistently identify DFT1 cells.

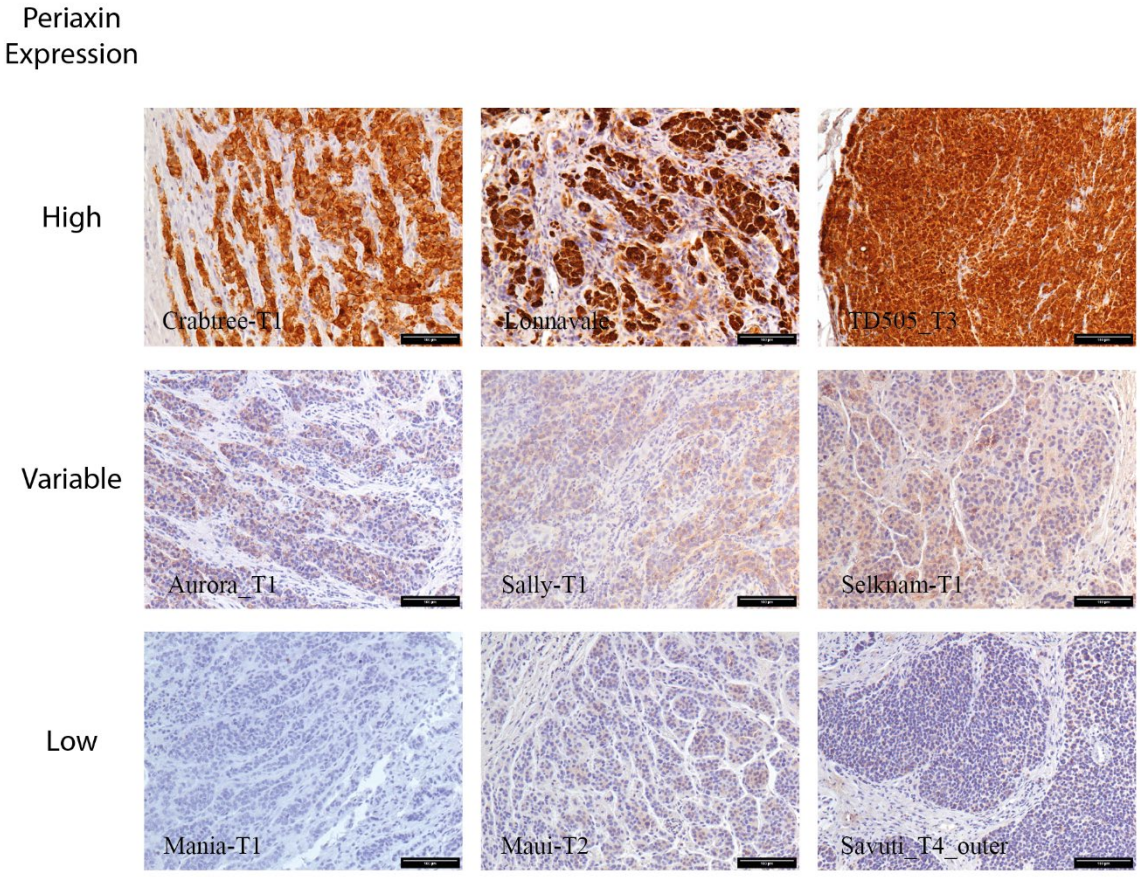

Figure 4.5 Periaxin expression by DFT1 is not consistent across tumours.

Example images of DFT1 tumour biopsies stained by IHC for Periaxin. Expression of periaxin, previously used as a strong marker for DFT1 cells, is highly variable in DFT1 tumours. Images were taken at 200× magnification. Positive cells are stained brown; nuclei are stained blue. Scale bars = 100 µm.

4.3 IFNγ expression correlates with classical MHC class I expression by DFT1 tumours.

To understand whether classical MHC class I expression by DFT1 cells is immunogenic, tumour biopsies were also stained for immune markers, IFNγ (n=51 tumours, from n=38 individuals), an inflammatory cytokine, and CD3 (n=42 tumours, from n=30 individuals), a cell surface marker for T cells. Some tumour sections were stained by master's student, Humaira Islam, under my supervision. IFNγ staining was quantified by assigning expression scores based on strength of staining, using the same method as for classical MHC class I staining. CD3 staining was classified based on number and density of CD3+ cells.

IFNγ expression and CD3 infiltration is present in DFT1 tumours (Figure 4.6). Most DFT1 tumours had IFNγ expression (84.3%), however, the level of expression in these tumours was low, as 51.0% of all tumours (26 tumours) were assigned an expression score of 1, and 27.5% of tumours (14 tumours) were assigned an expression score of 2. Many tumours had CD3+ cells present (42.9%, 18 tumours). All these tumours had CD3+ cells in the stroma, but only two tumours each were categorised as 'Some' and 'Many'. Only 14.3% (6 tumours) of DFT1 tumours stained had infiltration of CD3+ cells among tumour cells. None of these tumours were categorised as 'Some' or 'Many', with five tumours categorised as 'Very few' and one tumour as 'Few'.

We would expect immune responses from hosts to classical MHC class I expression by DFT1 cells. To investigate whether MHC class I expression by DFT1 correlates with immune activation in the tumour, expression scores were compared with IFNγ and CD3+ staining (Figure 4.7). A significance level of $p<0.05$ was used for all statistical tests. There was a strong correlation between IFNγ expression in DFT1 tumours and classical MHC class I expression by DFT1 tumour cells (Figure 4.7A; Spearman's rank correlation; rho=0.627, $t=8.68\text{x}10^{-7}$, $p<0.05$). However, there was no significant difference in classical MHC class I expression by DFT1 based on presence of CD3+ cells (Unpaired two-samples t-test; $t=0.325$), stromal CD3+ cells (One-way ANOVA; $t=0.594$), or CD3+ cells among tumour cells (Kruskal-Wallis rank sum test; $t=0.0808$); though analysis of CD3+ infiltration may be insufficient due to low missing values for higher CD3+ stromal and tumour classifications.

Investigating whether IFNγ expression corresponds with infiltration of CD3+ cells, IFNγ expression scores were compared to CD3+ classification (Figure 4.8). There was no significant difference for IFNγ expression by presence of CD3+ cells (Wilcoxon rank sum test; $t=0.0911$), stromal CD3+ cells (One-way ANOVA; $t=0.594$), or CD3+ cells in the tumour (Kruskal-Wallis rank sum test; $t=0.0872$).

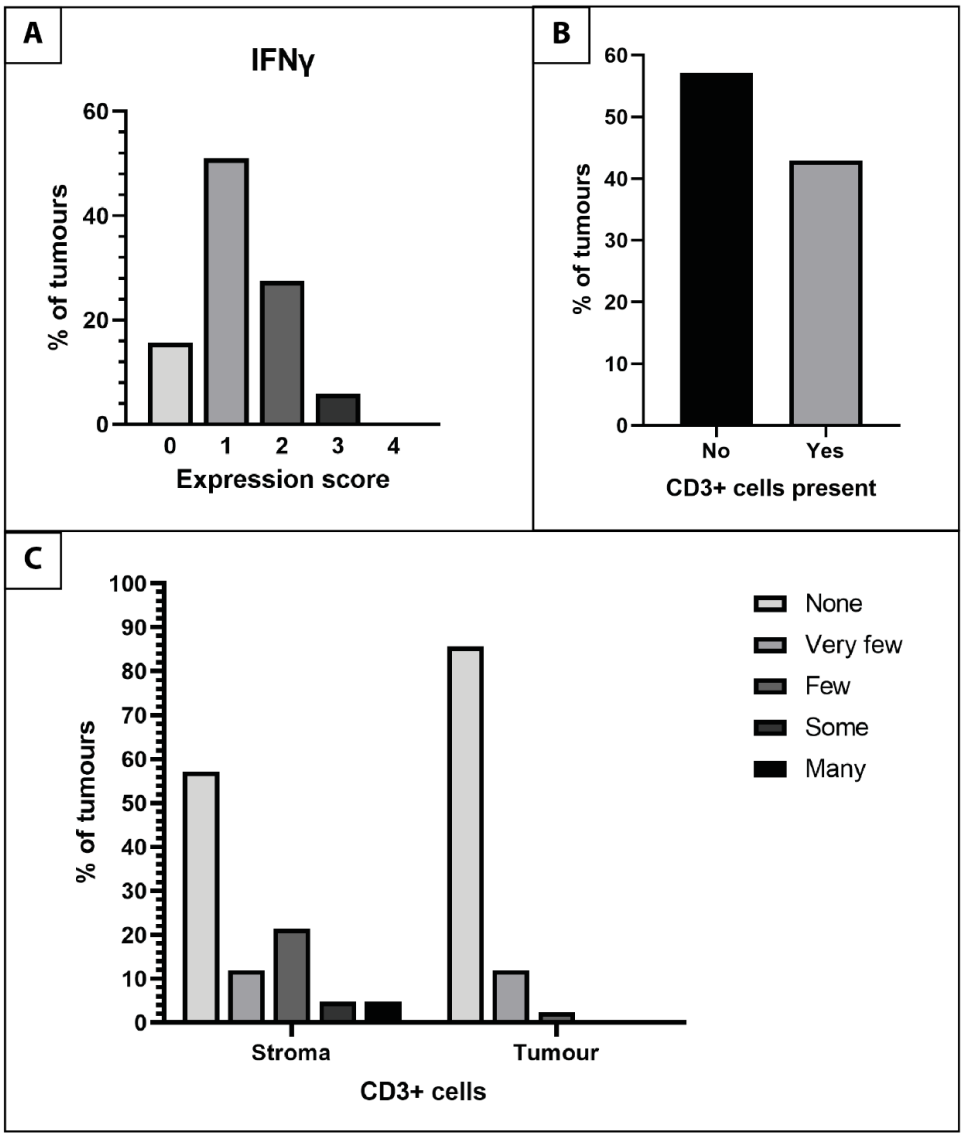

Figure 4.6 DFT1 tumours have limited immune activation.

Summary of immune markers for DFT1 tumours stained by IHC. **(A)** Percentage of DFT1 tumours (n=51) assigned each expression score for IFNγ staining by IHC. 0 = no IFNγ staining, 4 = strong IFNγ staining. **(B)** Percentage of DFT1 tumours (n=42) with CD3+ cells based on IHC staining. **(C)** Percentage of DFT1 tumours (n=42) for CD3+ cell classifications. Classifications were based on number and density of CD3+ cells in the stroma or among tumour cells.

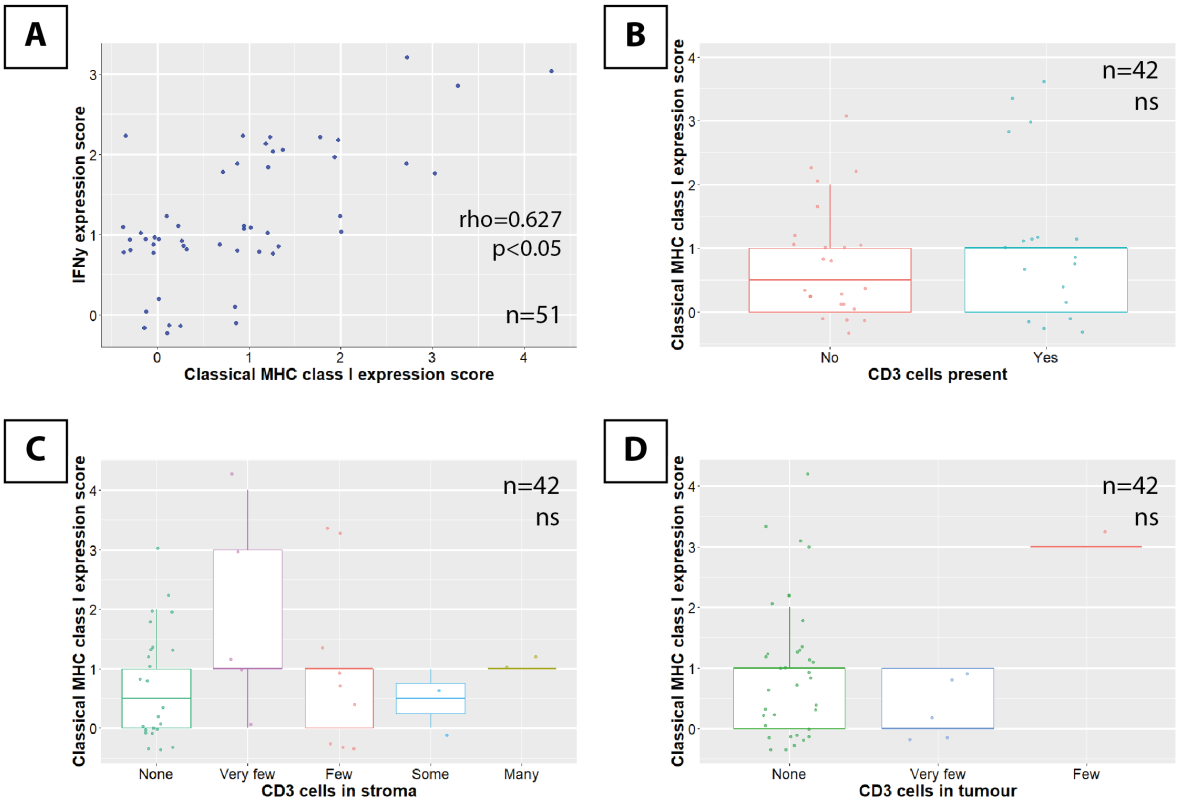

Figure 4.7 IFNγ expression correlates strongly with classical MHC class I expression by DFT1.

Classical MHC class I expression in DFT1 tumour biopsies compared with **(A)** IFNγ expression scores (n=51), **(B)** presence of CD3+ cells (n=42), **(C)** CD3+ cells in the stroma (n=42), or **(D)** CD3+ cells among tumour cells (n=42). Expression scores are based on the strength of IHC staining; 0 = no staining, 4 = very strong staining. Expression scores are discrete variables – jitter has been applied to the data points for visualisation. There is a strong positive correlation between classical MHC class I and IFNγ expression scores (rho=0.627, t=8.68x10^{-7}, p<0.05). None of the CD3 classifications are significant for differences in classical MHC class I expression. 'ns' = not significant (p>0.05).

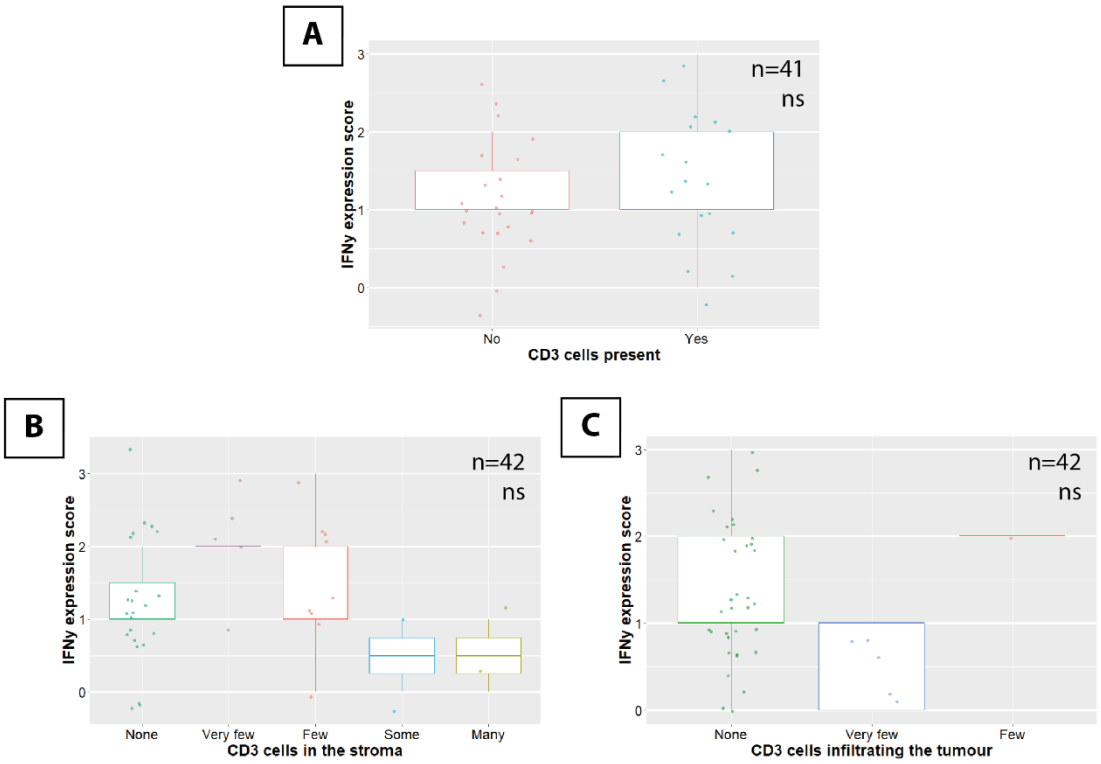

Figure 4.8 IFNγ expression does not correspond with infiltration of CD3+ cells in DFT1 tumours.

IFNγ expression in DFT1 tumour biopsies by **(A)** presence of CD3+ cells (n=41), **(B)** CD3+ cells in the stroma (n=41), and **(C)** CD3+ cells among tumour cells (n=41). Expression scores are based on the strength of IHC staining; 0 = no staining for IFNγ, 4 = very strong staining. Expression scores are discrete variables – jitter has been applied to the data points for visualisation. There are no significant differences in IFNγ expression for the CD3 classifications. 'ns' = not significant (p>0.05).

4.3.1 Variation in IFNγ expression between DFT1 tumours within the same individual is limited.

As is expected based on correlation with classical MHC class I expression by DFT1 cells, there is no clear correlation of IFNγ expression over time and expression is highly variable (Figure 4.9A). Like with classical MHC class I expression, IFNγ expression is similar between tumours infecting the same individual (Figure 4.9B), with most tumours having the same expression score or varying by an expression score of 1.

Two hosts, Haloumi and Mania, each have two tumours that vary by an expression score of 2; both with one tumour assigned an expression score of 0 and the other an expression score of 2. This variation may be due to different factors, such as, location on the face, or the tumours could have been inoculated at different times. It is interesting that two DFT1 tumours infecting the same devil can have different immune environments. For Haloumi, IFNγ expression directly correlates with classical MHC class I expression, where the tumour expressing classical MHC class I stained for IFNγ, and vice versa. However, in Mania, both tumours were assigned a classical MHC class I expression score of 1.

Orange was captured twice, with the same two tumours sampled each time. While these tumours had an MHC class I expression score of 0 when captured in February 2020, both tumours increased IFNγ expression by an expression score of 1 (one from 0 to 1, and the other from 1 to 2) between February 2020 and May 2020, corresponding with upregulation of classical MHC class I in one of these tumours.

As with classical MHC class I expression, there was no significant difference in IFNγ expression based on location, either by Broad Area (Wilcoxon rank sum test; t=0.899) or Area (Kruskal-Wallis rank sum test; t=0.389) (Appendix Figure C 2). There was also no significant difference in IFNγ expression based on sex (t=0.566) or secondary infection of the tumour (t=0.586) (Wilcoxon rank sum test), age (t=0.670), season (t=0.953) or tumour location (t=0.482) (Kruskal-Wallis rank sum test), and there was no correlation with host tumour load (Spearman's rank correlation; t=0.652) (Appendix Figure C 3). A significance level of $p<0.05$ was used for all statistical tests.

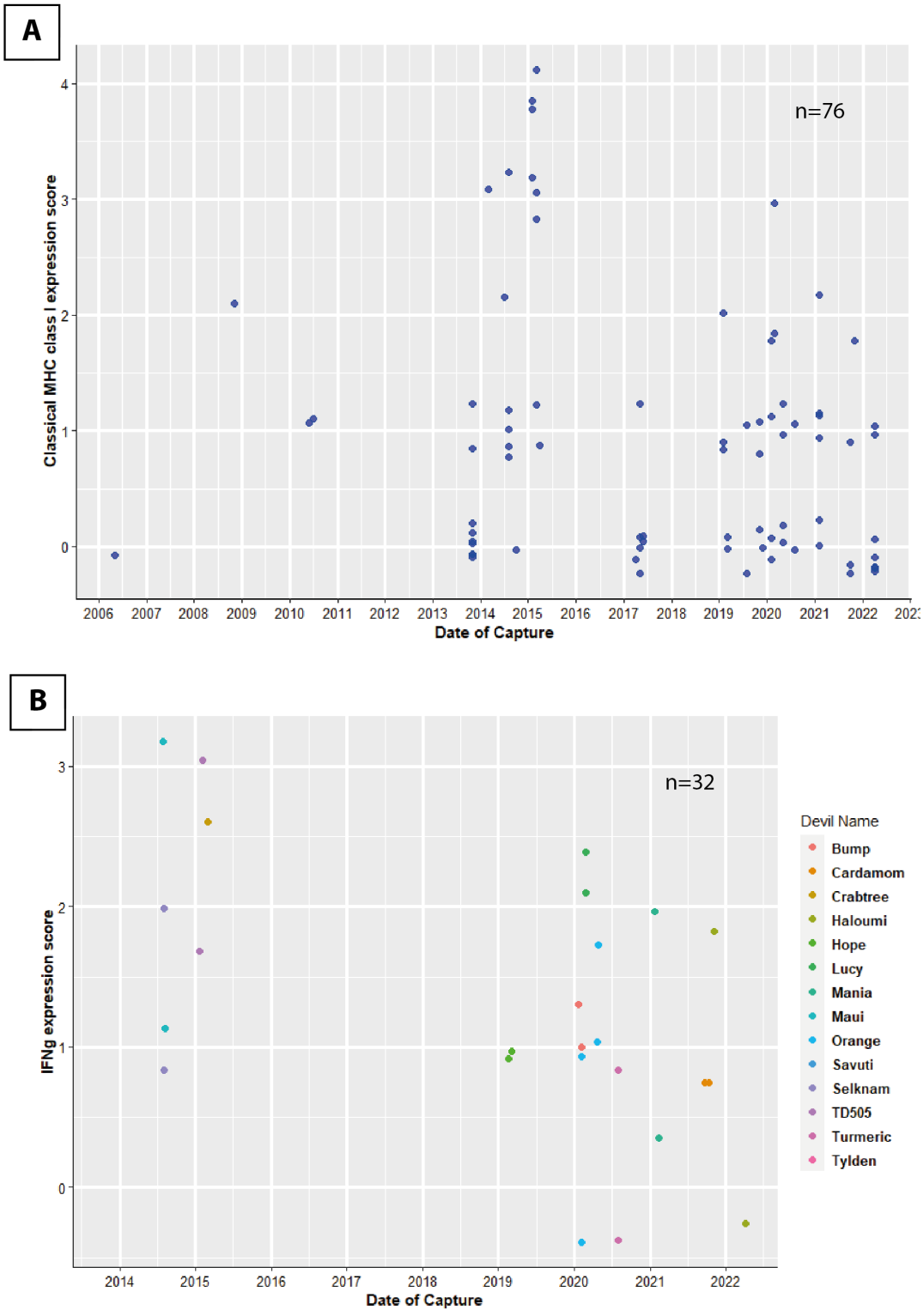

Figure 4.9 IFNγ expression in DFT1 tumours varies little within individuals.

IFNγ expression in DFT1 tumour biopsies over time, plotted against the sample collection date. Showing (A) all stained DFT1 tumours (n=76), and (B) highlighting multiple tumours that came from the same host (n=32 tumours from n=14 individuals). Expression scores are based on the strength of IHC staining. 0 = no staining for IFNγ, 4 = very strong staining. Expression scores are discrete variables – jitter has been applied to the data points for visualisation.

4.4 Discussion

To investigate classical MHC class I expression in DFT1, 76 DFT1 tumours (collected between May 2006 – April 2022) were stained by IHC. Previously only two DFT1 tumours had been stained in relation to classical MHC class I expression (Siddle et al., 2013), thus this study significantly broadens our understanding of class I expression by DFT1.

Based on IHC expression scores, DFT1 tumours are variable for classical MHC class I expression and there is no correlation over time. This is surprising, as all DFT1 tumours were thought to lack classical MHC class I expression as an immune evasion mechanism (Siddle et al., 2013). Therefore, immune evasion by DFT1 cells may be more complex than originally thought, potentially utilising multiple mechanisms to avoid the host immune system.

4.4.1 Total classical MHC class I loss is not an immune evasion mechanism employed by all DFT1 tumours.

It was previously presumed all DFT1 tumours were negative for classical MHC class I expression, due to IHC staining of primary tumours and experiments investigating expression in three DFT1 cells lines (Siddle et al., 2013). Surprisingly, while there were DFT1 tumours that were negative for classical MHC class I expression, some DFT1 primary biopsies stained positively (55.3%, n=76). Therefore, loss of classical MHC class I is not universal for DFT1 cells, and these tumours may be utilising other mechanisms for immune evasion.

DFT1 tumours that expressed classical MHC class I mostly had low levels of expression; 34.2% of all tumours were assigned an expression score of 1 (n=76). This could be due to hemizygous deletion in β_2m (Stammnitz et al., 2018) resulting in lower classical MHC class I expression, however some DFT1 tumours were assigned higher expression scores of 3 and 4 (Figure 4.1). It could also be that in tumours expressing classical MHC class I, there is a benefit to lower levels on the cell surface, as there is a lower chance of recognition by T cells.

IFNγ expression in DFT1 tumours was positively correlated with classical MHC class I expression by DFT1 tumour cells, which could indicate that classical MHC class I expression by DFT1 promotes an inflammatory tumour environment. However, expression of IFNγ is low in most tumours (expression score of 1 in 51.0%, n=51). Furthermore, IFNγ expression does not promote infiltration of CD3+ cells into DFT1 tumours (Figure 4.8).

Despite reports of increased tolerance to DFT1 infection in female devils (Margres et al., 2018; Ruiz-Aravena et al., 2018), there was no difference in classical MHC class I or IFNγ expression

between male and female devils, nor do classical MHC class I expression levels vary for female devils over time (See Figure 4.2B). It may be that recognition of classical MHC class I expressed by DFT1 cells and expression of IFNγ do not play a role in DFT1 tolerance in female devils. Conversely, these female devils may not have developed tolerance to DFT1.

4.4.2 Classical MHC class I expression in DFT1 may be plastic in response to environmental pressures.

Sample numbers are low pre-2013, and very few samples exist from the period after DFT1's emergence (Pearse and Swift, 2006), therefore we have limited data on how classical MHC class I expression by DFT1 has evolved over time. As DFT1 has spread across Tasmania, it has evolved into distinct subclones, or clades, with certain clades becoming dominant in different regions of Tasmania (Kwon et al., 2020). Therefore, the variation in classical MHC class I expression may be due to different clades having evolved different levels of classical MHC class I expression. While there was no significant difference between classical MHC class I by tumours in the North-West versus the South-East (Figure 4.4), sample numbers for the North-West are low (n=17), including three tumours from inoculated or induced devils, and only two areas are being compared. In addition, multiple clades exist in a region (Kwon et al., 2020); as such, a more detailed method to investigate classical MHC class I in different clades would be through genetic analysis of the tumour to group tumours by clades.

Another possible explanation for the variation in classical MHC class I expression by DFT1 is plasticity in MHC class I expression in response to environmental factors, such as host immune responses. This plasticity could be due to epigenetic mutations in components of the APP, where classical MHC class I expression can be upregulated by exposure to cytokines, such as IFNγ (Siddle et al., 2013). For example, in the devil, Orange, both tumours increased in classical MHC class I expression between sampling in February 2020 and May 2020, which indicates DFT1 cells can change their classical MHC class I expression. Modulation of classical MHC class I expression is a mechanism employed by CTVT throughout its infection of a host, where expression is up- and downregulated dependent on the stage of infection (Belov, 2011; Murgia et al., 2006).

Both clade-dependent and plastic classical MHC class I expression could explain the variable expression in tumours infecting the same host (Figure 4.2A). Tumours that vary from each other may belong to different clades, or the tumours are exposed to slightly different environmental pressures and alter their classical MHC class I expression accordingly. It is also likely that multiple factors are affecting classical MHC class I by DFT1, therefore both situations could be at play in the population.

Interestingly, DFT1 tumours have variable periaxin expression. DFT1 cells have previously been found to be consistently high for periaxin expression and periaxin was used as a specific marker for DFT1 (Murchison et al., 2010). However, many tumours lacked or were variable for expression based on IHC staining (Figure 4.5). These findings are important for future experiments, as periaxin can no longer be used as a sole marker for DFT1 cells, and for interpreting previous results, as older tumours also stained negative for periaxin (for example Savuti T4 from 2011). DFT1 cells express periaxin because they originate from a myelinating (differentiated) Schwann cell (Murchison et al., 2010; Owen et al., 2021). As periaxin is only expressed in differentiated cells, loss in DFT1 may indicate DFT1 is dedifferentiated in these tumours. DFT1 cells were found to have dedifferentiated in DFT1 tumours that had escaped the immune system in vaccinated devils (Patchett et al., 2021). Dedifferentiation of DFT1 cells could increase plasticity of classical MHC class I expression in tumours.

4.4.3 Implications and future study

Understanding the immune response, if any, against DFT1 is vital to understanding how the cancer evades the host immune system to transmit among the population, and how to design therapeutic interventions. Previously, it was believed that all DFT1 cells had totally downregulated MHC class I to evade the immune system, however, many DFT1 tumours have stained positively for classical MHC class I expression. Therefore, evasion of host T cell responses by DFT1 is not as straightforward as previously suggested. Further work is needed to establish whether classical MHC class I molecules are expressed on the surface of DFT1 cells for recognition by immune cells. If so, investigation into how these cells avoid the host immune system is warranted. Additionally, host-tumour mismatch should be investigated for DFT1 tumours, as host immune recognition could contribute to differences in classical MHC class I expression between tumours.

Chapter 5 MHC class I genotyping of DFT hosts to assess the role of host-tumour mismatch in MHC class I loss

5.1 Introduction

An immune response against transmissible cancers is expected due to disparate MHC class I alleles between cancer cells and their host. Despite expression of cell surface classical MHC class I (Caldwell et al., 2018), DFT2 is able to spread among Tasmanian devils with little to no T cell infiltration in DFT2 tumours (Caldwell et al., 2018). Variability in classical MHC class I expression by DFT2 cells in tumour biopsies (Caldwell et al., 2018, see Chapter 3 - Section 3.2), and the total loss of classical MHC class I in some tumours observed by IHC staining (see Chapter 3 – Section 3.2), suggests there is selective pressure for MHC class I loss, which likely arises from host immune recognition of classical MHC class I alleles expressed by the tumour but not the host.

The variability of classical MHC class I expression by DFT2 tumours suggests that DFT2 is in the process of losing classical MHC class I expression as it spreads through the population. This may be due to selective pressure from the host immune system in response to unrecognised, non-self tumour MHC class I alleles. We predict that where classical MHC class I expression is high in a tumour, the host would have a similar MHC class I genotype, and where classical MHC class I has been lost, there would be mismatch between tumour and host classical MHC class I.

Previous studies suggested that DFT1 tumours evaded the host immune system through complete loss of classical MHC class I from the cell surface. However, IHC staining of primary biopsies has shown not all DFT1 tumours are MHC class I negative (see Chapter 4 – Section 4.2). MHC class I loss in DFT1 is due to epigenetic downregulation of β2m and TAP and has been shown to be reversible with inflammatory cytokines and epigenetic modification (Burr et al., 2019; Siddle et al., 2013), therefore it is possible classical MHC class I is being upregulated in response to the local tumour environment. As with DFT2, selective pressure for downregulation of classical MHC class I in DFT1 cells is likely greater in hosts with a mismatched MHC class I genotype to the cancer.

To investigate whether classical MHC class I mismatch between tumour and host is driving MHC class I loss by DFT1 and DFT2, we examined the MHC class I allotypes in 29 host samples and compared these to the DFT1 and DFT2 allotypes. Host samples were collected from individuals trapped in the d'Entrecasteaux peninsula, in conjunction with tumour sampling. This is integrated

with examination of MHC class I expression in DFT1 and DFT2 primary tumours in Chapter 3 and Chapter 4. Classical MHC class I genes were amplified by RT-PCR using RNA extracted from ear biopsies. The amplified product was sequenced using an Illumina MiSeq and reads aligned to Tasmanian devil classical MHC class I allele, SahaI*27. Host classical MHC class I genotypes were compared to known DFT alleles to assign hosts as matched or mismatched. Mismatch data was then assessed against tumour expression scores to determine whether there is a correlation between host-tumour MHC class I mismatch and classical MHC class I loss by tumour cells.

5.1.1 Aims and objectives

This chapter addresses Hypothesis 1, "DFT2 is losing MHC class I expression during progression through the devil population" (see Chapter 1 – Section 1.5):

> Aim 3: Investigate classical MHC class I mismatch between tumour and host as a driver of MHC class I loss by DFT2.

The objectives of this chapter are:

1. Genotype DFT hosts for classical MHC class I by Next Generation Sequencing.
2. Compare classical MHC class I genotype of DFTs to that of their hosts to identify mismatched alleles.
3. Examine whether there is a correlation between host-tumour mismatch and tumour classical MHC class I expression.

5.2 Sequencing reveals Tasmanian devils have between two and five classical MHC class I alleles.

To investigate host-tumour classical MHC class I mismatch in DFTs, 29 DFT hosts (matched to tumours stained in Chapter 3) collected between September 2016 and May 2019, along with a DFT1 cell line, 4906_IFNγ, and a DFT2 cell line, RV, were sequenced by NGS using cDNA for classical MHC class I. To upregulate classical MHC class I expression for sequencing in 4906, the cells were treated with IFNγ prior to RNA extraction. See Table D 1 for samples used for classical MHC class I genotyping; for further sample information see Table A 1.

Forward reads were assigned against Tasmanian devil classical MHC class I alleles previously identified (Caldwell and Siddle, 2017). Reverse reads were not used for analysis as they were of lower quality and had fewer reads than the forward data set. Raw forward reads, prior to processing, had a mean of 163,118 per replicate (range 69,001 – 494,077 reads). After processing,

the mean assigned reads per replicate were 106,906 (range 32,822 – 342,618), shown in Figure 5.1. On average, the number of assigned reads was 65.4% of the raw reads.

The experimental design aimed to achieve 100,000 reads per sample, with 3 replicates per sample. This allowed comparison between replicates; alleles that were found in only one replicate were regarded as artefacts and the replicate discarded. A high threshold for reproducibility is important when dealing with a duplicated locus known for its high level of polymorphism. During analysis, two samples, Simone and Willie, were removed as all three replicates were discordant for alleles called. This left 27 DFT host samples: 11 DFT1 hosts and 16 DFT2 hosts. Five of these samples, Cyprus, Harry, Pooh, Selma, and Snowball, had a replicate discarded (n=2) as it did not match the alleles called for the other two replicates. For the other samples, the alleles called matched across all three replicates (n=3).

The DFT cell lines acted as a control to validate sequencing analysis as the MHC class I alleles in these samples have been previously defined with this primer set (Caldwell et al., 2018). Variant calling correctly assigned DFT1, 4906_IFNγ and DFT2, RV classical MHC class I alleles, matching previous sequencing of these cell lines (Caldwell et al., 2018; Gastaldello et al., 2021); SahaI*27, SahaI*35, SahaI*46, and SahaI*90 for DFT1, and SahaI*27, SahaI*35, SahaI*74, and SahaI*90 for DFT2.

Out of the 34 classical MHC class I alleles from Caldwell and Siddle (2017), 14 alleles were called across the 29 samples (shown in Figure 5.2). In addition, two alleles were identified that were not in the allele list taken from Caldwell and Siddle (2017). These sequences were BLAST on NCBI for matches to existing Tasmanian devil nucleotide sequences. One sequence matched with 100% sequence identity for 3 previously identified classical MHC class I alleles, SahaI*37 (GQ411487.1), SahaI*72 (GQ411480.1), and SahaI*79 (GQ411445.1). As the amplicon was not long enough to distinguish between these 3 alleles, the sequence was named SahaI*37/72/79 for analysis. The second sequence did not match any existing alleles, and was named SahaI*103, to follow on from new alleles identified by Tovar et al. (2017). SahaI*37/72/79 was found in two individuals, Krum and Summer, and SahaI*103 appeared in one individual, Tibet.

Sequencing analysis found devils express between two and five classical MHC class I alleles (Figure 5.3). Only one sample, Taco, had two alleles called, and the most common number of alleles was four.

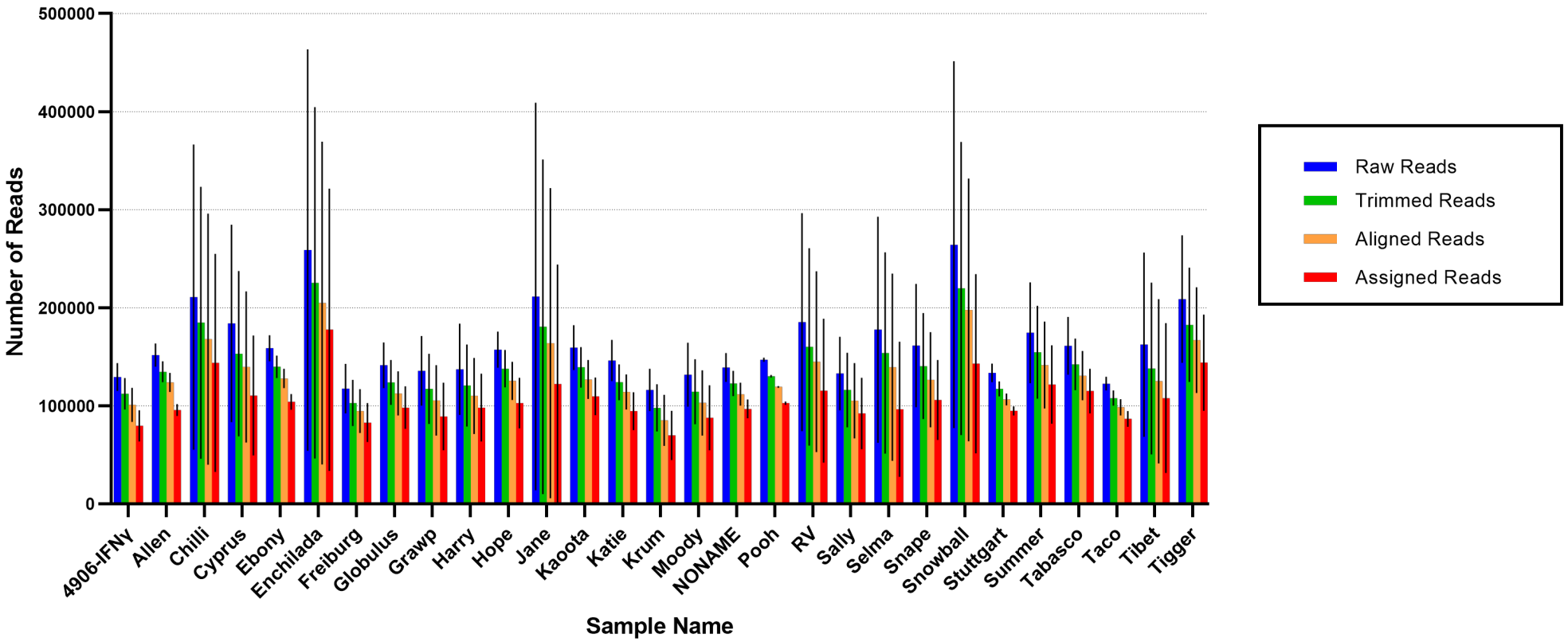

Figure 5.1 Number of reads for classical MHC class I sequencing.

Mean read numbers for Tasmanian devil samples sequenced for classical MHC class I genes using Illumina MiSeq. Raw reads are the forward reads from sequencing (blue), trimmed reads (green), aligned reads (yellow) and assigned reads (red) show the culling of reads during sample processing. Black bars represent standard deviation. Cyprus, Harry, Pooh, Selma, and Snowball are n=2. All other samples are n=3. Created using GraphPad.

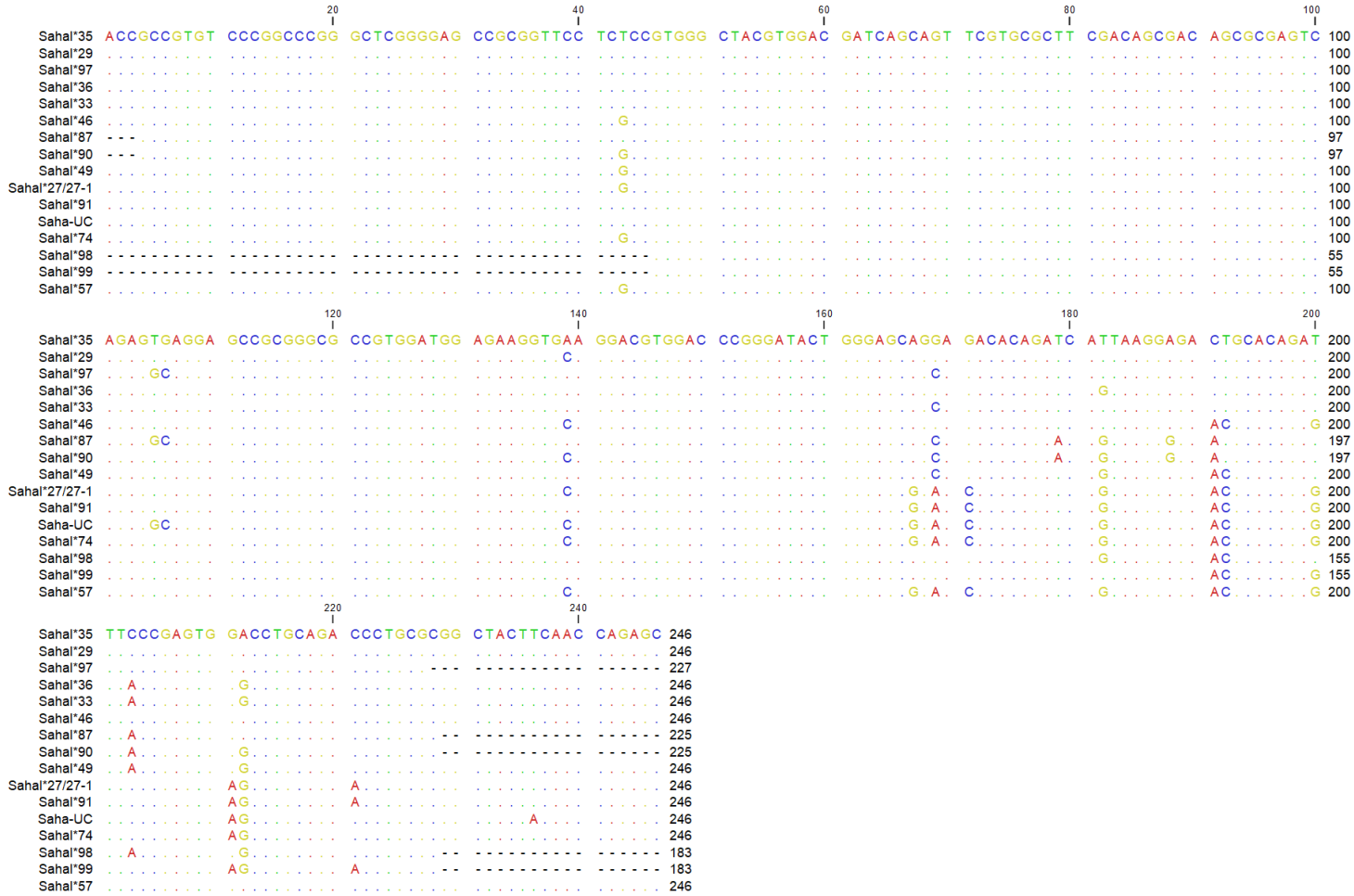

Figure 5.2 Classical MHC class I nucleotide alignment of unique alleles called for Tasmanian devil and DFT sequencing.

Sequences span exon 2 to exon 3 of the MHC class I gene. Alignment created in CLC Main Workbench 22.0.

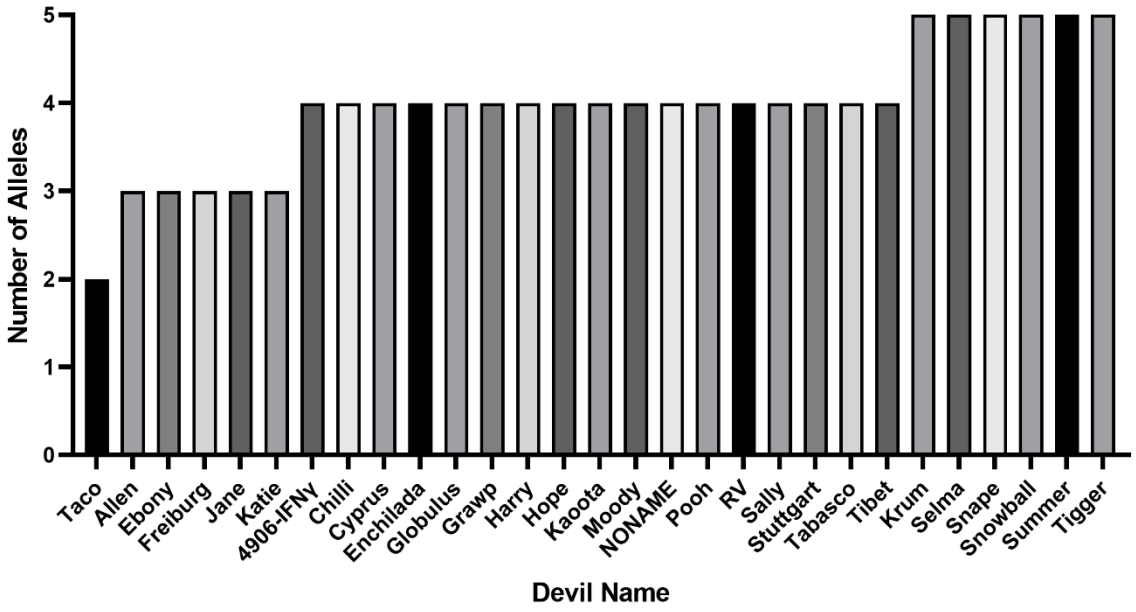

Figure 5.3 Number of classical MHC class I alleles per sample

The number of classical MHC class I alleles called per sample, based on nucleotide sequences from Illumina sequencing. Tasmanian devil samples had between two and five classical MHC class I alleles, where the mean was 4. Created using GraphPad.

5.3 All devils share a common classical MHC class I allele.

Strikingly, of the 27 individuals sequenced, all devils expressed SahaI*27 (shown in Figure 5.4) including the DFT cell lines. The allele with the next highest expression in the population is SahaI*35 at 66.7% (18 devils), then SahaI*29 at 55.6% (15 devils). The other 13 alleles were found in 33.3% of the devils or less (≤9 devils). These results indicate that the diversity of classical MHC class I expression in the d'Entrecasteaux peninsula is limited. Interestingly, five of the six highest expressed classical MHC class I alleles in the devils sequenced are expressed by DFT1 and/or DFT2 – SahaI*27, SahaI*35, SahaI*46, SahaI*74, and SahaI*90.

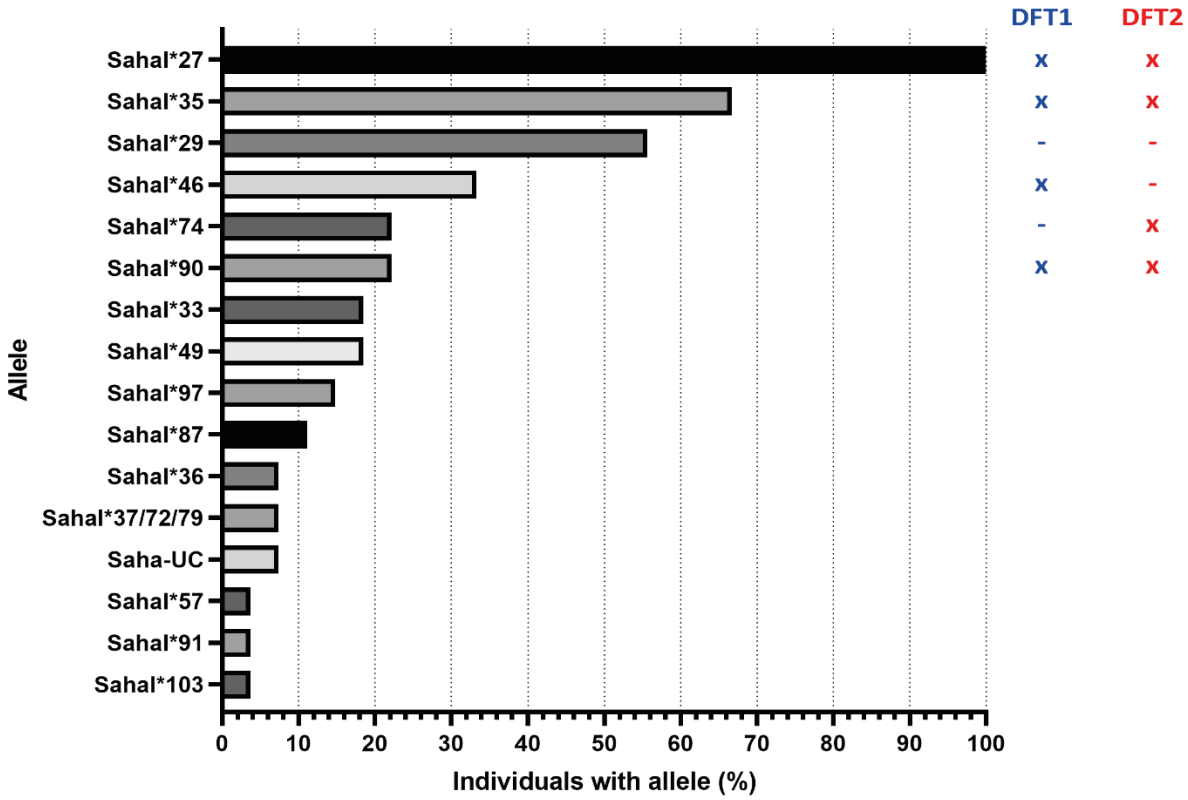

Figure 5.4 Tasmanian devils share a common classical MHC class I allele.

Bar chart showing the percentage of individuals, out of 27 DFT hosts sequenced, that express each classical MHC class I allele. SahaI*27/27-1 is expressed by all devils. Created using GraphPad. Crosses on the right indicate alleles expressed by DFT1 (blue) or DFT2 (red).

5.3.1 Few MHC class I alleles are mismatched between tumour and host.

To investigate mismatch between the classical MHC class I genotype of DFTs and their hosts, DFT alleles that were not expressed by their host were compared to the host genotype, as mismatched DFT alleles are most likely to be antigenic to the host devils. Amino acid sequences of mismatched DFT classical MHC class I alleles were compared to the sequences of host alleles for their closest match. The MHC class I alleles called from sequencing analysis were translated into amino acid sequences, shown in Figure 5.5, and percentage sequence identity and similarity between alleles calculated using Sequence Manipulation Suite: Ident and Sim ("Ident and Sim," 2020). Percentage sequence identity and similarity were calculated using sequences trimmed from position 2 to 75 in the amino acid alignment (Figure 5.5); except for comparisons to SahaI*37/72/79 and SahaI*103, which were calculated from position 16 to 75 to prevent skewed data due to missing residues. To compare alleles from a functional perspective, the number of mismatched residues at positions predicted to interact with the TCR or bind a peptide for presentation were calculated. Tasmanian devil classical MHC class I amino acid sequences were aligned with Human HLA-A (hla-a2.1; PDB: 3HLA_A, GI: 230875) and residues assigned based on postulated residues by Bjorkman and Parham (1990) (predicted TCR and peptide residues shown in Figure 5.5).

Tables for classical MHC class I allele comparisons; percentage sequence identity, percentage sequence similarity, mismatched TCR residues, and mismatched peptide residues are included in Appendix C (Table D 2 – D 5).

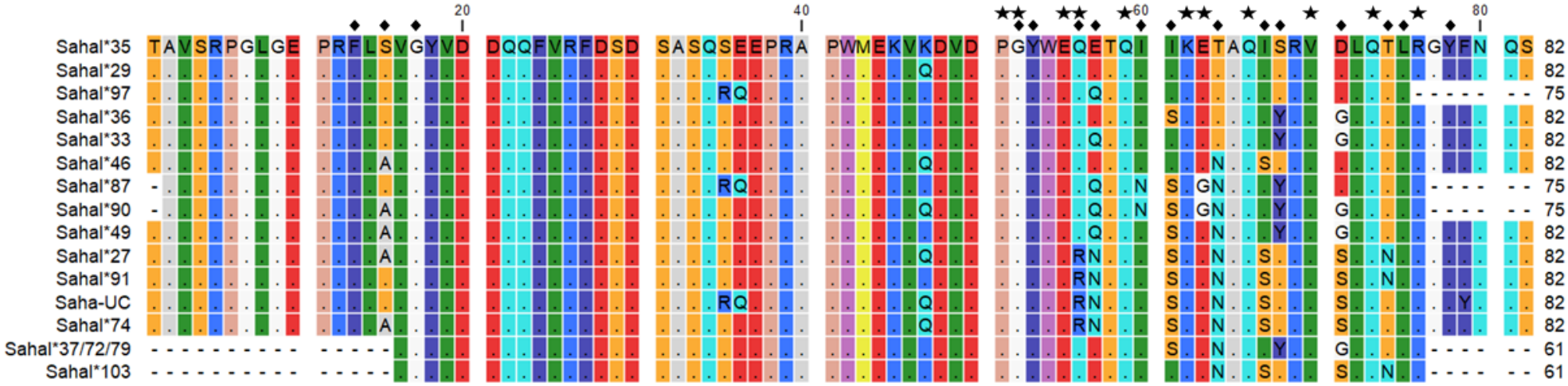

Figure 5.5 Amino acid alignment of classical MHC class I alleles

Alignment of amino acid sequences of classical MHC class I alleles expressed by DFT cell lines and Tasmanian devils sequenced from the d'Entrecasteaux peninsula. Stars indicate residues predicted to interact with the TCR, and diamonds indicate residues predicted to bind the peptide. Residue predictions were calculated by referencing Bjorkman and Parham (1990), Figure 4. Alignment created in CLC Main Workbench 22.0.

DFT1 and DFT2 classical MHC class I genotypes were compared with that of their hosts, to identify which DFT alleles were mismatched in each host. A DFT allele was termed mismatched if the allele was not expressed by the host. As all devils sequenced expressed SahaI*27 (Figure 5.4), this allele was not mismatched between DFTs and their hosts (Figure 5.6A). SahaI*35, the second highest expressed allele in the population, was rarely mismatched at 27.3% of DFT1 hosts (n=11) and 31.3% of DFT2 hosts (n=16). For DFT1, the two commonly mismatched alleles were SahaI*46 and SahaI*90, both mismatched in 72.7% of hosts. For DFT2, SahaI*74 and SahaI*90 were each mismatched in 75.0% of hosts.

The mismatched DFT alleles were compared to host alleles for the closest allele match in each host based on percentage amino acid sequence identity and similarity (Figure 5.6B). For SahaI*35 in DFT1, the closest host allele was always SahaI*29 (n=3), while in DFT2 (n=5), SahaI*29 was the closest host allele in 80% of mismatches, while in the other 20% of DFT2 hosts the closest allele was SahaI*33. Percentage amino acid sequence identity to SahaI*35 for SahaI*29 is 98.65% and for SahaI*33 is 95.95%. None of these mismatched residues occur at positions predicted to interact with the TCR, with the only major difference between the amino acids sequences being 3 residues predicted to bind the peptide (Figure 5.5). Therefore, even when mismatched, SahaI*35 has high similarity to most host classical MHC class I genotypes.

For DFT1, when SahaI*46 was mismatched (n=8), the closest host allele in 75% of mismatches was also SahaI*29, which appears to be commonly expressed in population, and had an amino acid sequence identity and similarity of 95.95%, which does not translate to residues predicted to interact with the TCR (Figure 5.5). In the other 25% of mismatches the closest host alleles were SahaI*57 and SahaI*74 (representing one individual each), which had 95.95% sequence identity and 94.59% sequence identity to SahaI*46, respectively, and both translated to one 'TCR residue' mismatch. For DFT2, in hosts where SahaI*74 was not expressed (n=12) the closest host allele was SahaI*27, which is expressed by all devils in the population. SahaI*27 is closely related to SahaI*74 at 98.65% sequence identity, with no mismatched residues occurring at 'TCR residues' and only 1 at a residue predicted to bind the peptide. Though SahaI*46 in DFT1 and SahaI*74 in DFT2 were mismatched in over 72% of hosts, they share sequence similarity with commonly expressed alleles in the population, therefore are unlikely to immunogenic to their hosts.

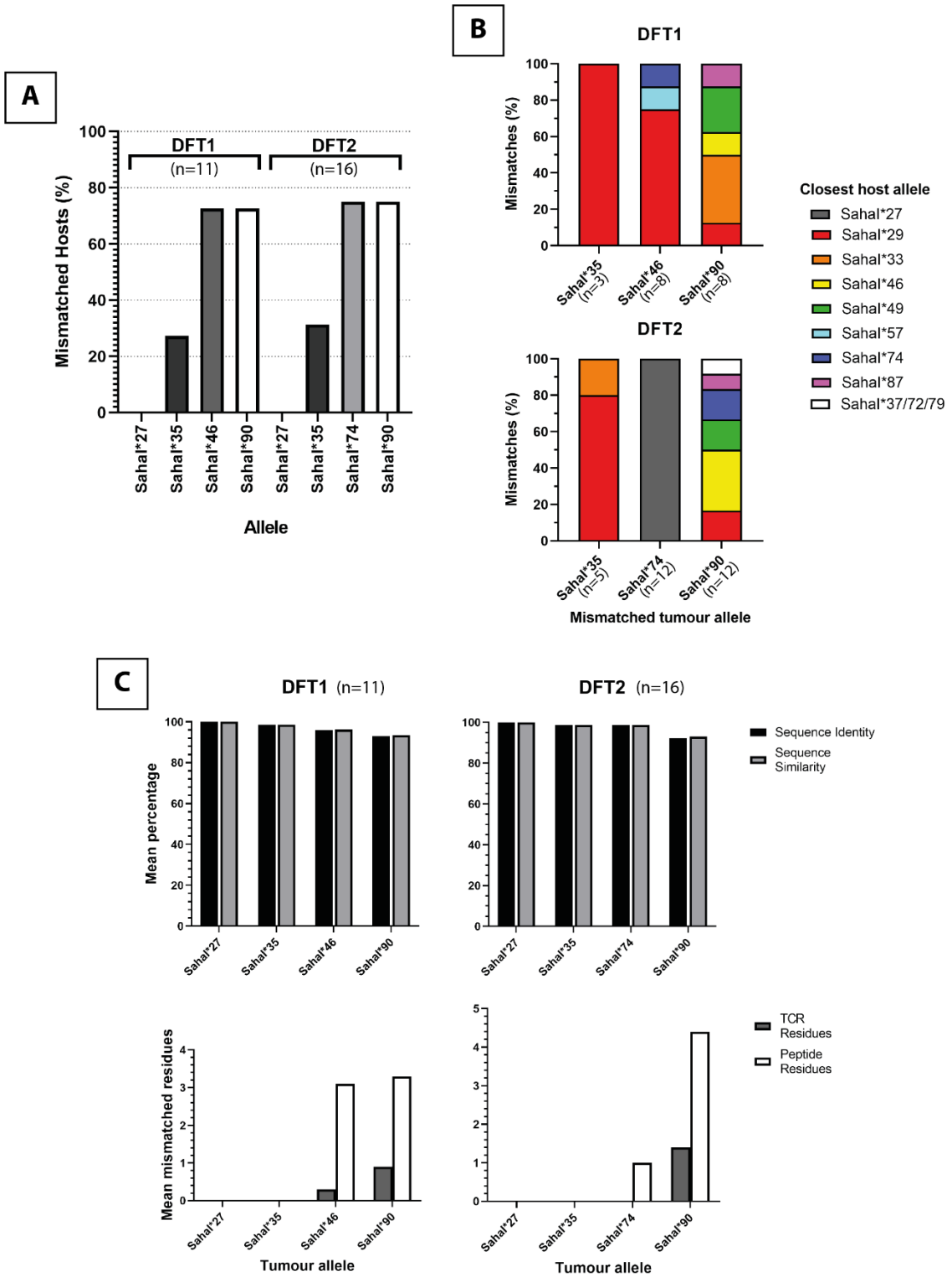

Figure 5.6 Classical MHC class I mismatches are uncommon between DFTs and their hosts.

DFT1 and DFT2 classical MHC class I genotypes compared with classical MHC class I alleles expressed by their hosts. **(A)** The percentage of hosts that do not express each DFT1 (n=11) and DFT2 (n=16) classical MHC class I allele. **(B)** The closest host allele for each DFT allele mismatch, based on percentage amino acid sequence identity and similarity (see Table D 2 and Table D 3), as a percentage of mismatches for that allele.

(C) Top - Graphs showing the mean percentage amino acid sequence identity and similarity for each DFT1 (**left**) and DFT2 (**right**) classical MHC class I allele to the closest allele in each host. **Bottom –** Graphs for the mean number of mismatched residues, that are predicted to interact with the TCR or bind peptide, between DFT1 (**left**) and DFT2 (**right**) alleles and their closest allelic match in each host. DFT1 (n=11), DFT2 (n=16). Created using GraphPad.

SahaI*90 was commonly mismatched in both DFT1 and DFT2 hosts. In mismatched DFT1 hosts (n=8) there were five different closest host allele matches, and for DFT2 hosts (n=12) there were 6; the closest host allele matches for both cancers ranged between 89.19% and 91.89% amino acid sequence identity to SahaI*90. SahaI*33 was the most common allele match in DFT1 hosts at 37.5% of mismatches, with a sequence identity of 91.89%. For DFT2 the most common allele was SahaI*46 (33.3% of mismatched hosts), which has 90.54% sequence identity.

Unlike other DFT alleles, SahaI*90 does not share similarity with classical MHC class I alleles that are highly expressed in the population, therefore it is potentially the most antigenic of the tumour alleles. This is reflected in the mean amino acid sequence identity/similarity and mean residue mismatches (Figure 5.6C). For each DFT allele, the closest host alleles were found, and the mean % sequence identity and similarity calculated. The DFT and host allele sequences were also compared at residue positions predicted to interact with the TCR or bind peptides for presentation (residue predictions based on Bjorkman and Parham, 1990). Key residues are illustrated in Figure 5.2 and residue comparisons between alleles shown in Table D 4 and Table D 5. SahaI*90 has the lowest mean sequence identity and similarity in DFT1 (92.94% and 93.39%) and DFT2 (92.18% and 93.15%). This corresponds with the highest mean residue mismatches, with 0.9 for TCR and 3.3 for peptide in DFT1 hosts, and 1.4 for TCR and 4.4 for peptide residues in DFT2.

As SahaI*27 has no mismatches in DFT hosts, it has 100% sequence similarity and 0.0 residue mismatches. SahaI*35, despite having 98.65% mean sequence identity in DFT1 and DFT2 to the closest host allele, this does not translate to TCR or peptide residue mismatches, so SahaI*35 is unlikely to elicit a T cell response. In DFT1, SahaI*46 had the second lowest mean sequence identity (95.76%), and while it had 3.1 mean peptide residue mismatches, this did not translate to TCR residue mismatches, at 0.3. SahaI*74 in DFT2 had the same mean sequence identity as SahaI*35 (98.65%), and similarly had 0.0 TCR residue mismatches and only 1.0 mean peptide residue mismatches.

To investigate whether there was a correlation between host-tumour mismatch and loss of classical MHC class I expression in tumours, allelic mismatch data described above was compared to classical MHC class I expression scores from matched tumours in Chapter 3. Not all host samples had stained tumours, but both DFT1 and DFT2 had 10 host samples with matched tumours. Some individuals had multiple tumours, which gave 11 stained tumours for DFT1 and 17 for DFT2. Tumour expression scores for classical MHC class I were compared to percentage sequence identity and mismatched residues, for each host overall and for frequently mismatched alleles, for example SahaI*90. The host expression of SahaI*27 and SahaI*90 was also plotted against classical MHC class I expression scores (Appendix Figure D 1 and Figure D 2). Across these data no correlation was found between classical MHC class I expression and host-tumour MHC class I mismatch (Spearman's correlation). However, analysis was limited by sample number. A significance level of $p<0.05$ was used for all statistical tests.

5.4 Host devils and tumour cells express higher levels of classical MHC class I molecules that are common in the population.

As classical MHC class I genes were amplified from cDNA for sequencing and the primers for classical MHC class I are expected to amplify alleles equally (Caldwell et al., 2018), read numbers correspond to the expression levels of each allele. SahaI*27, which is expressed in all samples (Figure 5.4), has the highest number of reads in all samples, shown in Figure 5.7, while other alleles have lower read numbers.

Total read numbers vary between samples, therefore, to visualise the allele expression levels, reads were plotted as a percentage of the total reads for each sample (Figure 5.7B) (scripts for analysis are available at https://doi.org/10.5258/SOTON/D3092). This further illustrates that SahaI*27 is highly expressed at an individual level, with 48.9% mean reads (range 28.3% - 75.0%) in Tasmanian devils (excluding cell lines).

Other common alleles in the population also have a higher percentage of read numbers than less common alleles (Figure 5.7B). SahaI*35 has a mean expression of 19.8%, SahaI*29 - 18.4%, and SahaI*46 - 20.0%, compared to a mean expression of 15.2% for all other alleles (excluding SahaI*27, SahaI*35, SahaI*29, and SahaI*46). SahaI*90, which is expressed by DFT1 and DFT2, and is commonly mismatched between tumour and host, has a mean expression of 17.1%, but was only expressed in six devils (22.2%) (Figure 5.4).

As is shown in Figure 5.7A, most devils that do not have SahaI*35, express closely related allele SahaI*29 (98.65% sequence identity). This is reflected in host mismatch data (Figure 5.6B), where the closest allele to SahaI*35 in most mismatched hosts is SahaI*29. These results highlight that there is high expression of common alleles in the population. SahaI*27, SahaI*35, and SahaI*29 are highly expressed in the population and by individuals, therefore SahaI*27 and SahaI*35 expression by DFTs not likely to be antigenic.

To probe allele expression levels in DFT cell lines (4906_IFNγ and RV), in Figure 5.8 percentage reads (tumour cell expression (%)) were plotted against mean host sequence identity (%), taken from percentage sequence identity in Figure 5.6C. DFT2 expresses much higher levels of SahaI*27 (57.7%) than other classical MHC class I alleles (between 10.9% and 18.6%). With SahaI*27 being highly expressed in the population and individuals, this allele has 100% sequence identity to hosts, therefore high levels of expression by DFT2 could be advantageous for host immune evasion. In DFT1, while SahaI*27 has the highest expression, it is not dissimilar from the other alleles; all DFT1 classical MHC class I alleles had expression levels between 18.8% – 33.4%.

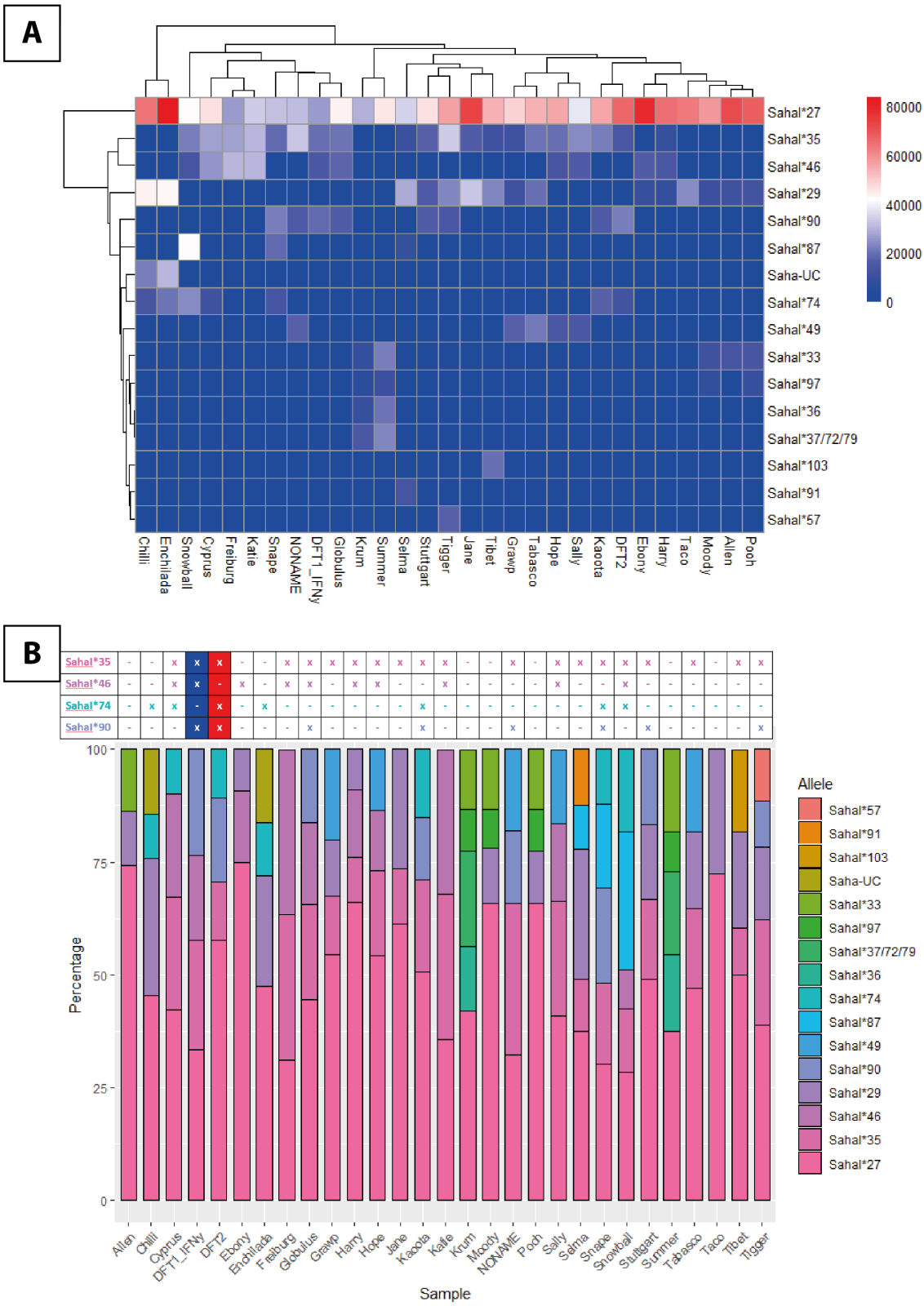

Figure 5.7 Tasmanian devils and DFTs express high levels of a common classical MHC class I allele, Sahal*27.

Data from classical MHC class I sequencing of Tasmanian devils from the d'Entrecasteaux peninsula, along with a DFT1 cell line treated with IFNγ, 4906_IFNγ, and a DFT2 cell line, RV. **(A)** Heatmap showing mean read numbers for each sample.

All samples n=3, except for Cyprus, Harry, Pooh, Selma, and Snowball, which are n=2. Generated using pheatmap package in R. **(B)** Graph presenting mean reads per allele as a percentage of the total reads for that sample. Generated using ggplot2 in R. Crosses in the table above represent DFT alleles expressed in each sample, except SahaI*27, which is expressed in all samples.

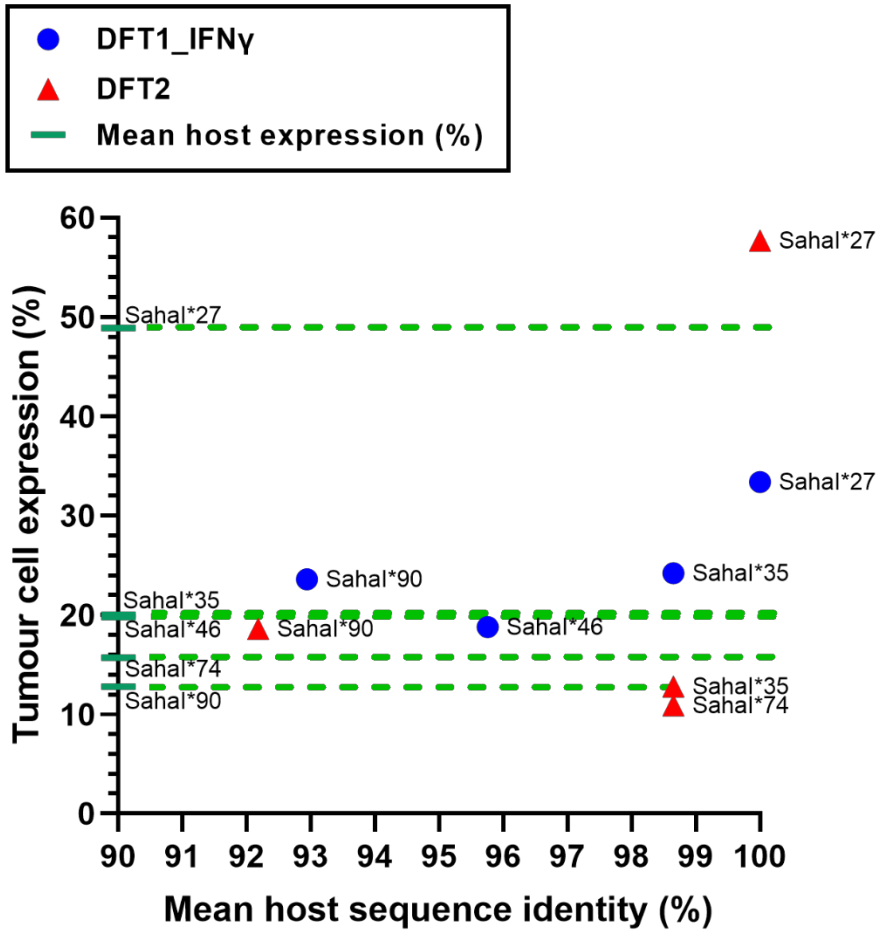

Figure 5.8 DFT2 has higher expression of SahaI*27 than other classical MHC class I alleles.

Mean reads from NGS sequencing of DFT1 cell line, 4906 treated with IFNγ and DFT2 cell line, RV, presented as a percentage of total reads for that sample (n=3). Percentage of reads for an allele represent relative expression by the cell line. Percentage expression is plotted against the mean host sequence identity (%) to the closest host allele in DFT1 (n=11) and DFT2 (n=16) hosts. Green dashed line shows the mean host expression of each DFT allele based on number of reads. Created using GraphPad.

5.5 Discussion

In this chapter, 27 Tasmanian devils from the d'Entrecasteaux peninsula were sequenced for classical MHC class I (captured between September 2016 – May 2019) for comparison to matched tumour samples. A common allele, SahaI*27, was expressed by all devils, and had the highest allele expression at an individual level (by read number), supporting previous sequencing of three DFT2 hosts (Caldwell et al., 2018). As SahaI*27 is expressed by both DFT1 and DFT2, widespread expression of this allele may facilitate immune evasion of these tumour cells.

It is important to note that SahaI*27 and SahaI*27-1 could not be distinguished from each other using the sequencing data. Therefore, SahaI*27 could represent two alleles in some samples if they express both SahaI*27 and SahaI*27-1, which may contribute to the high read numbers. However, SahaI*27 and SahaI*27-1 only differ by one non-synonymous substitution at a position not predicted to interact with the TCR or bind peptides, thus, from a functional perspective these allele sequences are identical. Alternatively, SahaI*27 reads could represent a single homozygous locus, however the pattern of read numbers does not support this.

This is the first use of NGS for RNA sequencing of Tasmanian devil MHC class I and increases the number of devils sequenced for classical MHC class I from the d'Entrecasteaux peninsula. Previously only three devils had been sequenced from this area (Caldwell et al., 2018), with Fentonbury being the closest site of large-scale MHC class I sequencing (Cheng et al., 2022, 2012).

The target level of sequencing depth was achieved, with a mean of 106,906 reads/sample (range 32,822 – 342,618) after processing. The genotype for a DFT1 and DFT2 cell line, used as controls, were accurately called across replicates, matching previous sequencing (Caldwell et al., 2018; Gastaldello et al., 2021). Between 2 – 5 alleles were called per individual. This fits with previous findings of between 1-6 (Cheng et al., 2022) and 2 – 7 (Siddle et al., 2010) classical MHC class I alleles in an individual. It is likely some of these devils have more classical MHC class I alleles, particularly Taco, which only had two (Figure 5.3). This could be due to polymorphic sites lying outside of the amplified region, or that alleles were missed during sequencing, though the latter is less likely due to the depth of sequencing. Further, as SahaI*27 was called for all samples, some samples will express SahaI*27 and SahaI*27-1, therefore they have an additional allele which could not be resolved from this data. For example, we know from previous work (Caldwell et al., 2018) that DFT1 and DFT2 express both SahaI*27 and SahaI*27-1, therefore 4906-IFNg and RV each have five classical MHC class I alleles.

Two alleles were identified that were not included in the list of alleles from Caldwell and Siddle (2017). These were named SahaI*37/72/79 and SahaI*103 for analysis in this thesis, expressed in

two and one individual(s) respectively. These alleles were called in all three replicates in the individuals they were expressed in. Additionally, SahaI*37/72/79 was identical to three previously identified classical MHC class I alleles, and SahaI*103 matched an allele identified by Cheng et al. (2022), UB*06:02:01:01, confirming these sequences are unlikely to be artefacts.

5.5.1 Genotyping the d'Entrecasteaux population identified key DFT alleles for immune activation and evasion.

There is widespread expression of common alleles in the d'Entrecasteaux population; SahaI*27 (100%), SahaI*35 (66.7%), and SahaI*29 (55.6%) - the later has high similarity to SahaI*35. As a result, the antigenicity of SahaI*27 and SahaI*35 expressed by DFT1 and DFT2 genomes is very low to null (see 5.3.1).

These results correspond with classical MHC class I sequencing of devil populations across Tasmania presented by Cheng et al. (2022). SahaI*27 and SahaI*35 could not be linked to a single allele found by Cheng et al. (2022), due to long-read sequencing identifying alleles with sequence variations outside of the exon 2 – 3 amplicons used for Illumina sequencing. However, SahaI*27 amplicon matched seven alleles (UB*08:01:01:01, UB*12:01:01:01, UC*01:01:01:01, UC*01:01:01:02, UC*01:02:01:01, UC*01:04:01:01, and UC*04:05:01:01), and the SahaI*35 amplicon also matched seven alleles (UA*02:01:01:01, UA*02:01:01:02, UA*02:01:01:03, UA*02:01:01:04, UA*02:03:01:01, UA*02:03:02:01, and UA*05:02:01:01). Some of these sequences were highly expressed across the devil population (Cheng et al., 2022), particularly alleles matched with SahaI*27 (UC*01:01).

As the full classical MHC class I sequence cannot be identified from the short read data, and SahaI*27 and SahaI*35 relate to multiple sequences identified by Cheng et al. 2022, it may be that these called alleles are representing multiple allele sequences across the population. The sequences that matched SahaI*27 share amino acid sequence identities of 97.59% – 100%, and the sequences matched with SahaI*35 had sequence identities of 99.31% - 100%. These differences in amino acid sequence do not translate to differences at residues predicted to interact with the TCR. In summary, while the overall sequence between these alleles would differ, the polymorphic region in the α1 – α2 domain, which interacts with the TCR, is identical between them. Therefore, SahaI*27 and SahaI*35 still represent high expression of the same functional allele in the population.

Interestingly, SahaI*90 was commonly mismatched between tumour and host for both DFT1 and DFT2. This allele lacks a similar allele that is widely expressed in the population, such as SahaI*35 and SahaI*29, resulting in the lowest sequence identity/similarity for both DFT1 and DFT2 alleles.

In addition, the sequence differences translate to the highest mismatches at TCR and peptide residues in both DFT1 and DFT2. Therefore, SahaI*90 is predicted to be the most immunogenic allele in both cancers and is a key target for the design of vaccines and immunotherapies.

In terms of DFT1, the application of classical MHC class I genotyping in this population could be limited, as it only covers devils sequenced from the d'Entrecasteaux peninsula, where DFT2 emerged. DFT1, however, originated in North-eastern Tasmania. As the cancer has spread across most of Tasmania, it may have encountered different selective pressures due to differing classical MHC class I diversity in other populations. However, the mean sequence identity and similarity are the same for the full list of alleles from Caldwell and Siddle (2017) (identity 91.2%, similarity 92.5%) versus the called alleles (identity 91.2%, similarity 92.7%). Sequencing by Cheng et al. (2022) across Tasmania also found there was only one population of devils with lower classical MHC class I diversity (South-west), which is geographically isolated. The other populations, separated into North-western and Eastern, had the same level of diversity. Therefore, the d'Entrecasteaux peninsula is likely to be fairly representative of diversity in the population.

5.5.2 DFT classical MHC class I expression is not as simple as mismatch with the current host.

Though there was no correlation found between classical MHC class I loss, or immune activation, and host-tumour mismatch, this does not mean there is no link between the two. The number of matched hosts and tumours available was limiting (n=10 each for DFT1 and DFT2), with several tumours coming from the same individual. As such, there is likely not enough samples to properly assess correlation.

In addition, tumour cells will have encountered multiple hosts prior to the individual they were infecting when the sample was taken; therefore, immune recognition from previous hosts will play a role in MHC class I expression of the tumour. Thus, host-tumour classical MHC class I mismatch is likely to play a role in expression of MHC class I by the tumour, but there may not be a direct correlation between DFT expression and the MHC class I genotype of the current host.

From work on allograft rejection in Tasmanian devils, we know they can reject matched and mismatched skin grafts (Kreiss et al., 2011), therefore limited diversity in devil classical MHC class I alleles shouldn't prevent an immune recognition of mismatched DFT alleles expressed by tumour cells. The generation of antibody responses against DFT1 classical MHC class I has been found in two wild devils (Pye et al., 2016a), and demonstrated during vaccine trials (Pye et al., 2018; Tovar et al., 2017). Despite this, immune responses against DFT1 appear to be rare in the wild.

The apparent lack of immune response against tumours expressing classical MHC class I suggests there are other factors at play than classical MHC class I expression alone. A possible mechanism employed by the tumour cells is up- and down-regulation of classical MHC class I within a single host depending on the stage the tumour is at. This is an adaptation observed in CTVT, where the tumour cells downregulate classical MHC class I expression during early stages of infection and expression is upregulated at a later stage in response to cytokines, by which point the cancer has already been transmitted to a new host (Belov, 2011; Murgia et al., 2006). While this has not been studied in DFT1 or DFT2, and modelling of DFTs in Tasmanian devils is limited as they are an endangered species; DFT1 epigenetically downregulates classical MHC class I, and expression can be restored to the cell surface by treatment with inflammatory cytokine, IFNγ (Siddle et al., 2013) or overexpression of transcriptional coactivator, NLRC5 (Ong et al., 2021). For DFT2, our current cell lines are from early in the emergence of DFT2 (Pye et al., 2016b), therefore newer cell lines would be needed to investigate.

5.5.3 High expression of a common allele is advantageous for DFT2.

Based on relative read data, DFT2 expresses higher levels of SahaI*27 (57.7%) than other classical MHC class I alleles; agreeing with previous sequencing of DFT2 cell lines (Caldwell et al., 2018). This is also reflected in higher expression of SahaI*27 heavy chains by DFT2 cells (Gastaldello et al., 2021). As SahaI*27 is highly expressed both in the population and at an individual level, this allele is the least immunogenic; expression of this allele by DFT2 above other classical MHC class I could prevent host immune recognition by ‘shielding’ other alleles against recognition by T cells.

High expression of SahaI*27 may be an advantage afforded by the founder devil, as some individuals express high levels of SahaI*27 (Figure 5.7B). Or it could have evolved over time, either through upregulation of SahaI*27, or downregulation of other classical MHC class I alleles in response to immune pressures. The modulation of specific MHC class I alleles by cancer cells is well documented (Dhatchinamoorthy et al., 2021; Jongsma et al., 2021), however, this is often through loss of expression, such as loss of heterozygosity or modifications to the peptide presentation pathway, while upregulation of classical MHC class I alleles is not common in cancer. Current DFT2 cell lines were taken from tumours early in the emergence of the cancer (Pye et al., 2016b); therefore, it would be interesting to study allele expression levels in DFT2 cells taken from more recent tumours.

5.5.4 Classical MHC class I alleles were downregulated by DFT1.

While DFT1 also expresses 2 alleles common in the population, SahaI*27 and SahaI*35, it expresses similar levels of all four assigned alleles at the RNA level, which could be an artificial finding due to upregulation of the genes by IFNγ treatment. However, isolation of MHC class I heavy chains found the highest allele expressed by DFT1 (treated with IFNγ) was SahaI*35, with a low level of SahaI*90 and no expression of other classical MHC class I (Gastaldello et al., 2021). This variation in protein expression, despite roughly equal transcription, could be historical, where DFT1 downregulated expression of specific alleles prior to a total loss of MHC class I via epigenetic modification (Siddle et al., 2013).

Of interest is the lack of SahaI*27 expression at the protein level, as, based on population sequencing, the expression of SahaI*27 is unlikely to result in an immune response. This could indicate that DFT1 emerged in an area with lower expression levels of SahaI*27 in the population, resulting in immune recognition by hosts lacking the allele, and subsequent downregulation by DFT1. DFT1 might not have had the same advantage as DFT2 of expressing MHC class I alleles that are common in the area it emerged. Combined with the rapid spread across Tasmania, DFT1 may have been exposed to stronger selective pressure from the immune system than DFT2, which lead to total downregulation of classical MHC class I.

5.5.5 Implications and further study

The results presented in this chapter indicate the expression of common alleles in the population confers an advantage to DFT2 for evading the host immune system. DFT2 expressed high levels of an allele expressed in all devils sequenced. This was based on a cell line developed early in the evolution of DFT2, therefore newer cell lines are needed to investigate how classical MHC class I expression levels have changed as the tumour cells spread through the population, particularly as there is total loss of classical MHC class I expression in some DFT2 tumours (shown in Chapter 3).

Conversely, despite expressing RNA for all four assigned alleles (following IFNγ treatment) at equal levels, DFT1 only expresses heavy chains for two alleles. This may reduce the likelihood of host recognition when classical MHC class I is upregulated. While there is the chance of T cell recognition of mismatched alleles, upregulation of classical MHC class I may be upregulated in response to the local immune environment, like CTVT, and prevent activation of NK cells in response to lack of MHC class I on the cell surface.

No correlation was found between host-tumour classical MHC class I mismatch and classical MHC class I expression by tumour cells, however, sample numbers were low. To confidently draw

conclusions about the effect of host-tumour mismatch as an ongoing driver of MHC class I loss by DFT2, more host samples need to be sequenced with matched tumour samples. Gaining a greater understanding of MHC class I host-tumour mismatch is important for understanding how DFTs are evolving, and is important for the development of vaccines. Based on these results, SahaI*90 is the best MHC class I candidate for a vaccine target.

Chapter 6 Investigation of non-classical MHC class I expression in DFT1

6.1 Introduction

Downregulation of classical MHC class I by DFT1 cells explains the lack of T cell response to these tumours. However, an NK cell response to a lack of MHC class I on the cell surface, called 'missing self', would be expected. Tasmanian devils have functional NK cells (Brown et al., 2011) but an immune response against DFT1 is rarely observed. Plasticity in classical MHC class I expression afforded by epigenetic mutations in the peptide presentation pathway (Burr et al., 2019; Siddle et al., 2013) could allow DFT1 cells to upregulate expression in response to the local environment. This would overcome NK cell activation but would once again put tumour cells at risk of T cell recognition. Thus, we would expect strong selective pressure from the host immune system for development of further immune evasion mechanisms in DFT1 cells.

Some cancers upregulate non-classical MHC class I molecules to induce immunotolerance (Kochan et al., 2013), as non-classical MHC class I have a role in immunosuppression; for example, they are expressed by trophoblasts at the maternal-foetal barrier in the placenta to prevent rejection of the foetus by the maternal immune system (Djurisic and Hviid, 2014; Tersigni et al., 2020). Non-classical MHC class I molecules often have limited polymorphisms, so are less likely to be recognised as 'non-self' by T cells, while their expression on the cell surface provides an inhibitory ligand for NK cells (Allen and Hogan, 2013).

Previous studies have found expression of non-classical MHC class I in DFT1 tumours. A DFT1 tissue biopsy expressed devil non-classical Saha-UD and Saha-UK (Cheng and Belov, 2014). However, whether the expression originated in host or tumour cells was not confirmed in this study. Further, Saha-UD heavy chain protein was confirmed in a DFT1 cell line treated with IFNγ (Gastaldello et al., 2021). We hypothesise that, in DFT1 tumours where classical MHC class I has been downregulated, non-classical MHC class I molecules could be upregulated to prevent an NK cell response to 'missing self'.

To investigate non-classical MHC class I expression by DFT1 tumours, 76 tumour biopsies were stained by IHC for non-classical MHC class I molecules, Saha-UD and Saha-UK. Antibodies against devil non-classical, Saha-UD and Saha-UK were generated in our lab previously (Caldwell, 2018; Caldwell et al., 2018). The anti-Saha-UK antibody was validated by Caldwell et al. (2018), and the Saha-UD antibody screened during my master's degree (Hussey, 2018), but was not validated. In

this chapter, the anti-Saha-UD antibody was validated using Western blots to test antibody specificity and IHC controls. As with classical MHC class I staining (see Chapter 3), IHC staining of tumour biopsies was quantified via expression scoring based on strength of staining, using semi-automated image analysis. Serial sections of tumours were used for IHC, enabling comparison between classical and non-classical MHC class I expression scores. Non-classical MHC class I expression scores were assessed in relation to immune markers, IFNγ and CD3, to assess whether they are immunosuppressive in DFT1 tumours.

6.1.1 Aims and objectives

This chapter addresses Hypothesis 2, "DFT1 expresses non-classical MHC class I to evade the host immune response" (see Chapter 1 – Section 1.5):

> Aim 5: Investigate non-classical MHC class I expression in primary DFT1 tumours.
>
> Aim 6: Investigate whether non-classical MHC class I expression correlates with a 'colder' tumour immune environment.

The objectives of this chapter are:

1. Validate an antibody against devil non-classical MHC class I, Saha-UD.
2. Stain DFT1 biopsies by IHC using devil-specific non-classical MHC class I antibodies, Saha-UD and Saha-UK.
3. Compare classical and non-classical MHC class I expression scores.
4. Compare non-classical MHC class I expression to IHC staining for immune markers (CD3 and IFNγ)

6.2 Anti-Saha-UD antibody, α-14-37-3, specifically bind recombinant non-classical Saha-UD protein.

Monoclonal antibodies against devil non-classical, Saha-UD were previously generated by Caldwell (2018) and screened by Hussey (2018). Screening of eight Saha-UD antibodies using FFPE devil spleen samples identified two antibodies that give strong staining by IHC with minimal background staining (Hussey, 2018; Hussey et al., 2022). These two antibodies, α-14-37-3 (labelled as UD(3) in Figure 6.1) and α-14-37-5 (UD(5)), were tested for their specificity to Saha-UD via Western blot.

A recombinant protein was produced for non-classical, Saha-UD to run as a positive control for Saha-UD antibodies. Coomassie gels and Western blots showing induction of Saha-UD

recombinant protein production are shown in Appendix Figure E 1. Recombinant Saha-UD heavy chain protein was stained with the UD(3) and UD(5) antibodies, along with a pan specific anti-Saha-UA-UB-UC antibody, α-UA/UB/UC_15-25-8, and an anti-Saha-UK antibody, α-UK_15-29-1 (Caldwell et al., 2018) (hereafter referred to as UABC and UK antibodies respectively) as negative controls (Figure 6.1A). UD(3) and UD(5) both identified Saha-UD recombinant protein, giving bands at ~44 kDa, the size expected for the recombinant protein. UD(5) produced stronger staining, but also stained for multiple bands above and below the ~44 kDa band for Saha-UD, which were not seen on the UD(3) blot. This was likely non-specific staining of other proteins in the bacterial lysate, as the Saha-UD recombinant protein was not purified prior to Western blot analysis. The UABC and UK antibodies both gave a very faint band for Saha-UD, validating that these antibodies do not have a strong affinity for non-classical Saha-UD.

Recombinant MHC class I heavy chain proteins, classical Saha-UC and non-classical Saha-UK, previously produced in our lab (Caldwell, 2018), were probed with the anti-Saha-UD antibodies to exclude the possibility of cross-reactivity with closely related devil MHC class I heavy chain proteins (Figure 6.1B). As expected, the UABC and UK antibodies stained for Saha-UC (~38 kDa) and Saha-UK (~35 kDa) recombinant proteins respectively, with the UK antibody also binding weakly to the Saha-UC protein. For their respective proteins, there were additional bands at a lower molecular weight. As these were purified recombinant protein samples, the bands are likely due to protein degradation resulting from freeze-thawing. This was tested by running the proteins on an SDS-PAGE gel and staining with Coomassie Blue, where the same bands were observed (Appendix Figure E 2). The UD(3) antibody produced very faint bands for Saha-UC and Saha-UK recombinant proteins. As devil classical MHC class I molecules have a high sequence similarity (Caldwell and Siddle, 2017), the result observed for Saha-UC is expected to reflect all classical MHC class I. Therefore, these results indicate the UD(3) antibody does not have a strong binding affinity for either classical MHC class I or non-classical Saha-UK and is specific for non-classical Saha-UD. The UD(5) antibody didn't produce a band for Saha-UK protein, however it did stain for Saha-UC (~38 kDa), therefore it is not a specific antibody against non-classical MHC class I, Saha-UD (Figure 6.1B).

To further validate the specificity of the UD(3) antibody, serial lymph node samples were stained using a mouse IgG2a isotype control antibody and a secondary only control (Figure 6.1C). As Saha-UD antibody, α-14-37-3 was specific for recombinant Saha-UD heavy chain (Figure 6.1A&B) and produced negative secondary and isotype controls (Figure 6.1C), it was used to investigate Saha-UD expression in DFT1 FFPE tumour biopsies by IHC.

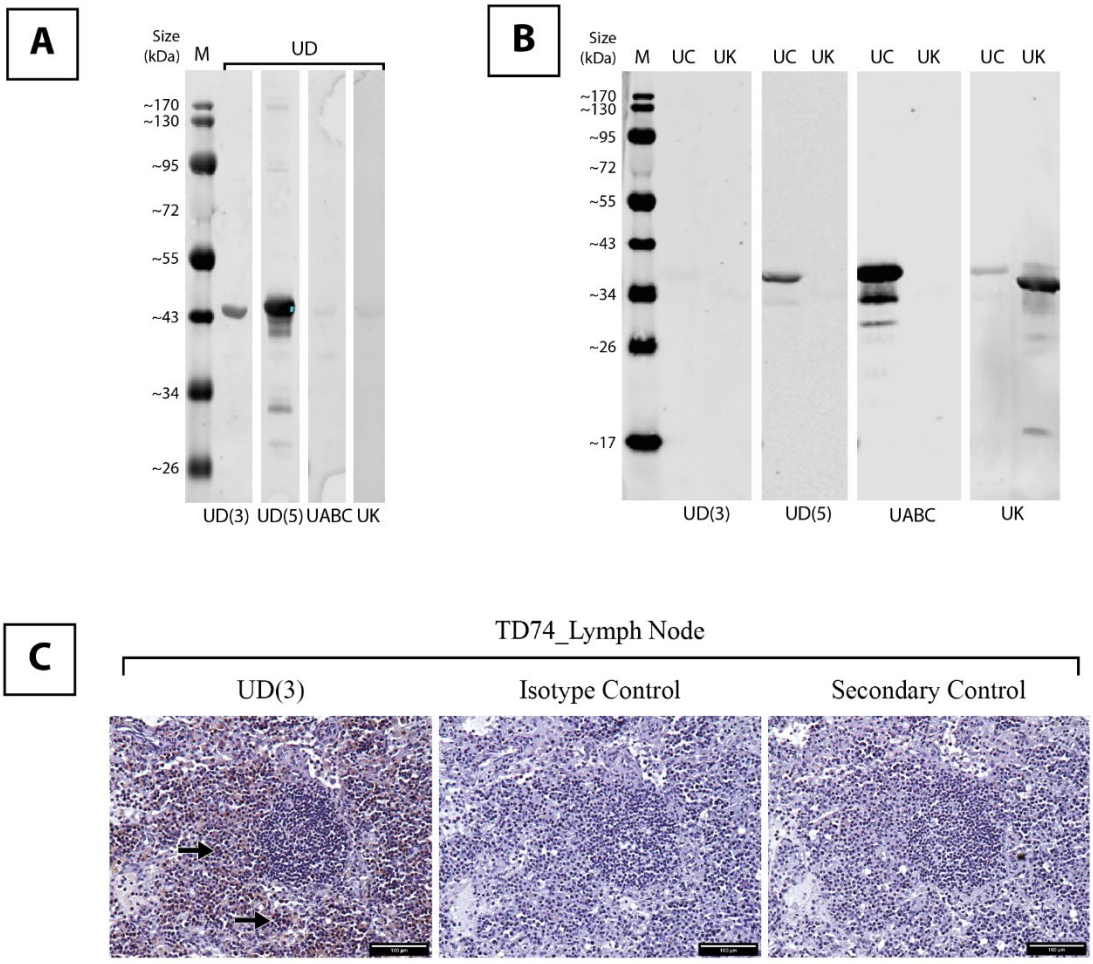

Figure 6.1 Non-classical, Saha-UD antibody α-14-37-3 is specific for Saha-UD recombinant protein.

(A) & (B) Two anti-Saha-UD antibodies, clones α-UD_14-37-3 (UD(3)) and α-UD_14-37-5 (UD(5)) were screened by Western blot for protein specificity. Blots were stained with antibodies against classical Saha-UA, -UB, and -UC (UABC), α-UA/UB/UC_15-25-8, and non-classical Saha-UK (UK), α-UK_15-29-1, as positive controls for their respective proteins and negative controls for other MHC class I. Blots were run with: **(A)** recombinant Saha-UD heavy chain protein, **(B)** recombinant Saha-UC and Saha-UK heavy chain proteins. **(C)** Formalin-fixed paraffin-embedded Tasmanian devil submandibular lymph node samples were stained by immunohistochemistry with the α-UD_14-37-3 (UD(3)) anti-Saha-UD antibody, along with secondary antibody only and an IgG2a isotype antibody as controls. Images were taken at 200x magnification. Positive cells are stained brown, nuclei are stained blue. Black arrows indicate cells with positive staining. Scale bars = 100 µm.

6.3 DFT1 tumour cells express non-classical, Saha-UD and Saha-UK

To investigate Saha-UD expression in DFT1, the validated UD(3) antibody (α-14-37-3) was used to stain 76 DFT1 tumour biopsies (supplied by Dr Rodrigo Hamede and Prof Gregory Woods, University of Tasmania) by IHC, collected from 56 individuals between May 2006 – April 2022. Some tumour sections were stained by master's students, Ella Milne and Neve Prowting, under my supervision. To quantify IHC staining, an expression score was generated based on the strength of staining in areas of tumour cells, with 0 indicating no staining, and 4 representing strong staining. Expression scores were assigned by automated image analysis in Image J and Fiji (see Methods Section 2.5.2), and manually checked for accuracy.

IHC analysis confirmed Saha-UD is expressed by DFT1 tumour cells (Figure 6.2); though expression levels are variable, and it is not expressed by all tumours. Levels of Saha-UD expression by DFT1 tumours appears to have changed little over time, however analysis is limited due to low sample numbers pre-2013.

Saha-UD was expressed in 61 DFT1 tumours (80.3%) (see Figure 6.3). Lower expression levels were common, with 46.1% (35 tumours) assigned an expression score of 1, and 19.7% (15 tumours) an expression score of 2. Higher expression scores of 3 and 4 were least common, at 10.5% (8 tumours) and 3.9% (3 tumours), respectively.

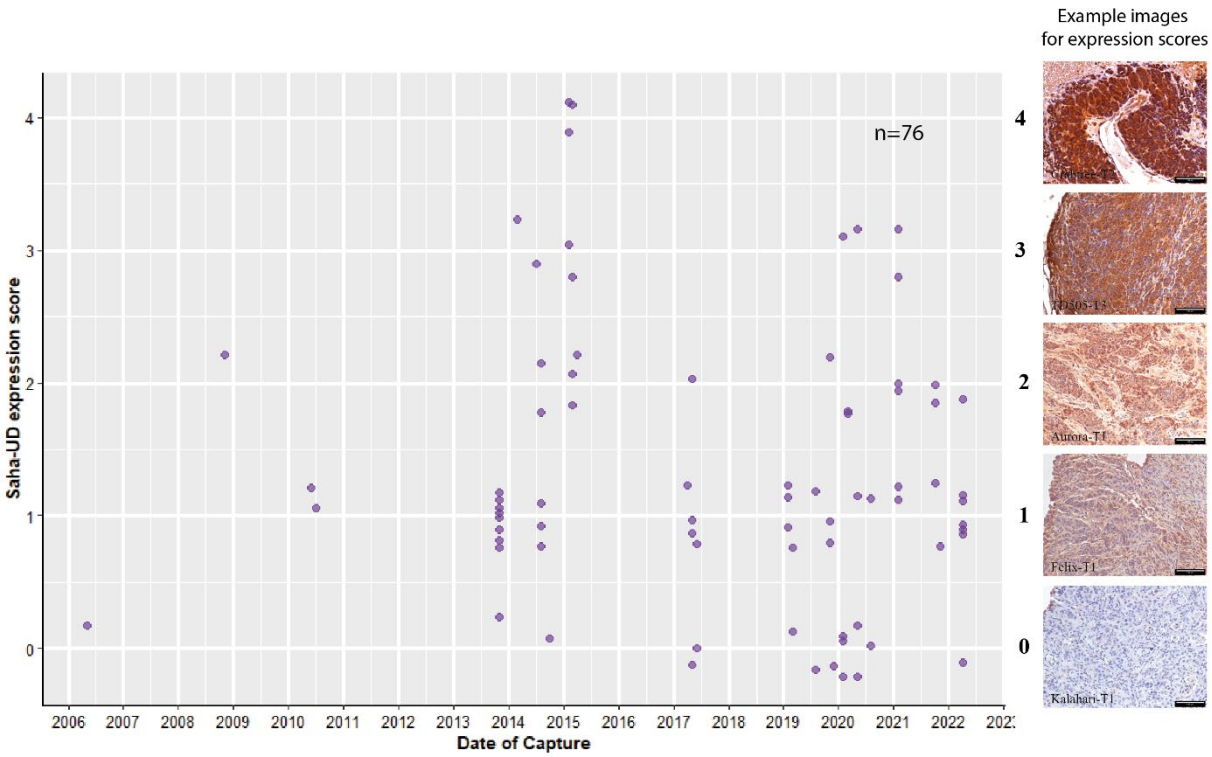

Figure 6.2 Non-classical, Saha-UD expression is highly variable in DFT1 tumours.

Non-classical, Saha-UD expression in DFT1 tumour biopsies over time (n=76). Saha-UD expression scores, based on the strength of IHC staining, are plotted against the sample collection date (Date of Capture). 0 = no staining for classical MHC class I, 4 = very strong staining. Expression scores are discrete variables – jitter has been applied to the data points for visualisation. Example images for expression scores are shown to the right of the graph. IHC images were taken at 200x magnification. Positive cells are stained brown; nuclei are stained blue. Scale bars = 100 µm.

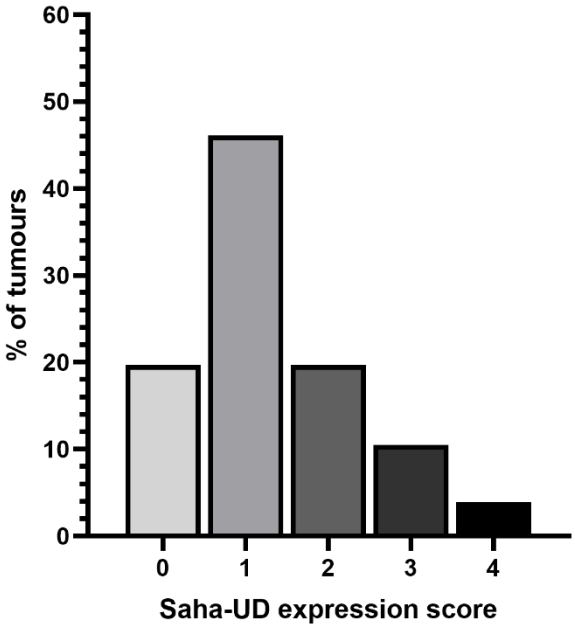

Figure 6.3 Most DFT1 tumours express non-classical, Saha-UD.

Percentage of DFT1 tumours (n=76) assigned each expression score for non-classical MHC class I, Saha-UD staining by IHC. 0 = no IFNγ staining, 4 = strong IFNγ staining.

To verify positive Saha-UD expression observed by IHC, 10 primary DFT1 samples stored in RNAlater, taken from the same tumours stained by IHC, were tested by RT-PCR (Figure 6.4). Included in this analysis were 3 DFT1 cell lines (DFT1_1426, DFT1_4906, and DFT1_C5065), and devil spleen (Spleen_TD209) as a positive control. Samples were amplified using primers specific for Saha-UD and a ribosomal protein, RPL13A, as a control (primers detailed in Table 2.4). Consistent with previous results, DFT1 cell lines were positive for Saha-UD heavy chain (Caldwell et al., 2018; Gastaldello et al., 2021; Pye et al., 2016b). All DFT1 primary tumours were positive by IHC and RT-PCR, confirming the results obtained with the UD(3) antibody. Tumours negative for Saha-UD were not tested by RT-PCR, as samples stored in RNAlater were not available. These results confirm Saha-UD expression in DFT1 tumours from different individuals, but it is difficult to compare expression levels as, based on the IHC results, some contamination from host cells is expected in the biopsies.

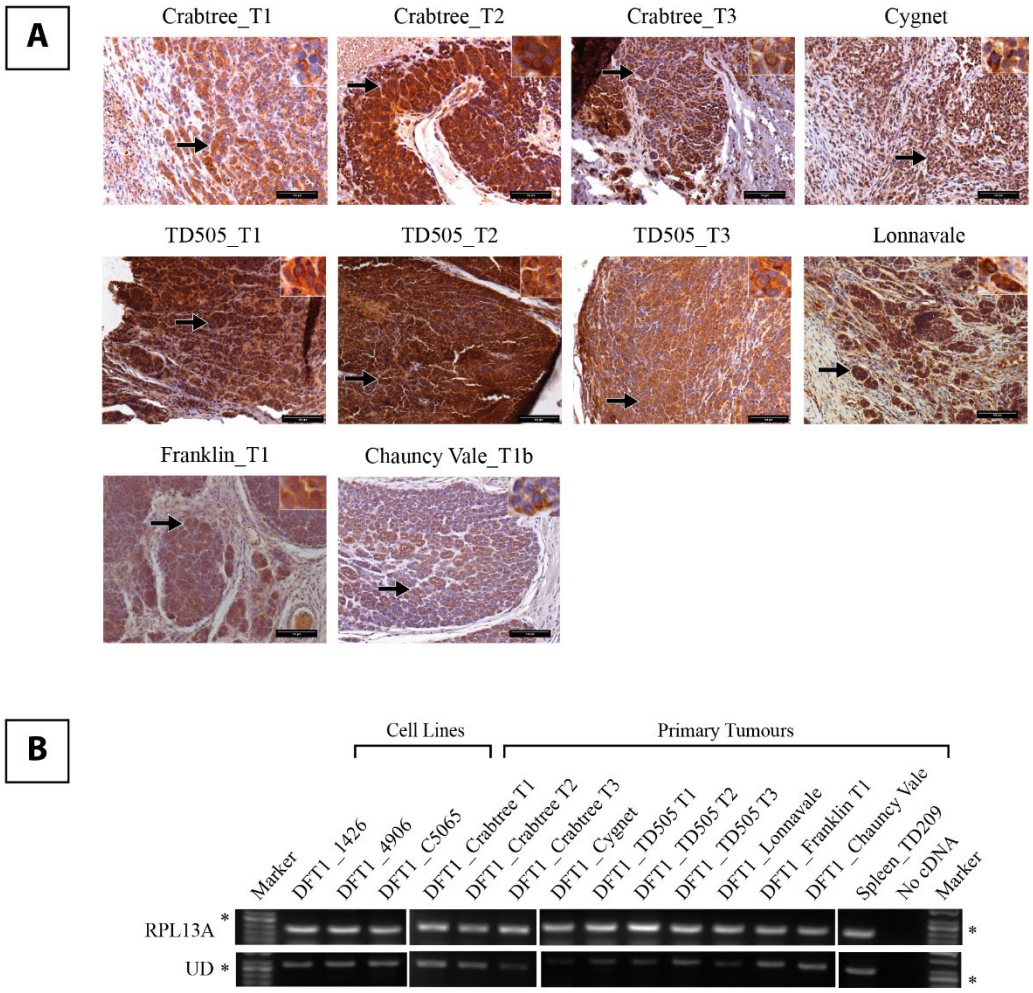

Figure 6.4 Confirmation of non-classical MHC class I expression detected by a Saha-UD antibody.

(A) Immunohistochemistry (IHC) staining of formalin-fixed paraffin-embedded (FFPE) DFT1 tumour samples using anti-Saha-UD antibody, α-14-37-3. Black arrows indicate DFT1 tumour cells with positive staining for Saha-UD. Images taken at 200x magnification. Positive cells are stained brown, nuclei are stained blue. Scale bars = 100 µm. **(B)** RT-PCR for Saha-UD on DFT cell lines and primary tumours, matched to DFT1 tumours stained by IHC. RPL13A, encoding a ribosomal protein, was used as a loading control. A no cDNA control is included for each. Asterisks indicate 300 bp on the DNA ladder.

Seventy-four DFT1 biopsies (collected from 56 individuals) were also stained for expression of non-classical MHC class I, Saha-UK, using antibody clone α-15-29-1, previously used in our lab (Caldwell et al., 2018), by IHC. Tumours were analysed using the same expression scoring method as classical MHC class I and non-classical, Saha-UD, described above.

Thirty-seven DFT1 tumours stained positively for non-classical, Saha-UK. Expression scores for Saha-UK are less variable than Saha-UD, and Saha-UK expression scores do appear to increase over time (Figure 6.5), however, this may be an artefact of low sample numbers for earlier dates. Overall, DFT1 tumours were assigned lower expression scores (Figure 6.6), with over half of tumours negative for expression (expression score of 0) at 50.7% (38 tumours). Most tumours that stained for Saha-UK were assigned an expression score of 1 (36.0%, 27 tumours). Only 10.7% (8 tumours) and 2.7% (2 tumours) were assigned expression scores of 2 and 3, respectively, and no tumours had an expression score of 4.

It is important to note that differences in expression scores between Saha-UD and Saha-UK might not be reflective of different expression levels between the two proteins. These differences may be the result of different antibody affinities between Saha-UD and Saha-UK; therefore, their expression scores cannot be directly compared.

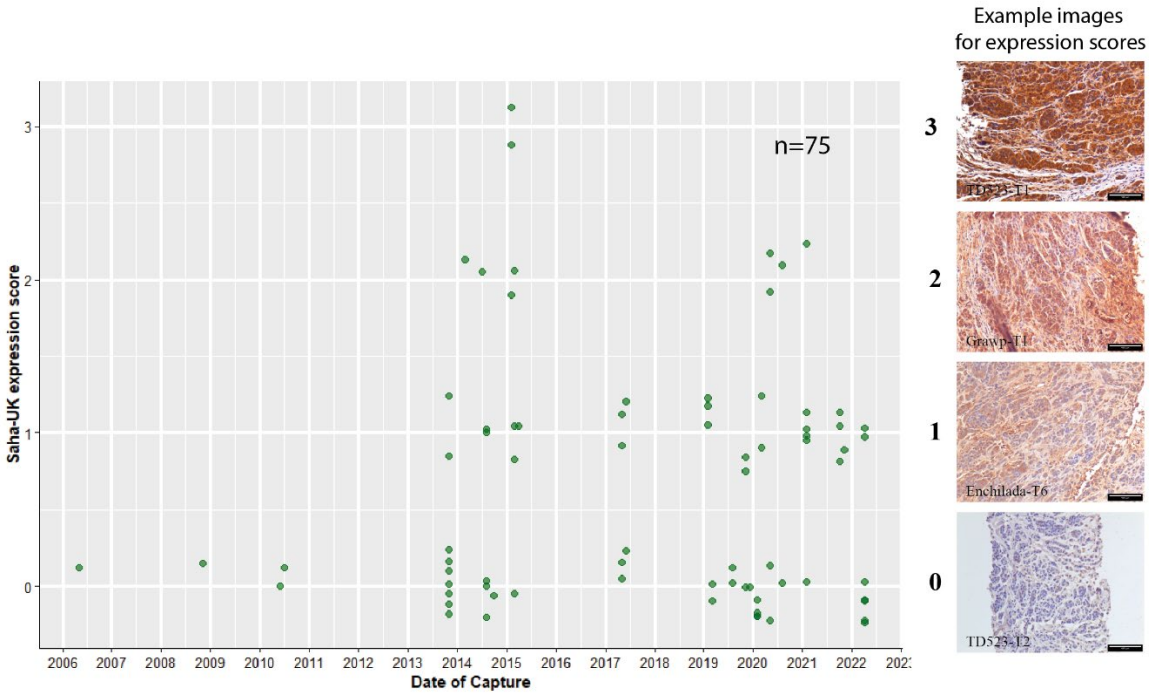

Figure 6.5 Some DFT1 tumours express non-classical, Saha-UK.

Non-classical, Saha-UK expression in DFT1 tumour biopsies over time (n=75). Saha-UK expression scores, based on the strength of IHC staining, are plotted against the sample collection date (Date of Capture). 0 = no staining for classical MHC class I, 4 =

very strong staining. Expression scores are discrete variables – jitter has been applied to the data points for visualisation. Example images for expression scores are shown to the right of the graph. IHC images were taken at 200x magnification. Positive cells are stained brown; nuclei are stained blue. Scale bars = 100 μm.

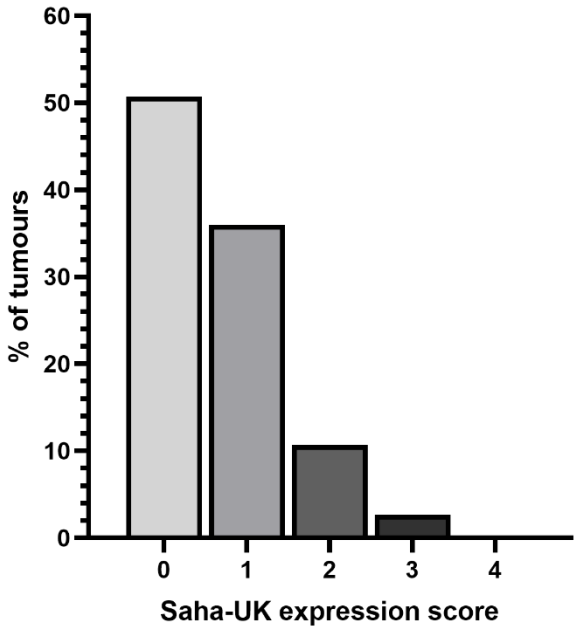

Figure 6.6 Non-classical, Saha-UK expression in DFT1 tumours is low.

Percentage of DFT1 tumours (n=75) assigned each expression score for non-classical MHC class I, Saha-UK staining by IHC. 0 = no IFNγ staining, 4 = strong IFNγ staining.

6.3.1 MHC class I expression is variable within tumours.

Thirty-three biopsies were collected at the same time as another biopsy from the same devil (n=14). As these tumours are exposed to the same immune system, it is interesting to study whether they differ in non-classical MHC class I expression. For Saha-UD, there are only slight differences in expression scores between biopsies taken from the same host (Figure 6.7A). The majority of biopsies (82.4%) taken from the same devil have the same expression score or differ by an expression score of 1. However, there are two devils, Bump and Orange, whose tumours differ by an expression score of 3. Both devils have a tumour negative for Saha-UD and a tumour with an expression score of 3. Orange was capture twice; the first time (February 2020), both

tumours were negative for Saha-UD, while from the second captured (May 2020), one tumour had developed high Saha-UD expression (score of 3).

In addition to the variations in Saha-UD expression between DFT1 tumours, there was heterogeneity within tumours (Figure 6.7B). Heterogeneity was classed as samples that contained tumour cells with high-moderate Saha-UD expression and tumour cells that were low-negative. At least 17 tumours (50%) had intra-tumour heterogeneity for non-classical Saha-UD expression, where strong/moderate Saha-UD-positive tumour cells neighbour tumour cells with weaker staining, or no staining at all. For over half of these tumours, this was observed throughout the tumour, for example, Crabtree T3, Nudibranch T1, TD505 T2, and TD505 T3 (Figure 6.7B). Other tumours had areas with consistent Saha-UD expression, either positive or negative, in addition to areas with interspersed tumour cells of varying Saha-UD expression, as observed in Crabtree T1, Crabtree T2, Grommit, and Maui T1 (Figure 6.7B). Interestingly, there was no clear pattern for areas that were high expressing and areas that were low or negative.

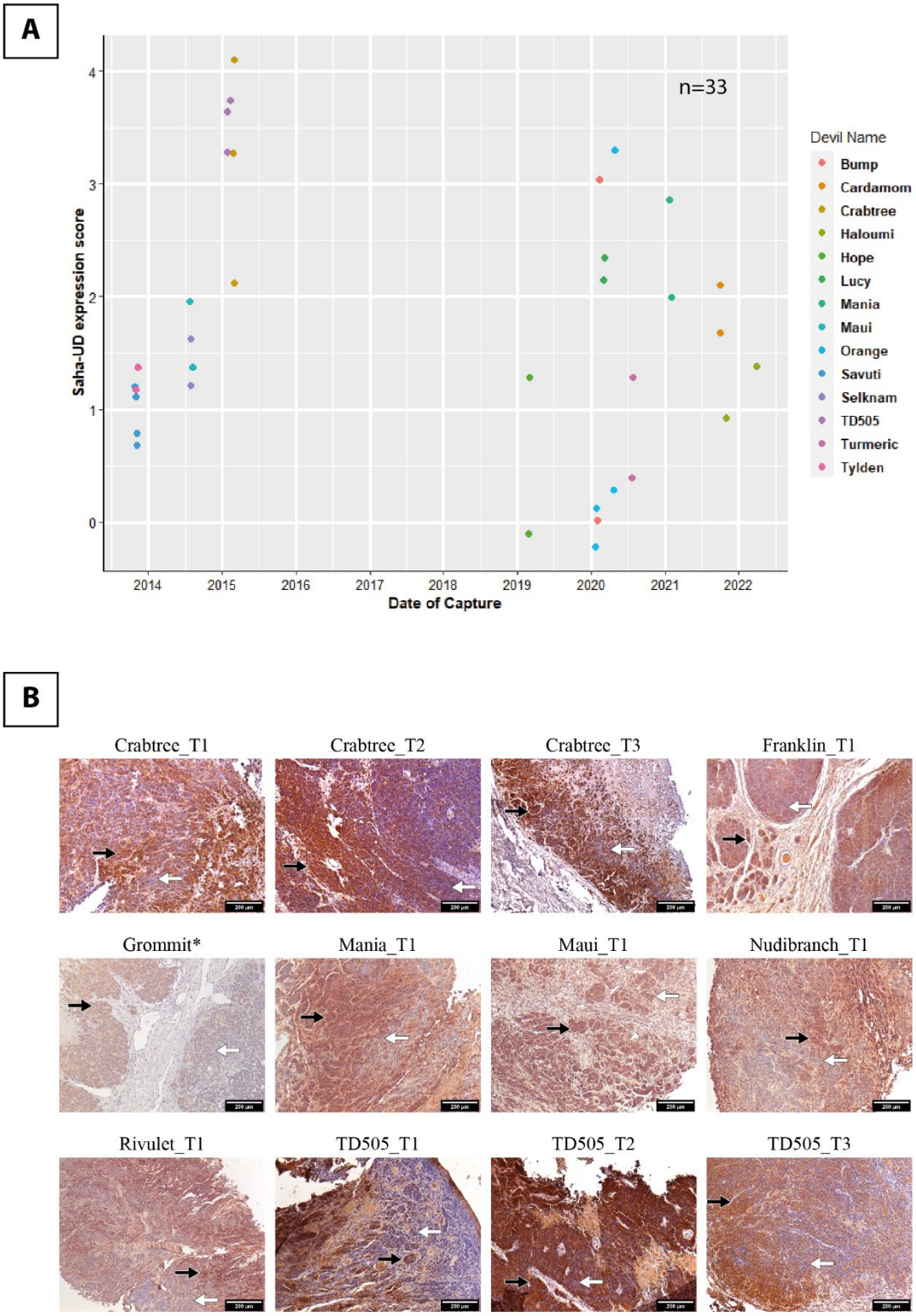

Figure 6.7 Non-classical, Saha-UD expression can be highly variable within DFT1 tumours.

(A) Non-classical MHC class I, Saha-UD expression in DFT1 tumour biopsies over time, for samples collected from the same host (n=33). Saha-UD expression scores, based on the strength of IHC staining, are plotted against the sample collection date (Date of Capture). 0 = no staining for classical MHC class I, 4 = very strong staining. Expression scores are discrete variables – jitter has been applied to the data points

for visualisation. **(B)** IHC images for FFPE DFT1 tumour samples showing heterogeneous intra-tumour staining for Saha-UD. Black arrows indicate DFT1 tumour cells with strong staining for Saha-UD, white arrows indicate DFT1 tumour cells that are negative or have lower levels of staining for Saha-UD. Images taken at 100x magnification. Positive cells are stained brown, nuclei are stained blue. Scale bars = 100 µm.

For Saha-UK, tumours in the same host have the same expression score or vary by an expression score of 1, the same as observed for Saha-UD (Figure 6.8A). There were two devils whose tumours had a greater difference in expression scores: Orange and TD505. Both devils have two tumour biopsies, one negative and the another assigned an expression score of 2. Orange was captured twice and, as with Saha-UD, both biopsies from the first capture in February 2020 were negative for Saha-UK, while on the second capture (May 2020) one tumour had a higher expression score of 2 for Saha-UK. Interestingly, the hosts with tumours that varied by an expression score of greater than 1 for Saha-UD (Figure 6.7A) or Saha-UK (Figure 6.8A) were not the same hosts that varied by an expression score of greater than 1 for classical MHC class I (Figure 4.2A).

Some DFT1 tumours were also heterogenous for Saha-UK expression (Figure 6.8B). There were fewer heterogenous tumours for Saha-UK (five tumours) than Saha-UD, but this may be because there are few tumours expressing Saha-UK. As with Saha-UD, all heterogenous tumours had higher expressing tumours cells near lower expressing, or negative, tumour cells. Two tumours, Rivulet T1 and Turmeric T1 (Figure 6.8B), also had areas of tumour cells that were consistently negative or positive for Saha-UK, in addition to areas with neighbouring heterogenous cells.

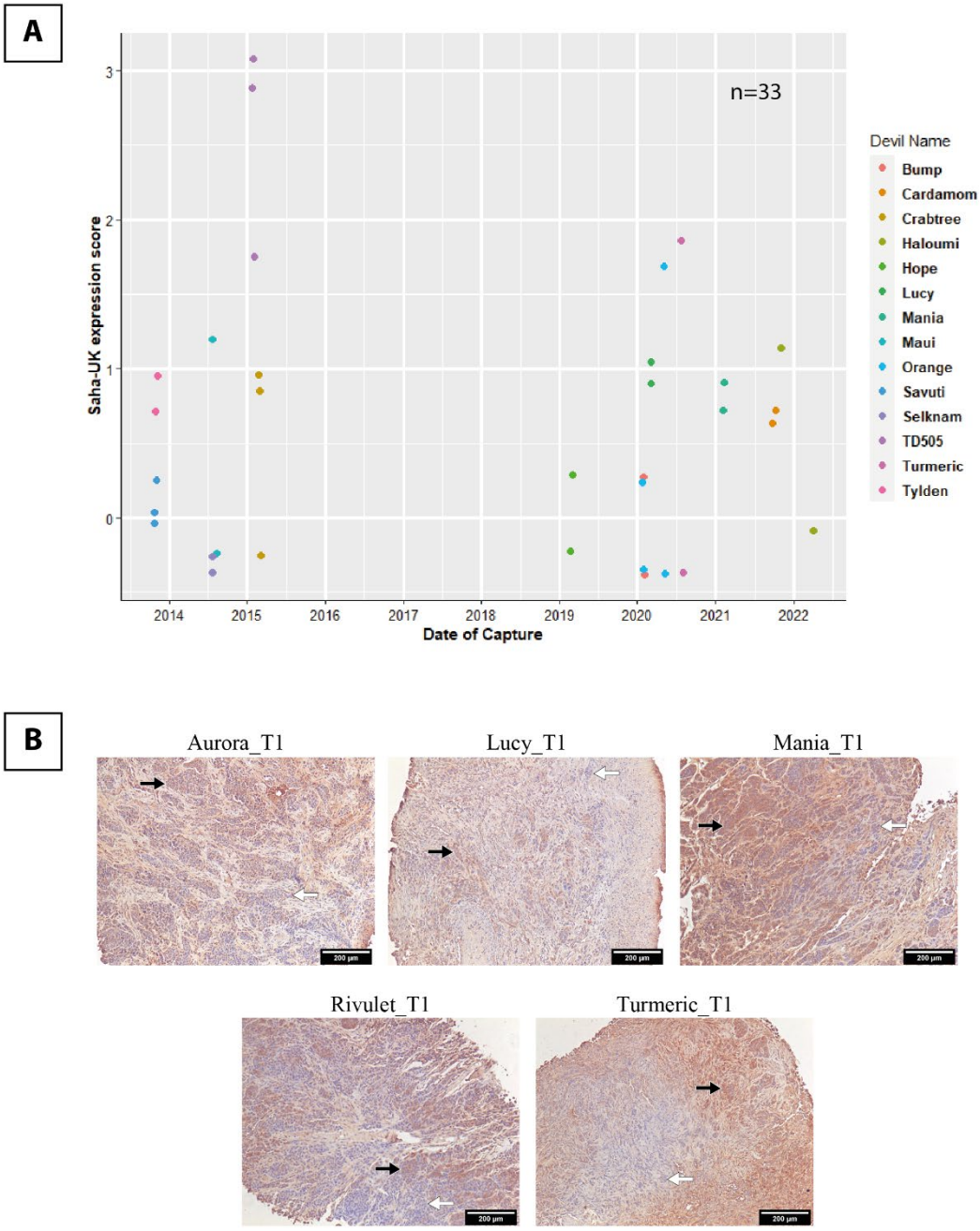

Figure 6.8 Non-classical, Saha-UK expression can vary within DFT1 tumours.

(A) Non-classical MHC class I, Saha-UK expression in DFT1 tumour biopsies over time, for samples collected from the same host (n=33). Saha-UK expression scores, based on the strength of IHC staining, are plotted against the sample collection date (Date of Capture). 0 = no staining for classical MHC class I, 4 = very strong staining. Expression scores are discrete variables – jitter has been applied to the data points for visualisation. **(B)** IHC images for FFPE DFT1 tumour samples showing heterogeneous intra-tumour staining for Saha-UK. Black arrows indicate DFT1 tumour cells with strong staining for Saha-UK, white arrows indicate DFT1 tumour cells that are negative or have lower levels of staining for Saha-UD. Images taken at

100x magnification. Positive cells are stained brown, nuclei are stained blue. Scale bars = 100 µm.

Non-classical MHC class I expression by DFT1 was investigated as an immunomodulatory mechanism for preventing recognition of 'missing self' due to a lack of classical MHC class I expression. As some DFT1 tumours were heterogenous for expression of non-classical Saha-UD and Saha-UK, DFT1 tumours were assessed for classical MHC class I heterogeneity. If non-classical MHC class I expression is being upregulated to protect tumour cells that have lost classical MHC class I expression, we would expect areas of higher non-classical MHC class I expression in heterogeneous tumour to correlate with areas of lower classical MHC class I.

As expected, some DFT1 tumours were heterogenous for classical MHC class I expression (examples shown in Figure 6.9). Of the 14 tumours heterogenous for classical MHC class I, seven were also heterogenous for either non-classical, Saha-UD or Saha-UK. Two of these tumours were also heterogeneous for Saha-UK, Aurora T1 and Mania T1. Mania T1 was also heterogeneous for Saha-UD, along with five other tumours: Crabtree T2, Franklin T1, Maui T1, TD505 T3, and Tiarna. Serial sections of tumour biopsies were stained by IHC to enable comparison between MHC class I staining. For tumours that were heterogenous for both classical and non-classical (either Saha-UD or Saha-UK), while not identical, both had similar patterns of expression, where classical and non-classical MHC class I were expressed in similar areas (except for Aurora T1 and Franklin T1).

As tumours are not always heterogeneous for both classical and non-classical MHC class I, expression of non-classical MHC class I is not solely based on classical MHC class I expression in the tumour. However, correlation in expression patterns between DFT1 tumours that are heterogeneous for both classical MHC class I and non-classical Saha-UD, suggests Saha-UD can be related to that of classical MHC class I expression by tumour cells, whether directly or indirectly.

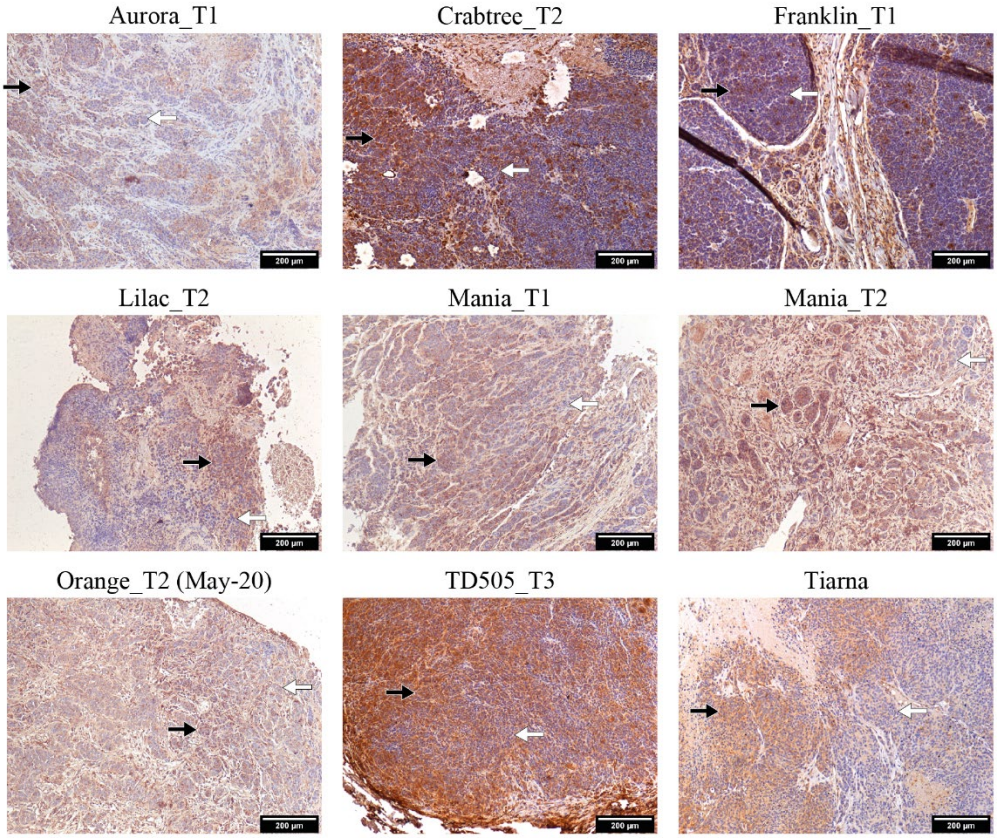

Figure 6.9 Classical MHC class I expression can be highly variable within DFT1 tumours.

IHC images for FFPE DFT1 tumour samples showing heterogeneous intra-tumour staining for Classical MHC class I. Black arrows indicate DFT1 tumour cells with strong staining, white arrows indicate DFT1 tumour cells that are negative or have lower levels of staining for classical MHC class I. Images taken at 100x magnification. Positive cells are stained brown, nuclei are stained blue. Scale bars = 100 µm.

6.4 Non-classical expression by DFT1 correlates with classical MHC class I expression.

Based on our hypothesis that non-classical Saha-UD is upregulated in DFT1 tumours to prevent NK cell activation due to 'missing self', we would expect higher levels of Saha-UD expression when there is lower classical MHC class I expression. To compare expression of classical MHC class I Saha-UA, -UB and -UC with that of non-classical Saha-UD (n=76) and Saha-UK (n=75), serial sections of DFT1 tumours were stained, and the expression scores plotted against each other (Figure 6.10).

Instead of an inverse correlation between classical and non-classical MHC class I expression, predicted by the hypothesis, a strong positive correlation was observed for both Saha-UD (Figure 6.10A; Spearman's correlation, rho=0.167, t=3.04x10^{-9}, p<0.05) and Saha-UK (Figure 6.10B; Spearman's correlation, rho=0.532, t=9.22x10^{-7}, p<0.05). Despite a positive correlation between classical and non-classical MHC class I expression, classical MHC class I and non-classical, Saha-UD or Saha-UK are not always co-expressed in a tumour. Notably, 22 tumours (28.9%) expressed low levels of Saha-UD, but not classical MHC class I. This fits the hypothesis that non-classical MHC class I will be upregulated when classical MHC class I expression is lost by tumour cells. There were also eight (10.7%) tumours that expressed non-classical, Saha-UK, which did not express classical MHC class I. However, the majority of tumours do not follow this pattern.

Expression scores were also compared between non-classical, Saha-UD and Saha-UK (Figure 6.11). There was a strong positive correlation between Saha-UD and Saha-UK expression (Spearman's correlation, rho=0.626, t=1.95x10^{-9}, p<0.05). Twenty-four DFT1 tumours (32.0%) expressed Saha-UD and not Saha-UK, while only one tumour expressed Saha-UK and not Saha-UD.

This could be due to differences in antibody affinities, which is unconfirmed. However, recombinant protein titration by Western blot indicates anti-Saha-UK antibody, α-UK_15-29-1, has a higher affinity for its target protein than anti-Saha-UD antibody, α-14-37-3 (Appendix Figure E 3). If antibody affinity by Western blot is reflective of affinity by IHC, DFT1 tumours more frequently express Saha-UD than Saha-UK *in vivo*. Potentially indicating non-classical MHC class I, Saha-UD is more valuable for immune evasion than Saha-UK.

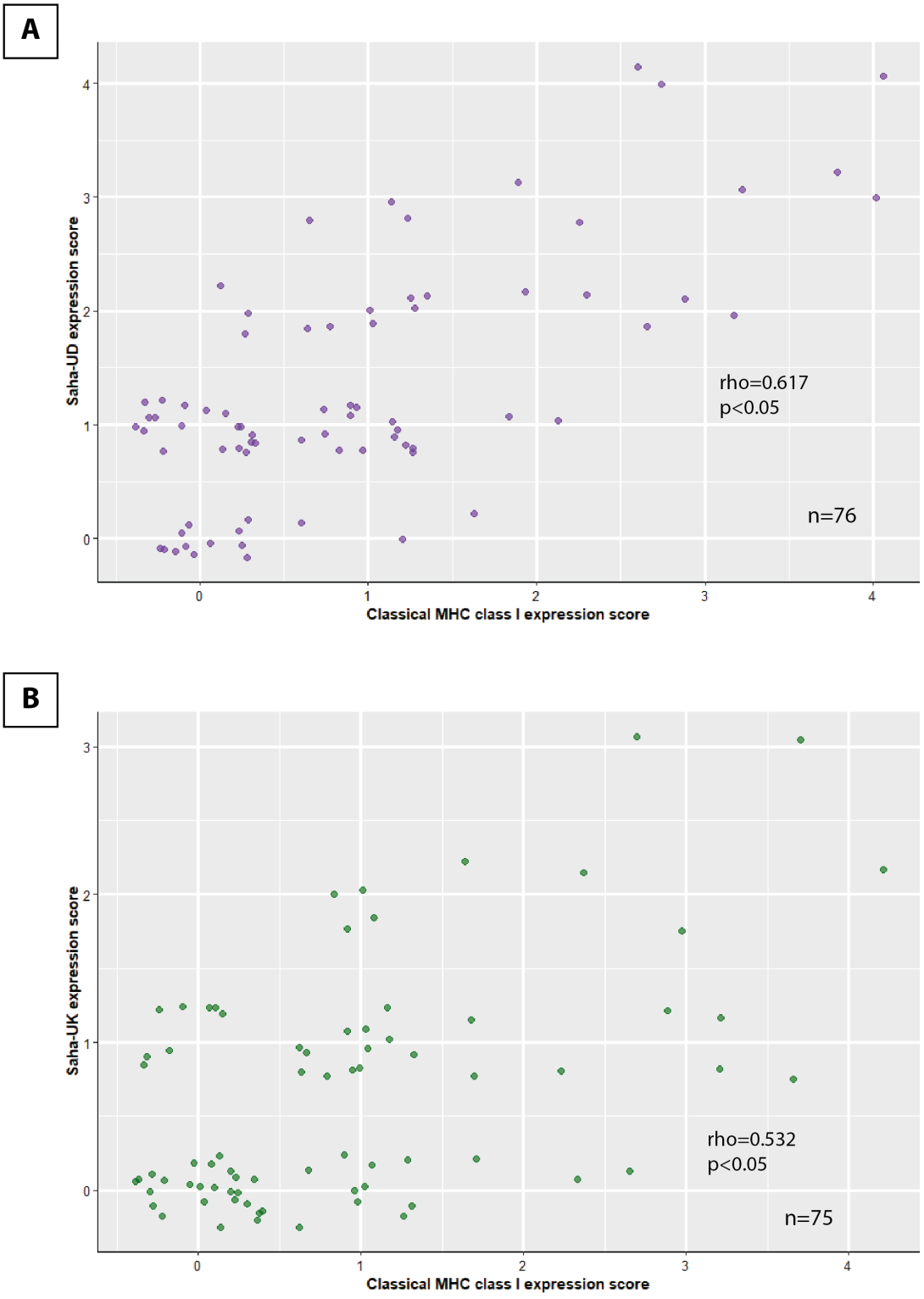

Figure 6.10 Non-classical MHC class I expression correlates with classical MHC class I in DFT1 tumours.

Non-classical, **(A)** Saha-UD (n=76) and **(B)** Saha-UK (n=75) expression in DFT1 tumour biopsies compared with Classical MHC class I expression scores. Expression scores are based on the strength of IHC staining; 0 = no staining, 4 = very strong staining. Expression scores are discrete variables – jitter has been applied to the data points

for visualisation. Both Saha-UD (rho=0.617, t=3.04x10^{-9}) and Saha-UK (rho=0.532, t=9.22x10^{-7}) expression have a strong positive correlation with classical MHC class I (Spearman's correlation, p<0.05).

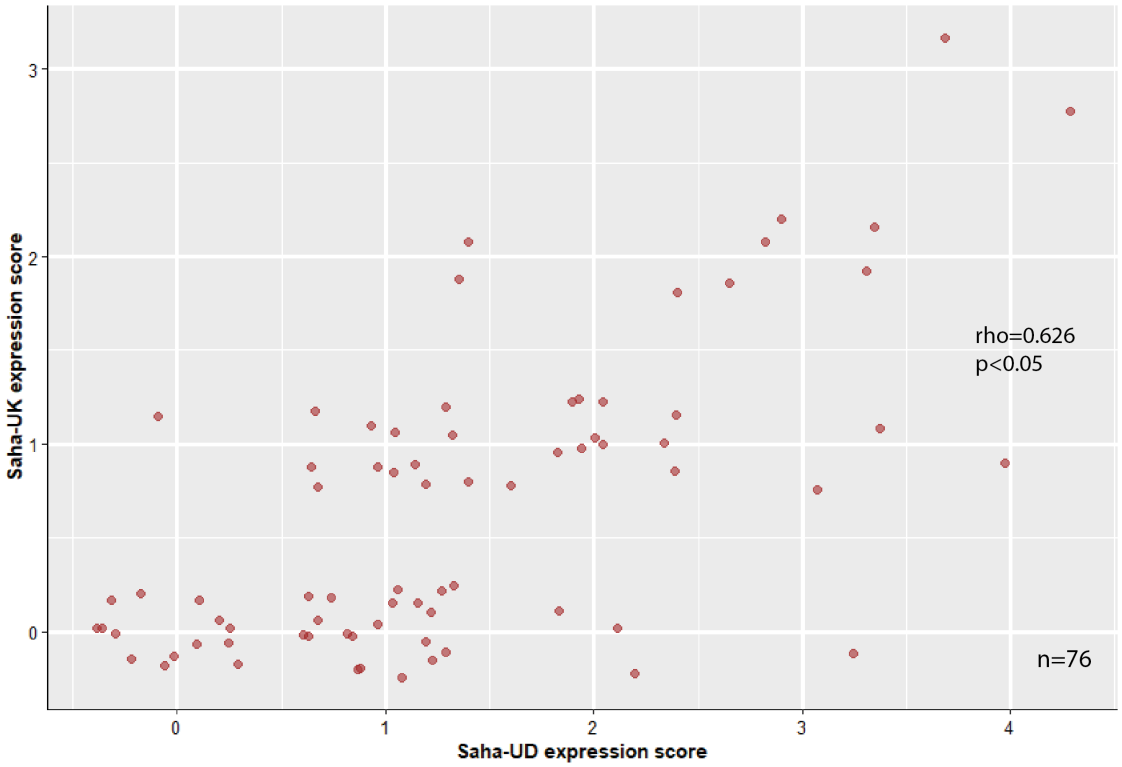

Figure 6.11 Non-classical, Saha-UD and Saha-UK expression correlate with each other in DFT1 tumours.

Expression of non-classical MHC class I, Saha-UK and Saha-UD expression scores in DFT1 tumour biopsies compared with each other (n=76). Expression scores are based on the strength of IHC staining; 0 = no staining, 4 = very strong staining. Expression scores are discrete variables – jitter has been applied to the data points for visualisation. Expression of Saha-UD and Saha-UK have a strong positive correlation (Spearman's correlation, rho=0.626, t=1.95x10^{-9}, p<0.05).

6.5 Immune markers (IFNγ and CD3)

To investigate whether non-classical MHC class I expression has an immunoregulatory function in DFT1 tumours, non-classical MHC class I expression scores were compared to IHC staining for immune markers, IFNγ, an inflammatory cytokine, and CD3, a marker for T cells. If non-classical expression creates an immunosuppressive tumour environment, low levels of IFNγ and CD3 would be expected.

Unexpectedly, both non-classical, Saha-UD (rho=0.415, t=2.48x10^{-3}) and Saha-UK (rho=0.383, t=6.01x10^{-3}) expression by DFT1 tumour cells have a positive correlation with IFNγ expression (Spearman's correlation, $p<0.05$) (Figure 6.12A and Figure 6.13A). In addition, there is higher non-classical MHC class I expression, Saha-UD (t=4.47x10^{-3}) and Saha-UK (t=4.48x10^{-2}), when CD3+ cells are present in the tumour biopsy (Wilcoxon rank sum test, $p<0.05$) (Figure 6.12B and Figure 6.13B). Looking at the location of CD3+ cells, there was a significant difference in Saha-UD expression for CD3+ cells in the stroma (Kruskal-Wallis rank sum test; t=0.0125, $p<0.05$) (Figure 6.12C). However, there was no significant difference between any of these groups when using Dunn's test adjusted for pairwise comparison. There was no significance for Saha-UD based on CD3+ cells in the tumour (Figure 6.12D), and no significance for Saha-UK expression for CD3+ cells in either stroma or tumour (Wilcoxon rank sum test, $p<0.05$) (Figure 6.13C&D). A significance level of $p<0.05$ was used for all statistical tests. The lack of significance for CD3+ cells in the stroma or tumour, despite being significant for CD3+ cells present in the biopsy, is likely due to there being too many categories for the sample number.

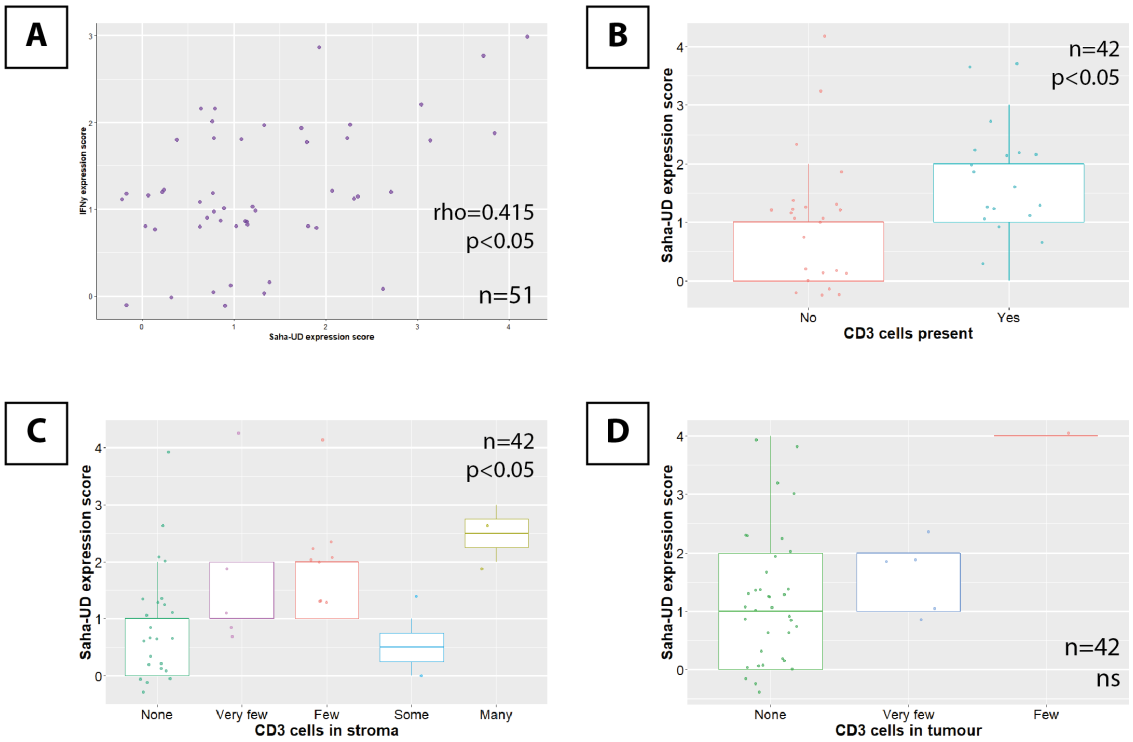

Figure 6.12 Non-classical, Saha-UD expression correlates with IFNγ expression in DFT1 tumours.

Non-classical, Saha-UD expression in DFT1 tumour biopsies compared with **(A)** IFNγ expression scores (n=51), **(B)** presence of CD3+ cells (n=42), **(C)** CD3+ cells in the stroma (n=42), or **(D)** CD3+ cells among tumour cells (n=42). Expression scores are based on the strength of IHC staining; 0 = no staining, 4 = very strong staining. Expression scores are discrete variables – jitter has been applied to the data points for visualisation. There is a positive correlation between Saha-UD and IFNγ expression scores (rho=0.415, t=2.48x10^{-3}, p<0.05). There was also a significant difference in Saha-UD expression for CD3+ cells present (t=4.47x10^{-3}) and CD3+ cells in the stroma (t=1.25x10^{-2}), but not for CD3+ cells in the tumour. 'ns' = not significant (p>0.05).

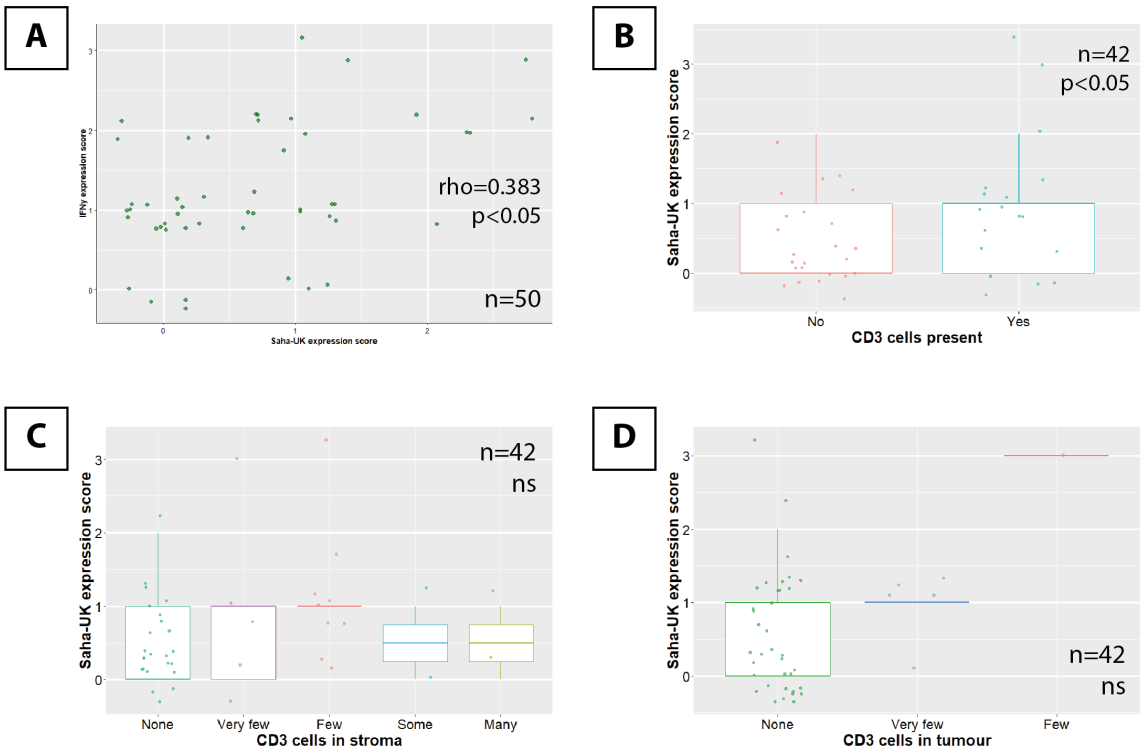

Figure 6.13 Non-classical, Saha-UK expression correlates with IFNγ expression in DFT1 tumours.

Non-classical, Saha-UK expression in DFT1 tumour biopsies compared with **(A)** IFNγ expression scores (n=50), **(B)** presence of CD3+ cells (n=42), **(C)** CD3+ cells in the stroma (n=42), or **(D)** CD3+ cells among tumour cells (n=42). Expression scores are based on the strength of IHC staining; 0 = no staining, 4 = very strong staining. Expression scores are discrete variables – jitter has been applied to the data points for visualisation. There is a positive correlation between Saha-UD and IFNγ expression scores (rho=0.383, t=6.01x10^{-3}, p<0.05). There was also a significant difference in Saha-UD expression for CD3+ cells present (p = 4.48x10^{-2}), but not for CD3+ cells in the stroma or tumour. 'ns' = not significant (p>0.05).

6.5.1 Classical and non-classical MHC class I expression by DFT1 does not correlate with tumour volume.

It was noted that many tumours heterogeneous for MHC class I expression were biopsies taken from larger tumours, such as Crabtree T1, Crabtree T2, Grommit, Franklin T1, and TD505 T3. Additionally, large tumours from devils, Crabtree and TD505 were high expressing for classical MHC class I and non-classical, Saha-UD. To investigate whether there was a difference in MHC class I or IFNγ expression by tumour volume, expression scores for non-classical, Saha-UD (n=52), non-classical, Saha-UK (n=52), classical MHC class I (n=52), and IFNγ (n=44), were plotted against tumour volume (mm^3) (Appendix Figure E 4). A significance level of $p<0.05$ was used for all statistical tests. There is no correlation between tumour volume and MHC class I or IFNγ expression (Spearman's correlation). However, most tumour volume data was for smaller tumours, which may have skewed the analysis.

6.5.2 Non-classical MHC class I expression in DFT1 tumours does not correlate with host and tumour factors.

There may be differences in non-classical MHC class I expression based on location; as different DFT1 clades have become dominant in different regions of Tasmania (Kwon et al., 2020). Non-classical MHC class I expression by DFT1 tumour cells based on location was investigated using the Area and Broad Area groupings of sample sites previously assigned for classical MHC class I analysis in Section 4.2.1 (see Figure 4.4A). A significance level of $p<0.05$ was used for all statistical tests. There was no significant difference in non-classical, Saha-UD expression by DFT1 (Figure 6.14A ; n=76) for either Broad Area (Wilcoxon rank sum test; t=0.569) or Area (Kruskal-Wallis rank sum test; t=0.379). Saha-UK expression by DFT1 (Figure 6.14B; n=75) did not differ by Area (Kruskal-Wallis rank sum test; t=0.0643), however there was a significant difference between expression for Broad Area (Wilcoxon rank sum test; t=0.0102, $p<0.05$), with the mean in the South-East being higher than the North-West. While this might be a result of lower sample numbers, it could indicate that there are differences in Saha-UK expression between DFT1 clades circulating in these areas.

Other factors were also investigated for effect on non-classical MHC class I by DFT1: sex of the host, age, host tumour load, season, secondary infection of the tumour, and tumour location, which could all influence host immune response and may translate to differences in non-classical MHC class I expression. There was no difference in Saha-UD expression in DFT1 based on age (t=0.305), season (t=0.551), or tumour location (t=0.426) (Kruskal-Wallis rank sum test), sex of host (t=0.765) or secondary infection (t=0.932) (Wilcoxon rank sum test), and there was no

correlation between classical MHC class I expression scores and tumour load (Spearman's rank correlation; *t*=0.884) (Appendix Figure E 5). The same was found for Saha-UK, with no significance for age (*t*=0.186), season (*t*=0.291), or tumour location (*t*=0.0635) (Kruskal-Wallis rank sum test), sex of host (*t*=0.112) or secondary infection (*t*=0.858) (Wilcoxon rank sum test), and there was no correlation between classical MHC class I expression scores and tumour load (Spearman's rank correlation; *t*=0.817) (Appendix Figure E 6).

Non-classical MHC class I expression by DFT1 tumour cells was also assessed compared to classical MHC class I host-tumour mismatch data from Chapter 4, to investigate whether non-classical MHC class I is upregulated in response to host recognition of tumour classical MHC class I alleles. No correlation was found for Saha-UD (Appendix Figure E 7) or Saha-UK (Appendix Figure E 8) in relation to host-tumour classical MHC class I mismatch, either for percentage sequence identity or mismatched TCR residues, or host expression levels of classical MHC class I, SahaI*27, or SahaI*90 (Spearman’s correlation).

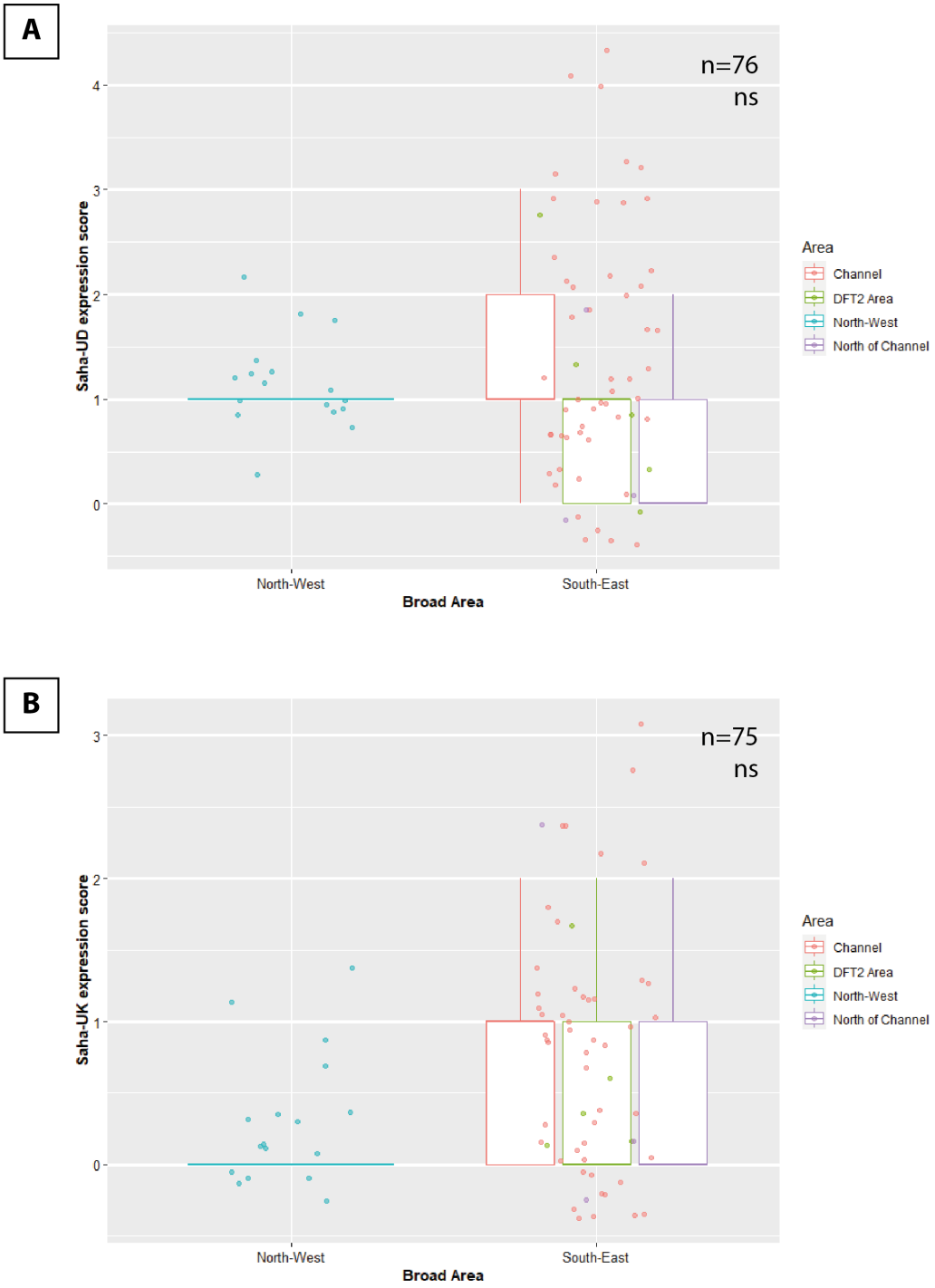

Figure 6.14 Non-classical MHC class I expression is not associated with area of sample collection.

Non-classical, **(A)** Saha-UD and **(B)** Saha-UK expression by DFT1 tumours based on the area of sample collection. A map of Tasmania showing the sample sites included in 'Broad Area' and 'Area' is shown in Figure 4.4A. Non-classical MHC class I expression is based on the strength of IHC staining. 0 = no staining, 4 = very strong staining. Expression scores are discrete variables – jitter has been applied to the data

points for visualisation. There is no significant difference in IFNγ expression by Broad Area or Area. 'ns' = not significant (p>0.05).

6.6 Discussion

6.6.1 Non-classical MHC class I is widely expressed in DFT1 tumours.

A specific monoclonal antibody against devil non-classical Saha-UD (α-UD_14-37-3), previously generated (Caldwell, 2018) and screened in our lab (Hussey, 2018; Hussey et al., 2022), has been validated, which shows little cross-reactivity with other devil recombinant MHC class I proteins (classical Saha-UC and non-classical Saha-UK). This antibody was used by IHC to confirm Saha-UD expression in DFT1 tumours, though expression varies between tumours. Saha-UD expression in 10 of the DFT1 biopsies was also confirmed by RT-PCR using Saha-UD specific primers.

Both non-classical, Saha-UD and Saha-UK are expressed by DFT1 tumour cells, though expression of varies between (Figure 6.3) and within (Figure 6.7 and Figure 6.8) tumours. Expression of non-classical Saha-UD heavy chain has previously been found in three DFT1 cell lines (Caldwell et al., 2018; Gastaldello et al., 2021; Pye et al., 2016b) and this study provides the first evidence of Saha-UD expression in primary DFT1 biopsies. Based on IHC staining, Saha-UD expression is common in DFT1 tumours from different individuals, with 80.3% of tumours (n=76) expressing Saha-UD. In contrast, Saha-UK expression is less common in DFT1 tumours (49.3%, n=75). Previously three tumours were stained for Saha-UK expression, Chauncy Vale, Lonnavale, and Franklin (Caldwell, 2018); this study increases the number and timespan of DFT1 tumours stained by IHC for Saha-UK. mRNA expression has also been confirmed in DFT1 cell line, 4906 (Caldwell et al., 2018) and a DFT1 biopsy (Cheng and Belov, 2014), but there was no Saha-UK heavy chain from β_2m pulldown on IFNγ-treated 4906 (Gastaldello et al., 2021), therefore, it is possible this MHC class I heavy chain does not bind β_2m and may have a role other than peptide presentation.

6.6.2 Non-classical expression by DFT1 tumours may play a role in preventing recognition of classical MHC class I molecules.

Based on our original hypothesis, loss of classical MHC class I would be expected to correlate with gain of non-classical expression to avoid NK cell activation against 'missing self'. While some DFT1 tumours (28.9%, n=76) expressed non-classical Saha-UD when there was no classical MHC class I expression, both non-classical Saha-UD and Saha-UK have a strong positive correlation with classical MHC class I expression by DFT1 tumour cells.

Though these results do not support our hypothesis, non-classical Saha-UD expression may still play a role in immune evasion of DFT1. Given that classical MHC class I expression in DFT1 is antigenic (Tovar et al., 2017) and we have found that Saha-UD is often expressed when there is classical MHC class I, non-classical Saha-UD could be creating an immunosuppressive environment to prevent host recognition. *Saha-UD* alleles are under purifying selection, resulting in very few polymorphisms, therefore immune responses to Saha-UD molecules on the cell surface are unlikely. In humans, expression of non-classical HLA-E, HLA-F, and HLA-G by extravillous trophoblasts induces maternal immunotolerance of foetal cells, preventing recognition of paternal alloantigens via the classical HLA-C molecules (Djurisic and Hviid, 2014; Tersigni et al., 2020). We postulate that Saha-UD binds peptides, due to the similarity to classical MHC class I sequences (Cheng et al., 2012; Cheng and Belov, 2014), and is expressed at the cell surface, as it binds β2m (Gastaldello et al., 2021); so, it is possible that Saha-UD is providing an immunosuppressive signal to the immune system.

Non-classical, Saha-UD and Saha-UK also have a positive correlation with each other. As classical MHC class I, and non-classical, Saha-UD and Saha-UK expression are all positively correlated with each other, it may be that these MHC class I molecules are all passively upregulated by a common driver. Alternatively, non-classical MHC class I may be specifically upregulated for immune suppression. The latter is more likely, as classical and non-classical MHC class I are not always co-expressed in tumours. Particularly classical MHC class I is often expressed when Saha-UK is not (Figure 6.10B) and Saha-UD is often expressed when classical MHC class I is not (Figure 6.10A), suggesting non-classical MHC class I is upregulated independently of classical MHC class I. Supporting this, non-classical Saha-UD expression is most likely to be controlled by a separate pathway to classical MHC class I as it lacks many upstream promoters present for the classical MHC class I genes, notably an IFNγ response element (Cheng et al., 2012). In contrast, Saha-UK does have an IFNγ response element (Cheng et al., 2012), therefore we would expect upregulation of both classical MHC class I and non-classical, Saha-UK in response to local inflammation.

6.6.3 There is plasticity in non-classical MHC class I expression.

In addition to variation in non-classical MHC class I expression between DFT1 tumours, there was also intra-tumour heterogeneity in some tumours. Heterogeneity was mainly observed for Saha-UD, in 22.4% of tumours (n=76). Lower levels of heterogeneity for Saha-UK (6.7%, n=75) may be due to lower levels of staining overall compared to Saha-UD. Some variation was also observed for Saha-UD (Figure 6.7A) and Saha-UK (Figure 6.8A) expression between tumours infecting the same individual.

In one devil, Orange, who was captured twice, there was an increase in Saha-UD and Saha-UK expression in one of the two tumour biopsies. This tumour was negative for both non-classical, Saha-UD and Saha-UK when captured in February 2020, but had increased to expression scores of 3 and 2 for Saha-UD (Figure 6.7A) and Saha-UK (Figure 6.7B), respectively, when re-captured in May 2020. These differences in expression score could be upregulation of non-classical MHC class I by the tumour, or, as it has been shown that DFT1 tumours can be heterogeneous for expression of non-classical MHC class I, this may be due to sampling of a different area of the tumour. Either way, these results support intra-tumour variation of DFT1 tumours for non-classical MHC class I expression.

The variation in Saha-UD and Saha-UK expression may be due to the individual interactions of tumours with the host immune system. Expression of Saha-UD is higher in Christine (expression score of 2) than Grommit and Tiarna (expression score of 1), despite all developing after inoculation with cell line C5065, and Grommit and Tiarna both show intra-tumour heterogeneity. Intra-tumour heterogeneity observed in DFT1 tumours highlights that Saha-UD expression may be plastic in response to local tissue conditions, such as infiltrating immune cells. It has been shown that DFT1 cells exhibit mesenchymal plasticity in response to immune activation following immunisation (Patchett et al., 2021), changing to a dedifferentiated, immunosuppressive state. Though MHC class I expression was not investigated, it could be controlled by similar pathways. However, Saha-UD is located in a different region to the classical MHC class I genes and is missing many upstream regulatory elements present for classical MHC class I, including an interferon stimulated response element (Cheng et al., 2012). Thus, its response to local inflammation is predicted to be limited.

If non-classical MHC class I expression were solely dependent on the local immune environment, patterns of heterogeneity within the tumour would be expected. However, this was not seen in most tumours. Some tumours had small areas with slightly higher Saha-UD expression on the outside of clusters of tumour cells, which might be expected if Saha-UD were being upregulated in response to infiltrating immune cells, but this was not conclusive or present throughout the tumour. Thus, Saha-UD expression is likely to be associated with a combination of the sublineage of DFT1, the history of host devils encountered by the tumour cells and the specific interactions with the current host devil immune system. This is highlighted by varying levels of Saha-UD expression in different DFT1 tumours infecting the same devil (see Figure 6.7 and Figure 6.8). These tumours may originate from bite wounds from different devils and/or derive from infection with different clades of DFT1 (Kwon et al., 2020). Tumour cells may have been subjected to different selective pressures as they moved through the population prior to infection in the current devil, which may produce differential interactions with the host immune system. This is

akin to evolution observed in other emerging pathogens as they spread through a population; acquiring mutations and genetic changes in response to the pressures of the host environments they encounter, which leads to the development of variants.

As Saha-UK expression by DFT1 tumours was significantly higher in the South-East than the North-West, this may reflect the genetic evolution of the cancer as it has spread across Tasmania. The biopsy samples in this study are derived from two broad geographical areas in Tasmania: the North-West, including 3 devils captured from the North-West and inoculated with DFT1 cell line, C5065, obtained from Eastern Tasmania in 2005, and wild tumours collected from locations in and around the d'Entrecasteaux peninsula, in the South-East (See Figure 4.4A). Though sample number is limiting, it is possible the variation in Saha-UK expression is due to genetic differences between DFT1 tumours in these areas (Kwon et al., 2020). Recent genotyping of DFT1 tumours has found that early in its clonal evolution, DFT1 developed into multiple clades, some of which have persisted and become dominant in particular geographic areas (Kwon et al., 2020; Stammnitz et al., 2023), therefore, Saha-UK expression may be reflective of DFT1 sublineages. In contrast, there is no significant difference for classical MHC class I or Saha-UD expression by area. While expression of these MHC class I could be affected by their sublineages, this suggests classical MHC class I and Saha-UD expression is more plastic than Saha-UK.

DFT1 tumours were also heterogenous for classical MHC class I expression. This may be due to plasticity in classical MHC class I expression, afforded by epigenetic mutations in genes for components of the peptide presentation pathway (Burr et al., 2019; Siddle et al., 2013), which can be upregulated by cytokines, for example IFNγ. This would be a similar progression as observed in the transmissible cancer in dogs, CTVT, which regulates expression of MHC class I during infection of a single host, with MHC class I downregulated during its progressive growth phase and upregulated in response to cytokines during the regressive phase (Belov, 2011; Murgia et al., 2006). An alternative scenario is that subclonal lineages of DFT1 are emerging that express classical MHC class I. MHC class I expression on DFT1 cells has been shown to elicit an immune response in devils (Tovar et al., 2017), therefore emergence of MHC class I-positive tumours may contribute to recent findings of devil immune responses (Pye et al., 2016a) and tolerance to DFT1 (Margres et al., 2018).

Despite DFT1 tumours being heterogeneous for expression of classical MHC class I, and non-classical, Saha-UD and Saha-UK, heterogeneity for these MHC class I were not always found in the same tumours. Therefore, expression of classical and non-classical MHC class I is not directly linked, supporting the conclusion that non-classical MHC class I expression is controlled independently to classical MHC class I.

6.6.3.1 Non-classical MHC class I expression could be upregulated in response to an inflammatory tumour environment

As non-classical MHC class I expression in DFT1 tumours was hypothesised to be immunoregulatory, it is expected to correlate with a 'colder' tumour environment. However, both Saha-UD and Saha-UK expression by DFT1 cells have a positive correlation with markers for immune activation, IFNγ and CD3. As Saha-UD does not have a interferon stimulated response element (Cheng et al., 2012), it is not predicted to be upregulated by IFNγ directly. However, as classical MHC class I expression by DFT1 can be upregulated by IFNγ (Siddle et al., 2013), non-classical MHC class I molecules may be upregulated with classical MHC class I, or upregulated in response to host recognition of MHC class I via other cytokines or signalling molecules.

Non-classical MHC class I expression is unlikely to be in response to the presence of CD3+ cells directly, as the number of CD3+ cells is low and there is little infiltration into the tumour. However, there is an association between non-classical expression and the presence of CD3+ cells, supporting the correlation with IFNγ and the association of non-classical expression with an inflammatory environment. The lack of CD3+ cells infiltrating the tumour when observed in the biopsy also suggests that expression of non-classical MHC class I by DFT1 cells in these tumours may be immunoregulatory.

Correlation of non-classical MHC class I expression with immune markers indicates Saha-UD and Saha-UK may be upregulated due to a host immune response against tumour classical MHC class I. Surprisingly, there was no correlation between Saha-UD or Saha-UK expression by DFT1 and host-tumour mismatch. This may indicate that non-classical MHC class I expression is not related to host recognition of disparate tumour alleles, or that DFT1 classical MHC class I alleles have the potential to be immunogenic in all hosts and there are other factors affecting host immune responses against DFT1 classical MHC class I.

6.6.4 Implications and further study

In summary, non-classical MHC class I, Saha-UD and Saha-UK are expressed by DFT1 tumour cells, though expression is variable. Due to its widespread expression, high heterogeneity between and within tumours, and its expression in the absence of classical MHC class expression, Saha-UD is most of interest.

Some tumours express Saha-UD, but not classical MHC class I, supporting the hypothesis that non-classical MHC class I is upregulated to prevent an immune response against 'missing self'. However, most DFT1 tumours have a positive correlation between classical and non-classical MHC

class I expression, where non-classical MHC class I is expressed when classical MHC class I is expressed. Though this does not fit the hypothesis, non-classical MHC class I may still have an immunosuppressive role in DFT1, by masking classical MHC class I molecules on DFT1 cells from recognition by the host immune system.

An outstanding question for tumours that lack classical and non-classical MHC class I expression is, how are they evading immune activation of NK cells to 'missing self'? Possibly, they are expressing other non-classical MHC class I molecules to inhibit NK cells, or other immune modulators, such as cytokines. Another possibility is that expression of MHC class I by DFT1 cells is plastic in response to the local environment, similar to CTVT (Belov, 2011; Murgia et al., 2006), and is upregulated in response to immune activation, though this needs further investigation.

To investigate potential roles for Saha-UD in immune evasion, further work is needed to confirm its ligand binding properties and interactions with immune cells. It should also be established whether Saha-UD or Saha-UK are expressed at the surface of DFT1 cells for immune recognition. If they are expressed at the cell surface, expression levels of Saha-UD and Saha-UK should be compared with classical MHC class I to assess whether they are masking host recognition of polymorphic alleles.

In addition, a wider range of DFT1 samples from different areas should be studied to investigate whether there are differences in non-classical MHC class I expression, in different locations or by DFT1 clades. As non-classical MHC class I expression appears to be important in DFT1 tumours, expression of Saha-UD has been found in DFT2 cell lines (Caldwell et al., 2018; Gastaldello et al., 2021), and Saha-UK expression in cell lines (Caldwell et al., 2018) and a limited number of biopsies, expression should be investigated in a wider range of DFT2 biopsies.

Chapter 7 Final discussion

7.1 Final discussion

In this thesis, I investigated two hypotheses (see Section 1.5):

1) DFT2 is losing MHC class I expression during progression through the devil population.
2) DFT1 expresses non-classical MHC class I to evade the host immune response.

To address Hypothesis 1, classical MHC class I expression was investigated in a wider range of DFT2 biopsies sampled across the current range of the disease and spanning the time frame since DFT2 emergence (2014 – 2020). To quantify expression of MHC class I molecules, an expression score was generated, assigned using semi-automated image analysis. Thirty-four DFT2 biopsies were stained for classical MHC class I expression by IHC (Aim 1), revealing variable expression between tumours, some infecting the same individual. This may indicate loss over time and, based on Hypothesis 1, it is possible that classical MHC class I loss is the result of DFT2 infecting devils with a mismatched MHC class I genotype, driving immune escape by DFT2. To investigate immune responses to DFT2 tumours, an antibody against IFNγ was validated for use by IHC (previously generated and screened by Alison Caldwell (2018)). This antibody showed variable expression of IFNγ across DFT2 tumours that was positively correlated with classical MHC class I expression (Aim 2). However, there was no link between the level of classical MHC class I allelic mismatch between tumour and host and classical MHC class I expression by DFT2 cells (Aim 3).

To investigate Hypothesis 2, 76 DFT1 biopsies were stained for classical and non-classical MHC class I by IHC, expanding the number and timeframe of DFT1 tumour biopsies investigated for MHC class I expression (Aims 4 & 5). Surprisingly, classical MHC class I expression was variable in DFT1 tumours, which were previously thought to be constitutively negative as a mechanism for immune evasion (Siddle et al., 2013). Classical MHC class I expression by DFT1 cells correlated with IFNγ expression in the tumour, suggesting classical MHC class I may be upregulated in response to local inflammation. To investigate non-classical, Saha-UD expression, the specificity of an anti-Saha-UD antibody, previously generated by Alison Caldwell (2018) and screened during my master's thesis (Hussey, 2018), was validated. Staining of DFT1 tumours for non-classical, Saha-UD and Saha-UK confirmed variable expression of both MHC class I proteins, with this being the first evidence of Saha-UD expression in DFT1 tumour biopsies by IHC.

As non-classical MHC class I expression was hypothesised to prevent NK cell activation against classical MHC class I-negative DFT1 cells, correlation between classical and non-classical

expression were investigated. Unexpectedly there was a positive correlation between classical and non-classical MHC class I expression, suggesting it might have a role in immune evasion when classical MHC class I is on the cell surface. Based on the hypothesis that non-classical MHC class I expression is immunosuppressive in DFT1, a negative correlation with immune activation markers would be expected. While there was no association with CD3+ cells, which may be due to low sample numbers, there was a positive correlation with both Saha-UD and Saha-UK expression by DFT1 cells and IFNγ expression (Aim 6), contrary to the hypothesis.

7.1.1 DFT1 may express immunosuppressive markers to evade the host immune system.

As transmissible cancers transmit as allografts between individuals, they are under strong selective pressure for evolution of immune escape mechanisms, as they need to avoid the immune system of each host they infect. Therefore, transmissible cancers provide an interesting model for the study of cancer evolution. Tasmanian devils are of particular interest, as they are the only known mammal to have developed two transmissible cancers, and both developed recently in comparison to CTVT (Murchison et al., 2014; Novinski, 1874). As these cancers arose at different times, DFT1 circulating for around three decades and DFT2 only one decade (Hawkins et al., 2006; Pearse and Swift, 2006; Pye et al., 2016b; Stammnitz et al., 2023), we are studying these cancers at different stages in their evolution.

DFT1 was thought to have developed a consistent mechanism for avoidance of host T cell responses, by removing MHC class I from the cell surface, via epigenetic downregulation of components of the peptide presentation pathway (Burr et al., 2019; Siddle et al., 2013). However, IHC staining of DFT1 tumours shows classical MHC class I expression is highly variable. Expression levels were often low, which may be due to their hemizygous deletion at the β_2m loci (Stammnitz et al., 2018). Despite this, some tumours stained strongly for classical MHC class I, thus, lower levels of expression may be due to epigenetic expression or other mechanisms, such as selective loss of alleles, to reduce the immunogenicity of DFT1 cells.

Regardless of the level of classical MHC class I expression, these results challenge our understanding of how DFT1 cancer cells avoid recognition by the host immune system. As epigenetic mutations in the APP allow for up- and downregulation of classical MHC class molecules. It may be that DFT1 modulates its MHC class I expression based on the local immune environment, akin to CTVT (Hsiao et al., 2008; Pérez et al., 1998). It has been shown that DFT1 can mutate in response to immune activation, as EMT was observed by DFT1 cells in immunised devils treated with immunotherapy (Patchett et al., 2021), and loss of periaxin expression, a marker of differentiated Schwann cells, has been observed in this thesis. Therefore, the ability of DFT1 to

transiently change its MHC class I expression levels, may be key to immune evasion in transmissible cancers.

Interestingly, there was a positive correlation between classical MHC class I expression and the expression of non-classical MHC class I genes, Saha-UD and Saha-UK by DFT1 cells. Though the function of these non-classical genes in Tasmanian devils is unknown, the expression of non-classical MHC class I molecules in humans can be associated with immunosuppressive or regulatory functions, both in their regular function, such as in the placenta (Rapacz-Leonard et al., 2014), and their pathological function in cancer cells (Kochan et al., 2013). Non-classical MHC class I molecules may also play an indirect role in immune evasion by DFT1 tumours. For example, in contrast to the classical MHC class I genes in devils, *Saha-UD* does not have an IFNγ stimulated response element upstream of its start codon (Cheng et al., 2012), thus, it is unlikely to be upregulated in response to local inflammation as classical MHC class I would. It is possible that Saha-UD expression is specifically upregulated in DFT1 tumour cells to protect against recognition of classical MHC class I molecules, though further work is needed to identify immune ligand and function for Saha-UD. In contrast, Saha-UK has an IFNγ stimulated response element (Cheng et al., 2012), therefore may be transiently upregulated with classical MHC class I in response to an inflammatory tumour environment. This is highlighted by Saha-UK sharing a similar expression score profile to classical MHC class I in DFT1 tumours, while Saha-UD has a different profile with higher expression scores (Figure 7.1). Combined with lower expression levels in DFT1 tumours, this indicates Saha-UK may not play a key role in immune evasion by DFT1 cells. However, as its function has not been determined, Saha-UK cannot be discounted from immunosuppression in DFT1.

Based on these results, immune evasion by DFT1 is not as straightforward as total MHC class I loss, which was previously thought to be the main mechanism utilised by DFT1 cells. An alternative hypothesis for DFT1 immune evasion, illustrated in Figure 7.2, is that classical MHC class I molecules are up- and downregulated by DFT1 cells in response to the local immune environment. When classical MHC class I is upregulated, non-classical is upregulated as well, as a mechanism to shield classical MHC class I molecules from recognition by the host immune system. This model has similarities to the regulation of MHC expression found during the transmission and growth of CTVTs in dogs.

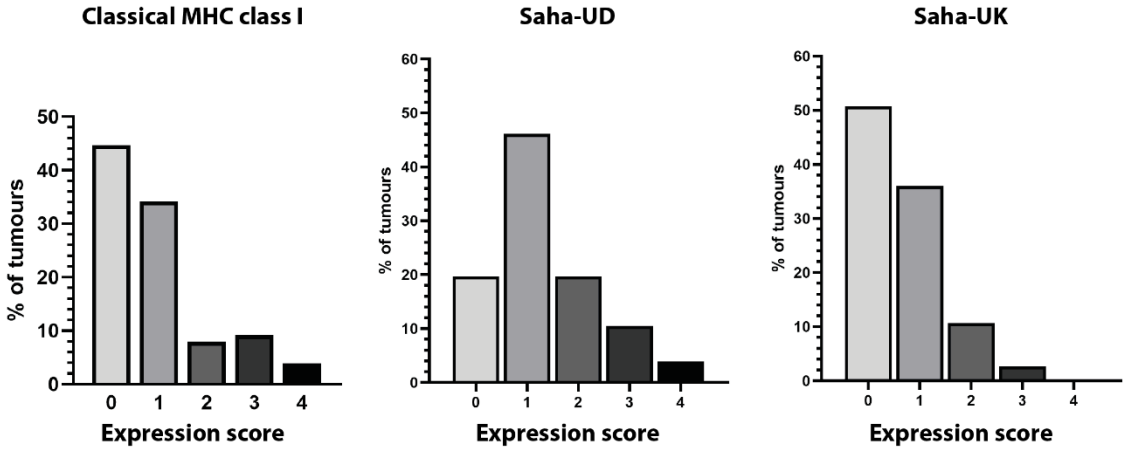

Figure 7.1 DFT1 tumours have a similar expression profile for classical MHC class I and non-classical Saha-UK expression.

Percentage of DFT1 tumours (n=76) assigned each expression score for classical MHC class I, non-classical Saha-UD, and non-classical Saha-UK staining by IHC. 0 = no staining, 4 = strong staining.

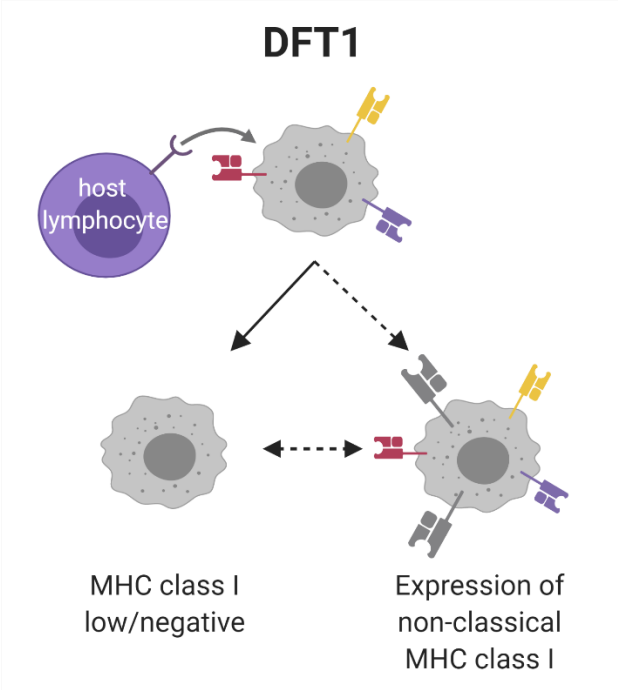

Figure 7.2 Non-classical MHC class I molecules are upregulated by DFT1 cells to shield classical MHC class I molecules from host immune recognition.

It was previously thought that there was total downregulation of classical MHC class I by DFT1 cells in all tumours (Siddle et al., 2013) to avoid T cell activation (shown by

the solid arrow). However, results in this thesis show classical MHC class I expression by DFT1 tumour cells is variable and positively correlates with non-classical MHC class I expression. Therefore, it is hypothesised that DFT1 cells can modulate classical MHC class I expression on the cell surface via epigenetic modifications in the response the immune environment, and when classical MHC class I is expressed, so is non-classical MHC class I to shield against immune recognition and suppress the host immune system.

As immune responses are complex, it is likely DFT1 molecules have developed multiple mechanisms for immune evasion, such as co-expression of non-classical and classical MHC class I, along with the ability to regulate MHC class I expression on the cell surface. As DFT1 cells express PD-L1 in response to IFNγ treatment (Flies et al., 2016), it appears DFT1 creates an immunosuppressive environment to prevent recognition of classical MHC class I molecules at the cell surface. How DFT1 cells avoid NK cell activation in response to 'missing self' is an outstanding question. In this thesis it was shown that some DFT1 tumours express Saha-UD when there is a lack of classical MHC class I expression, which may suppress NK cells responses; but this was not consistent across tumours, therefore other mechanisms may be utilised. It is important to note that, although functional cytotoxic NK cell responses have been identified in Tasmanian devils (Brown et al., 2011), their NK cells may function differently to eutherian mammals, therefore further work is need to characterise Tasmanian devil NK cells.

Understanding how DFT1 evades the immune system, particularly in relation to classical MHC, is important for vaccine design. An enabling characteristic in cancer is genetic instability (Hanahan and Weinberg, 2000), which results in the ability of cancer cells to become resistant to therapy (Bai et al., 2020; Bukowski et al., 2020; Cree and Charlton, 2017; Mansoori et al., 2017), therefore therapies are often used in conjunction. Not inhibiting immunosuppressive mechanisms in DFT1 may contribute to the lack of long-term protective immune responses in immunised devils in previous vaccination trials (Kreiss et al., 2015; Tovar et al., 2017). Considering this, targeting multiple immune evasion mechanisms in DFT1 should help the effectiveness of vaccines and reduce the chances of immune escape by the cancer.

7.1.2 Widespread downregulation of classical MHC class I by DFT2

DFT2 is earlier in its evolution compared to the other two transmissible cancers infecting mammals, predicted to have emerged between 2009 – 2012 (Stammnitz et al., 2023). A previous study (n=6) found all DFT2 tumours expressed classical MHC class I, most with high expression; though two had slightly lower expression levels (Caldwell et al., 2018). Expression of MHC class I by DFT2 cells should initiate an immune response due to disparate classical MHC class I between tumour and host. Therefore, we would expect downregulation of classical MHC class I due to host immune responses.

Results in this thesis show classical MHC class I is still expressed by most DFT2 cells; however, expression levels are low in some of these tumours, and some tumours have totally lost classical MHC class I expression. Therefore, there may be selective pressure for loss or downregulation of MHC class I expression in DFT2 cells. For example, in response to immune inflammation. Though classical MHC class I and IFNγ expression scores were positively correlated in DFT1 and DFT2, only in DFT2 do they share a similar expression score profile (Figure 7.3). This could suggest that there is local tumour inflammation in response to classical MHC class I expression by DFT2, or that IFNγ expression is upregulating classical MHC class I expression by tumour cells. Notably, there was no correlation between downregulation of classical MHC class I expression and host-tumour genotype mismatch.

This lack of correlation may be explained by evolution of DFT2 cells as they move through the population. Cancer cells gain beneficial mutations based on selective pressures, such as from the immune system (Dunn et al., 2004, 2002; McGranahan et al., 2017; Schreiber et al., 2011). Selective pressures can result in subclonal heterogenous cell populations within a tumour (Caldas, 2012). It has been shown by deep sequencing, that some subclones will become extinct or dormant, while others persist, with some providing beneficial mutations for metastasis (Campbell et al., 2010; Shah et al., 2012; Yachida et al., 2010). This is a useful model for understanding evolution of transmissible cancers, with ‘metastases’ occurring on a larger scale – between devils. This concept of cancer evolution in DFT2 is illustrated in Figure 7.4. Recently it was discovered that DFT2 developed into two clades early in its evolution (Stammnitz et al., 2023), supporting the idea that DFT2 could develop subclones within the population.

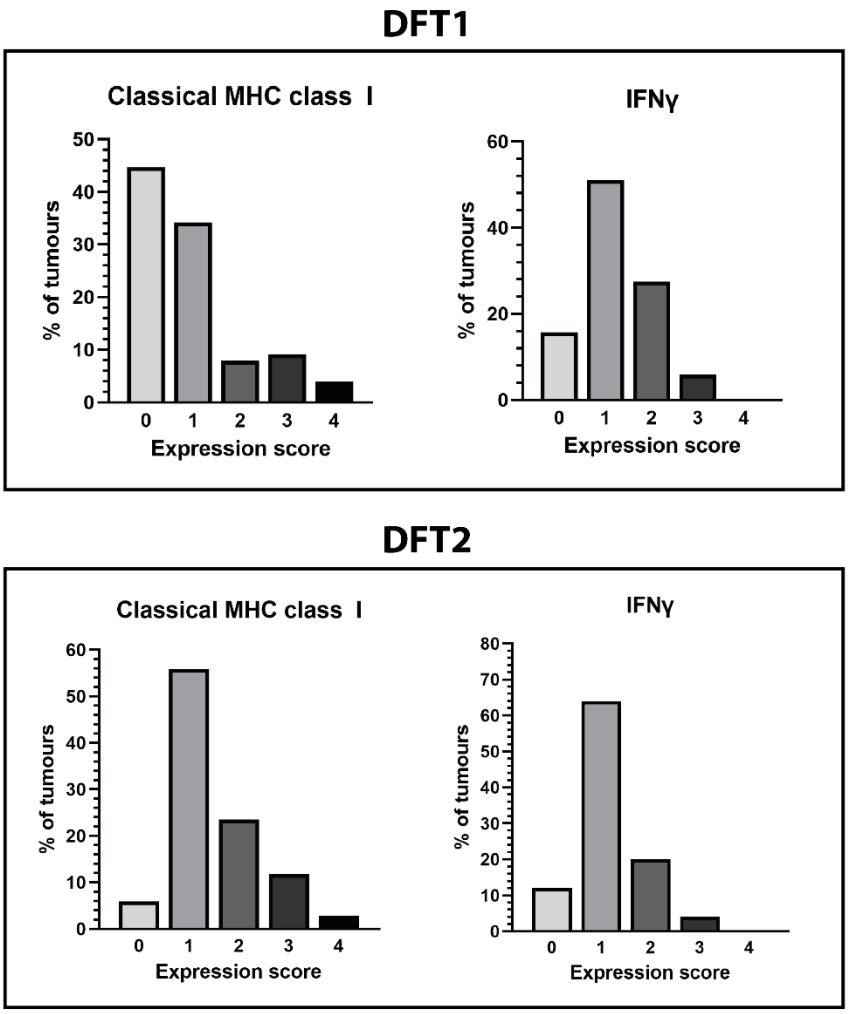

Figure 7.3 Classical MHC class I and IFNγ expression have a similar expression profile in DFT2 tumours.

Percentage of DFT1 tumours (n=76) and DFT2 tumours (n=34) assigned each expression score for classical MHC class I and IFNγ staining by IHC. 0 = no staining, 4 = strong staining.

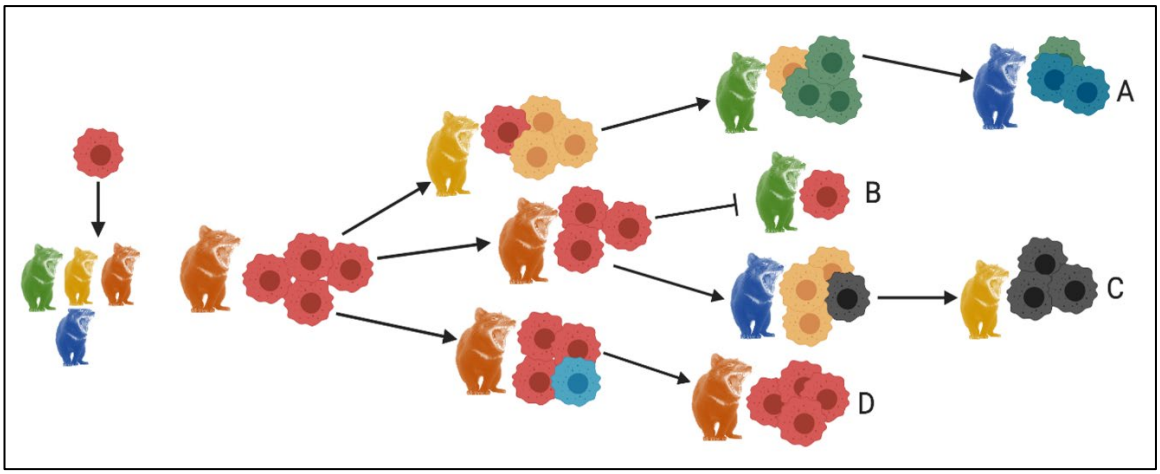

Figure 7.4 Classical MHC class I expression profile of DFT2 cells may be dependent on its clonal history.

As cancers evolve, they can develop into subclones based on their genetic mutations. Mutations, such as MHC class I expression profiles, can aid or hinder transmission through the population. **Subclone A** mutates with each host it infects, gaining mutations that confer survival in the current host. **Subclone B** does not gain beneficial mutations and can only survive in Tasmanian devils with a similar MHC class I genotype, therefore it is eliminated upon transmission to a host with disparate MHC class I alleles. **Subclone C** develops a trump mutation, which enables transmission among all devils. **Subclone D** continues to transmit among devils with a similar MHC class I genotype, therefore there is no selective pressure for mutation of MHC class I expression.

Changes to MHC class I expression will be occurring as DFT2 moves through the population. As a result, MHC class I loss may be historical in certain DFT2 subclones, based on immune responses from previous hosts they have infected. Therefore, classical MHC class I expression is more complicated than the host DFT2 cells are currently infecting. Findings in this thesis that MHC class I expression by DFT2 cells is variable, and there is no clear correlation over time or based on host-tumour mismatch, supports the theory that subclones may have developed, or are currently developing, with different MHC class I profiles.

Variability in classical MHC class I expression in DFT2 highlights the heterogeneity in cancer cells, particularly during the evolution of a transmissible cancer. If classical MHC class I expression profiles differ between cells, potentially modulated using different mechanisms, this presents a challenge when generating therapeutics and vaccines against DFT2. Therefore, vaccines may not be effective against all DFT2 cells, within a single tumour or between tumours. As a result, a better understanding of DFT2 classical MHC class I modulation mechanisms is needed before

disease management is implemented, as premature vaccination could select for development of additional immune escape mechanisms.

7.1.2.1 Epigenetic downregulation of classical MHC class I may be common in transmissible cancers

Downregulation of classical MHC class I has been observed in all three transmissible cancers occurring in mammals (Belov, 2011; Caldwell et al., 2018; Hsiao et al., 2008; Murchison, 2009; Siddle et al., 2013) and is a common occurrence in somatic cancers (Campoli and Ferrone, 2008; Dhatchinamoorthy et al., 2021; Hicklin et al., 1999). In transmissible cancers, cancer cells expressing classical MHC class I should be highly antigenic targets for the host immune system, due to differing MHC class I genotypes; and it has been shown that transmissible cancer cells expressing MHC class I generate immune responses from their hosts (Hsiao et al., 2008; Pérez et al., 1998; Pye et al., 2018; Tovar et al., 2017). Therefore, loss of MHC class I is highly beneficial for avoidance of immune responses, particularly T cell-mediated responses.

Though the mechanism of downregulation in DFT2 is not known, and may vary between subclonal populations, it is possible this may be due to epigenetic downregulation. Both CTVT and DFT1, older cancer lineages than DFT2, epigenetically downregulate MHC class I (Belov, 2011; Hsiao et al., 2008; Siddle et al., 2013), DFT1 downregulates MHC class I expression via PRC2, a conserved mechanism in cancers of neuroendocrine origin (Burr et al., 2019), however, this mechanism was not identified in DFT2 cell lines (Owen et al., 2021). Loss of MHC class I by structural mutations would prevent T cells responses but puts the cancer at risk of responses from other immune cells, thus epigenetic mutations provide plasticity in MHC class I expression. This may be the key to success of transmissible cancers. In CTVT, cancer cells can downregulate MHC class I during early infection (Hsiao et al., 2008), though the epigenetic mechanism has not been defined, enabling a latent period to transmit to the next host prior to elimination by the current host immune system. Epigenetic modifications in the APP may have similar function in DFT1, as MHC class I expression in tumours is variable, enabling up- and down-regulation of MHC class I in response to the local immune environment. Considering this, we may find that persisting DFT2 subclones also have epigenetic downregulation of MHC class I. While this enables immune escape by cancer cells, the ability to upregulate MHC class I expression is hopeful for the generation of vaccines.

7.1.3 A common MHC class I allele likely facilitates spread of transmissible cancers in Tasmanian devils.

Limited infiltration of CD3+ cells into DFT1 and DFT2 tumours was observed. And, even when CD3+ cells were present, they were mostly low density and restricted to the stroma. Analysis of infiltration by CD3+ cells may be limited due to sample number, though previous studies have also found limited lymphocyte infiltration (Caldwell et al., 2018; Loh et al., 2006).

While immune responses can be generated against DFT1 (Kreiss et al., 2015; Pye et al., 2018, 2016a; Tovar et al., 2017), vaccination against DFT1 has only been protective in a few cases (Tovar et al., 2017). Though there is enough genetic diversity for Tasmanian devils to reject matched skin grafts (Kreiss et al., 2011), perhaps the immune response is ineffective, owing to their restricted diversity (Cheng et al., 2012; Morris et al., 2013; Siddle et al., 2007a). As a result, even if an immune response is generated against DFTs, it may not be protective, giving the tumour time to evolve new escape mechanisms.

The generation of protective immune responses may be hindered by the expression of a classical MHC class I allele, SahaI*27, that is commonly expressed in the devil population, and also expressed by DFT1 and DFT2. While these results agree with previous findings of widespread expression of SahaI*27 (Caldwell et al. 2018, Cheng et al. 2022), SahaI*27-negative host samples are needed to show its true prevalence. Interestingly, not only is this allele commonly expressed, but it also has higher expression than other alleles in many individuals. Based on the findings in this thesis, there was no correlation found between higher expression of SahaI*27 by the host and immune activation against DFTs (though sample numbers were limiting). However, high expression of SahaI*27 in DFT2 could reduce the chance of immune recognition by hosts, as it would have lower immunogenicity than other classical MHC class I alleles. The possible fixation of this allele and its high expression will be important to confirm across the devil range as it may reflect past selective pressures on the devil immune system.

From host classical MHC class I genotyping a common allele was identified in DFT1 and DFT2 that is most frequently mismatched between tumour and host, SahaI*90. This is an important discovery for vaccine design and could be utilised to generate a dual vaccine for DFT1 and DFT2.

7.2 Future work

To further our understanding of immune evasion mechanisms by DFTs, and apply this knowledge to vaccine design, additional studies are required. In DFT2, the mechanism of MHC class I downregulation needs to be established, to understand whether classical MHC class I expression

can be restored in these tumours. In addition, it is not understood if, in tumours with lower MHC class I expression, any MHC class I is expressed at the cell surface. If downregulation of MHC class I heavy chain protein expression is sufficient to significantly reduce cell surface expression, this will have implications on our understanding of immune evasion by DFTs.

To determine whether non-classical MHC class I expression is immunosuppressive, the immune ligand and function for Saha-UD and Saha-UK needs to be identified. Additionally, NK cell responses to DFT1 tumours should be investigated, as activation is still expected against tumours that lack MHC class I expression. If NK cell responses are not observed, DFT1 may be employing additional immune evasion mechanisms that need to be explored.

To assist future studies into immune evasion mechanisms by DFT1 and DFT2, it would be beneficial to establish new DFT cell lines, as cancer lineages will evolve over time.

7.3 Conclusions

Classical MHC class I expression is highly variable in DFT1 and DFT2, suggesting cancer cells are modulating their MHC class I expression in response to selective pressure from the host immune system. Understanding the immune response, if any, against DFTs is vital to understanding how they evade the host immune system to transmit among the population. We hypothesise classical MHC class I expression is downregulated in DFT2 due to host immune recognition of mismatched tumour classical MHC class I alleles; and in DFT1, that non-classical MHC class I is upregulated to suppress host immune responses against classical MHC class I.

Classical MHC class I expression by DFT cells positively correlates with IFNγ expression in the tumour. Supporting *in vitro* findings that classical MHC class I can be upregulated by cytokines in DFT1 cells (Siddle et al., 2013). The ability to upregulate classical MHC class I expression in DFT1 tumours is important for vaccine design, as previous immunisation trials have found MHC class I expression is required for an effective immune response against DFT1 (Pye et al., 2018, 2016a; Tovar et al., 2017). Though it is important to note that non-classicals may be upregulated in inflammatory tumours as an immunosuppressive mechanism, which would need to be targeted in vaccine design.

Varying classical MHC class I expression in DFT2 tumours, and the positive correlation of classical MHC class I expression with IFNγ, suggests classical MHC class I loss may also be epigenetic in DFT2, therefore, reversible. While the mechanism of downregulation is still to be established in DFT2 cells, epigenetic downregulation would be hopeful for the development of vaccines against DFT2; providing an intervention to reduce disease spread among an already endangered species.

Appendix A Samples and antibodies

Table A 1 List of Tasmanian devil samples.

Devil name	Other identifiers	Microchip number	Tissue sample	Tumour type	Date collected	Location
Allen		982000410416915	Ear biopsy	N/a	Feb-19	Sandfly
Allen		982000410416915	Tumour 1	DFT1	Feb-19	Sandfly
Aurora		900164001721539	Tumour 1	DFT1	Apr-22	Sandfly
Bump		982000410416748	Tumour 1	DFT1	Feb-20	Sandfly
Bump		982000410416748	Tumour 2	DFT1	Feb-20	Sandfly
Cardamom		982000405976309	Tumour 1	DFT1	Oct-21	Sandfly
Cardamom		982000405976309	Tumour 2	DFT1	Oct-21	Sandfly
Chauncy Vale			Tumour 1b	DFT1	Mar-15	Chauncy Vale
Chilli		982000405797498	Ear biopsy	N/a	Dec-17	Woodbridge
Chilli		982000405797498	Tumour 2	DFT2	Jul-18	Woodbridge
Christine	TD111		Tumour	DFT1	Nov-08	Woolnorth
Clytemnestra		982000405977507	Tumour 1	DFT1	Nov-19	Sandfly
Crabtree	TD507	SDD000000100315	Tumour 1	DFT1	Mar-15	Crabtree
Crabtree	TD507	SDD000000100315	Tumour 2	DFT1	Mar-15	Crabtree
Crabtree	TD507	SDD000000100315	Tumour 3	DFT1	Mar-15	Crabtree
Cygnet	TD467		Tumour	DFT1	Mar-14	Cygnet
Cyprus		982000356584128	Ear biopsy	N/a	May-17	Woodbridge
Cyprus		982000356584128	Tumour 1	DFT1	Jun-17	Woodbridge
Danni		982000405982644	Tumour 1	DFT1	Feb-21	Sandfly
Ebony		982000410416500	Ear biopsy	N/a	May-18	Woodbridge

Devil name	Other identifiers	Microchip number	Tissue sample	Tumour type	Date collected	Location
Ebony		982000410416500	Tumour 2	DFT2	May-19	Woodbridge
Enchilada		982000405794795	Ear biopsy	N/a	Dec-17	Woodbridge
Enchilada		982000405794795	Tumour 3	DFT2	Nov-18	Woodbridge
Enchilada		982000405794795	Tumour 4	DFT2	Nov-18	Woodbridge
Enchilada		982000405794795	Tumour 5	DFT2	Nov-18	Woodbridge
Enchilada		982000405794795	Tumour 6	DFT2	Nov-18	Woodbridge
Enchilada		982000405794795	Tumour 10	DFT2	Nov-18	Woodbridge
Enchilada		982000405794795	Tumour 13	DFT2	Nov-18	Woodbridge
Felix		982000405976006	Tumour 1	DFT1	Nov-19	Woodbridge
Franklin			Tumour 1	DFT1	Apr-15	Franklin
Freiburg		982000410416829	Ear biopsy	N/a	Jul-18	Woodbridge
Gaza		982000190605291	Tumour 1	DFT1	Nov-13	West Pencil Pine
Globulus		982000410327612	Ear biopsy	N/a	Feb-19	Woodbridge
Globulus		982000410327612	Tumour 1	DFT2	Feb-19	Woodbridge
Grawp		982000365601023	Ear biopsy	N/a	Aug-16	Woodbridge
Grawp		982000365601023	Tumour 1	DFT2	Aug-17	Woodbridge
Grawp		982000365601023	Tumour 2	DFT2	Aug-17	Woodbridge
Grawp		982000365601023	Tumour 4	DFT2	Aug-17	Woodbridge
Grommit	TD184	982009105175123	Tumour	DFT1	Jun-10	Granville Harbour
Haloumi		956000011775873	Tumour 1	DFT1	Nov-21	Sandfly
Haloumi		956000011775873	Tumour 1	DFT1	Apr-22	Sandfly
Hannah		982000410415096	Tumour 1	DFT1	No-19	Sandfly
Harry		982000402820066	Ear biopsy	N/a	Jul-16	Woodbridge

Devil name	Other identifiers	Microchip number	Tissue sample	Tumour type	Date collected	Location
Hope		982000410417268	Ear biopsy	N/a	Feb-19	Sandfly
Hope		982000410417268	Tumour 1	DFT1	Mar-19	Sandfly
Hope		982000410417268	Tumour 2	DFT1	Mar-19	Sandfly
Jaarlsberg		956000011770023	Tumour 5	DFT1	Apr-22	Sandfly
Jane		982000405797721	Ear biopsy	N/a	May-17	Longley
Jane		982000405797721	Tumour T1	DFT1	May-17	Longley
Jesus		982000405975909	Tumour 1	DFT1	Feb-21	Sandfly
Jules		982000405979192	Tumour 1	DFT1	Feb-21	Sandfly
Kalahari		982009104909961	Tumour 1	DFT1	Nov-13	West Pencil Pine
Kaoota		982000356710852	Ear biopsy	N/a	May-17	Snug Tiers
Kaoota		982000356710852	Tumour 1	DFT1	May-17	Snug Tiers
Katie		982000365120047	Ear biopsy	N/a	Aug-16	Woodbridge
Krum		982000365611366	Ear biopsy	N/a	Aug-16	Woodbridge
Lake		900164001721569	Tumour 1	DFT1	Apr-22	Sandfly
Laurasia		982000405975852	Tumour 1	DFT2	Nov-19	Woodbridge
Lilac		982000405978832	Tumour 2	DFT1	Aug-19	Sandfly
Limpopo		982000167786788	Tumour 3 outer	DFT1	Nov-13	West Pencil Pine
Lonnavale	TD489		Tumour	DFT1	Jul-14	Lonnavale
Lucy		982000409860848	Tumour 1	DFT1	Mar-20	Sandfly
Lucy		982000409860848	Tumour 3	DFT1	Mar-20	Sandfly
Lutruwita		982000405978718	Tumour 2	DFT1	May-20	Sandfly
Magnolia		982000405983123	Tumour 1	DFT1	May-20	Sandfly
Mania		982000405978676	Tumour 1	DFT1	Feb-21	Sandfly

Devil name	Other identifiers	Microchip number	Tissue sample	Tumour type	Date collected	Location
Mania		982000405978676	Tumour 2	DFT1	Feb-21	Sandfly
Margaret	812	982000356483454	Tumour 1	DFT2	Jan-15	Snug
Marsh		900164001721556	Tumour 1	DFT1	Apr-22	Sandfly
Maui		982000167814762	Tumour 1	DFT1	Aug-14	West Pencil Pine
Maui		982000167814762	Tumour 2	DFT1	Aug-14	West Pencil Pine
Moody		982000410416671	Ear biopsy	N/a	Feb-19	Sandfly
Moody		982000410416671	Tumour 1	DFT1	Feb-19	Sandfly
NO NAME	ST67	982000363392739	Ear biopsy	N/a	Jun-17	Snug Tiers
NO NAME	ST67	982000363392739	Tumour 1	DFT2	Jun-17	Snug Tiers
Nudibranch		956000011763603	Tumour 1	DFT1	Apr-22	Sandfly
Orange		982000405975935	Tumour 1	DFT1	Feb-20	Sandfly
Orange		982000405975935	Tumour 1	DFT1	May-20	Sandfly
Orange		982000405975935	Tumour 2	DFT1	Feb-20	Sandfly
Orange		982000405975935	Tumour 2	DFT1	May-20	Sandfly
Paprika		982000405975892	Tumour 1	DFT1	Oct-21	Sandfly
Peach		982000405986087	Tumour 1	DFT2	May-20	Woodbridge
Peach		982000405986087	Tumour 2	DFT2	May-20	Woodbridge
Persia		900006000169079	Tumour 2	DFT1	Aug-14	West Pencil Pine
Pooh		982000405826904	Ear biopsy	N/a	May-17	Longley
Pooh		982000405826904	Tumour 1	DFT1	May-17	Longley
Purple		982000405979273	Tumour 1	DFT1	Aug-19	Sandfly
Red Velvet	202	982000190608331	Tumour 1	DFT2	Mar-14	Cygnet

Devil name	Other identifiers	Microchip number	Tissue sample	Tumour type	Date collected	Location
Rivulet		900164001721558	Tumour 1	DFT1	Feb-21	Sandfly
Sally		982000405914882	Ear biopsy	N/a	Jun-17	Sandfly
Sally		982000405914882	Tumour 1	DFT1	Feb-19	Sandfly
Sarafina		982000190530043	Tumour 1	DFT2	Nov-19	Woodbridge
Sarafina		982000190530043	Tumour 3	DFT2	Nov-19	Woodbridge
Savuti		982009104919599	Tumour 1	DFT1	Nov-13	West Pencil Pine
Savuti		982009104919599	Tumour 4 deep	DFT1	Nov-13	West Pencil Pine
Savuti		982009104919599	Tumour 4 mid	DFT1	Nov-13	West Pencil Pine
Savuti		982009104919599	Tumour 4 outer	DFT1	Nov-13	West Pencil Pine
Sea Cucumber		956000011762664	Tumour 1	DFT1	Apr-22	Sandfly
Selknam		982000190532966	Tumour 1	DFT1	Aug-14	West Pencil Pine
Selknam		982000190532966	Tumour 3	DFT1	Aug-14	West Pencil Pine
Selma		982000365112286	Ear biopsy	N/a	Apr-17	Southwood Road
Selma		982000365112286	Tumour 1	DFT1	Apr-17	Southwood Road
Simone		982000405909352	Tumour 1	DFT1	Jun-17	Snug Tiers
Snape		982000365120134	Ear biopsy	N/a	Aug-16	Woodbridge
Snape		982000365120134	Tumour 2	DFT2	Dec-17	Woodbridge
Snowball		982000405826357	Ear biopsy	N/a	Apr-17	Woodbridge

Devil name	Other identifiers	Microchip number	Tissue sample	Tumour type	Date collected	Location
Snowball		982000405826357	Tumour 1	DFT2	May-18	Woodbridge
Snug	203: TD500	982000356526917	Tumour 2	DFT2	Oct-14	Snug
Stuttgart		982000410416957	Ear biopsy	N/a	Jul-19	Woodbridge
Summer		982000405827802	Ear biopsy	N/a	Jul-17	Woodbridge
Tabasco		982000190607683	Ear biopsy	N/a	Dec-17	Woodbridge
Tabasco		982000190607683	Tumour 1	DFT2	Jun-18	Woodbridge
Taco		982000405792676	Ear biopsy	N/a	Dec-17	Woodbridge
Taco		982000405792676	Tumour 2	DFT2	Feb-18	Woodbridge
Tarrabeh		982000405979168	Tumour 1	DFT1	Dec-19	Sandfly
TD74			Lymph node	N/a	May-06	Tea Tree
TD74			Tumour 1	DFT1	May-06	Tea Tree
TD388			Tumour 1	DFT1	Nov-14	Carlton
TD505	Grove	982000356444429	Tumour 1	DFT1	Feb-15	Grove
TD505	Grove	982000356444429	Tumour 2	DFT1	Feb-15	Grove
TD505	Grove	982000356444429	Tumour 3	DFT1	Feb-15	Grove
TD523	638		Tumour 1	DFT2	Jun-15	Snug
TD523	638		Tumour 2	DFT2	Jun-15	Snug
TD547	807	R00000020151130	Tumour 1	DFT2	Oct-15	Cygnet
Teufel	818	982000167740522	Tumour 1	DFT2	Jan-15	Snug
Tiarna	TD182	982009105183213	Tumour	DFT1	Jul-10	Temma
Tibet		982000361993284	Ear biopsy	N/a	Sep-16	Woodbridge
Tigger		982000405851834	Ear biopsy	N/a	May-17	Longley
Tigger		982000405851834	Tumour 1	DFT1	May-17	Longley

Devil name	Other identifiers	Microchip number	Tissue sample	Tumour type	Date collected	Location
Turmeric		982000405978433	Tumour 1	DFT1	Aug-20	Sandfly
Turmeric		982000405978433	Tumour 2	DFT1	Aug-20	Sandfly
Tylden		982000190610576	Tumour deep	DFT1	Nov-13	West Pencil Pine
Tylden		982000190610576	Tumour mid	DFT1	Nov-13	West Pencil Pine
Violet		982000405976000	Tumour 1	DFT2	Feb-20	Woodbridge
Yellow		982000405978457	Tumour 1	DFT2	Feb-20	Woodbridge
Yellow		982000405978457	Tumour 2	DFT2	Feb-20	Woodbridge
Zeus		982000405978208	Tumour 1	DFT2	May-20	Woodbridge
Zeus		982000405978208	Tumour 2	DFT2	May-20	Woodbridge

Table A 2 List of cell lines.

Sample Name	Other Identifiers	Reference
DFT1_1426	DFTD_1426; 86T	Siddle et al., 2013; Murchison et al., 2012
DFT1_4906	DFTD_4906; 88T	Siddle et al., 2013
DFT1_C5065	DFTD_C5065; 87T	Siddle et al., 2013
DFT2_RV	TD467; 202T1	Pye et al., 2016
DFT2_SN	TD500; 203T1	Pye et al., 2016
CHO		
CHO_SahaIFNγ		Siddle et al., 2013

Table A 3 List of primary antibodies used for IHC and Western blot.

Antibody	Referred to as in this thesis	Clone/catalogue number	Dilution for IHC	Dilution for Western blot	Reference/supplier
CD3		A045229-2	1:50	N/a	Dako/Agilent
Classical MHC class I Saha-UA, -UB and -UC	UABC	α-UA/UB/UC_15-25-8	Neat supernatant	Neat supernatant	Caldwell et al. 2018
His		TA15088	N/a	1 µg/ml	Origene
IFNγ		α-IFNγ_13-44-6	Neat supernatant	Neat supernatant	Caldwell 2018
Myc (9E10)		13-2500	N/a	1.25 µg/ml	Thermo scientific
Non-classical MHC class I Saha-UD (1)		α-UD_14-37-1	Neat supernatant	N/a	This thesis
Non-classical MHC class I Saha-UD (2)		α-UD_14-37-2	Neat supernatant	N/a	This thesis
Non-classical MHC class I Saha-UD (3)	UD(3)	α-UD_14-37-3	Neat supernatant	Neat supernatant	This thesis
Non-classical MHC class I Saha-UD (4)		α-UD_14-37-4	Neat supernatant	N/a	This thesis
Non-classical MHC class I Saha-UD (5)	UD(5)	α-UD_14-37-5	Neat supernatant	Neat supernatant	This thesis
Non-classical MHC class I Saha-UD (6)		α-UD_14-37-6	Neat supernatant	N/a	This thesis

Antibody	**Referred to as in this thesis**	**Clone/catalogue number**	**Dilution for IHC**	**Dilution for Western blot**	**Reference/supplier**
Non-classical MHC class I Saha-UD (7)		α-UD_14-37-7	Neat supernatant	N/a	This thesis
Non-classical MHC class I Saha-UD (8)		α-UD_14-37-8	Neat supernatant	N/a	This thesis
Non-classical MHC class I Saha-UK	UK	α-UK_15-29-1	Neat supernatant	Neat supernatant	Caldwell et al. 2018
Mouse IgG2a kappa isotype control (eBM2a)	IgG2a	14-4724-82	1 µg/ml	N/a	Invitrogen (ThermoFisher)
Periaxin		HPA001868	0.667 µg/ml	N/a	Sigma-Aldrich

Appendix B Classical MHC class I expression in DFT2

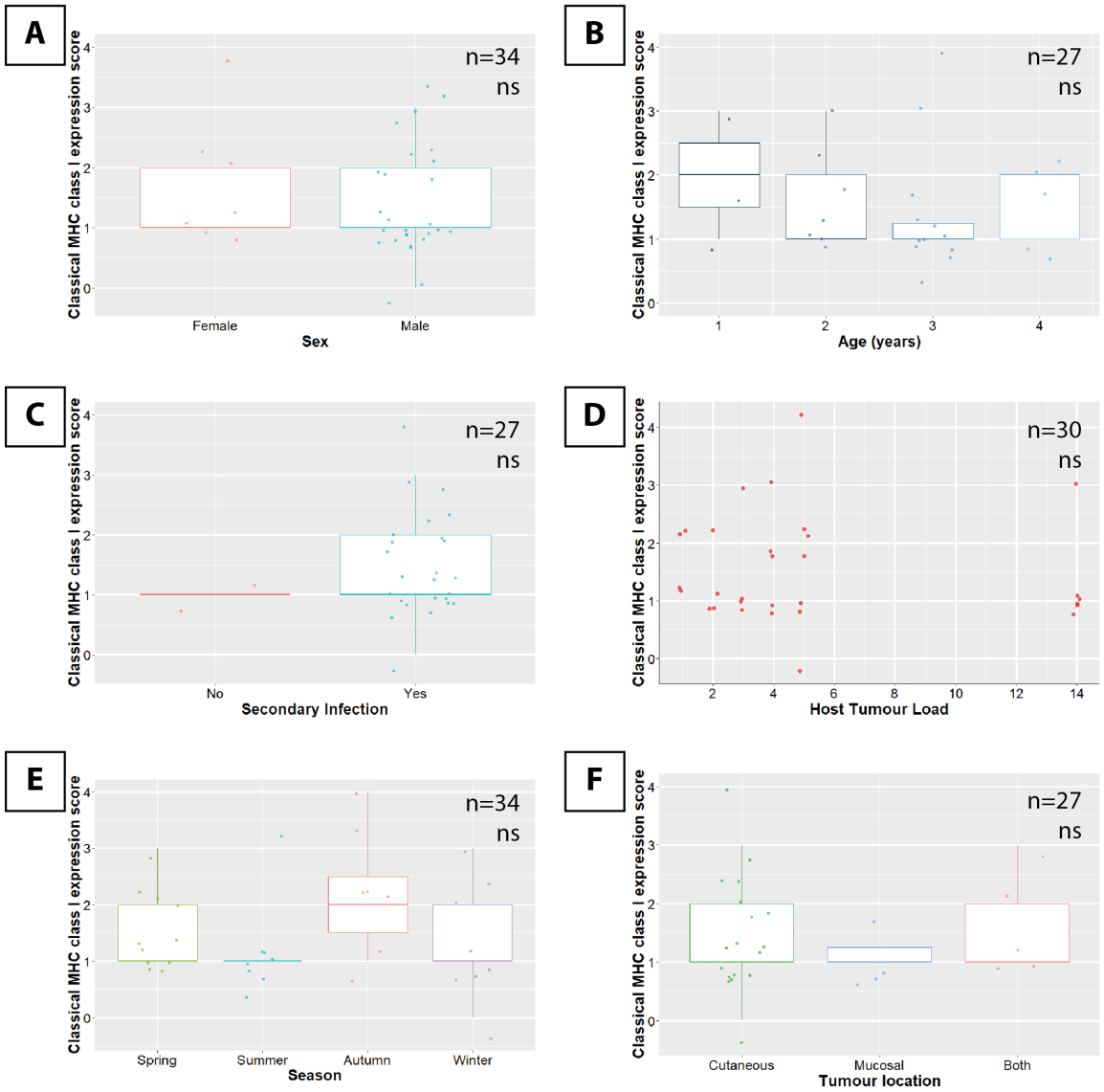

Figure B 1 Classical MHC class I expression by DFT2 tumours does not correspond with host factors, season, or tumour location.

Classical MHC class I expression in DFT2 tumour biopsies by **(A)** sex of host (n=34), **(B)** age of host (years) (n=27), **(C)** secondary infection of the tumour (n=27), **(D)** host tumour load (n=30), **(E)** season of sample collection (n=34), and **(F)** tumour location (whether the tumour was cutaneous or mucosal) (n=27). Classical MHC class I expression scores are based on the strength of IHC staining for Saha-UA, -UB, and -UC. 0 = no staining for classical MHC class I, 4 = very strong staining. Expression scores are discrete variables – jitter has been applied to the data points for visualisation. None of these factors are significant for differences in classical MHC class I expression. 'ns' = not significant ($p>0.05$).

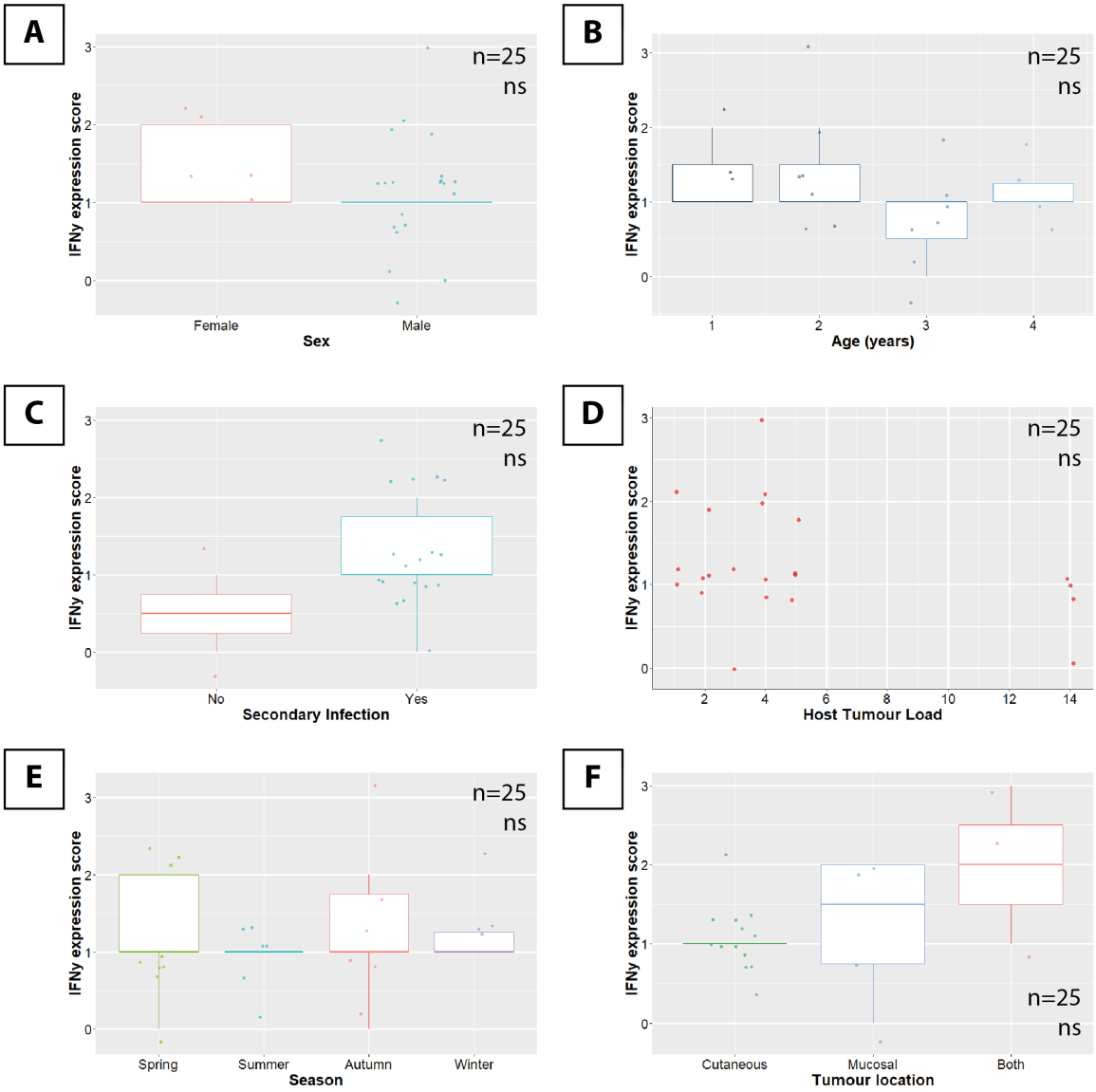

Figure B 2 IFNγ expression in DFT2 tumours does not correlate with host factors, season, or tumour location.

IFNγ expression in DFT2 tumour biopsies by **(A)** sex of host (n=25), **(B)** age of host (years) (n=21), **(C)** secondary infection of the tumour (n=20), **(D)** host tumour load (n=22), **(E)** season of sample collection (n=25), and **(F)** tumour location (whether the tumour was cutaneous or mucosal) (n=20). Expression scores are based on the strength of IHC staining. 0 = no staining for IFNγ, 4 = very strong staining. Expression scores are discrete variables – jitter has been applied to the data points for visualisation. None of these factors are significant for differences in IFNγ expression. 'ns' = not significant ($p>0.05$).

Appendix C Classical MHC class I expression in DFT1

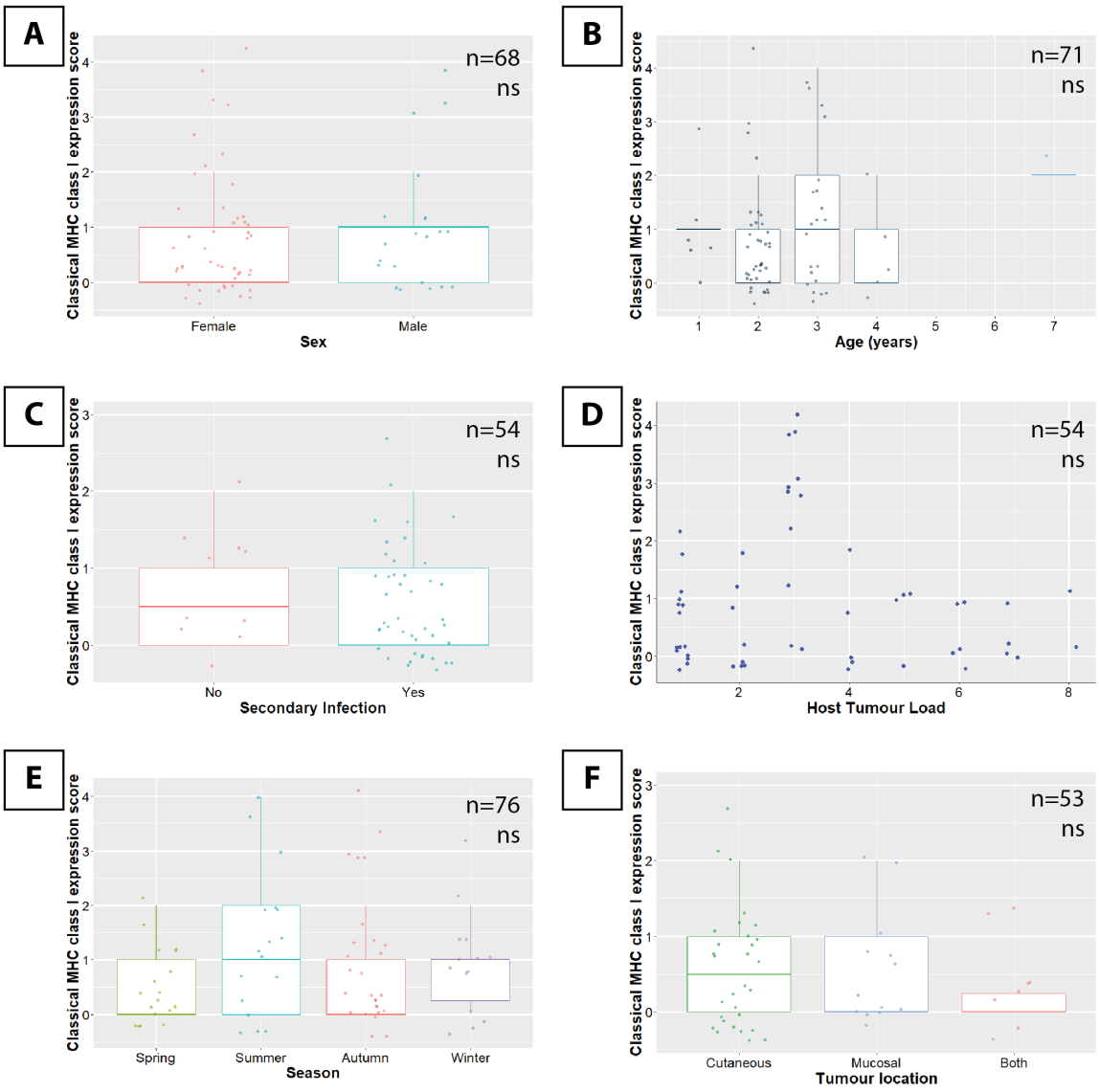

Figure C 1 Classical MHC class I expression by DFT1 does not vary by host factors, season, or tumour location.

Classical MHC class I expression in DFT1 tumour biopsies by **(A)** sex of host (n=68), **(B)** age of host (years) (n=71), **(C)** secondary infection of the tumour (n=54), **(D)** host tumour load (n=54), **(E)** season of sample collection (n=76), and **(F)** tumour location (whether the tumour was cutaneous or mucosal) (n=53). Classical MHC class I expression scores are based on the strength of IHC staining for Saha-UA, -UB, and -UC. 0 = no staining for classical MHC class I, 4 = very strong staining. Expression scores are discrete variables – jitter has been applied to the data points for

visualisation. None of these factors are significant for differences in classical MHC class I expression. ‘ns’ = not significant (p>0.05).

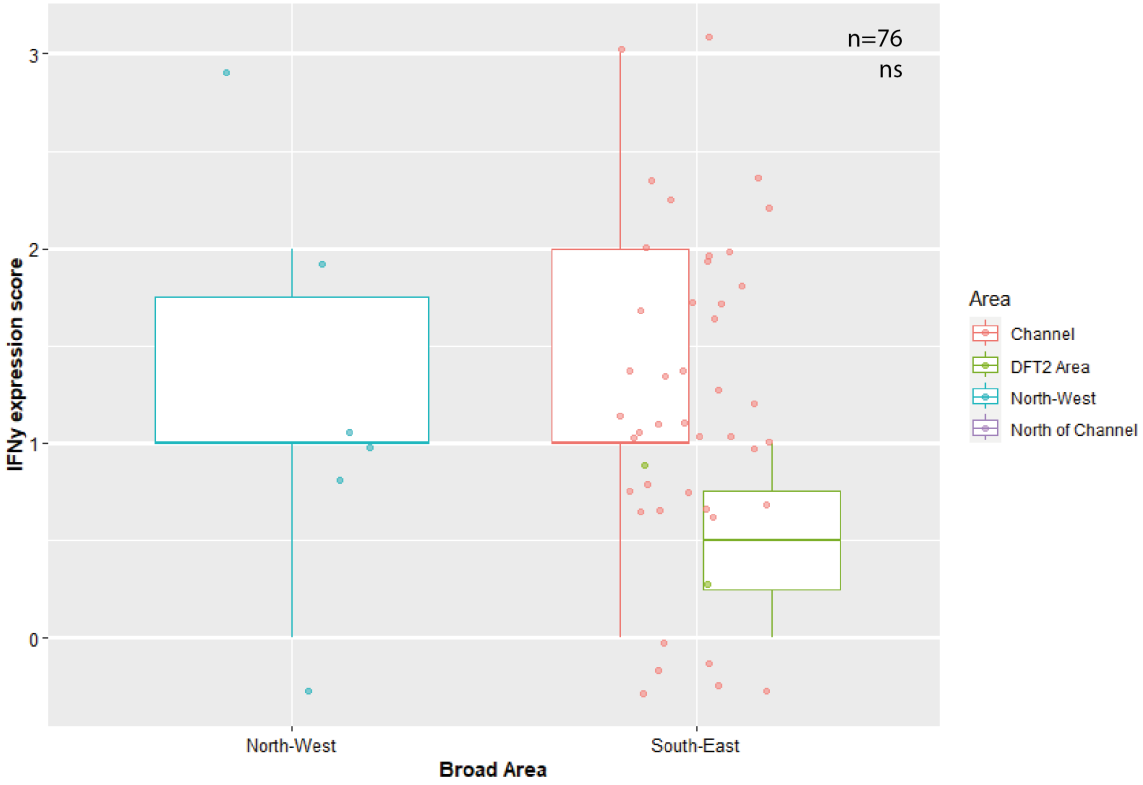

Figure C 2 IFNγ expression in DFT1 tumours does not vary by location.

IFNγ expression by DFT1 tumours (n=76) based on the area of sample collection. A map of Tasmania showing the sample sites included in Broad Area and Area is shown in Figure 4.4A. IFNγ expression is based on the strength of IHC staining. 0 = no staining for IFNγ, 4 = very strong staining. Expression scores are discrete variables – jitter has been applied to the data points for visualisation. There is no significant difference in IFNγ expression by Broad Area or Area. ‘ns’ = not significant (p>0.05).

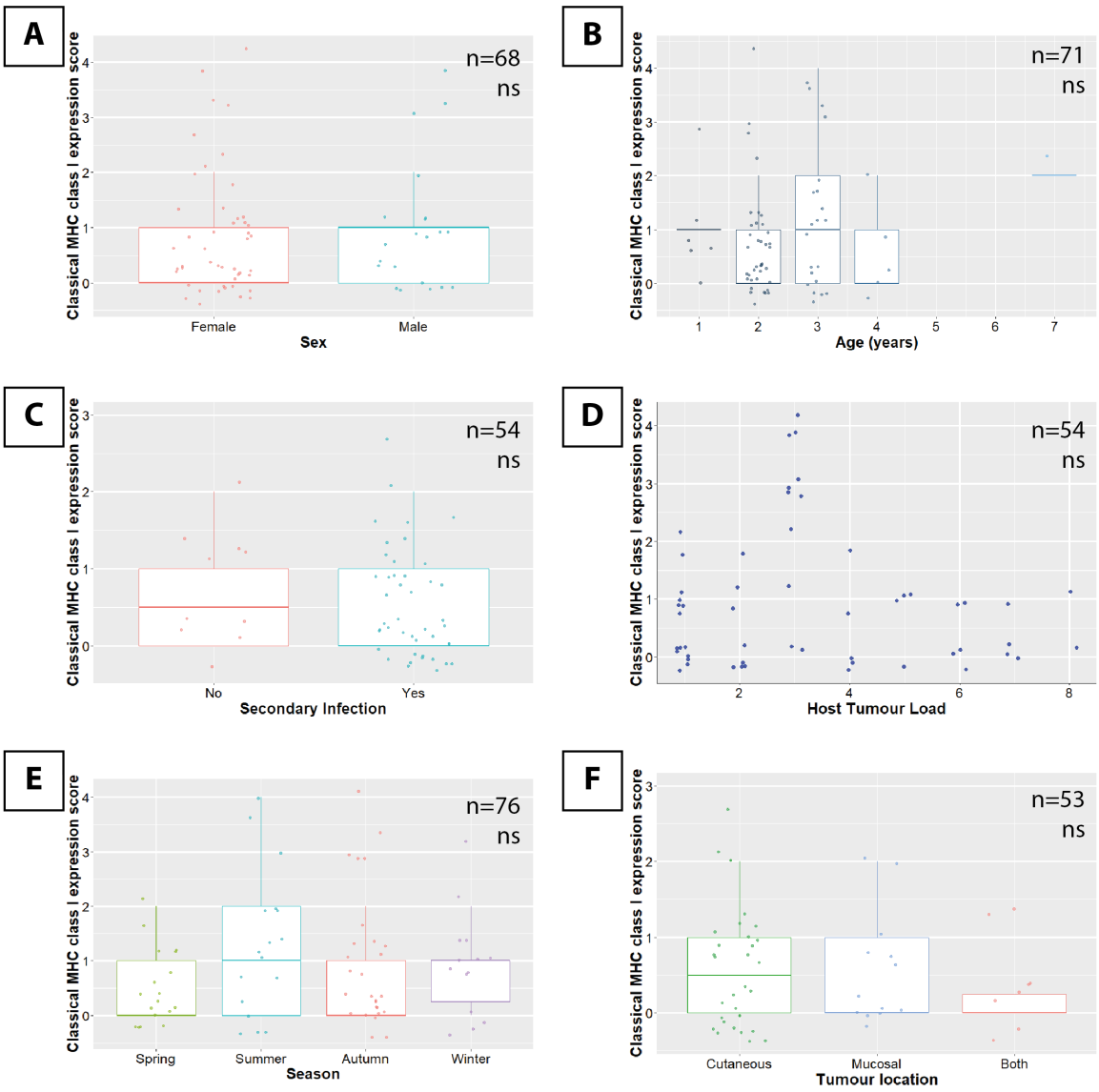

Figure C 3 IFNγ expression in DFT1 tumours does not correspond with host factor, season, or tumour location.

IFNγ expression in DFT1 tumour biopsies by **(A)** sex of host (n=42), **(B)** age of host (years) (n=42), **(C)** secondary infection of the tumour (n=33), **(D)** host tumour load (n=36), **(E)** season of sample collection (n=42), and **(F)** tumour location (whether the tumour was cutaneous or mucosal) (n=33). Expression scores are based on the strength of IHC staining. 0 = no staining for IFNγ, 4 = very strong staining. Expression scores are discrete variables – jitter has been applied to the data points for visualisation. None of these factors are significant for differences in IFNγ expression. 'ns' = not significant ($p>0.05$).

Appendix D Classical MHC class I host genotyping

Table D 1 Samples used for classical MHC class I genotyping.

Sample name	Sample type	Infected with	Included in analysis
4906_IFNγ	Cell line	N/a	Yes
Allen	Ear biopsy	DFT1	Yes
Chilli	Ear biopsy	DFT2	Yes
Cyprus	Ear biopsy	DFT1	Yes
Ebony	Ear biopsy	DFT2	Yes
Enchilada	Ear biopsy	DFT2	Yes
Freiburg	Ear biopsy	DFT2	Yes
Globulus	Ear biopsy	DFT2	Yes
Grawp	Ear biopsy	DFT2	Yes
Harry	Ear biopsy	DFT2	Yes
Hope	Ear biopsy	DFT1	Yes
Jane	Ear biopsy	DFT1	Yes
Kaoota	Ear biopsy	DFT1	Yes
Katie	Ear biopsy	DFT2	Yes
Krum	Ear biopsy	DFT2	Yes
Moody	Ear biopsy	DFT1	Yes
NONAME	Ear biopsy	DFT2	Yes
Pooh	Ear biopsy	DFT1	Yes
RV	Cell line	N/a	Yes
Sally	Ear biopsy	DFT1	Yes
Selma	Ear biopsy	DFT1	Yes
Simone	Ear biopsy	DFT1	No

Sample name	Sample type	Infected with	Included in analysis
Snape	Ear biopsy	DFT2	Yes
Snowball	Ear biopsy	DFT2	Yes
Stuttgart	Ear biopsy	DFT1	Yes
Summer	Ear biopsy	DFT2	Yes
Tabasco	Ear biopsy	DFT2	Yes
Taco	Ear biopsy	DFT2	Yes
Tibet	Ear biopsy	DFT2	Yes
Tigger	Ear biopsy	DFT1	Yes
Willie	Ear biopsy	DFT2	No

Table D 2 Percentage sequence identity for classical MHC class I amino acid sequences.

Table showing cassical MHC class I alleles called from sequencing of DFT cell lines and Tasmanian devils from the d'Entrecasteaux peninsula. Purple indicates alleles expressed by DFT1 and DFT2, blue indicates an allele expressed by DFT1 only, red indicates an allele expressed by DFT2 only. Amino acid sequences shown in Figure 5.5. Percentages calculated using Sequence Manipulation Suite: Ident and Sim ("Ident and Sim," 2020).

Allele Name	Sahal*35	Sahal*29	Sahal*97	Sahal*36	Sahal*33	Sahal*46	Sahal*87	Sahal*90	Sahal*49	Sahal*27	Sahal*91	Saha-UC	Sahal*74	Sahal*57	Sahal*37/72/79	Sahal*103
Sahal*35		98.65	95.95	95.95	95.95	94.59	89.19	87.84	91.89	87.84	90.54	87.84	89.19	90.54	93.33	93.33
Sahal*29	98.65		94.59	94.59	94.59	95.95	87.84	89.19	90.54	89.19	89.19	89.19	90.54	91.89	91.67	91.67
Sahal*97	95.95	94.59		91.89	94.59	90.54	93.24	86.49	90.54	85.14	87.84	90.54	86.49	87.84	88.33	88.33
Sahal*36	95.95	94.59	91.89		97.30	90.54	90.54	91.89	95.95	87.84	90.54	87.84	89.19	89.19	98.33	90.00
Sahal*33	95.95	94.59	94.59	97.30		90.54	90.54	91.89	95.95	86.49	89.19	86.49	87.84	87.84	95	90.00
Sahal*46	94.59	95.95	90.54	90.54	90.54		86.49	90.54	91.89	93.24	90.54	90.54	94.59	95.95	91.67	95.00
Sahal*87	89.19	87.84	93.24	90.54	90.54	86.49		93.24	91.89	83.78	86.49	89.19	85.14	86.49	90	83.33
Sahal*90	87.84	89.19	86.49	91.89	91.89	90.54	93.24		95.95	89.19	86.49	86.49	90.54	90.54	93.33	85.00
Sahal*49	91.89	90.54	90.54	95.95	95.95	91.89	91.89	95.95		90.54	90.54	87.84	91.89	91.89	98.33	90.00
Sahal*27	87.84	89.19	85.14	87.84	86.49	93.24	83.78	89.19	90.54		97.30	94.59	98.65	97.30	88.33	93.33
Sahal*91	90.54	89.19	87.84	90.54	89.19	90.54	86.49	86.49	90.54	97.30		94.59	95.95	94.59	90.00	95.00
Saha-UC	87.84	89.19	90.54	87.84	86.49	90.54	89.19	86.49	87.84	94.59	94.59		95.95	94.59	86.67	88.33
Sahal*74	89.19	90.54	86.49	89.19	87.84	94.59	85.14	90.54	91.89	98.65	95.95	95.95		98.65	90.00	91.67
Sahal*57	90.54	91.89	87.84	89.19	87.84	95.95	86.49	90.54	91.89	97.30	94.59	94.59	98.65		90.00	90.00
Sahal*37/72/79	93.33	91.67	88.33	98.33	95.00	91.67	90.00	93.33	98.33	88.33	90.00	86.67	90.00	90.00		91.67
Sahal*103	93.33	91.67	88.33	90.00	90.00	95.00	83.33	85.00	90.00	93.33	95.00	88.33	91.67	90.00	91.67	

Table D 3 Percentage sequence similarity for classical MHC class I amino acid sequences.

Table showing classical MHC class I alleles called from sequencing of DFT cell lines and Tasmanian devils from the d'Entrecasteaux peninsula. Purple indicates alleles expressed by DFT1 and DFT2, blue indicates an allele expressed by DFT1 only, red indicates an allele expressed by DFT2 only. Amino acid sequences shown in Figure 5.5. Percentages calculated using Sequence Manipulation Suite: Ident and Sim ("Ident and Sim," 2020).

Allele Name	Sahal*35	Sahal*29	Sahal*97	Sahal*36	Sahal*33	Sahal*46	Sahal*87	Sahal*90	Sahal*49	Sahal*27	Sahal*91	Saha-UC	Sahal*74	Sahal*57	Sahal*37/72/79	Sahal*103
Sahal*35		98.65	98.65	95.95	97.30	94.59	91.89	89.19	93.24	89.19	91.89	90.54	90.54	91.89	93.33	93.33
Sahal*29	98.65		97.30	94.59	95.95	95.95	90.54	90.54	91.89	90.54	90.54	91.89	91.89	93.24	91.67	91.67
Sahal*97	98.65	97.30		94.59	95.95	93.24	93.24	87.84	91.89	87.84	90.54	91.89	89.19	90.54	91.67	91.67
Sahal*36	95.95	94.59	94.59		98.65	90.54	93.24	93.24	97.30	89.19	91.89	90.54	90.54	90.54	98.33	90.00
Sahal*33	97.30	95.95	95.95	98.65		91.89	91.89	91.89	95.95	87.84	90.54	89.19	89.19	89.19	96.67	91.67
Sahal*46	94.59	95.95	93.24	90.54	91.89		89.19	91.89	93.24	94.59	91.89	93.24	95.95	97.30	91.67	95.00
Sahal*87	91.89	90.54	93.24	93.24	91.89	89.19		94.59	93.24	86.49	89.19	90.54	87.84	89.19	93.33	86.67
Sahal*90	89.19	90.54	87.84	93.24	91.89	91.89	94.59		95.95	90.54	87.84	89.19	91.89	91.89	95.00	86.67
Sahal*49	93.24	91.89	91.89	97.30	95.95	93.24	93.24	95.95		91.89	91.89	90.54	93.24	93.24	100.00	91.67
Sahal*27	89.19	90.54	87.84	89.19	87.84	94.59	86.49	90.54	91.89		97.30	95.95	98.65	97.30	90.00	95.00
Sahal*91	91.89	90.54	90.54	91.89	90.54	91.89	89.19	87.84	91.89	97.30		95.95	95.95	94.59	91.67	96.67
Saha-UC	90.54	91.89	91.89	90.54	89.19	93.24	90.54	89.19	90.54	95.95	95.95		97.30	95.95	90.00	91.67
Sahal*74	90.54	91.89	89.19	90.54	89.19	95.95	87.84	91.89	93.24	98.65	95.95	97.30		98.65	91.67	93.33
Sahal*57	91.89	93.24	90.54	90.54	89.19	97.30	89.19	91.89	93.24	97.30	94.59	95.95	98.65		91.67	91.67
Sahal*37/72/79	93.33	91.67	91.67	98.33	96.67	91.67	93.33	95.00	100.00	90.00	91.67	90.00	91.67	91.67		91.67
Sahal*103	93.33	91.67	91.67	90.00	91.67	95.00	86.67	86.67	91.67	95.00	96.67	91.67	93.33	91.67	91.67	

Table D 4 Number of mismatched TCR residues for classical MHC class I amino acid sequences.

Table showing the number of residues predicted to interact with the TCR (assigned based on Bjorkman and Parham (1990)) that are mismatched between classical MHC class I alleles. Alleles shown were called from sequencing of DFT cell lines and Tasmanian devils from the d'Entrecasteaux peninsula. Purple indicates alleles expressed by DFT1 and DFT2, blue indicates an allele expressed by DFT1 only, red indicates an allele expressed by DFT2 only. Amino acid sequences shown in Figure 5.5.

Allele Name	Sahal*35	Sahal*29	Sahal*97	Sahal*36	Sahal*33	Sahal*46	Sahal*87	Sahal*90	Sahal*49	Sahal*27	Sahal*91	Saha-UC	Sahal*74	Sahal*57	Sahal*37/72/79	Sahal*103
Sahal*35		0	0	0	0	0	1	1	0	1	1	1	1	1	0	0
Sahal*29	0		0	0	0	0	1	1	0	1	1	1	1	1	0	0
Sahal*97	0	0		0	0	0	1	1	0	1	1	1	1	1	0	0
Sahal*36	0	0	0		0	0	1	1	0	1	1	1	1	1	0	0
Sahal*33	0	0	0	0		0	1	1	0	1	1	1	1	1	0	0
Sahal*46	0	0	0	0	0		1	1	0	1	1	1	1	1	0	0
Sahal*87	1	1	1	1	1	1		0	1	2	2	2	2	2	1	1
Sahal*90	1	1	1	1	1	1	0		1	2	2	2	2	2	1	1
Sahal*49	0	0	0	0	0	0	1	1		1	1	1	1	1	0	0
Sahal*27	1	1	1	1	1	1	2	2	1		0	0	0	0	1	1
Sahal*91	1	1	1	1	1	1	2	2	1	0		0	0	0	1	1
Saha-UC	1	1	1	1	1	1	2	2	1	0	0		0	0	1	1
Sahal*74	1	1	1	1	1	1	2	2	1	0	0	0		0	1	1
Sahal*57	1	1	1	1	1	1	2	2	1	0	0	0	0		1	1
Sahal*37/72/79	0	0	0	0	0	0	1	1	0	1	1	1	1	1		0
Sahal*103	0	0	0	0	0	0	1	1	0	1	1	1	1	1	0	

Table D 5 Number of mismatched peptide binding residues for classical MHC class I amino acid sequences.

Table showing the number of residues predicted to bind a peptide for presentation (assigned based on Bjorkman and Parham (1990)) that are mismatched between classical MHC class I alleles. Alleles shown were called from sequencing of DFT cell lines and Tasmanian devils from the d'Entrecasteaux peninsula. Purple indicates alleles expressed by DFT1 and DFT2, blue indicates an allele expressed by DFT1 only, red indicates an allele expressed by DFT2 only. Amino acid sequences shown in Figure 5.5.

Allele Name	Sahal*35	Sahal*29	Sahal*97	Sahal*36	Sahal*33	Sahal*46	Sahal*87	Sahal*90	Sahal*49	Sahal*27	Sahal*91	Saha-UC	Sahal*74	Sahal*57	Sahal*37/72/79	Sahal*103
Sahal*35		0	1	3	3	3	5	7	6	8	7	7	7	6	4	4
Sahal*29	0		1	3	3	3	5	7	6	8	7	7	7	6	4	4
Sahal*97	1	1		4	2	4	4	6	5	8	7	6	7	6	5	5
Sahal*36	3	3	4		2	6	4	4	3	8	7	6	7	7	1	6
Sahal*33	3	3	2	2		6	4	4	3	9	8	7	8	8	3	6
Sahal*46	3	3	4	6	6		7	6	5	5	6	5	4	3	4	2
Sahal*87	5	5	4	4	4	7		2	3	7	7	6	7	6	3	7
Sahal*90	7	7	6	4	4	6	2		1	7	8	7	6	6	2	7
Sahal*49	6	6	5	3	3	5	3	1		6	7	6	5	5	1	6
Sahal*27	8	8	8	8	9	5	7	7	6		1	2	1	2	6	3
Sahal*91	7	7	7	7	8	6	7	8	7	1		1	2	3	6	3
Saha-UC	7	7	6	6	7	5	6	7	6	2	1		1	2	5	4
Sahal*74	7	7	7	7	8	4	7	6	5	1	2	1		1	5	4
Sahal*57	6	6	6	7	8	3	6	6	5	2	3	2	1		5	5
Sahal*37/72/79	4	4	5	1	3	4	3	2	1	6	6	5	5	5		5
Sahal*103	4	4	5	6	6	2	7	7	6	3	3	4	4	5	5	

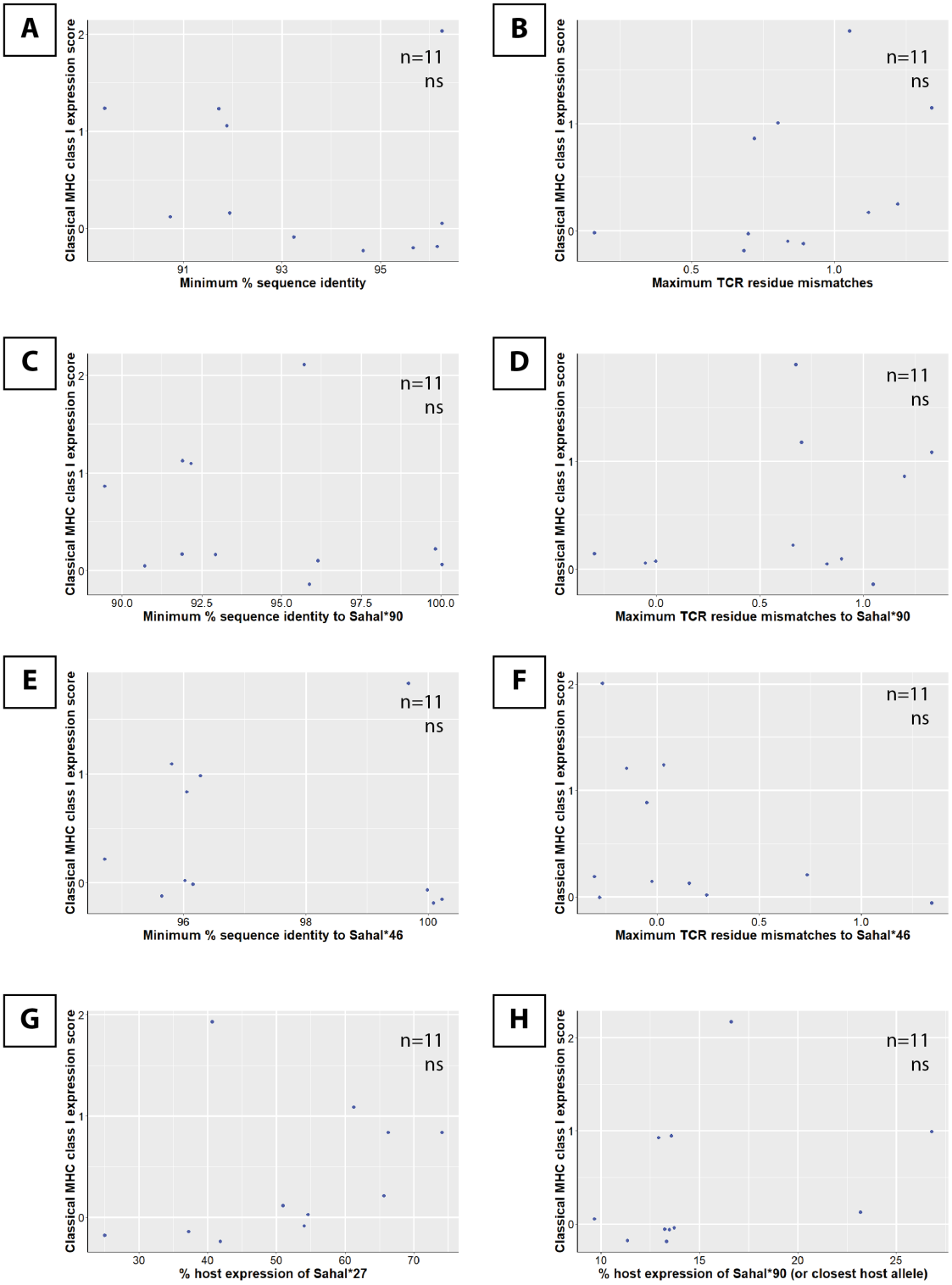

Figure D 1 Classical MHC class I expression does not correlate with host-tumour classical MHC class I mismatch in DFT1.

DFT1 hosts were genotyped for classical MHC class I, at the α1-α2 domains (exons 2-3) by NGS. Host genotypes were compared with DFT1 to assess the level of mismatch between host and tumour classical MHC class I alleles. TCR residues predicted to interact with the TCR were based on Bjorkman and Parham (1990). Graphs show

classical MHC class I expression in DFT1 tumour biopsies (n=11) compared with **(A)** minimum % sequence identity between host and DFT1 classical MHC class I alleles, **(B)** maximum mismatches between host and tumour MHC class I alleles at residues predicted to interact with the TCR, **(C)** minimum host % sequence identity and **(D)** maximum TCR residue mismatches to DFT1 allele SahaI*90, **(E)** minimum host % sequence identity and **(F)** maximum TCR residue mismatches to DFT1 allele SahaI*46, **(G)** % host expression of common allele, SahaI*27, and **(H)** % host expression of commonly mismatched allele, SahaI*90 (or the closest matched allele in the host). Classical MHC class I expression scores are based on the strength of IHC staining. 0 = no staining, 4 = very strong staining. Expression scores are discrete variables – jitter has been applied to the data points for visualisation. None of these factors are significant for differences in classical MHC class I expression (Spearman's correlation). 'ns' = not significant ($p>0.05$).

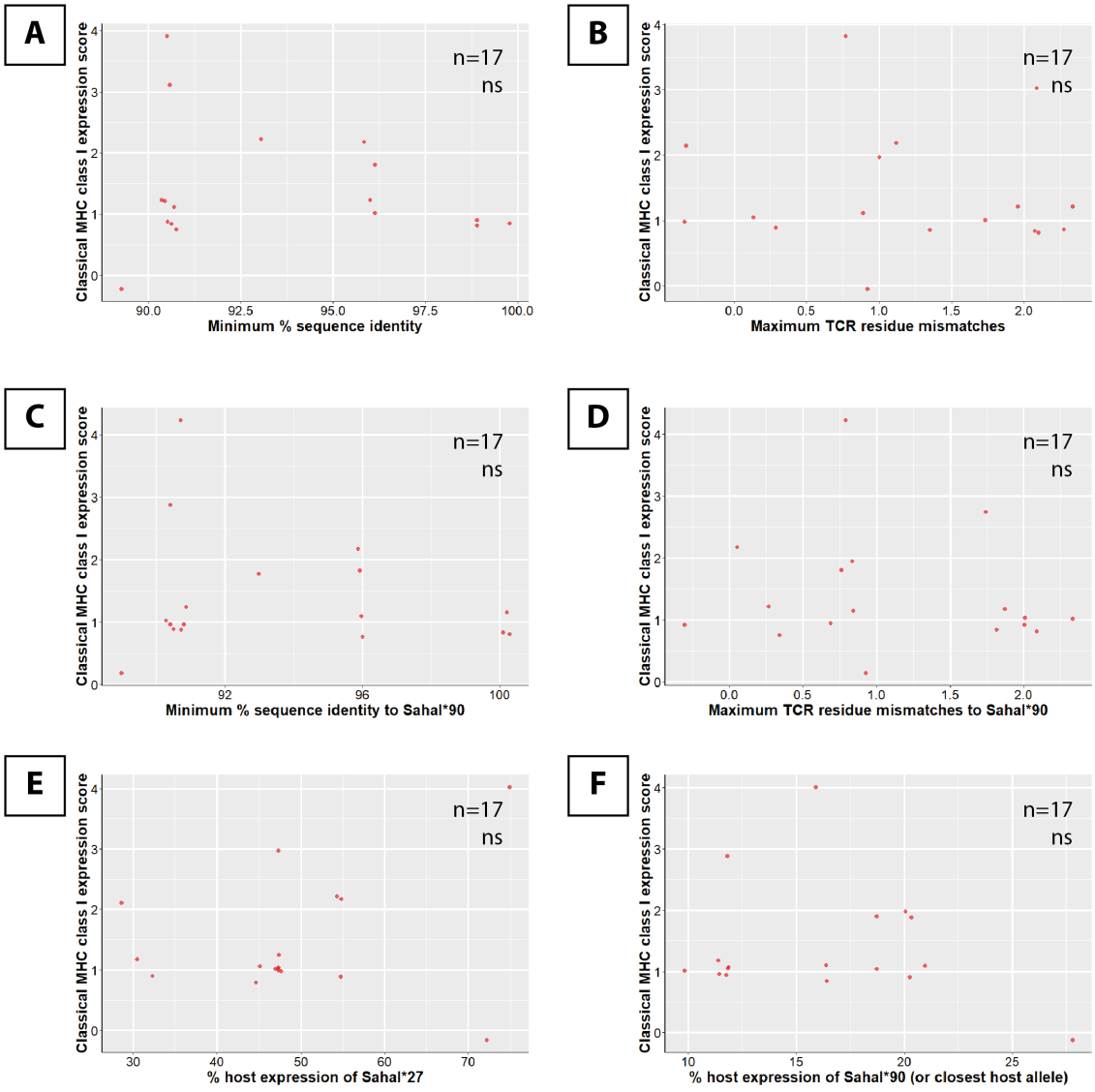

Figure D 2 Classical MHC class I expression does not correlate with host-tumour classical MHC class I mismatch in DFT2.

DFT2 hosts were genotyped for classical MHC class I, at the α1-α2 domains (exons 2-3) by NGS. Host genotypes were compared with DFT2 to assess the level of mismatch between host and tumour classical MHC class I alleles. TCR residues predicted to interact with the TCR were based on Bjorkman and Parham (1990). Graphs show classical MHC class I expression in DFT2 tumour biopsies (n=17) compared with **(A)** minimum % sequence identity between host and DFT2 classical MHC class I alleles, **(B)** maximum mismatches between host and tumour MHC class I alleles at residues predicted to interact with the TCR, **(C)** minimum host % sequence identity and **(D)** maximum TCR residue mismatches to DFT2 allele SahaI*90, **(E)** % host expression of common allele, SahaI*27, and **(F)** % host expression of commonly mismatched allele, SahaI*90 (or the closest matched allele in the host). Classical MHC class I expression

scores are based on the strength of IHC staining. 0 = no staining, 4 = very strong staining. Expression scores are discrete variables – jitter has been applied to the data points for visualisation. None of these factors are significant for differences in classical MHC class I expression (Spearman's correlation). 'ns' = not significant ($p>0.05$).

Appendix E Non-classical expression in DFT1

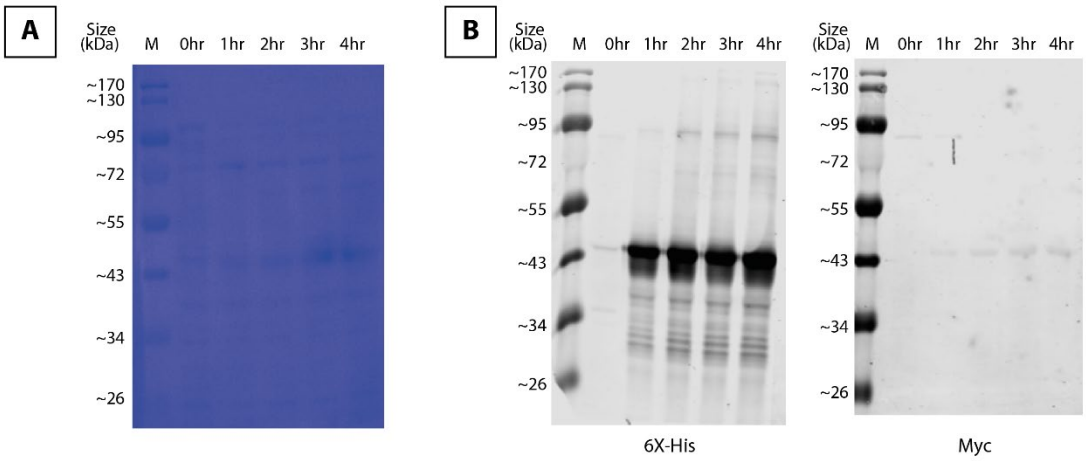

Figure E 1 Coomassie and Western blots confirming Saha-UD protein production.

Recombinant Saha-UD heavy chain production was induced in Rosetta pLysS cells by the addition of 1mM IPTG. Culture media was collected every 1 hr and run on an SDS-PAGE gel and either **(A)** stained with Coomassie blue, or transferred to a Western blot and stained for **(B)** 6X-His tag and myc. All show an increase in band at ~45 kDa, indicating Saha-UD heavy chain expression has been induced.

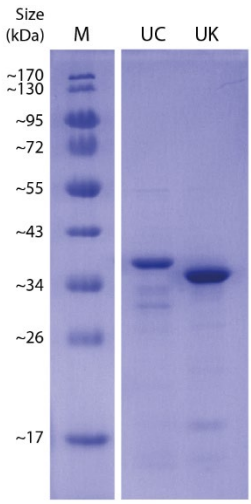

Figure E 2 Recombinant heavy chain proteins for classical Saha-UC and non-classical Saha-UK, analysed on an SDS-PAGE gel stained with Coomassie blue.

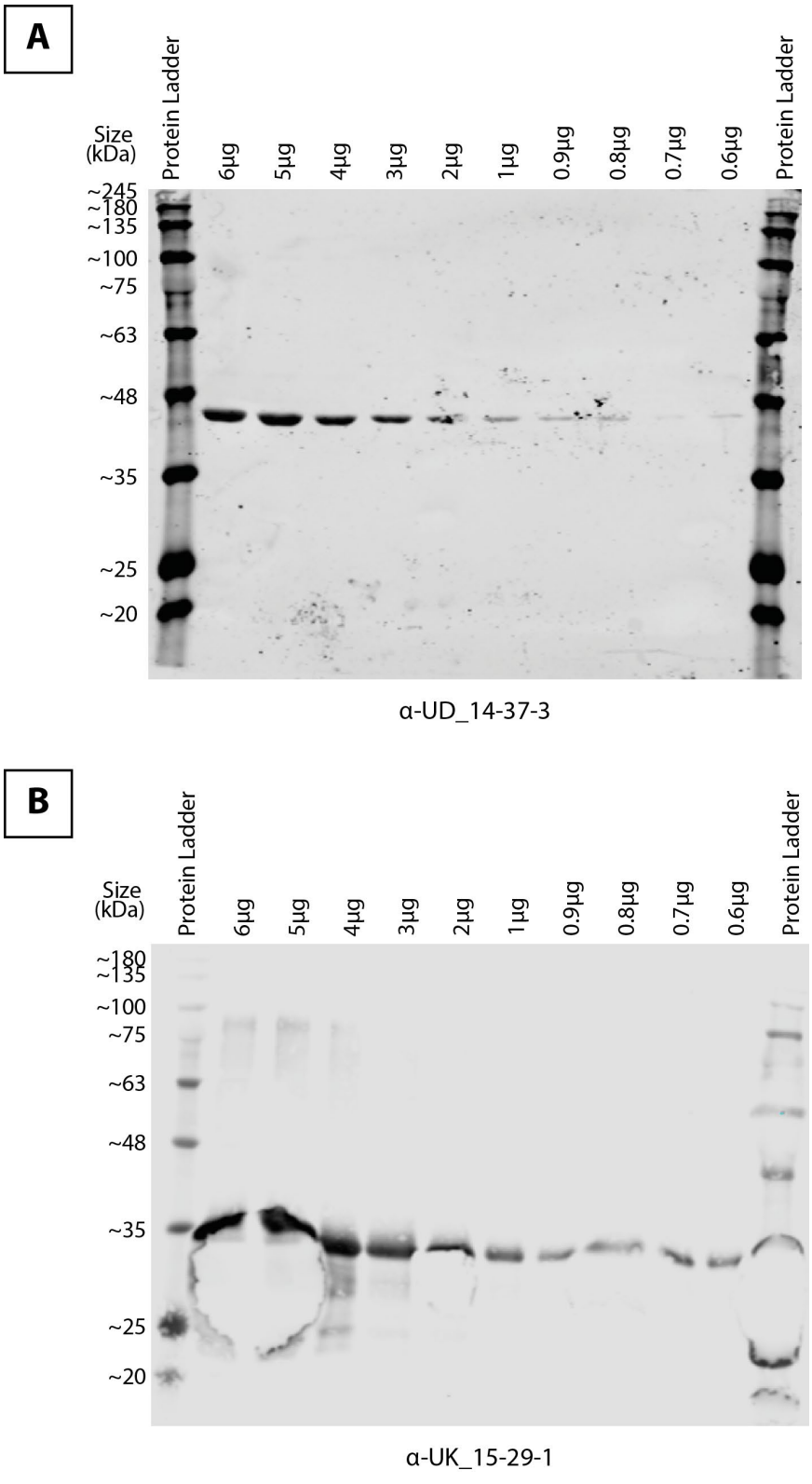

Figure E 3 Antibody affinity for antibodies against non-classical MHC class I, Saha-UD and Saha-UK.

Protein titration of recombinant MHC class I heavy chain proteins for analysis of antibody specificity by Western blot. **(A)** Recombinant non-classical, Saha-UD heavy chain, stained with antibody α-UD_14-37-3. **(B)** Recombinant non-classical, Saha-UK heavy chain, stained with antibody α-UK_15-29-1.

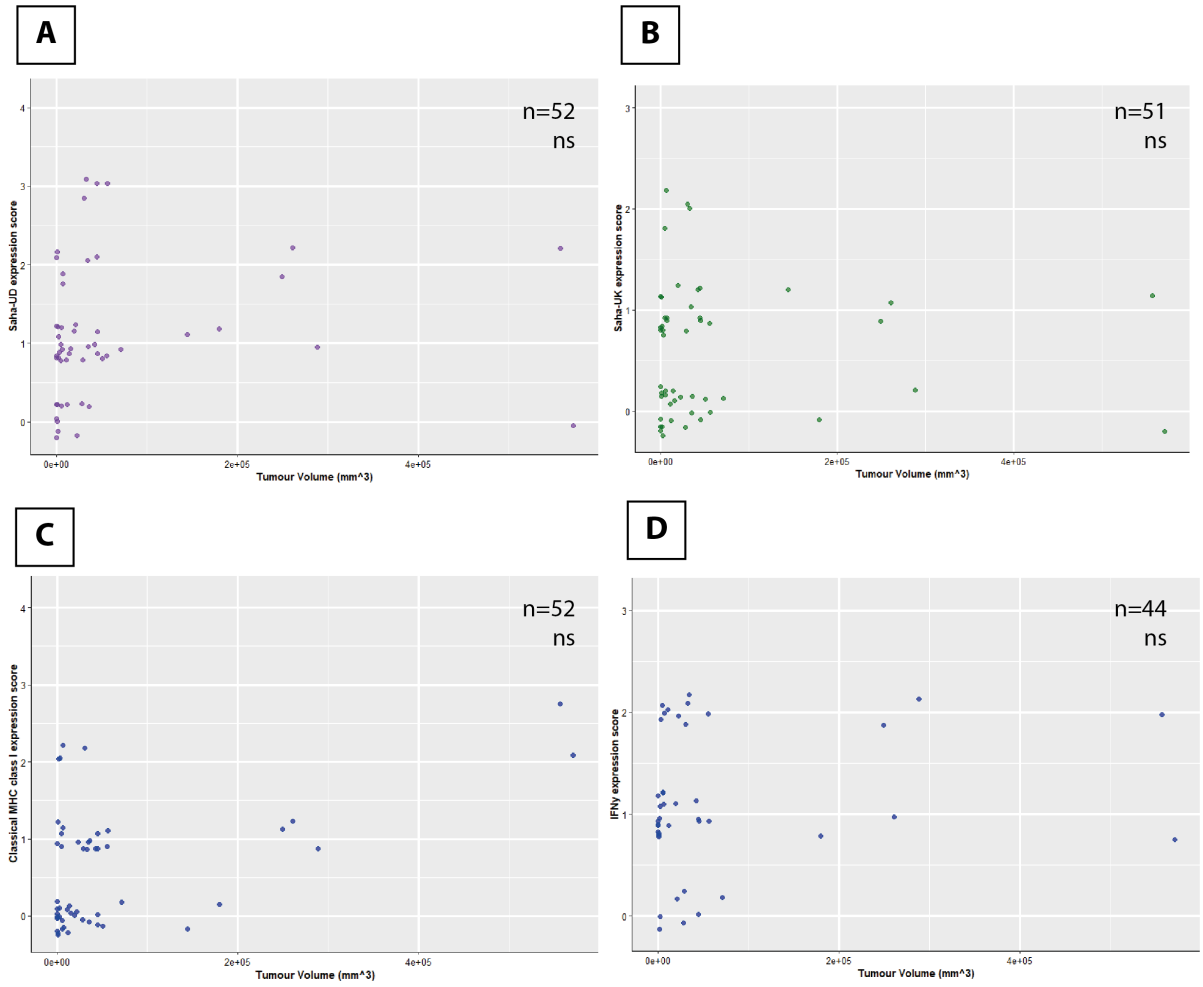

Figure E 4 Tumour volume does not correlate with MHC class I expression by DFT1 tumour cells or IFNγ expression in DFT1 tumours.

Expression of **(A)** non-classical, Saha-UD (n=52), **(B)** non-classical MHC class I, Saha-UK (n=51), **(C)** Classical MHC class I (n=52), and **(A)** immune marker, IFNγ (n=44) in DFT1 tumour biopsies compared with tumour volume in mm^3. Expression scores are based on the strength of IHC staining; 0 = no staining, 4 = very strong staining. Expression scores are discrete variables – jitter has been applied to the data points for visualisation. There is no correlation between MHC class I or IFNγ and tumour volume (Spearman's correlation). 'ns' = not significant (p>0.05).

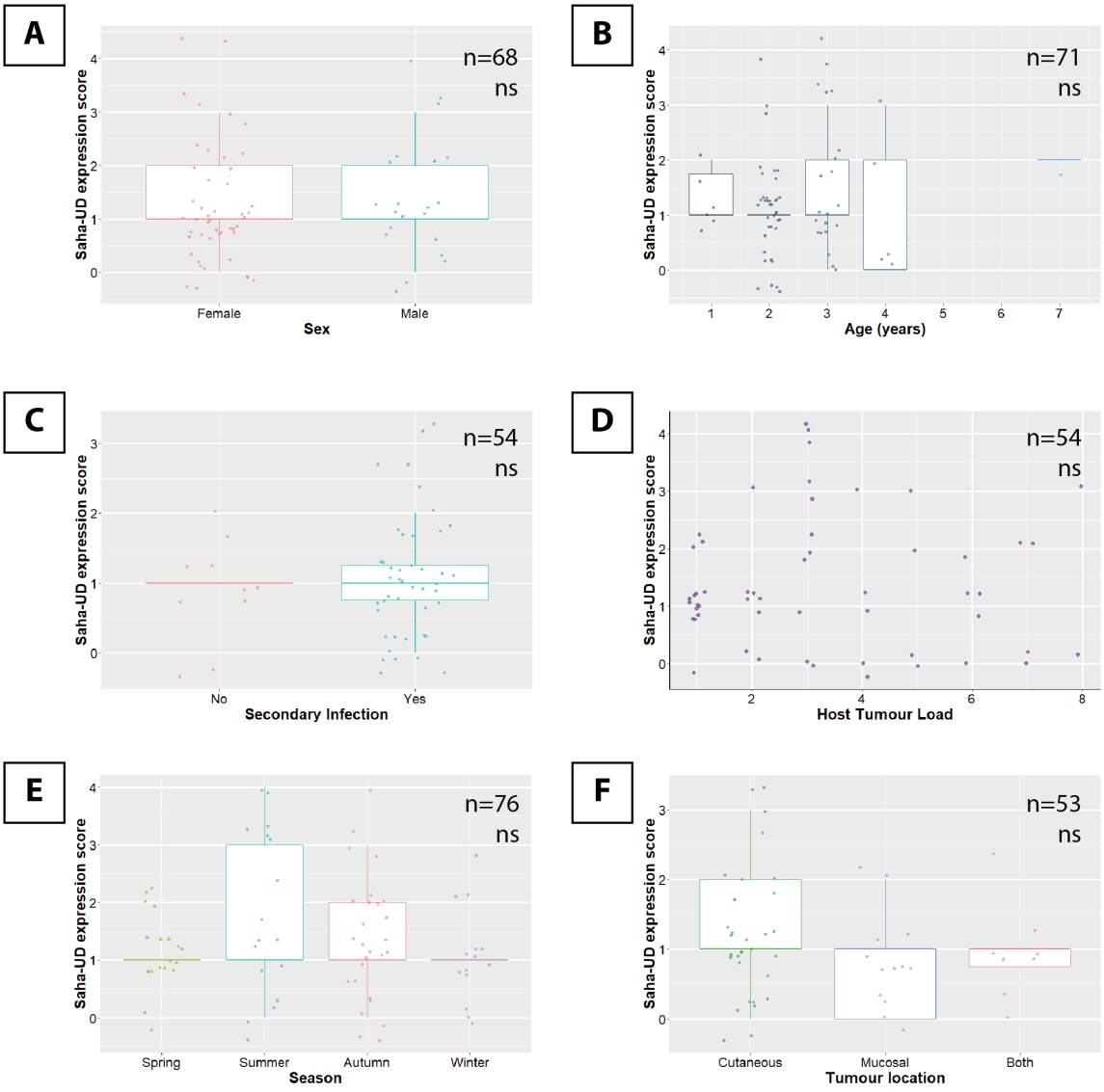

Figure E 5 Non-classical, Saha-UD expression in DFT1 tumours does not correlate with host factors, season, or tumour location.

Non-classical, Saha-UD expression in DFT1 tumour biopsies by **(A)** sex of host (n=68), **(B)** age of host (years) (n=71), **(C)** secondary infection of the tumour (n=54), **(D)** host tumour load (n=54), **(E)** season of sample collection (n=76), and **(F)** tumour location (whether the tumour was cutaneous or mucosal) (n=53). Saha-UD expression scores are based on the strength of IHC staining. 0 = no staining for Saha-UD, 4 = very strong staining. Expression scores are discrete variables – jitter has been applied to the data points for visualisation. None of these factors are significant for differences in classical MHC class I expression. 'ns' = not significant ($p>0.05$).

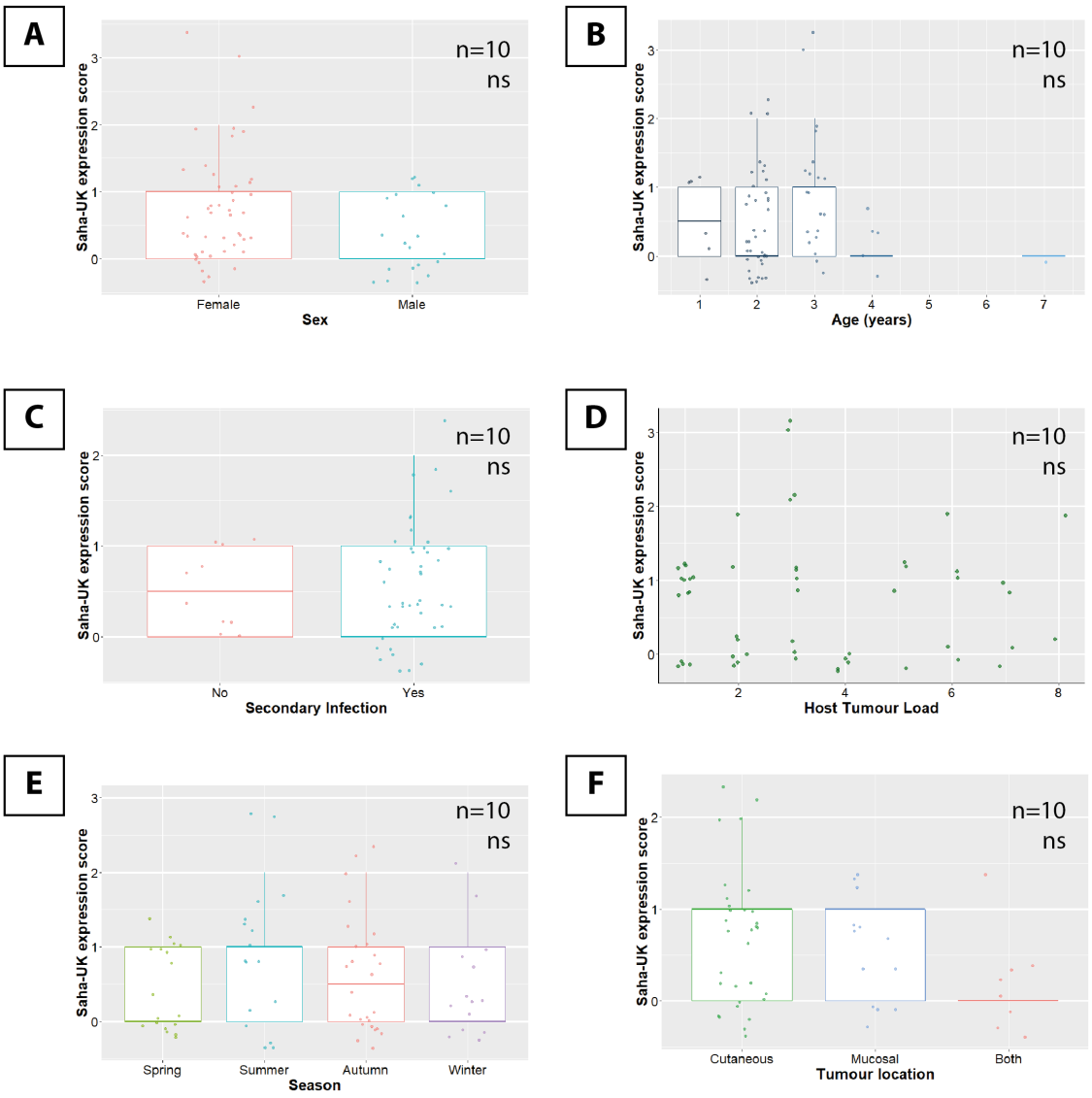

Figure E 6 Non-classical, Saha-UK expression in DFT1 tumours does not correlate with host factors, season, or tumour location.

Non-classical, Saha-UK expression in DFT1 tumour biopsies by **(A)** sex of host (n=67), **(B)** age of host (years) (n=70), **(C)** secondary infection of the tumour (n=53), **(D)** host tumour load (n=53), **(E)** season of sample collection (n=75), and **(F)** tumour location (whether the tumour was cutaneous or mucosal) (n=52). Saha-UK expression scores are based on the strength of IHC staining. 0 = no staining for Saha-UK, 4 = very strong staining. Expression scores are discrete variables – jitter has been applied to the data points for visualisation. None of these factors are significant for differences in classical MHC class I expression. 'ns' = not significant (p>0.05).

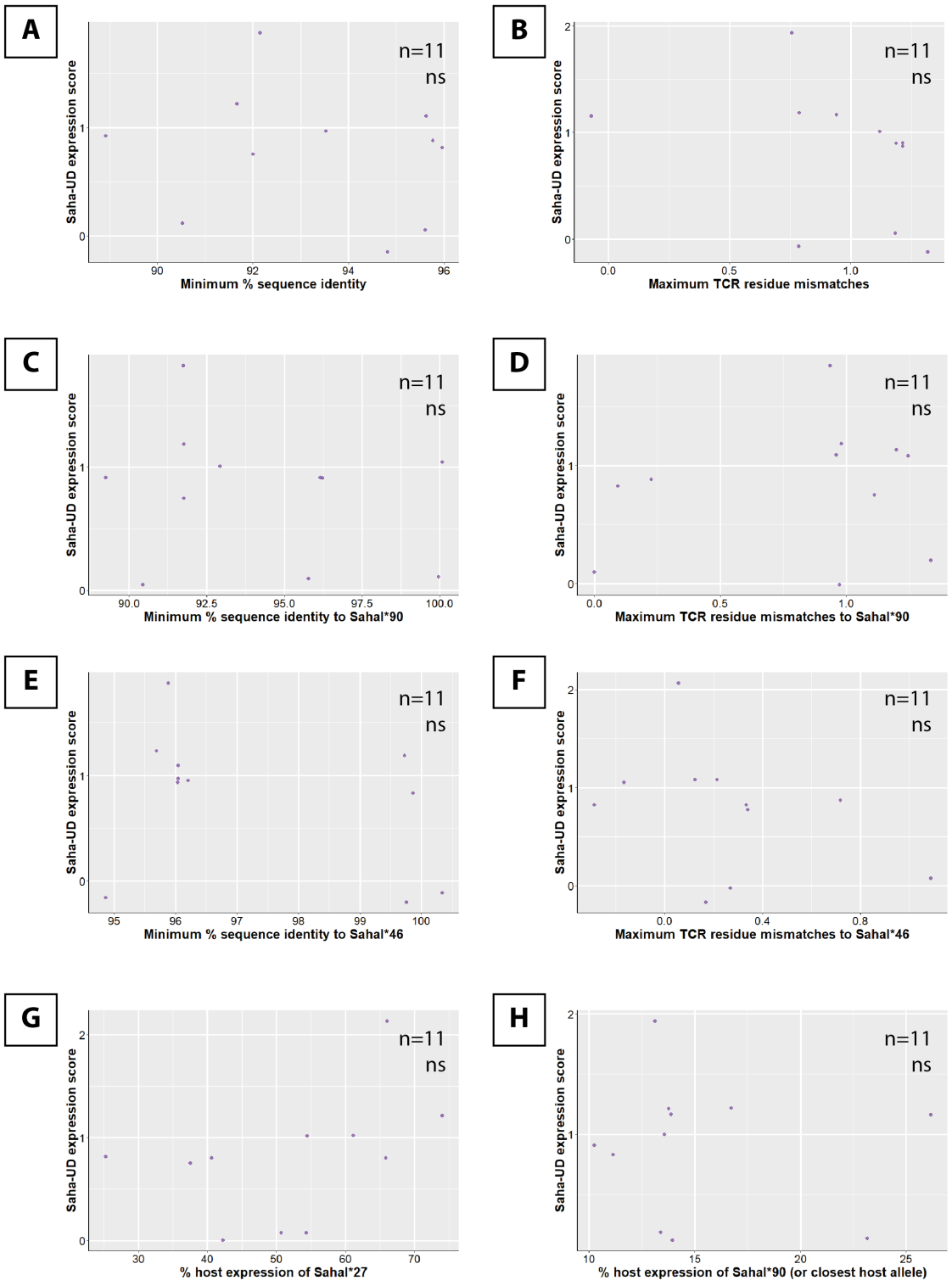

Figure E 7 Non-classical Saha-UD expression does not correlate with host-tumour classical MHC class I mismatch in DFT1.

DFT1 hosts were genotyped for classical MHC class I, at the α1-α2 domains (exons 2-3) by NGS. Host genotypes were compared with DFT1 to assess the level of mismatch between host and tumour classical MHC class I alleles. TCR residues predicted to interact with the TCR were based on Bjorkman and Parham (1990). Graphs show

non-classical, Saha-UD expression in DFT1 tumour biopsies (n=11) compared with **(A)** minimum % sequence identity between host and DFT1 classical MHC class I alleles, **(B)** maximum mismatches between host and tumour MHC class I alleles at residues predicted to interact with the TCR, **(C)** minimum host % sequence identity and **(D)** maximum TCR residue mismatches to DFT1 allele SahaI*90, **(E)** minimum host % sequence identity and **(F)** maximum TCR residue mismatches to DFT1 allele SahaI*46, **(G)** % host expression of common allele, SahaI*27, and **(H)** % host expression of commonly mismatched allele, SahaI*90 (or the closest matched allele in the host). Saha-UD expression scores are based on the strength of IHC staining. 0 = no staining for Saha-UD, 4 = very strong staining. Expression scores are discrete variables – jitter has been applied to the data points for visualisation. None of these factors are significant for differences in classical MHC class I expression (Spearman's correlation). 'ns' = not significant ($p>0.05$).

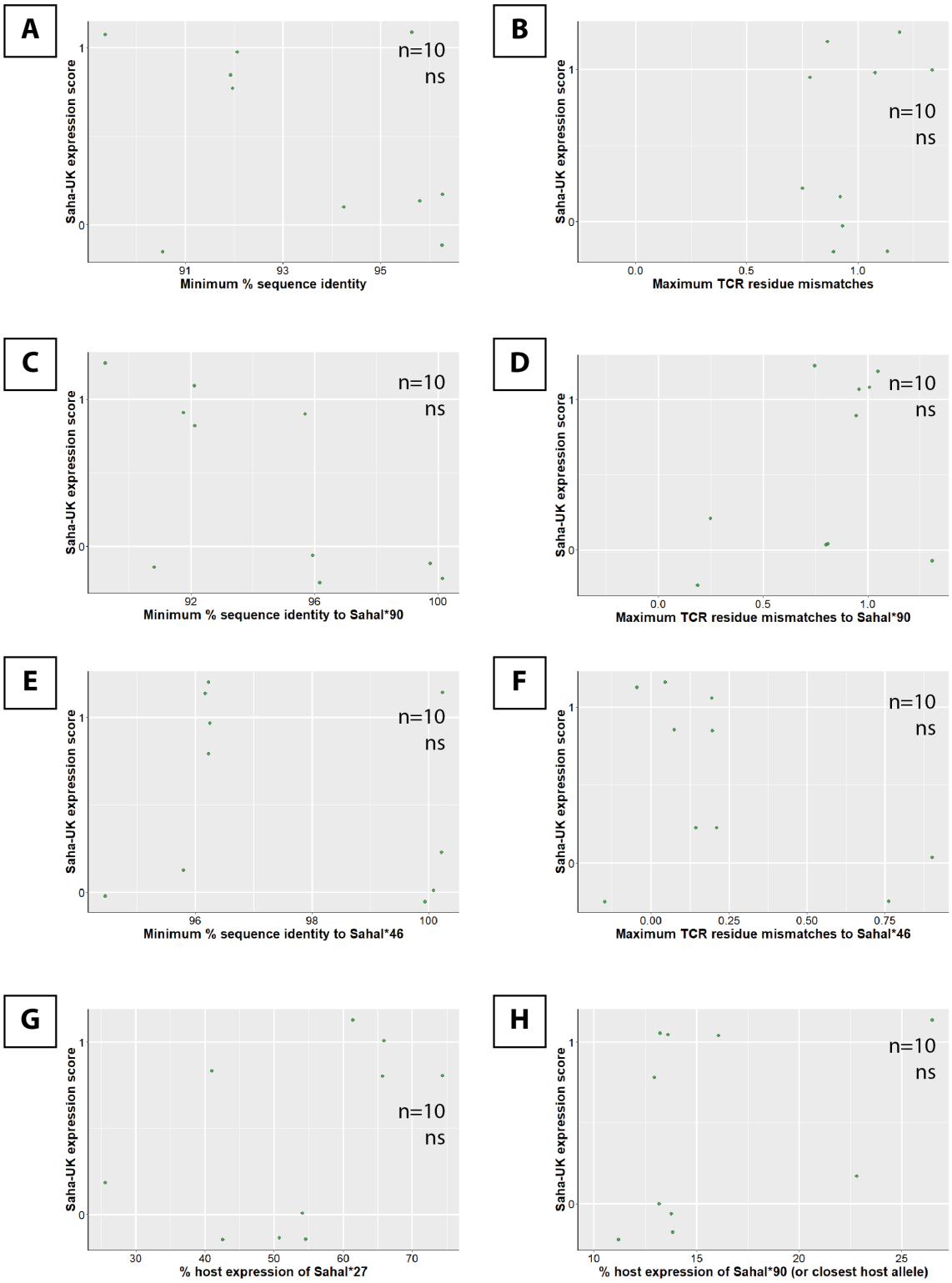

Figure E 8 Non-classical Saha-UK expression does not correlate with host-tumour classical MHC class I mismatch in DFT1.

DFT1 hosts were genotyped for classical MHC class I, at the α1-α2 domains (exons 2-3) by NGS. Host genotypes were compared with DFT1 to assess the level of mismatch between host and tumour classical MHC class I alleles. TCR residues predicted to

interact with the TCR were based on Bjorkman and Parham (1990). Graphs show non-classical, Saha-UK expression in DFT1 tumour biopsies (n=10) compared with **(A)** minimum % sequence identity between host and DFT1 classical MHC class I alleles, **(B)** maximum mismatches between host and tumour MHC class I alleles at residues predicted to interact with the TCR, **(C)** minimum host % sequence identity and **(D)** maximum TCR residue mismatches to DFT1 allele SahaI*90, **(E)** minimum host % sequence identity and **(F)** maximum TCR residue mismatches to DFT1 allele SahaI*46, **(G)** % host expression of common allele, SahaI*27, and **(H)** % host expression of commonly mismatched allele, SahaI*90 (or the closest matched allele in the host). Saha-UK expression scores are based on the strength of IHC staining. 0 = no staining for Saha-UK, 4 = very strong staining. Expression scores are discrete variables – jitter has been applied to the data points for visualisation. None of these factors are significant for differences in classical MHC class I expression (Spearman's correlation). 'ns' = not significant ($p>0.05$).

List of References

Agaugué, S., Carosella, E.D., Rouas-Freiss, N., 2011. Role of HLA-G in tumor escape through expansion of myeloid-derived suppressor cells and cytokinic balance in favor of Th2 versus Th1/Th17. Blood 117, 7021–7031. https://doi.org/10.1182/blood-2010-07-294389

Alberts, B., Johnson, A., Lewis, J., Raff, M., Roberts, K., Walter, P., 2002. T Cells and MHC Proteins. Mol. Biol. Cell 4th Ed.

Allen, R.L., Hogan, L., 2013. Non-Classical MHC Class I Molecules (MHC-Ib), in: eLS. American Cancer Society. https://doi.org/10.1002/9780470015902.a0024246

Andrews, S., 2010. FastQC: A Quality Control Tool for High Throughput Sequence Data [WWW Document]. URL https://www.bioinformatics.babraham.ac.uk/projects/fastqc/

Arpinati, L., Scherz-Shouval, R., 2023. From gatekeepers to providers: regulation of immune functions by cancer-associated fibroblasts. Trends Cancer 9, 421–443. https://doi.org/10.1016/j.trecan.2023.01.007

Bai, R., Chen, N., Li, L., Du, N., Bai, L., Lv, Z., Tian, H., Cui, J., 2020. Mechanisms of Cancer Resistance to Immunotherapy. Front. Oncol. 10, 1290. https://doi.org/10.3389/fonc.2020.01290

Barnes, T.A., Amir, E., 2017. HYPE or HOPE: the prognostic value of infiltrating immune cells in cancer. Br. J. Cancer 117, 451–460. https://doi.org/10.1038/bjc.2017.220

Belov, K., 2011. The role of the Major Histocompatibility Complex in the spread of contagious cancers. Mamm. Genome 22, 83–90. https://doi.org/10.1007/s00335-010-9294-2

Bierie, B., Moses, H.L., 2010. Transforming growth factor beta (TGF-β) and inflammation in cancer. Cytokine Growth Factor Rev., Inflammation and Cancer 21, 49–59. https://doi.org/10.1016/j.cytogfr.2009.11.008

Bjorkman, P.J., Parham, P., 1990. Structure, Function, and Diversity of Class I Major Histocompatibility Complex Molecules. Annu. Rev. Biochem. 59, 253–288. https://doi.org/10.1146/annurev.bi.59.070190.001345

Blees, A., Januliene, D., Hofmann, T., Koller, N., Schmidt, C., Trowitzsch, S., Moeller, A., Tampé, R., 2017. Structure of the human MHC-I peptide-loading complex. Nature 551, 525–528. https://doi.org/10.1038/nature24627

Blum, J.S., Wearsch, P.A., Cresswell, P., 2013. Pathways of Antigen Processing. Annu. Rev. Immunol. 31, 443–473. https://doi.org/10.1146/annurev-immunol-032712-095910

Bolger, A.M., Lohse, M., Usadel, B., 2014. Trimmomatic: a flexible trimmer for Illumina sequence data. Bioinformatics 30, 2114–2120. https://doi.org/10.1093/bioinformatics/btu170

Bossard, C., Bézieau, S., Matysiak-Budnik, T., Volteau, C., Laboisse, C.L., Jotereau, F., Mosnier, J.-F., 2012. HLA-E/β2 microglobulin overexpression in colorectal cancer is associated with recruitment of inhibitory immune cells and tumor progression. Int. J. Cancer 131, 855–863. https://doi.org/10.1002/ijc.26453

Braud, V.M., Allan, D.S., McMichael, A.J., 1999. Functions of nonclassical MHC and non-MHC-encoded class I molecules. Curr. Opin. Immunol. 11, 100–108.

Brigl, M., Brenner, M.B., 2004. CD1: Antigen Presentation and T Cell Function. Annu. Rev. Immunol. 22, 817–890. https://doi.org/10.1146/annurev.immunol.22.012703.104608

Brown, G.K., Kreiss, A., Lyons, A.B., Woods, G.M., 2011. Natural Killer Cell Mediated Cytotoxic Responses in the Tasmanian Devil. PLoS ONE 6. https://doi.org/10.1371/journal.pone.0024475

Brown, R.S., Wolke, R.E., Saila, S.B., Brown, C.W., 1978. Prevalence of neoplasia in 10 New England populations of the soft-shell clam (Mya arenaria). Ann. N. Y. Acad. Sci. 298, 522–534. https://doi.org/10.1111/j.1749-6632.1977.tb19287.x

Bukowski, K., Kciuk, M., Kontek, R., 2020. Mechanisms of Multidrug Resistance in Cancer Chemotherapy. Int. J. Mol. Sci. 21, 3233. https://doi.org/10.3390/ijms21093233

Burnet, F.M., 1970. The concept of immunological surveillance. Prog. Exp. Tumor Res. 13, 1–27. https://doi.org/10.1159/000386035

Burr, M.L., Sparbier, C.E., Chan, K.L., Chan, Y.-C., Kersbergen, A., Lam, E.Y.N., Azidis-Yates, E., Vassiliadis, D., Bell, C.C., Gilan, O., Jackson, S., Tan, L., Wong, S.Q., Hollizeck, S., Michalak, E.M., Siddle, H.V., McCabe, M.T., Prinjha, R.K., Guerra, G.R., Solomon, B.J., Sandhu, S., Dawson, S.-J., Beavis, P.A., Tothill, R.W., Cullinane, C., Lehner, P.J., Sutherland, K.D., Dawson, M.A., 2019. An Evolutionarily Conserved Function of Polycomb Silences the MHC Class I Antigen Presentation Pathway and Enables Immune Evasion in Cancer. Cancer Cell 36, 385–401. https://doi.org/10.1016/j.ccell.2019.08.008

Caldas, C., 2012. Cancer sequencing unravels clonal evolution. Nat. Biotechnol. 30, 408–410. https://doi.org/10.1038/nbt.2213

Caldwell, A., 2018. Investigating the molecular mechanisms behind immune escape and recognition of two genetically distinct contagious cancers in the Tasmanian devil (Doctoral Thesis). University of Southampton.

Caldwell, A., Coleby, R., Tovar, C., Stammnitz, M.R., Kwon, Y.M., Owen, R.S., Tringides, M., Murchison, E.P., Skjødt, K., Thomas, G.J., Kaufman, J., Elliott, T., Woods, G.M., Siddle, H.V., 2018. The newly-arisen Devil facial tumour disease 2 (DFT2) reveals a mechanism for the emergence of a contagious cancer. eLife 7, e35314. https://doi.org/10.7554/eLife.35314

Caldwell, A., Siddle, H.V., 2017. The role of MHC genes in contagious cancer: the story of Tasmanian devils. Immunogenetics 69, 537–545. https://doi.org/10.1007/s00251-017-0991-9

Calon, A., Espinet, E., Palomo-Ponce, S., Tauriello, D.V.F., Iglesias, M., Céspedes, M.V., Sevillano, M., Nadal, C., Jung, P., Zhang, X.H.-F., Byrom, D., Riera, A., Rossell, D., Mangues, R., Massagué, J., Sancho, E., Batlle, E., 2012. Dependency of Colorectal Cancer on a TGF-β-Driven Program in Stromal Cells for Metastasis Initiation. Cancer Cell 22, 571–584. https://doi.org/10.1016/j.ccr.2012.08.013

Campbell, P.J., Yachida, S., Mudie, L.J., Stephens, P.J., Pleasance, E.D., Stebbings, L.A., Morsberger, L.A., Latimer, C., McLaren, S., Lin, M.-L., McBride, D.J., Varela, I., Nik-Zainal, S.A., Leroy, C., Jia, M., Menzies, A., Butler, A.P., Teague, J.W., Griffin, C.A., Burton, J., Swerdlow, H., Quail, M.A., Stratton, M.R., Iacobuzio-Donahue, C., Futreal, P.A., 2010. The patterns and dynamics of genomic instability in metastatic pancreatic cancer. Nature 467, 1109–1113. https://doi.org/10.1038/nature09460

Campoli, M., Ferrone, S., 2008. HLA antigen changes in malignant cells: epigenetic mechanisms and biologic significance. Oncogene 27, 5869–5885. https://doi.org/10.1038/onc.2008.273

Chancellor, A., Gadola, S.D., Mansour, S., 2018. The versatility of the CD1 lipid antigen presentation pathway. Immunology 154, 196–203. https://doi.org/10.1111/imm.12912

Cheng, Y., Belov, K., 2014. Characterisation of non-classical MHC class I genes in the Tasmanian devil (Sarcophilus harrisii). Immunogenetics 66, 727–735. https://doi.org/10.1007/s00251-014-0804-3

Cheng, Y., Grueber, C., Hogg, C.J., Belov, K., 2022. Improved high-throughput MHC typing for non-model species using long-read sequencing. Mol. Ecol. Resour. 22, 862–876. https://doi.org/10.1111/1755-0998.13511

Cheng, Y., Stuart, A., Morris, K., Taylor, R., Siddle, H., Deakin, J., Jones, M., Amemiya, C.T., Belov, K., 2012. Antigen-presenting genes and genomic copy number variations in the Tasmanian devil MHC. BMC Genomics 13, 87. https://doi.org/10.1186/1471-2164-13-87

Cohen, D., 1985. The canine transmissible venereal tumor: a unique result of tumor progression. Adv. Cancer Res. 43, 75–112. https://doi.org/10.1016/s0065-230x(08)60943-4

Cree, I.A., Charlton, P., 2017. Molecular chess? Hallmarks of anti-cancer drug resistance. BMC Cancer 17, 10. https://doi.org/10.1186/s12885-016-2999-1

Curiel, T.J., Coukos, G., Zou, L., Alvarez, X., Cheng, P., Mottram, P., Evdemon-Hogan, M., Conejo-Garcia, J.R., Zhang, L., Burow, M., Zhu, Y., Wei, S., Kryczek, I., Daniel, B., Gordon, A., Myers, L., Lackner, A., Disis, M.L., Knutson, K.L., Chen, L., Zou, W., 2004. Specific recruitment of regulatory T cells in ovarian carcinoma fosters immune privilege and predicts reduced survival. Nat. Med. 10, 942–949. https://doi.org/10.1038/nm1093

Danecek, P., Bonfield, J.K., Liddle, J., Marshall, J., Ohan, V., Pollard, M.O., Whitwham, A., Keane, T., McCarthy, S.A., Davies, R.M., Li, H., 2021. Twelve years of SAMtools and BCFtools. GigaScience 10, giab008. https://doi.org/10.1093/gigascience/giab008

Das, U., Das, A.K., 2000. Review of Canine Transmissible Venereal Sarcoma. Vet. Res. Commun. 24, 545–556. https://doi.org/10.1023/A:1006491918910

Derré, L., Corvaisier, M., Charreau, B., Moreau, A., Godefroy, E., Moreau-Aubry, A., Jotereau, F., Gervois, N., 2006. Expression and Release of HLA-E by Melanoma Cells and Melanocytes: Potential Impact on the Response of Cytotoxic Effector Cells. J. Immunol. 177, 3100–3107. https://doi.org/10.4049/jimmunol.177.5.3100

Dhatchinamoorthy, K., Colbert, J.D., Rock, K.L., 2021. Cancer Immune Evasion Through Loss of MHC Class I Antigen Presentation. Front. Immunol. 12.

Djurisic, S., Hviid, T.V.F., 2014. HLA Class Ib Molecules and Immune Cells in Pregnancy and Preeclampsia. Front. Immunol. 5. https://doi.org/10.3389/fimmu.2014.00652

D'Souza, M.P., Adams, E., Altman, J.D., Birnbaum, M.E., Boggiano, C., Casorati, G., Chien, Y., Conley, A., Eckle, S.B.G., Früh, K., Gondré-Lewis, T., Hassan, N., Huang, H., Jayashankar, L., Kasmar, A.G., Kunwar, N., Lavelle, J., Lewinsohn, D.M., Moody, B., Picker, L., Ramachandra, L., Shastri, N., Parham, P., McMichael, A.J., Yewdell, J.W., 2019. Casting a wider net: Immunosurveillance by nonclassical MHC molecules. PLOS Pathog. 15, e1007567. https://doi.org/10.1371/journal.ppat.1007567

Dunker, K., Schlaf, G., Bukur, J., Altermann, W.W., Handke, D., Seliger, B., 2008. Expression and regulation of non-classical HLA-G in renal cell carcinoma. Tissue Antigens 72, 137–148. https://doi.org/10.1111/j.1399-0039.2008.01090.x

Dunn, G.P., Bruce, A.T., Ikeda, H., Old, L.J., Schreiber, R.D., 2002. Cancer immunoediting: from immunosurveillance to tumor escape. Nat. Immunol. 3, 991–998. https://doi.org/10.1038/ni1102-991

Dunn, G.P., Old, L.J., Schreiber, R.D., 2004. The Immunobiology of Cancer Immunosurveillance and Immunoediting. Immunity 21, 137–148. https://doi.org/10.1016/j.immuni.2004.07.017

Durrant, R., Hamede, R., Wells, K., Lurgi, M., 2021. Disruption of Metapopulation Structure Reduces Tasmanian Devil Facial Tumour Disease Spread at the Expense of Abundance and Genetic Diversity. Pathogens 10, 1592. https://doi.org/10.3390/pathogens10121592

Epstein, B., Jones, M., Hamede, R., Hendricks, S., McCallum, H., Murchison, E.P., Schönfeld, B., Wiench, C., Hohenlohe, P., Storfer, A., 2016. Rapid evolutionary response to a transmissible cancer in Tasmanian devils. Nat. Commun. 7. https://doi.org/10.1038/ncomms12684

Flies, A.S., Lyons, A.B., Corcoran, L.M., Papenfuss, A.T., Murphy, J.M., Knowles, G.W., Woods, G.M., Hayball, J.D., 2016. PD-L1 Is Not Constitutively Expressed on Tasmanian Devil Facial Tumor Cells but Is Strongly Upregulated in Response to IFN-γ and Can Be Expressed in the Tumor Microenvironment. Front. Immunol. 7.

Freeman, G.J., Long, A.J., Iwai, Y., Bourque, K., Chernova, T., Nishimura, H., Fitz, L.J., Malenkovich, N., Okazaki, T., Byrne, M.C., Horton, H.F., Fouser, L., Carter, L., Ling, V., Bowman, M.R., Carreno, B.M., Collins, M., Wood, C.R., Honjo, T., 2000. Engagement of the PD-1 immunoinhibitory receptor by a novel B7 family member leads to negative regulation of lymphocyte activation. J. Exp. Med. 192, 1027–1034. https://doi.org/10.1084/jem.192.7.1027

Gabrilovich, D.I., Nagaraj, S., 2009. Myeloid-derived suppressor cells as regulators of the immune system. Nat. Rev. Immunol. 9, 162–174. https://doi.org/10.1038/nri2506

Ganguly B, Das U, Das A. K, 2016. Canine transmissible venereal tumour: a review. Vet. Comp. Oncol. 14, 1–12. https://doi.org/10.1111/vco.12060

Garrison, E., Marth, G., 2012. Haplotype-based variant detection from short-read sequencing. https://doi.org/10.48550/arXiv.1207.3907

Gastaldello, A., Ramarathinam, S.H., Bailey, A., Owen, R., Turner, S., Kontouli, N., Elliott, T., Skipp, P., Purcell, A.W., Siddle, H.V., 2021. The immunopeptidomes of two transmissible cancers and their host have a common, dominant peptide motif. Immunology n/a. https://doi.org/10.1111/imm.13307

Gibbons Johnson, R.M., Dong, H., 2017. Functional Expression of Programmed Death-Ligand 1 (B7-H1) by Immune Cells and Tumor Cells. Front. Immunol. 8, 961. https://doi.org/10.3389/fimmu.2017.00961

Gudmundsdottir, H., Wells, A.D., Turka, L.A., 1999. Dynamics and requirements of T cell clonal expansion in vivo at the single-cell level: effector function is linked to proliferative capacity. J. Immunol. Baltim. Md 1950 162, 5212–5223.

Hamede, R.K., McCallum, H., Jones, M., 2013. Biting injuries and transmission of Tasmanian devil facial tumour disease. J. Anim. Ecol. 82, 182–190. https://doi.org/10.1111/j.1365-2656.2012.02025.x

Hamede, R.K., Mccallum Hamish, Jones Menna, 2008. Seasonal, demographic and density-related patterns of contact between Tasmanian devils (Sarcophilus harrisii): Implications for

transmission of devil facial tumour disease. Austral Ecol. 33, 614–622. https://doi.org/10.1111/j.1442-9993.2007.01827.x

Hamilton, D.H., McCampbell, K.K., Palena, C., 2018. Loss of the Cyclin-Dependent Kinase Inhibitor 1 in the Context of Brachyury-Mediated Phenotypic Plasticity Drives Tumor Resistance to Immune Attack. Front. Oncol. 8.

Han, Y., Liu, D., Li, L., 2020. PD-1/PD-L1 pathway: current researches in cancer. Am. J. Cancer Res. 10, 727–742.

Hanahan, D., 2022. Hallmarks of Cancer: New Dimensions. Cancer Discov. 12, 31–46. https://doi.org/10.1158/2159-8290.CD-21-1059

Hanahan, D., Weinberg, R.A., 2011. Hallmarks of Cancer: The Next Generation. Cell 144, 646–674. https://doi.org/10.1016/j.cell.2011.02.013

Hanahan, D., Weinberg, R.A., 2000. The Hallmarks of Cancer. Cell 100, 57–70. https://doi.org/10.1016/S0092-8674(00)81683-9

Hawinkels, L.J. a. C., Paauwe, M., Verspaget, H.W., Wiercinska, E., van der Zon, J.M., van der Ploeg, K., Koelink, P.J., Lindeman, J.H.N., Mesker, W., ten Dijke, P., Sier, C.F.M., 2014. Interaction with colon cancer cells hyperactivates TGF-β signaling in cancer-associated fibroblasts. Oncogene 33, 97–107. https://doi.org/10.1038/onc.2012.536

Hawkins, C.E., Baars, C., Hesterman, H., Hocking, G.J., Jones, M.E., Lazenby, B., Mann, D., Mooney, N., Pemberton, D., Pyecroft, S., Restani, M., Wiersma, J., 2006. Emerging disease and population decline of an island endemic, the Tasmanian devil Sarcophilus harrisii. Biol. Conserv., Infectious Disease and Mammalian Conservation 131, 307–324. https://doi.org/10.1016/j.biocon.2006.04.010

Hawkins, C.E., McCallum, H., Mooney, N., Jones, M., Holdsworth, M., 2008. Sarcophilus Harrisii. The IUCN Red List of Threatened Species 2008: e.T40540A10331066. http://dx.doi.org/10.2305/IUCN.UK.2008.RLTS.T40540A10331066.en

Hicklin, D.J., Marincola, F.M., Ferrone, S., 1999. HLA class I antigen downregulation in human cancers: T-cell immunotherapy revives an old story. Mol. Med. Today 5, 178–186. https://doi.org/10.1016/S1357-4310(99)01451-3

Hino, R., Kabashima, K., Kato, Y., Yagi, H., Nakamura, M., Honjo, T., Okazaki, T., Tokura, Y., 2010. Tumor cell expression of programmed cell death-1 ligand 1 is a prognostic factor for malignant melanoma. Cancer 116, 1757–1766. https://doi.org/10.1002/cncr.24899

Hiraki, A., Fujii, N., Murakami, T., Kiura, K., Aoe, K., Yamane, H., Masuda, K., Maeda, T., Sugi, K., Darzynkiewicz, Z., Tanimoto, M., Harada, M., 2004. High Frequency of Allele-specific Down-regulation of HLA class I Expression in Lung Cancer Cell Lines. Anticancer Res. 24, 1525–1528.

Hsiao, Y.-W., Liao, K.-W., Chung, T.-F., Liu, C.-H., Hsu, C.-D., Chu, R.-M., 2008. Interactions of host IL-6 and IFN-γ and cancer-derived TGF-β1 on MHC molecule expression during tumor spontaneous regression. Cancer Immunol. Immunother. 57, 1091–1104. https://doi.org/10.1007/s00262-007-0446-5

Hsiao, Y.-W., Liao, K.-W., Hung, S.-W., Chu, R.-M., 2002. Effect of tumor infiltrating lymphocytes on the expression of MHC molecules in canine transmissible venereal tumor cells. Vet. Immunol. Immunopathol. 87, 19–27.

Hubert, J.-N., Zerjal, T., Hospital, F., 2018. Cancer- and behavior-related genes are targeted by selection in the Tasmanian devil (Sarcophilus harrisii). PLOS ONE 13, e0201838. https://doi.org/10.1371/journal.pone.0201838

Hudson, K., Cross, N., Jordan-Mahy, N., Leyland, R., 2020. The Extrinsic and Intrinsic Roles of PD-L1 and Its Receptor PD-1: Implications for Immunotherapy Treatment. Front. Immunol. 11.

Hulpke, S., Tampé, R., 2013. The MHC I loading complex: a multitasking machinery in adaptive immunity. Trends Biochem. Sci. 38, 412–420. https://doi.org/10.1016/j.tibs.2013.06.003

Hussey, K., 2018. Investigating Major Histocompatibility (MHC) Class I Expression in Two Contagious Cancers Infecting Tasmanian Devils (Masters Thesis). University of Southampton.

Hussey, K., Caldwell, A., Kreiss, A., Skjødt, K., Gastaldello, A., Pye, R., Hamede, R., Woods, G.M., Siddle, H.V., 2022. Expression of the Nonclassical MHC Class I, Saha-UD in the Transmissible Cancer Devil Facial Tumour Disease (DFTD). Pathogens 11, 351. https://doi.org/10.3390/pathogens11030351

Ident and Sim [WWW Document], 2020. URL https://www.bioinformatics.org/sms2/ident_sim.html (accessed 9.20.23).

Idos, G.E., Kwok, J., Bonthala, N., Kysh, L., Gruber, S.B., Qu, C., 2020. The Prognostic Implications of Tumor Infiltrating Lymphocytes in Colorectal Cancer: A Systematic Review and Meta-Analysis. Sci. Rep. 10, 3360. https://doi.org/10.1038/s41598-020-60255-4

Iwai, Y., Hamanishi, J., Chamoto, K., Honjo, T., 2017. Cancer immunotherapies targeting the PD-1 signaling pathway. J. Biomed. Sci. 24, 26. https://doi.org/10.1186/s12929-017-0329-9

James, S., Jennings, G., Kwon, Y.M., Stammnitz, M., Fraik, A., Storfer, A., Comte, S., Pemberton, D., Fox, S., Brown, B., Pye, R., Woods, G., Lyons, B., Hohenlohe, P.A., McCallum, H., Siddle, H., Thomas, F., Ujvari, B., Murchison, E.P., Jones, M., Hamede, R., 2019. Tracing the rise of malignant cell lines: Distribution, epidemiology and evolutionary interactions of two transmissible cancers in Tasmanian devils. Evol. Appl. 12, 1772–1780. https://doi.org/10.1111/eva.12831

Janeway, C.A., Travers, P., Walport, M., Shlomchik, M.J., 2001. T cell-mediated cytotoxicity, in: Immunobiology: The Immune System in Health and Disease. 5th Edition. Garland Science.

Jiang, H., Canfield, S.M., Gallagher, M.P., Jiang, H.H., Jiang, Y., Zheng, Z., Chess, L., 2010. HLA-E–restricted regulatory CD8+ T cells are involved in development and control of human autoimmune type 1 diabetes. J. Clin. Invest. 120, 3641–3650. https://doi.org/10.1172/JCI43522

Jiang, M., Chen, J., Zhang, W., Zhang, R., Ye, Y., Liu, P., Yu, W., Wei, F., Ren, X., Yu, J., 2017. Interleukin-6 Trans-Signaling Pathway Promotes Immunosuppressive Myeloid-Derived Suppressor Cells via Suppression of Suppressor of Cytokine Signaling 3 in Breast Cancer. Front. Immunol. 8.

Jongsma, M.L.M., Neefjes, J., Spaapen, R.M., 2021. Playing hide and seek: Tumor cells in control of MHC class I antigen presentation. Mol. Immunol. 136, 36–44. https://doi.org/10.1016/j.molimm.2021.05.009

Jorgovanovic, D., Song, M., Wang, L., Zhang, Y., 2020. Roles of IFN-γ in tumor progression and regression: a review. Biomark. Res. 8, 49. https://doi.org/10.1186/s40364-020-00228-x

Kärre, K., Ljunggren, H.G., Piontek, G., Kiessling, R., 1986. Selective rejection of H–2-deficient lymphoma variants suggests alternative immune defence strategy. Nature 319, 675–678. https://doi.org/10.1038/319675a0

Kent, M.L., Wilkinson, M.T., Drum, A.S., Elston, R.A., 1991. Failure of transmission of hemic neoplasia of bay mussels, Mytilus trossulus, to other bivalve species. J. Invertebr. Pathol. 57, 435–436. https://doi.org/10.1016/0022-2011(91)90148-J

Kochan, G., Escors, D., Breckpot, K., Guerrero-Setas, D., 2013. Role of non-classical MHC class I molecules in cancer immunosuppression. Oncoimmunology 2. https://doi.org/10.4161/onci.26491

Koppensteiner, L., Mathieson, L., O'Connor, R.A., Akram, A.R., 2022. Cancer Associated Fibroblasts - An Impediment to Effective Anti-Cancer T Cell Immunity. Front. Immunol. 13. https://doi.org/10.3389/fimmu.2022.887380

Kozakiewicz, C.P., Fraik, A.K., Patton, A.H., Ruiz-Aravena, M., Hamilton, D.G., Hamede, R., McCallum, H., Hohenlohe, P.A., Margres, M.J., Jones, M.E., Storfer, A., 2021. Spatial variation in gene expression of Tasmanian devil facial tumors despite minimal host transcriptomic response to infection. BMC Genomics 22, 698. https://doi.org/10.1186/s12864-021-07994-4

Kreiss, A., Brown, G.K., Tovar, C., Lyons, A.B., Woods, G.M., 2015. Evidence for induction of humoral and cytotoxic immune responses against devil facial tumor disease cells in Tasmanian devils (Sarcophilus harrisii) immunized with killed cell preparations. Vaccine 33, 3016–3025. https://doi.org/10.1016/j.vaccine.2015.01.039

Kreiss, A., Cheng, Y., Kimble, F., Wells, B., Donovan, S., Belov, K., Woods, G.M., 2011. Allorecognition in the Tasmanian Devil (Sarcophilus harrisii), an Endangered Marsupial Species with Limited Genetic Diversity. PLoS ONE 6. https://doi.org/10.1371/journal.pone.0022402

Krovi, S.H., Gapin, L., 2016. Structure and function of the non-classical major histocompatibility complex molecule MR1. Immunogenetics 68, 549–559. https://doi.org/10.1007/s00251-016-0939-5

Kwon, Y.M., Gori, K., Park, N., Potts, N., Swift, K., Wang, J., Stammnitz, M.R., Cannell, N., Baez-Ortega, A., Comte, S., Fox, S., Harmsen, C., Huxtable, S., Jones, M., Kreiss, A., Lawrence, C., Lazenby, B., Peck, S., Pye, R., Woods, G., Zimmermann, M., Wedge, D.C., Pemberton, D., Stratton, M.R., Hamede, R., Murchison, E.P., 2020. Evolution and lineage dynamics of a transmissible cancer in Tasmanian devils. PLOS Biol. 18, e3000926. https://doi.org/10.1371/journal.pbio.3000926

Kwon, Y.M., Stammnitz, M.R., Wang, J., Swift, K., Knowles, G.W., Pye, R.J., Kreiss, A., Peck, S., Fox, S., Pemberton, D., Jones, M.E., Hamede, R., Murchison, E.P., 2018. Tasman-PCR: a genetic diagnostic assay for Tasmanian devil facial tumour diseases. R. Soc. Open Sci. 5, 180870. https://doi.org/10.1098/rsos.180870

Lane, A., Cheng, Y., Wright, B., Hamede, R., Levan, L., Jones, M., Ujvari, B., Belov, K., 2012. New Insights into the Role of MHC Diversity in Devil Facial Tumour Disease. PLOS ONE 7, e36955. https://doi.org/10.1371/journal.pone.0036955

Langmead, B., Salzberg, S.L., 2012. Fast gapped-read alignment with Bowtie 2. Nat. Methods 9, 357–359. https://doi.org/10.1038/nmeth.1923

Langmead, B., Wilks, C., Antonescu, V., Charles, R., 2019. Scaling read aligners to hundreds of threads on general-purpose processors. Bioinformatics 35, 421–432. https://doi.org/10.1093/bioinformatics/bty648

Lanier, L.L., 2005. Nk Cell Recognition. Annu. Rev. Immunol. 23, 225–274. https://doi.org/10.1146/annurev.immunol.23.021704.115526

Lanier, L.L., 1998. Follow the Leader: NK Cell Receptors for Classical and Nonclassical MHC Class I. Cell 92, 705–707. https://doi.org/10.1016/S0092-8674(00)81398-7

Lazenby, B.T., Tobler, M.W., Brown, W.E., Hawkins, C.E., Hocking, G.J., Hume, F., Huxtable, S., Iles, P., Jones, M.E., Lawrence, C., Thalmann, S., Wise, P., Williams, H., Fox, S., Pemberton, D., 2018. Density trends and demographic signals uncover the long-term impact of transmissible cancer in Tasmanian devils. J. Appl. Ecol. 55, 1368–1379. https://doi.org/10.1111/1365-2664.13088

Lee, I., Wang, L., Wells, A.D., Dorf, M.E., Ozkaynak, E., Hancock, W.W., 2005. Recruitment of Foxp3+ T regulatory cells mediating allograft tolerance depends on the CCR4 chemokine receptor. J. Exp. Med. 201, 1037–1044. https://doi.org/10.1084/jem.20041709

Liao, K.-W., Hung, S.-W., Hsiao, Y.-W., Bennett, M., Chu, R.-M., 2003. Canine transmissible venereal tumor cell depletion of B lymphocytes: molecule(s) specifically toxic for B cells. Vet. Immunol. Immunopathol. 92, 149–162.

Lin, A., Yan, W.-H., Xu, H.-H., Gan, M.-F., Cai, J.-F., Zhu, M., Zhou, M.-Y., 2007. HLA-G expression in human ovarian carcinoma counteracts NK cell function. Ann. Oncol. Off. J. Eur. Soc. Med. Oncol. 18, 1804–1809. https://doi.org/10.1093/annonc/mdm356

Lin, C.M., Gill, R.G., 2016. Direct and indirect allograft recognition: pathways dictating graft rejection mechanisms. Curr. Opin. Organ Transplant. 21, 40–44. https://doi.org/10.1097/MOT.0000000000000263

Lin, E.Y., Gouon-Evans, V., Nguyen, A.V., Pollard, J.W., 2002. The Macrophage Growth Factor CSF-1 in Mammary Gland Development and Tumor Progression. J. Mammary Gland Biol. Neoplasia 7, 147–162. https://doi.org/10.1023/A:1020399802795

Liu, C.-C., Wang, Y.-S., Lin, C.-Y., Chuang, T.-F., Liao, K.-W., Chi, K.-H., Chen, M.-F., Chiang, H.-C., Chu, R.-M., 2008. Transient downregulation of monocyte-derived dendritic-cell differentiation, function, and survival during tumoral progression and regression in an in vivo canine model of transmissible venereal tumor. Cancer Immunol. Immunother. CII 57, 479–491. https://doi.org/10.1007/s00262-007-0386-0

Ljunggren, H.-G., Kärre, K., 1990. In search of the 'missing self': MHC molecules and NK cell recognition. Immunol. Today 11, 237–244. https://doi.org/10.1016/0167-5699(90)90097-S

Ljunggren, H.-G., Kärre, K., 1985. Host resistance directed selectively against H-2-deficient lymphoma variants. Analysis of the mechanism. J. Exp. Med. 162, 1745–1759.

Loh, R., Bergfeld, J., Hayes, D., O'Hara, A., Pyecroft, S., Raidal, S., Sharpe, R., 2006. The Pathology of Devil Facial Tumor Disease (DFTD) in Tasmanian Devils (Sarcophilus harrisii). Vet. Pathol. 43, 890–895. https://doi.org/10.1354/vp.43-6-890

Lu, L., Zhang, A.Y., Camp, W.L., Qian, S., 2010. Natural killer cell induction of tolerance, in: Natural Killer Cells. Academic Press, pp. 617–631. https://doi.org/10.1016/B978-0-12-370454-2.00047-8

Maine, C.J., Aziz, N.H.A., Chatterjee, J., Hayford, C., Brewig, N., Whilding, L., George, A.J.T., Ghaem-Maghami, S., 2014. Programmed death ligand-1 over-expression correlates with malignancy and contributes to immune regulation in ovarian cancer. Cancer Immunol. Immunother. CII 63, 215–224. https://doi.org/10.1007/s00262-013-1503-x

Mansoori, B., Mohammadi, A., Davudian, S., Shirjang, S., Baradaran, B., 2017. The Different Mechanisms of Cancer Drug Resistance: A Brief Review. Adv. Pharm. Bull. 7, 339–348. https://doi.org/10.15171/apb.2017.041

Margres, M.J., Jones, M., Epstein, B., Kerlin, D.H., Comte, S., Fox, S., Fraik, A.K., Hendricks, S.A., Huxtable, S., Lachish, S., Lazenby, B., O'Rourke, S.M., Stahlke, A.R., Wiench, C.G., Hamede, R., Schönfeld, B., McCallum, H., Miller, M.R., Hohenlohe, P.A., Storfer, A., 2018. Large-effect loci affect survival in Tasmanian devils (Sarcophilus harrisii) infected with a transmissible cancer. Mol. Ecol. 27, 4189–4199. https://doi.org/10.1111/mec.14853

Marín, R., Ruiz-Cabello, F., Pedrinaci, S., Méndez, R., Jiménez, P., Geraghty, D.E., Garrido, F., 2003. Analysis of HLA-E expression in human tumors. Immunogenetics 54, 767–775. https://doi.org/10.1007/s00251-002-0526-9

Mateo, D.R., MacCallum, G.S., Davidson, J., 2016. Field and laboratory transmission studies of haemic neoplasia in the soft-shell clam, Mya arenaria, from Atlantic Canada. J. Fish Dis. 39, 913–927. https://doi.org/10.1111/jfd.12426

McCallum, H., Jones, M., Hawkins, C., Hamede, R., Lachish, S., Sinn, D.L., Beeton, N., Lazenby, B., 2009. Transmission dynamics of Tasmanian devil facial tumor disease may lead to disease-induced extinction. Ecology 90, 3379–3392. https://doi.org/10.1890/08-1763.1

McCallum, H., Tompkins, D.M., Jones, M., Lachish, S., Marvanek, S., Lazenby, B., Hocking, G., Wiersma, J., Hawkins, C.E., 2007. Distribution and Impacts of Tasmanian Devil Facial Tumor Disease. EcoHealth 4, 318. https://doi.org/10.1007/s10393-007-0118-0

McGranahan, N., Rosenthal, R., Hiley, C.T., Rowan, A.J., Watkins, T.B.K., Wilson, G.A., Birkbak, N.J., Veeriah, S., Loo, P.V., Herrero, J., Swanton, C., Swanton, C., Jamal-Hanjani, M., Veeriah, S., Shafi, S., Czyzewska-Khan, J., Johnson, D., Laycock, J., Bosshard-Carter, L., Rosenthal, R., Gorman, P., Hynds, R.E., Wilson, G., Birkbak, N.J., Watkins, T.B.K., McGranahan, N., Horswell, S., Mitter, R., Escudero, M., Stewart, A., Loo, P.V., Rowan, A., Xu, H., Turajlic, S., Hiley, C., Abbosh, C., Goldman, J., Stone, R.K., Denner, T., Matthews, N., Elgar, G., Ward, S., Costa, M., Begum, S., Phillimore, B., Chambers, T., Nye, E., Graca, S., Bakir, M.A., Joshi, K., Furness, A., Aissa, A.B., Wong, Y.N.S., Georgiou, A., Quezada, S., Hartley, J.A., Lowe, H.L., Herrero, J., Lawrence, D., Hayward, M., Panagiotopoulos, N., Kolvekar, S., Falzon, M., Borg, E., Marafioti, T., Simeon, C., Hector, G., Smith, A., Aranda, M., Novelli, M., Oukrif, D., Janes, S.M., Thakrar, R., Forster, M., Ahmad, T., Lee, S.M., Papadatos-Pastos, D., Carnell, D., Mendes, R., George, J., Navani, N., Ahmed, A., Taylor, M., Choudhary, J., Summers, Y., Califano, R., Taylor, P., Shah, R., Krysiak, P., Rammohan, K., Fontaine, E., Booton, R., Evison, M., Crosbie, P., Moss, S., Idries, F., Joseph, L., Bishop, P., Chaturved, A., Quinn, A.M., Doran, H., Leek, A., Harrison, P., Moore, K., Waddington, R., Novasio, J., Blackhall, F., Rogan, J., Smith, E., Dive, C., Tugwood, J., Brady, G., Rothwell, D.G., Chemi, F., Pierce, J., Gulati, S., Naidu, B., Langman, G., Trotter, S., Bellamy, M., Bancroft, H., Kerr, A., Kadiri, S., Webb, J., Middleton, G., Djearaman, M., Fennell, D., Shaw, J.A., Quesne, J.L., Moore, D., Nakas, A., Rathinam, S., Monteiro, W., Marshall, H., Nelson, L., Bennett, J., Riley, J., Primrose, L., Martinson, L., Anand, G., Khan, S., Amadi, A., Nicolson, M., Kerr, K., Palmer, S., Remmen, H., Miller, J., Buchan, K., Chetty, M., Gomersall, L., Lester, J., Edwards, A., Morgan, F., Adams, H., Davies, H., Kornaszewska, M., Attanoos, R., Lock, S., Verjee, A., MacKenzie, M., Wilcox, M., Bell, H., Hackshaw, A., Ngai, Y., Smith, S., Gower, N., Ottensmeier, C., Chee, S., Johnson, B., Alzetani, A., Shaw, E., Lim, E., Sousa, P.D., Barbosa,

M.T., Bowman, A., Jordan, S., Rice, A., Raubenheimer, H., Proli, C., Cufari, M.E., Ronquillo, J.C., Kwayie, A., Bhayani, H., Hamilton, M., Bakar, Y., Mensah, N., Ambrose, L., Devaraj, A., Buderi, S., Finch, J., Azcarate, L., Chavan, H., Green, S., Mashinga, H., Nicholson, A.G., Lau, K., Sheaff, M., Schmid, P., Conibear, J., Ezhil, V., Ismail, B., Irvin-sellers, M., Prakash, V., Russell, P., Light, T., Horey, T., Danson, S., Bury, J., Edwards, J., Hill, J., Matthews, S., Kitsanta, Y., Suvarna, K., Fisher, P., Keerio, A.D., Shackcloth, M., Gosney, J., Postmus, P., Feeney, S., Asante-Siaw, J., Aerts, H.J.W.L., Dentro, S., Dessimoz, C., 2017. Allele-Specific HLA Loss and Immune Escape in Lung Cancer Evolution. Cell 171, 1259-1271.e11. https://doi.org/10.1016/j.cell.2017.10.001

Mehta, A.M., Jordanova, E.S., Kenter, G.G., Ferrone, S., Fleuren, G.-J., 2008. Association of antigen processing machinery and HLA class I defects with clinicopathological outcome in cervical carcinoma. Cancer Immunol. Immunother. 57, 197–206. https://doi.org/10.1007/s00262-007-0362-8

Menier, C., Rouas-Freiss, N., Carosella, E.D., 2008. The HLA-G non classical MHC class I molecule is expressed in cancer with poor prognosis. Implications in tumour escape from immune system and clinical applications [WWW Document]. Atlas Genet. Cytogenet. Oncol. Haematol. URL https://atlasgeneticsoncology.org/deep-insight/20070/the-hla-g-non-classical-mhc-class-i-molecule-is-expressed-in-cancer-with-poor-prognosis-implications-in-tumour-escape-from-immune-system-and-clinical-applications (accessed 10.28.23).

Metzger, M.J., Reinisch, C., Sherry, J., Goff, S.P., 2015. Horizontal Transmission of Clonal Cancer Cells Causes Leukemia in Soft-Shell Clams. Cell 161, 255–263. https://doi.org/10.1016/j.cell.2015.02.042

Metzger, M.J., Villalba, A., Carballal, M.J., Iglesias, D., Sherry, J., Reinisch, C., Muttray, A.F., Baldwin, S.A., Goff, S.P., 2016. Widespread transmission of independent cancer lineages within multiple bivalve species. Nature 534, 705–709. https://doi.org/10.1038/nature18599

Morandi, F., Levreri, I., Bocca, P., Galleni, B., Raffaghello, L., Ferrone, S., Prigione, I., Pistoia, V., 2007. Human neuroblastoma cells trigger an immunosuppressive program in monocytes by stimulating soluble HLA-G release. Cancer Res. 67, 6433–6441. https://doi.org/10.1158/0008-5472.CAN-06-4588

Moretta, A., Bottino, C., Vitale, M., Pende, D., Biassoni, R., Mingari, M.C., Moretta, L., 1996. Receptors for Hla Class-I Molecules in Human Natural Killer Cells. Annu. Rev. Immunol. 14, 619–648. https://doi.org/10.1146/annurev.immunol.14.1.619

Morris, K., Austin, J.J., Belov, K., 2013. Low major histocompatibility complex diversity in the Tasmanian devil predates European settlement and may explain susceptibility to disease epidemics. Biol. Lett. 9, 20120900. https://doi.org/10.1098/rsbl.2012.0900

Muenst, S., Schaerli, A.R., Gao, F., Däster, S., Trella, E., Droeser, R.A., Muraro, M.G., Zajac, P., Zanetti, R., Gillanders, W.E., Weber, W.P., Soysal, S.D., 2014. Expression of programmed death ligand 1 (PD-L1) is associated with poor prognosis in human breast cancer. Breast Cancer Res. Treat. 146, 15–24. https://doi.org/10.1007/s10549-014-2988-5

Murchison, E.P., 2009. Clonally transmissible cancers in dogs and Tasmanian devils. Oncogene 27, S19–S30. https://doi.org/10.1038/onc.2009.350

Murchison, E.P., Schulz-Trieglaff, O.B., Ning, Z., Alexandrov, L.B., Bauer, M.J., Fu, B., Hims, M., Ding, Z., Ivakhno, S., Stewart, C., Ng, B.L., Wong, W., Aken, B., White, S., Alsop, A., Becq, J., Bignell, G.R., Cheetham, R.K., Cheng, W., Connor, T.R., Cox, A.J., Feng, Z.-P., Gu, Y., Grocock, R.J., Harris, S.R., Khrebtukova, I., Kingsbury, Z., Kowarsky, M., Kreiss, A., Luo, S.,

Marshall, J., McBride, D.J., Murray, L., Pearse, A.-M., Raine, K., Rasolonjatovo, I., Shaw, R., Tedder, P., Tregidgo, C., Vilella, A.J., Wedge, D.C., Woods, G.M., Gormley, N., Humphray, S., Schroth, G., Smith, G., Hall, K., Searle, S.M.J., Carter, N.P., Papenfuss, A.T., Futreal, P.A., Campbell, P.J., Yang, F., Bentley, D.R., Evers, D.J., Stratton, M.R., 2012. Genome Sequencing and Analysis of the Tasmanian Devil and Its Transmissible Cancer. Cell 148, 780–791. https://doi.org/10.1016/j.cell.2011.11.065

Murchison, E.P., Tovar, C., Hsu, A., Bender, H.S., Kheradpour, P., Rebbeck, C.A., Obendorf, D., Conlan, C., Bahlo, M., Blizzard, C.A., Pyecroft, S., Kreiss, A., Kellis, M., Stark, A., Harkins, T.T., Marshall Graves, J.A., Woods, G.M., Hannon, G.J., Papenfuss, A.T., 2010. The Tasmanian Devil Transcriptome Reveals Schwann Cell Origins of a Clonally Transmissible Cancer. Science 327, 84–87. https://doi.org/10.1126/science.1180616

Murchison, E.P., Wedge, D.C., Alexandrov, L.B., Fu, B., Martincorena, I., Ning, Z., Tubio, J.M.C., Werner, E.I., Allen, J., De Nardi, A.B., Donelan, E.M., Marino, G., Fassati, A., Campbell, P.J., Yang, F., Burt, A., Weiss, R.A., Stratton, M.R., 2014. Transmissible dog cancer genome reveals the origin and history of an ancient cell lineage. Science 343, 437–440. https://doi.org/10.1126/science.1247167

Murgia, C., Pritchard, J.K., Kim, S.Y., Fassati, A., Weiss, R.A., 2006. Clonal Origin and Evolution of a Transmissible Cancer. Cell 126, 477–487. https://doi.org/10.1016/j.cell.2006.05.051

Neefjes, J., Jongsma, M.L.M., Paul, P., Bakke, O., 2011. Towards a systems understanding of MHC class I and MHC class II antigen presentation. Nat. Rev. Immunol. 11, 823–836. https://doi.org/10.1038/nri3084

Novinski, M.A., 1874. Zur Frage über die Impfung der Krebsigen Geschwülste. Zentralbl Med Wissensch 14, 790–791.

Ong, C.E.B., Patchett, A.L., Darby, J.M., Chen, J., Liu, G.-S., Lyons, A.B., Woods, G.M., Flies, A.S., 2021. NLRC5 regulates expression of MHC-I and provides a target for anti-tumor immunity in transmissible cancers. J. Cancer Res. Clin. Oncol. https://doi.org/10.1007/s00432-021-03601-x

Owen, R.S., 2019. Investigating Cellular Origins to Identify Peptide Vaccine Targets in two Independent Transmissible Tumours Circulating in the Tasmanian Devil (Sarcophilus harrisii). University of Southampton.

Owen, R.S., Ramarathinam, S.H., Bailey, A., Gastaldello, A., Hussey, K., Skipp, P.J., Purcell, A.W., Siddle, H.V., 2021. The differentiation state of the Schwann cell progenitor drives phenotypic variation between two contagious cancers. PLOS Pathog. 17, e1010033. https://doi.org/10.1371/journal.ppat.1010033

Papenfuss, A.T., Feng, Z.-P., Krasnec, K., Deakin, J.E., Baker, M.L., Miller, R.D., 2015. Marsupials and monotremes possess a novel family of MHC class I genes that is lost from the eutherian lineage. BMC Genomics 16, 535. https://doi.org/10.1186/s12864-015-1745-4

Pasche, B., 2001. Role of transforming growth factor beta in cancer. J. Cell. Physiol. 186, 153–168. https://doi.org/10.1002/1097-4652(200002)186:2<153::AID-JCP1016>3.0.CO;2-J

Pastushenko, I., Blanpain, C., 2019. EMT Transition States during Tumor Progression and Metastasis. Trends Cell Biol. 29, 212–226. https://doi.org/10.1016/j.tcb.2018.12.001

Patchett, A.L., Tovar, C., Blackburn, N.B., Woods, G.M., Lyons, A.B., 2021. Mesenchymal plasticity of devil facial tumour cells during in vivo vaccine and immunotherapy trials. Immunol. Cell Biol. n/a. https://doi.org/10.1111/imcb.12451

Patton, A.H., Lawrance, M.F., Margres, M.J., Kozakiewicz, C.P., Hamede, R., Ruiz-Aravena, M., Hamilton, D.G., Comte, S., Ricci, L.E., Taylor, R.L., Stadler, T., Leaché, A., McCallum, H., Jones, M.E., Hohenlohe, P.A., Storfer, A., 2020. A transmissible cancer shifts from emergence to endemism in Tasmanian devils. Science 370, eabb9772. https://doi.org/10.1126/science.abb9772

Pearse, A.-M., Swift, K., 2006. Allograft theory: Transmission of devil facial-tumour disease. Nature 439, 549. https://doi.org/10.1038/439549a

Pérez, J., J. Day, M., Mozos, E., 1998. Immunohistochemical study of the local inflammatory infiltrate in spontaneous canine transmissible venereal tumour at different stages of growth. Vet. Immunol. Immunopathol. 64, 133–147. https://doi.org/10.1016/S0165-2427(98)00131-7

Popova, N.V., Jücker, M., 2022. The Functional Role of Extracellular Matrix Proteins in Cancer. Cancers 14, 238. https://doi.org/10.3390/cancers14010238

Pye, R., Patchett, A., McLennan, E., Thomson, R., Carver, S., Fox, S., Pemberton, D., Kreiss, A., Baz Morelli, A., Silva, A., Pearse, M.J., Corcoran, L.M., Belov, K., Hogg, C.J., Woods, G.M., Lyons, A.B., 2018. Immunization Strategies Producing a Humoral IgG Immune Response against Devil Facial Tumor Disease in the Majority of Tasmanian Devils Destined for Wild Release. Front. Immunol. 9.

Pye, R.J., Hamede, R., Siddle, H.V., Caldwell, A., Knowles, G.W., Swift, K., Kreiss, A., Jones, M.E., Lyons, A.B., Woods, G.M., 2016a. Demonstration of immune responses against devil facial tumour disease in wild Tasmanian devils. Biol. Lett. 12. https://doi.org/10.1098/rsbl.2016.0553

Pye, R.J., Pemberton, D., Tovar, C., Tubio, J.M.C., Dun, K.A., Fox, S., Darby, J., Hayes, D., Knowles, G.W., Kreiss, A., Siddle, H.V.T., Swift, K., Lyons, A.B., Murchison, E.P., Woods, G.M., 2016b. A second transmissible cancer in Tasmanian devils. Proc. Natl. Acad. Sci. U. S. A. 113, 374–379. https://doi.org/10.1073/pnas.1519691113

Rapacz-Leonard, A., Dąbrowska, M., Janowski, T., 2014. Major Histocompatibility Complex I Mediates Immunological Tolerance of the Trophoblast during Pregnancy and May Mediate Rejection during Parturition. Mediators Inflamm. 2014, e579279. https://doi.org/10.1155/2014/579279

Rebbeck, C.A., Thomas, R., Breen, M., Leroi, A.M., Burt, A., 2009. Origins and Evolution of a Transmissible Cancer. Evolution 63, 2340–2349. https://doi.org/10.1111/j.1558-5646.2009.00724.x

Reeves, E., James, E., 2017. Antigen processing and immune regulation in the response to tumours. Immunology 150, 16–24. https://doi.org/10.1111/imm.12675

Ristich, V., Liang, S., Zhang, W., Wu, J., Horuzsko, A., 2005. Tolerization of dendritic cells by HLA-G. Eur. J. Immunol. 35, 1133–1142. https://doi.org/10.1002/eji.200425741

Rouas-Freiss, N., Moreau, P., Ferrone, S., Carosella, E.D., 2005. HLA-G Proteins in Cancer: Do They Provide Tumor Cells with an Escape Mechanism? Cancer Res. 65, 10139–10144. https://doi.org/10.1158/0008-5472.CAN-05-0097

Rouas-Freiss, N., Moreau, P., Menier, C., LeMaoult, J., Carosella, E.D., 2007. Expression of tolerogenic HLA-G molecules in cancer prevents antitumor responses. Semin. Cancer Biol. 17, 413–421. https://doi.org/10.1016/j.semcancer.2007.07.003

Ruiz-Aravena, M., Jones, M.E., Carver, S., Estay, S., Espejo, C., Storfer, A., Hamede, R.K., 2018. Sex bias in ability to cope with cancer: Tasmanian devils and facial tumour disease. Proc. R. Soc. B Biol. Sci. 285, 20182239. https://doi.org/10.1098/rspb.2018.2239

Sahai, E., Astsaturov, I., Cukierman, E., DeNardo, D.G., Egeblad, M., Evans, R.M., Fearon, D., Greten, F.R., Hingorani, S.R., Hunter, T., Hynes, R.O., Jain, R.K., Janowitz, T., Jorgensen, C., Kimmelman, A.C., Kolonin, M.G., Maki, R.G., Powers, R.S., Puré, E., Ramirez, D.C., Scherz-Shouval, R., Sherman, M.H., Stewart, S., Tlsty, T.D., Tuveson, D.A., Watt, F.M., Weaver, V., Weeraratna, A.T., Werb, Z., 2020. A framework for advancing our understanding of cancer-associated fibroblasts. Nat. Rev. Cancer 20, 174–186. https://doi.org/10.1038/s41568-019-0238-1

Salmon, H., Franciszkiewicz, K., Damotte, D., Dieu-Nosjean, M.-C., Validire, P., Trautmann, A., Mami-Chouaib, F., Donnadieu, E., 2012. Matrix architecture defines the preferential localization and migration of T cells into the stroma of human lung tumors. J. Clin. Invest. 122, 899–910. https://doi.org/10.1172/JCI45817

Schreiber, R.D., Old, L.J., Smyth, M.J., 2011. Cancer Immunoediting: Integrating Immunity's Roles in Cancer Suppression and Promotion. Science 331, 1565–1570. https://doi.org/10.1126/science.1203486

Sebti, Y., Le Maux, A., Gros, F., De Guibert, S., Pangault, C., Rouas-Freiss, N., Bernard, M., Amiot, L., 2007. Expression of functional soluble human leucocyte antigen-G molecules in lymphoproliferative disorders. Br. J. Haematol. 138, 202–212. https://doi.org/10.1111/j.1365-2141.2007.06647.x

Shah, S.P., Roth, A., Goya, R., Oloumi, A., Ha, G., Zhao, Y., Turashvili, G., Ding, J., Tse, K., Haffari, G., Bashashati, A., Prentice, L.M., Khattra, J., Burleigh, A., Yap, D., Bernard, V., McPherson, A., Shumansky, K., Crisan, A., Giuliany, R., Heravi-Moussavi, A., Rosner, J., Lai, D., Birol, I., Varhol, R., Tam, A., Dhalla, N., Zeng, T., Ma, K., Chan, S.K., Griffith, M., Moradian, A., Cheng, S.-W.G., Morin, G.B., Watson, P., Gelmon, K., Chia, S., Chin, S.-F., Curtis, C., Rueda, O.M., Pharoah, P.D., Damaraju, S., Mackey, J., Hoon, K., Harkins, T., Tadigotla, V., Sigaroudinia, M., Gascard, P., Tlsty, T., Costello, J.F., Meyer, I.M., Eaves, C.J., Wasserman, W.W., Jones, S., Huntsman, D., Hirst, M., Caldas, C., Marra, M.A., Aparicio, S., 2012. The clonal and mutational evolution spectrum of primary triple-negative breast cancers. Nature 486, 395–399. https://doi.org/10.1038/nature10933

Shankaran, V., Ikeda, H., Bruce, A.T., White, J.M., Swanson, P.E., Old, L.J., Schreiber, R.D., 2001. IFNγ and lymphocytes prevent primary tumour development and shape tumour immunogenicity. Nature 410, 1107–1111. https://doi.org/10.1038/35074122

Siddle, H.V., Kaufman, J., 2015. Immunology of naturally transmissible tumours. Immunology 144, 11–20. https://doi.org/10.1111/imm.12377

Siddle, H.V., Kreiss, A., Eldridge, M.D.B., Noonan, E., Clarke, C.J., Pyecroft, S., Woods, G.M., Belov, K., 2007a. Transmission of a fatal clonal tumor by biting occurs due to depleted MHC diversity in a threatened carnivorous marsupial. Proc. Natl. Acad. Sci. 104, 16221–16226. https://doi.org/10.1073/pnas.0704580104

Siddle, H.V., Kreiss, A., Tovar, C., Yuen, C.K., Cheng, Y., Belov, K., Swift, K., Pearse, A.-M., Hamede, R., Jones, M.E., Skjødt, K., Woods, G.M., Kaufman, J., 2013. Reversible epigenetic down-regulation of MHC molecules by devil facial tumour disease illustrates immune escape by a contagious cancer. Proc. Natl. Acad. Sci. 110, 5103–5108. https://doi.org/10.1073/pnas.1219920110

Siddle, H.V., Marzec, J., Cheng, Y., Jones, M., Belov, K., 2010. MHC gene copy number variation in Tasmanian devils: implications for the spread of a contagious cancer. Proc. R. Soc. B Biol. Sci. 277, 2001–2006. https://doi.org/10.1098/rspb.2009.2362

Siddle, H.V., Sanderson, C., Belov, K., 2007b. Characterization of major histocompatibility complex class I and class II genes from the Tasmanian devil (Sarcophilus harrisii). Immunogenetics 59, 753–760. https://doi.org/10.1007/s00251-007-0238-2

Sotomayor, E.M., Fu, Y.X., Lopez-Cepero, M., Herbert, L., Jimenez, J.J., Albarracin, C., Lopez, D.M., 1991. Role of tumor-derived cytokines on the immune system of mice bearing a mammary adenocarcinoma. II. Down-regulation of macrophage-mediated cytotoxicity by tumor-derived granulocyte-macrophage colony-stimulating factor. J. Immunol. 147, 2816–2823. https://doi.org/10.4049/jimmunol.147.8.2816

Stammnitz, M.R., Coorens, T.H.H., Gori, K.C., Hayes, D., Fu, B., Wang, J., Martin-Herranz, D.E., Alexandrov, L.B., Baez-Ortega, A., Barthorpe, S., Beck, A., Giordano, F., Knowles, G.W., Kwon, Y.M., Hall, G., Price, S., Pye, R.J., Tubio, J.M.C., Siddle, H.V.T., Sohal, S.S., Woods, G.M., McDermott, U., Yang, F., Garnett, M.J., Ning, Z., Murchison, E.P., 2018. The Origins and Vulnerabilities of Two Transmissible Cancers in Tasmanian Devils. Cancer Cell 33, 607-619.e15. https://doi.org/10.1016/j.ccell.2018.03.013

Stammnitz, M.R., Gori, K., Kwon, Y.M., Harry, E., Martin, F.J., Billis, K., Cheng, Y., Baez-Ortega, A., Chow, W., Comte, S., Eggertsson, H., Fox, S., Hamede, R., Jones, M., Lazenby, B., Peck, S., Pye, R., Quail, M.A., Swift, K., Wang, J., Wood, J., Howe, K., Stratton, M.R., Ning, Z., Murchison, E.P., 2023. The evolution of two transmissible cancers in Tasmanian devils. Science 380, 283–293. https://doi.org/10.1126/science.abq6453

Strakova, A., Murchison, E.P., 2014. The changing global distribution and prevalence of canine transmissible venereal tumour. BMC Vet. Res. 10, 168. https://doi.org/10.1186/s12917-014-0168-9

Sun, Y.-P., Ke, Y.-L., Li, X., 2023. Prognostic value of $CD8^+$ tumor-infiltrating T cells in patients with breast cancer: A systematic review and meta-analysis. Oncol. Lett. 25, 1–11. https://doi.org/10.3892/ol.2022.13625

Sunila, I., Farley, C.A., 1989. Environmental limits for survival of sarcoma cells from the soft-shell clam Mya arenaria. Dis. Aquat. Organ. 7, 111–115.

Taylor, B.C., Balko, J.M., 2022. Mechanisms of MHC-I Downregulation and Role in Immunotherapy Response. Front. Immunol. 13, 844866. https://doi.org/10.3389/fimmu.2022.844866

Terry, S., Buart, S., Tan, T.Z., Gros, G., Noman, M.Z., Lorens, J.B., Mami-Chouaib, F., Thiery, J.P., Chouaib, S., 2017. Acquisition of tumor cell phenotypic diversity along the EMT spectrum under hypoxic pressure: Consequences on susceptibility to cell-mediated cytotoxicity. OncoImmunology 6, e1271858. https://doi.org/10.1080/2162402X.2016.1271858

Tersigni, C., Meli, F., Neri, C., Iacoangeli, A., Franco, R., Lanzone, A., Scambia, G., Di Simone, N., 2020. Role of Human Leukocyte Antigens at the Feto-Maternal Interface in Normal and Pathological Pregnancy: An Update. Int. J. Mol. Sci. 21. https://doi.org/10.3390/ijms21134756

Tovar, C., Pye, R.J., Kreiss, A., Cheng, Y., Brown, G.K., Darby, J., Malley, R.C., Siddle, H.V.T., Skjødt, K., Kaufman, J., Silva, A., Morelli, A.B., Papenfuss, A.T., Corcoran, L.M., Murphy, J.M., Pearse, M.J., Belov, K., Lyons, A.B., Woods, G.M., 2017. Regression of devil facial tumour disease following immunotherapy in immunised Tasmanian devils. Sci. Rep. 7, 43827. https://doi.org/10.1038/srep43827

Tran, E., Robbins, P.F., Lu, Y.-C., Prickett, T.D., Gartner, J.J., Jia, L., Pasetto, A., Zheng, Z., Ray, S., Groh, E.M., Kriley, I.R., Rosenberg, S.A., 2016. T-Cell Transfer Therapy Targeting Mutant KRAS in Cancer. N. Engl. J. Med. 375, 2255–2262. https://doi.org/10.1056/NEJMoa1609279

Tsukamoto, K., Deakin, J.E., Graves, J.A.M., Hashimoto, K., 2013. Exceptionally high conservation of the MHC class I-related gene, MR1, among mammals. Immunogenetics 65, 115–124. https://doi.org/10.1007/s00251-012-0666-5

Vance, R.E., Kraft, J.R., Altman, J.D., Jensen, P.E., Raulet, D.H., 1998. Mouse CD94/NKG2A Is a Natural Killer Cell Receptor for the Nonclassical Major Histocompatibility Complex (MHC) Class I Molecule Qa-1b. J. Exp. Med. 188, 1841–1848. https://doi.org/10.1084/jem.188.10.1841

Varghese, F., Bukhari, A.B., Malhotra, R., De, A., 2014. IHC Profiler: An Open Source Plugin for the Quantitative Evaluation and Automated Scoring of Immunohistochemistry Images of Human Tissue Samples. PLOS ONE 9, e96801. https://doi.org/10.1371/journal.pone.0096801

Wang, D., Lin, J., Yang, Xu, Long, J., Bai, Y., Yang, Xiaobo, Mao, Y., Sang, X., Seery, S., Zhao, H., 2019. Combination regimens with PD-1/PD-L1 immune checkpoint inhibitors for gastrointestinal malignancies. J. Hematol. Oncol.J Hematol Oncol 12, 42. https://doi.org/10.1186/s13045-019-0730-9

Wischhusen, J., Friese, M.A., Mittelbronn, M., Meyermann, R., Weller, M., 2005. HLA-E Protects Glioma Cells from NKG2D-Mediated Immune Responses In Vitro: Implications for Immune Escape In Vivo. J. Neuropathol. Exp. Neurol. 64, 523–528. https://doi.org/10.1093/jnen/64.6.523

Wolpert, F., Roth, P., Lamszus, K., Tabatabai, G., Weller, M., Eisele, G., 2012. HLA-E contributes to an immune-inhibitory phenotype of glioblastoma stem-like cells. J. Neuroimmunol. 250, 27–34. https://doi.org/10.1016/j.jneuroim.2012.05.010

Woods, G.M., Kreiss, A., Belov, K., Siddle, H.V., Obendorf, D.L., Muller, H.K., 2007. The Immune Response of the Tasmanian Devil (Sarcophilus harrisii) and Devil Facial Tumour Disease. EcoHealth 4, 338–345. https://doi.org/10.1007/s10393-007-0117-1

Xue, J.-S., Ding, Z.-N., Meng, G.-X., Yan, L.-J., Liu, H., Li, H.-C., Yao, S.-Y., Tian, B.-W., Dong, Z.-R., Chen, Z.-Q., Hong, J.-G., Wang, D.-X., Li, T., 2022. The Prognostic Value of Natural Killer Cells and Their Receptors/Ligands in Hepatocellular Carcinoma: A Systematic Review and Meta-Analysis. Front. Immunol. 13, 872353. https://doi.org/10.3389/fimmu.2022.872353

Yachida, S., Jones, S., Bozic, I., Antal, T., Leary, R., Fu, B., Kamiyama, M., Hruban, R.H., Eshleman, J.R., Nowak, M.A., Velculescu, V.E., Kinzler, K.W., Vogelstein, B., Iacobuzio-Donahue, C.A., 2010. Distant metastasis occurs late during the genetic evolution of pancreatic cancer. Nature 467, 1114–1117. https://doi.org/10.1038/nature09515

Ye, S.-R., Yang, H., Li, K., Dong, D.-D., Lin, X.-M., Yie, S.-M., 2007. Human leukocyte antigen G expression: as a significant prognostic indicator for patients with colorectal cancer. Mod. Pathol. Off. J. U. S. Can. Acad. Pathol. Inc 20, 375–383. https://doi.org/10.1038/modpathol.3800751

Yevich, P.P., Barszez, C.A., 1977. Neoplasia in soft-shell clams (Mya arenaria) collected from oil-impacted sites. Ann N Acad Sci U. S. 298.

Yie, S.-M., Yang, H., Ye, S.-R., Li, K., Dong, D.-D., Lin, X.-M., 2007. Expression of human leukocyte antigen G (HLA-G) correlates with poor prognosis in gastric carcinoma. Ann. Surg. Oncol. 14, 2721–2729. https://doi.org/10.1245/s10434-007-9464-y

Yokokawa, J., Cereda, V., Remondo, C., Gulley, J.L., Arlen, P.M., Schlom, J., Tsang, K.Y., 2008. Enhanced Functionality of CD4+CD25highFoxP3+ Regulatory T Cells in the Peripheral Blood of Patients with Prostate Cancer. Clin. Cancer Res. 14, 1032–1040. https://doi.org/10.1158/1078-0432.CCR-07-2056

Yokoyama, W.M., 1995. Natural killer cell receptors specific for major histocompatibility complex class I molecules. | PNAS. PNAS 92, 3081–3085.

Yonemitsu, M.A., Giersch, R.M., Polo-Prieto, M., Hammel, M., Simon, A., Cremonte, F., Avilés, F.T., Merino-Véliz, N., Burioli, E.A., Muttray, A.F., Sherry, J., Reinisch, C., Baldwin, S.A., Goff, S.P., Houssin, M., Arriagada, G., Vázquez, N., Bierne, N., Metzger, M.J., 2019. A single clonal lineage of transmissible cancer identified in two marine mussel species in South America and Europe. eLife 8, e47788. https://doi.org/10.7554/eLife.47788

Zhang, S., Liu, W., Hu, B., Wang, P., Lv, X., Chen, S., Shao, Z., 2020. Prognostic Significance of Tumor-Infiltrating Natural Killer Cells in Solid Tumors: A Systematic Review and Meta-Analysis. Front. Immunol. 11, 1242. https://doi.org/10.3389/fimmu.2020.01242

Zou, W., 2006. Regulatory T cells, tumour immunity and immunotherapy. Nat. Rev. Immunol. 6, 295–307. https://doi.org/10.1038/nri1806